Understanding and Predicting Water Quality Impacts on Coagulation

Christina Clarkson Davis

Dissertation submitted to the faculty of
the Virginia Polytechnic Institute and State University
in partial fulfillment of the requirements for the degree of

Doctor of Philosophy
In
Civil Engineering

Marc Edwards, Chair
Matthew J. Eick
William R. Knocke
John C. Little
Peter J. Vikesland

September 12, 2014
Blacksburg, VA

Keywords: coagulation, natural organic matter, ferric chloride, calcium, silica, alkalinity, diffuse layer model

Understanding and Predicting Water Quality Impacts on Coagulation

Christina Clarkson Davis

ABSTRACT

Effective coagulation is critical to the production of safe, potable drinking water, but variations in the chemical composition of source water can present challenges in achieving targeted contaminant removal and predicting coagulation outcomes. A critical literature review describes factors affecting the hydrolysis reactions of metal salt coagulants and the resulting precipitates. Properties of two key contaminants, turbidity and natural organic matter (NOM), are explored in the context of removal during coagulation, and the influence of co-occurring ions is described. While it is apparent that NOM character determines the minimum achievable organic carbon residual, the effects of water quality—including pH, NOM character and concentration, and concentrations of synergistic and competitive ions—on overall coagulation efficacy and NOM removal may be underestimated. An experimental research plan was devised to investigate the influence of water quality in coagulation and provide data to support the development of a predictive coagulation model.

NOM is capable of interfering with ferric iron hydrolysis and influencing the size, morphology, and identity of precipitates. Conversely, calcium is known to increase the size and aggregation of Fe^{3+} precipitates and increase surface potential, leading to more effective coagulation and widening the pH range of treatment. Experiments and modeling were conducted to investigate the significance of the Fe/NOM ratio and the presence of calcium in coagulation. At the high Fe/NOM ratio, sufficient or excess ferric hydroxide was available for NOM removal, and coagulation proceeded according to expectations based upon the literature. At the low Fe/NOM ratio, however, NOM inhibited Fe^{3+} hydrolysis, reduced zeta potential, and suppressed the formation of filterable Fe flocs, leading to interference with effective NOM removal. In these dose-limited systems, equilibrating NOM with 1 mM Ca^{2+} prior to dosing with ferric chloride coagulant increased the extent of Fe^{3+} hydrolysis, increased zeta potential, decreased the fraction of colloidal Fe, and improved NOM removal. In dose-limited systems without calcium, complexation of Fe species by NOM appears to be the mechanism by which coagulation is disrupted. In systems with calcium, data and modeling indicate that calcium complexation by NOM neutralizes some of the negative organic charge and minimizes Fe complexation, making Fe hydrolysis species available for growth and effective coagulation.

Experiments were conducted to investigate the influence of aqueous silica and pH on the removal of natural organic matter (NOM) by coagulation with ferric chloride. Samples with preformed ferric hydroxide were also compared to samples coagulated in situ to assess the role of coprecipitation. The moderate (10 mg/L) and high (50 mg/L) SiO_2 concentrations both demonstrated interference with NOM removal at pH 6.5-7.5. In turn, NOM at 2 mg/L as DOC interfered with silica sorption at the moderate silica level and in

samples with preformed ferric hydroxide at the high silica level. The combination of NOM and high silica led to decreases in DOC sorption and unexpected increases in silica sorption in the coprecipitated samples. The fraction of colloidal Fe passing a 0.45-μm filter also increased in the coprecipitated samples with both NOM and high silica. It is hypothesized that the combination of NOM and high silica synergistically interfered with Fe precipitation and particle growth processes, with NOM having the greater effect at lower pH and shorter reaction times, and silica exerting greater influence at higher pH and longer reaction time. Direct competition for surface sites and electrostatic repulsion were also influential.

An overall goal for this research was the development of a quantitative coagulation model. Previous attempts to model coagulation have been limited by the inherent complexities of simultaneously predicting ligand sorption, metal complexation, floc surface charge, and particle removal. A diffuse layer (DLM) surface complexation model was formulated to simultaneously predict sorption of NOM and other key species, including silica, calcium, and carbonate alkalinity. Predictions of surface potential were used to estimate zeta potential and resulting regimes of effective aggregation and turbidity removal. The model provided good predictive ability for data from bench-scale experiments with synthetic water and jar tests of nine U.S. source waters. Under most conditions, the model provides excellent capability for predicting NOM sorption, calcium sorption, and particle destabilization and adequate capability for predicting silica sorption. Model simulations of hypothetical scenarios and experimental results help to explain practical observations from the literature. The DLM can be optimized to site-specific conditions and expanded to include sorption of additional species, such as arsenic.

.

DEDICATION

In memory of my grandparents,

Raymond V. and Laura L. Bond

and

In honor of the One who made the way

Every good and perfect gift is from above,
coming down from the Father of the heavenly lights,
who does not change like shifting shadows.
James 1:17

ACKNOWLEDGEMENTS

I extend my sincere gratitude and thanks to Dr. Marc Edwards. I appreciate his diligence in training and guiding me, and I admire his example of generosity, integrity, and commitment to public health and science. I feel extremely fortunate that he agreed to serve as my advisor and mentor, and I will always remember and appreciate his efforts.

I also appreciate the contributions of my committee members, Dr. William Knocke, Dr. John Little, Dr. Peter Vikesland, and Dr. Matt Eick. Their helpful suggestions and encouragement shaped and improved this research.

I thank Caitlin Grotke and Samantha Fisher for their assistance in the laboratory. Dr. Jeff Parks and other members of the Edwards Research Group kindly provided instrumental analyses, and Dr. Hsiao-wen Chen isolated the fulvic acid used in this research.

The following sources of financial support are gratefully acknowledged. This funding was critical to my ability to pursue this doctoral program.

- US EPA Science to Achieve Results (STAR) Graduate Fellowship Program
- Virginia Tech Department of Civil and Environmental Engineering Via Fellowship Program
- National Water Research Institute (NWRI) Graduate Fellowship Program
- American Water Works Association (AWWA) Larson Aquatic Research Support (LARS) Fellowship and Thomas R. Camp Scholarship Programs
- Edna Bailey Sussman Foundation's Jeremy Herbstritt Memorial Internship Program
- Virginia Water Resources Research Center William R. Walker Graduate Research Fellowship Program
- Dr. Marc Edwards

Finally, I wish to thank my husband, children, family, and friends who have walked this journey with me. There are not enough words to describe the contributions of my husband, Mark. Over the years, he has not wavered in his encouragement, and he has sacrificially helped me pursue this goal without complaint. He constructed my lab space, solved my computer problems, answered statistical questions, acted as my sounding board, and embodied Ecclesiastes 4:9-10. I thank my children for their patience while I completed my dissertation and for the love and joy they bring to my life. My extended family and friends provided enthusiastic encouragement along the way, prayed for me, and even cared for my children. I am deeply thankful for the love and support that all of these people have shown to me.

ATTRIBUTION

Each of the four chapters in this dissertation was prepared for submission to a peer-reviewed journal. This work represents a collaborative effort between the author and her advisor, Dr. Marc Edwards. Thus, Dr. Edwards is included as a co-author on each manuscript. Dr, Edwards is the Charles Lunsford Professor of Civil and Environmental Engineering at Virginia Tech.

Dr. Hsiao-wen Chen contributed to and is a co-author for Chapter 4, "Simultaneous Prediction of NOM Removal and Particle Destabilization in Coagulation." Dr. Chen developed an Excel-based model that served as a forerunner to the one presented in Chapter 4. Dr. Chen also isolated and characterized the fulvic acid used in this research. Currently, Dr. Chen is a Research Manager at the Water Research Foundation in Denver, CO.

Table of Contents

List of Figures

List of Tables

Chapter 1. Coagulation with Hydrolyzing Metal Salts: Mechanisms and Water Quality Impacts

Christina C. Davis and Marc Edwards

Virginia Tech Department of Civil and Environmental Engineering,
407 Durham Hall, Blacksburg, VA 24060

Keywords: coagulation, alum, ferric chloride, ferric sulfate, natural organic matter, turbidity, arsenic

Abstract

Coagulation is a critical—but highly complex—process in drinking water treatment. Variations in pH, temperature, source water composition, coagulant type, and other conditions collectively influence the process and confound efforts to quantitatively predict coagulation outcomes. Yet, qualitative understanding is possible through synthesis of the extensive literature. This review describes hydrolysis reactions of metal salts and summarizes variables that influence the characteristics of the resulting precipitates. Thereafter, properties of two key contaminants, turbidity and natural organic matter (NOM), are explored in the context of removal during coagulation. Finally, the significance of source water quality and co-occurring ions is described.

Introduction

Although coagulation was practiced by ancient civilizations, it first appeared in its modern form in the late 19th century (Crittenden et al. 2005, LaNier 1976). Water purveyors initially implemented coagulation to facilitate effective turbidity removal by rapid filtration, but its role in the removal of organic color became more important during the latter half of the 20th century. Today, it is a critical process in most surface water treatment plants, facilitating effective reductions in turbidity, pathogens, and inorganic and organic contaminants.

While more than 100 years of research, design, and operational experience has yielded a qualitative understanding of contaminant removal trends, the drinking water community is still unable to quantitatively predict coagulation efficacy. Although significant gaps exist, synthesis of current knowledge is expected to improve conceptualization of the coagulation process. This review aims to summarize and clarify understanding of (1) coagulant hydrolysis reactions, (2) the characteristics and removal mechanisms of key contaminants, and (3) the role of water quality in coagulation.

Hydrolysis of Metal Salt Coagulants

Metal salt coagulants are well suited for treating negatively-charged natural organic matter (NOM) and turbidity and are therefore the most widely used coagulants in the U.S. Although prehydrolyzed varieties have gained in popularity over the last few decades, simple hydrolyzing salts—including alum, ferric chloride, and ferric sulfate—remain predominant.

Aluminum and ferric cations in acidic solutions are coordinated with six water molecules. In the pH range of water treatment, alum and ferric salts undergo rapid hydrolysis reactions in which OH^- ligands substitute for coordinated water molecules, forming mononuclear compounds. Upon the formation of aquo-hydroxo complexes, condensation reactions proceed by nucleophilic addition or substitution, leading to olation (Equation 1-1) (Jolivet 2000, Stumm and Morgan 1996).

$$M - OH + M - OH_2 \rightarrow M - OH - M + H_2O \quad (1\text{-}1)$$

Continued condensation reactions of charged species produce oligomeric cations, like $M_2(OH)_2^{4+}$ and $M_3(OH)_4^{5+}$, and polymers, such as the Al_{13} polycation. In contrast, zero-charge precursors, such as $M(OH)_{3(aq)}$, condense to form nuclei which may ultimately precipitate as solids (Baes and Mesmer 1986, Jolivet 2000, Stumm and Morgan 1996). The pH and coagulant dosages commonly associated with water treatment are conducive to the precipitation of amorphous solids, specifically aluminum hydroxide or ferrihydrite, a ferric oxyhydroxide (Cornell and Schwertmann 2003, Jolivet 2000).

Reaction kinetics and the stability of hydrolysis species are correlated with the degree of condensation. Hydrolyzed monomers form rapidly and reversibly, whereas additional time is required for the condensation of oligomers and polymers (Baes and Mesmer 1986, Stumm and Morgan 1996). Polymers, like the Al_{13} polycation, can be quite stable; in fact, the persistence of large polymers upon dilution is the basis for prehydrolyzed coagulants, such as polyaluminum chloride (PACl). Analogous to the hydroxylated species, the kinetics and stability associated with precipitated solids can be correlated with chemical structure. Compared to amorphous aluminum

and ferric (oxy)hydroxide precipitates, crystalline solids, such as gibbsite and goethite, are less soluble but their formation is kinetically slow. If water is dosed with aluminum or ferric iron in excess of the amorphous (oxy)hydroxide solubility limit, metastable, poorly-ordered solids rapidly precipitate (Stumm and Morgan 1996). Over longer periods of time, ranging from days to years, the amorphous solids convert to stable, crystalline structures through one or more pathways.

The regions over which the various species occur depend upon the coagulant concentration and pH. Although monomeric and polymeric hydrolysis species may contribute to effective coagulation in some waters, coagulation operations are generally carried out under conditions associated with precipitation of amorphous aluminum or ferric (oxy)hydroxide (Figure 1-1). The minimum solubility of the ferric solid occurs at an approximate pH of 8.0, while the solubility of the aluminum solid is minimized at about pH 6.0. However, the overall solubility of the ferric oxyhydroxide is much lower, such that even at pH 6.0, the solubility of ferric oxyhydroxide is nearly two orders of magnitude lower. Comparing the two solubility diagrams suggests that ferric coagulants may be more efficient when contaminant sorption is the dominant coagulation mechanism. However, aluminum coagulants may perform better in waters where charge neutralization and complexation are important coagulation mechanisms.

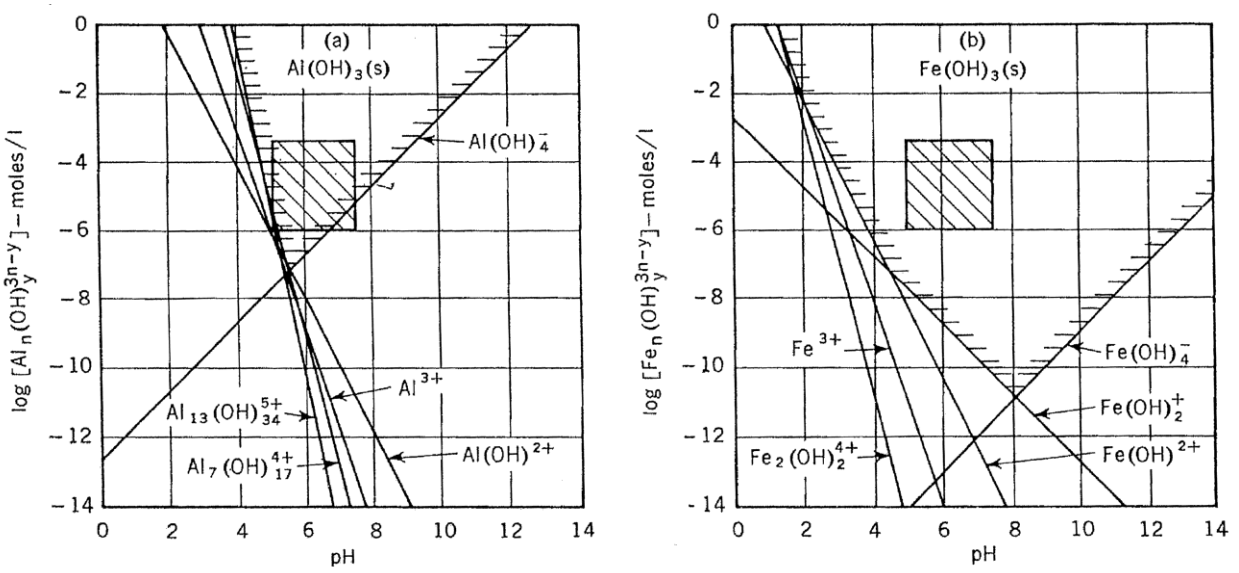

Figure 1-1. Equilibrium composition of solutions in contact with freshly precipitated $Al(OH)_3$ and $Fe(OH)_3$, calculated using representative values for the equilibrium constants for solubility and hydrolysis equilibria. Shaded areas are approximate operating regions in water treatment practice (Stumm and O'Melia 1968). Reprinted from Journal AWWA Vol. 60, No. 5, by permission. Copyright © 1968, American Water Works Association.

In addition to dose and pH effects, hydrolysis and precipitation reactions are influenced by water temperature, mixing, and solution chemistry. For example, numerous studies have demonstrated that colder water temperatures are detrimental to coagulation efficacy, with the negative effect more pronounced for alum than ferric-based coagulants (Hanson and Cleasby 1990, Morris and Knocke 1984). Van Benschoten and Edzwald (1990a) related temperature effects on turbidity, electrophoretic mobility (EM), and aluminum speciation to the ion product of water, which controls the supply of OH^- ions for hydrolysis reactions. Consequently, increasing the pH

in colder water can mitigate some of the negative effects of temperature (Hanson and Cleasby 1990, Kang and Cleasby 1995, Van Benschoten and Edzwald 1990a). Coagulation at colder temperatures has also been associated with slower aggregation kinetics (Kang and Cleasby 1995), smaller floc size (Morris and Knocke 1984), and reduced floc strength (Hanson and Cleasby 1990).

Inadequate mixing leads to localized pH gradients in solution, resulting in non-homogenous condensation reactions. Mixing has been linked to aluminum speciation, with more intense mixing favoring aluminum hydroxide precipitation, and poorer mixing associated with aluminum polymerization (Clark et al. 1993). Under conditions where precipitation occurs, microzones with higher OH^- concentrations experience more rapid hydrolysis, leading to a greater supply of nuclei for incorporation into the growing solid (Jolivet 2000). These zones produce larger precipitates, and the resulting suspension may exhibit a large distribution of particle sizes.

Turbidity

Turbidity may be defined as "an expression of the optical property that causes light to be scattered and absorbed rather than transmitted with no change in direction or flux level through the sample" (Eaton et al. 2005). Turbidity-causing material, including clays, silts, and microorganisms, frequently imparts a cloudy appearance to water and may be associated with other aesthetic concerns, such as color or taste. However, the greater significance of turbidity arises from the health risks associated with suspended organic matter, bacteria, and protozoans, as well as microorganisms that may be sorbed to the surfaces of otherwise innocuous particles and colloids. As a result of these risks, turbidity removal or reduction continues to be a primary objective of coagulation operations.

Mechanistically, turbidity removal by hydrolyzing metal salts occurs by charge neutralization or enmeshment by sweep floc (Dentel and Gossett 1988, Packham 1965, Shin et al. 2008, Stumm and O'Melia 1968). The hydrolysis species and specific mechanisms responsible for inducing coagulation depend upon a number of factors, including pC-pH conditions, particle surface area (Stumm and O'Melia 1968), and the presence of competing ligands that can shift the pH of precipitation (Stumm and Morgan 1962) or react with hydrolysis species (Shin et al. 2008). In waters with low initial turbidity, opportunities for particle collisions are limited, and sweep flocculation may be required for effective particle removal. However, Shin et al. (2008) demonstrated that low concentrations of NOM drastically lowered the minimum effective alum dose, essentially shifting the removal mechanism from sweep flocculation to charge neutralization.

Some researchers have summarized the different coagulation regimes with operational diagrams (Amirtharajah et al. 1993, Amirtharajah and Mills 1982). Yet variability in temperature, water chemistry, and metal speciation limit the practical usefulness of such diagrams. Ultimate determination of the governing mechanism typically relies on visual observation and measurements of zeta potential and residual turbidity.

Natural Organic Matter

Prior to the 1970s, the deleterious health effects of NOM in water supplies were unknown, and its presence was primarily viewed as an aesthetic problem (Black and Christman 1963). With the discovery of chlorinated disinfection byproducts (DBPs) (Rook 1974), however, NOM

removal became a priority for regulators and utilities. Additional issues associated with NOM include increased oxidant demand, membrane fouling, microbial regrowth, and distribution system corrosion.

Characteristics of NOM

NOM is a broad term employed to describe heterogeneous mixtures of organic compounds derived from both plant and animal sources. NOM is ubiquitous in natural waters, although levels—as measured by dissolved organic carbon (DOC) concentrations—can vary drastically (Table 1-1). The chemical composition of NOM also exhibits significant variation, depending upon the characteristics of the water body and the sources of organic carbon. Streams and rivers primarily receive allochthonous organic carbon, which is dominated by plant- and soil-based NOM (Thurman 1985), although treated wastewater discharges also contribute organic matter to receiving water bodies (Malcolm 1985). Lakes and reservoirs are subject to a combination of allochthonous and autochthonous organic carbon, with autochthonous NOM arising from algae, aquatic plants, and littoral sources (Malcolm 1985, Thurman 1985).

Table 1-1. Dissolved Organic Carbon Concentrations in Natural Waters

Water Type	DOC (mg/L)	Factors Influencing DOC Concentration
Groundwater	0.2 – 15	▪ Aquifer characteristics ▪ Recharge source
Streams & Rivers	1 – 60	▪ Climate ▪ Discharge ▪ Season (wet/dry)
Lake	1 – 50	▪ Trophic status

Source: Thurman 1985

Due to the complexity and variability of NOM, few generalizations can be made about the underlying molecular structures. Instead, fractions of NOM are generally classified according to physical and chemical characteristics, such as size and polarity. Most NOM compounds fall into one of six major chemical groups, specifically humic substances, hydrophilic acids, carbohydrates, carboxylic acids, amino acids, and hydrocarbons (Thurman 1985).

Drinking water research and operations tend to emphasize aquatic humic substances (AHSs) due to their prevalence, role as disinfection byproduct precursors, and amenability to coagulation. According to Thurman (1985), AHSs may be operationally defined as "colored, polyelectrolytic, organic acids isolated from water on XAD resins, weak-base ion-exchange resins, or a comparable procedure." AHSs are nonvolatile and comprise a substantial fraction of NOM in natural waters, typically contributing 30-50 percent of DOC in uncolored waters and 50-90 percent of DOC in organically colored waters (Thurman 1985). In isolation schemes utilizing XAD-8 resin, AHSs retained by the resin are classified as the hydrophobic acid fraction (Aiken et al. 1992, Leenheer 1981, Leenheer and Huffman 1976, Thurman and Malcolm 1981). Humic substances can be further categorized as humic acids (HAs), which precipitate at pH below 2.0, and fulvic acids (FAs), which remain soluble in acidic solution; FAs tend to occur at much higher concentrations than humic acids. Functional groups of AHSs include hydroxyl, carbonyl,

carboxyl, and phenolic hydroxyl, with the latter two groups controlling acidity (Thurman 1985). The tendency of HAs to precipitate in acidic solution is attributed to their lower carboxyl acidity, as compared to FAs (Thurman 1985).

FAs have a typical molecular weight (MW) within the range of 500-2000 Da, and HAs usually fall between 2000-5000 Da, although much higher HA sizes have been published (Swift 1999, Thurman 1985). While differences in experimental techniques have undoubtedly contributed to inconsistencies in the literature, the chemistry and conformation of humic substances are known to influence size measurements. HAs and FAs were historically viewed as macromolecular polyelectrolytes, capable of assuming a variety of conformations (Au et al. 1999, Stumm and Morgan 1996, Swift 1999, Thurman 1985). At acidic pH levels, where carboxylic and phenolic functional groups are completely or predominantly protonated, the humic polymers were thought to assume a coiled, compact arrangement (Figure 1-2); similar arrangements were expected to occur at high ionic strength conditions since deprotonated functional groups would presumably complex cations. At lower ionic strengths or higher pH levels, however, it was theorized that repulsion between deprotonated functional groups would yield a linear or flat conformation (Figure 1-2).

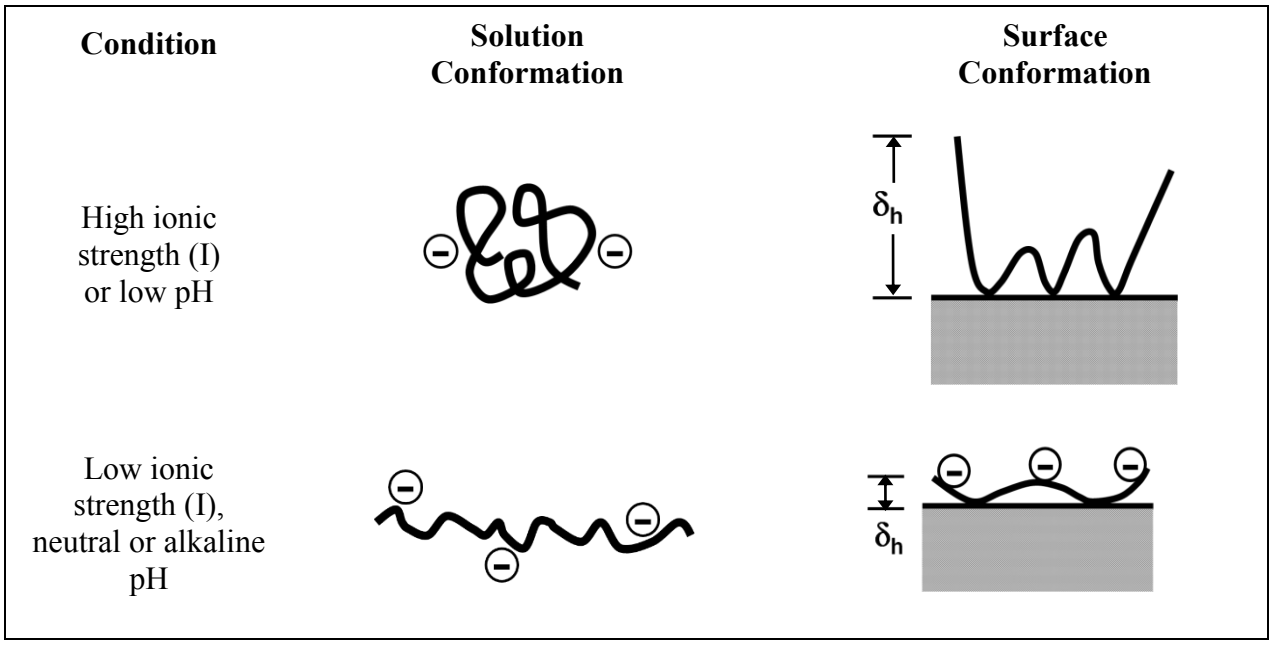

Figure 1-2. Schematic conceptualization of pH and ionic strength effects on the conformations of humic molecules. R_h: hydrodynamic radius. δ_h: hydrodynamic thickness. Redrawn from Stumm and Morgan 1996.

Simpson and co-workers (2002) used multi-dimensional nuclear magnetic resonance (NMR) to identify the major components of soil humic substances as aliphatic acids, ethers, esters, alcohols, aromatic lignin derived fragments, polysaccharides, and polypeptides. Many investigators have recently advanced the theory of supramolecular association, proposing that these units of relatively low MW aggregate under certain conditions (Baalousha et al. 2006, Diallo et al. 2005, Leenheer and Croue 2003, Maurice and Namjesnik-Dejanovic 1999, Piccolo 2001, Simpson et al. 2002, Sutton and Sposito 2005, Wilkinson et al. 1999).

Baalousha et al. (2006) used transmission electron microscopy (TEM) and photon correlation spectroscopy (PCS) to study the size of Suwannee River HA (SRHA) aggregates as a function of solution conditions. They concluded that SRHA consisted of basic units of less than 10 nm and that the extent of aggregation depended upon solution conditions. Testing at three pH levels revealed that aggregates at pH 4.5 were smaller than those formed at pH 7.5 and 9.3. Comparing the effect of metals, calcium promoted greater aggregation than sodium. Increasing ionic strength also generally resulted in larger aggregates, although exceptions were observed. Baalousha et al. (2006) also noted that supramolecular networks could exceed 0.45 μm, altering the classification of the network from "dissolved" to particulate. If humic substances do engage in supramolecular association, this phenomenon may explain conflicting reports in the literature regarding the nature of humic substances as either dissolved macromolecules or colloids.

Mechanisms of NOM Removal

The discovery of trihalomethanes (THMs), haloacetic acids (HAAs), and other DBPs launched several decades of intensive research aimed at identifying the best techniques and treatment schemes for mitigating the accompanying health risks. Attention quickly focused on coagulation-flocculation because (1) conventional treatment was already in use in many U.S. water treatment plants, and (2) early research demonstrated that coagulation was an effective technique for reducing total organic carbon (TOC) concentrations in many waters (Black and Christman 1963, Black et al. 1963). In 1998, the Environmental Protection Agency (EPA) named enhanced coagulation as a treatment technique for Stage 1 Disinfectants and Disinfection Byproducts Rule compliance. Yet, despite the voluminous literature and years of practical experience, the specific chemical interactions and mechanisms involved in NOM removal by coagulation have not been conclusively identified. Furthermore, mechanisms that have been proposed (Table 1-2) are typically restricted to semiempirical conditions, such as certain pH ranges.

Charge Neutralization/Precipitation. In the pH range of natural waters, the functional groups of humic substances are partially ionized, yielding anionic species. Coagulation by the charge neutralization/precipitation (CNP) mechanism assumes a discrete chemical reaction between soluble humic anions and the cationic species produced by aluminum or ferric hydrolysis. Possible end products of the reaction include soluble complexes and insoluble Al-NOM or Fe-NOM precipitates. Various investigators have suggested that the responsible species include aluminum monomers (Dempsey et al. 1984, Van Benschoten and Edzwald 1990a), ferric oligomers (Jung et al. 2005, Sieliechi et al. 2008, Vilge-Ritter et al. 1999), polymeric aluminum hydroxo complexes (Dempsey et al. 1984, Narkis and Rebhun 1977), and an "incipiently solid soluble phase" (Edwards and Amirtharajah 1985).

Table 1-2. Chronological Summary of NOM Coagulation Studies and Proposed Removal Mechanisms

Reference	Experiment	Organic Matter	Coagulant	Other Conditions	Conclusions
Hall and Packham 1965	Jar tests Optical density measured in filtered samples	FA and HA from Thames River, England	a) Ferric chloride b) Alum c) Aluminum chloride	Synthetic water Acid added with coagulant to maintain acid additions (meq) constant between tests Final pH controlled by varying $NaHCO_3$ and NaOH	CNP is consistent with optimal removal of humic substances in the pH range of 5-6
Narkis and Rebhun 1977	Details not provided	a) Aldrich HA (0-50 mg/L) b) Peat FA (Huleh Valley, Israel)	Alum	Details not provided	CNP and subsequent polymer bridging controls removal, with an optimal pH range of 5.8-6.7
Dempsey et al. 1984	Jar tests Measurement of UV_{254} absorbance and OC in filtered (0.2 μm) samples	FA from Dismal Swamp, VA	Alum or Aluminum chloride	Synthetic water Coagulant added simultaneously with acid (HCl) or base ($NaHCO_3$)	CNP by Al monomers prevails from pH 4.5-5.0 CNP by Al polymers prevails at pH<6.0 ADS of FA or FA-Al complexes controls removal at pH>6.25
Edwards and Amirtharajah 1985	Jar tests	Aldrich HA (4.0-37.5 mg/L)	Alum	Synthetic water 27-30 NTU turbidity (Min-U-Sil-30) $NaHCO_3$ (1 mg/L)	CNP active at pH<5.75 ADS active at pH>5.75

Table 1-2. Chronological Summary of NOM Coagulation Studies and Proposed Removal Mechanisms (Continued)

Reference	Experiment	Organic Matter	Coagulant	Other Conditions	Conclusions
Dempsey 1989	Sorption tests Solutions dosed with alum and sampled at 5 min, 1 h, 4 h, 1 day, and 7 days	FA from Lake Drummond, VA (0-84 mg/L as C)	Alum (1.05 mg/L as Al in most experiments)	Synthetic water pH adjustment with acid (HCl) or base (NaOH) prior to alum addition	$Al(OH)_{3(s)}$ precipitates under all p[Al]-pH conditions yielding FA removal ADS appears to be the predominant mechanism over the entire pH range associated with coagulation FA enhances $Al(OH)_{3(s)}$ precipitation at pH$\leq$5.0 Polymeric Al may contribute to removal, but its role is unclear
Van Benschoten and Edzwald 1990b	Complexation studies Measurement of filtered (0.22 μm) pH, Al speciation, and soluble UV_{254} absorbance	FA from Provencial Brook, MA (2.0 mg/L as C)	Alum (0.2-1.0 mg/L as Al)	Synthetic water I=0.002 M Initial pH=5.0 or 7.0, alum dosed, then pH adjusted to target	Proposed Al-FA complex with stoichiometry of $Al(OH)_{2.7}FA_{0.64}$ coincides with typical water treatment conditions $Al(OH)_{2.7}FA_{0.64}$ may represent a precursor to a solid phase (CNP mechanism) or it may sorb to precipitated $Al(OH)_{3(s)}$ (ADS mechanism) Order of chemical addition may have affected speciation and FA removal

Table 1-2. Chronological Summary of NOM Coagulation Studies and Proposed Removal Mechanisms (Continued)

Reference	Experiment	Organic Matter	Coagulant	Other Conditions	Conclusions
Dennett et al. 1996	Jar tests Measurement of UV_{254} absorbance and OC in filtered (1 μm) samples Fast atom bombardment mass spectroscopy (FABMS) analysis of non-removed DOM	Suwannee River DOM isolated by reverse osmosis (3.4, 6.8, and 13.0 mg/L as C)	Ferric chloride (10-100 mg/L)	Synthetic water Final pH varied $NaHCO_3$ dosed (1-100 mg/L as $CaCO_3$)	63-74% OC removal in jar test series with doses of 36-48 mg/L and final pH of 5.42-6.18 ADS mechanism active at all conditions CNP enhances removal of higher MW (>750 Da) organics at lower pH-higher dose conditions
Vilge-Ritter et al. 1999	Jar tests X-ray Absorption Spectroscopy (XAS) and Small Angle X-ray Scattering (SAXS) analysis of flocs	NOM in Seine River (4.0 mg/L as C) and Ribou Lake (8.4 mg/L as C), France	Ferric chloride (8.3 mg/L as Fe)	Natural waters from Seine River and Ribou Lake, France pH adjusted to 5.5 or 7.5 after coagulant addition	CNP by complexation of ferric oligomers active at pH 5.5 and 7.5 pH affects aggregate structure
Jung et al. 2005	Jar tests Transmission Electron Microscopy (TEM) analysis of flocs	AHSs isolated from Moselle River, France	Ferric nitrate	Synthetic water (30 mg/L of AHS, initial pH 6.0 or 8.0) Natural water from Moselle River, France (9.3 mg/L as C, initial pH 7.4)	CNP by complexation of ferric oligomers under all pH conditions pH effects related to conformational changes

Table 1-2. Chronological Summary of NOM Coagulation Studies and Proposed Removal Mechanisms (Continued)

Reference	Experiment	Organic Matter	Coagulant	Other Conditions	Conclusions
Shin et al. 2008	Jar tests Analysis of settled turbidity, filtered turbidity, and DOC (1.2-µm filter)	NOM from Dismal Swamp, VA	Alum	Synthetic water with varying initial concentrations of DOC and colloidal silica particles pH adjusted to target value (6.0 or 7.0) after alum addition	DOC dominates coagulant demand except at very high particle concentrations Linear relationship observed between initial DOC and minimum effective alum dose (MEAD) Estimated [OH]/[Al] ratios of 2.65 (pH 7) and 2.56 (pH 6) suggest at least some DOC removal occurs by CNP; ADS may also occur
Sieliechi et al. 2008	Jar tests X-ray microscopy (XRM) analysis of flocs	HA isolated from Nyong River sediments, Cameroon (10 mg/L as C)	Ferric chloride	Synthetic water (initial pH 6.0 or 8.0)	CNP by complexation of ferric oligomers under all pH conditions pH effects related to conformational changes

Key to Abbreviations

NOM: natural organic matter
CNP: charge neutralization/precipitation mechanism
ADS: adsorption mechanism
OC: organic carbon
FA: fulvic acid
HA: humic acid
DOM: dissolved organic matter
MW: molecular weight
AHS: aquatic humic substance

The CNP mechanism is similar to the adsorption/charge neutralization mechanism that governs coagulation of colloids under certain conditions. With respect to colloidal systems, Stumm and O'Melia (1968) established a stoichiometric relationship between colloid surface area and the ferric perchlorate dose required for charge neutralization. By analogy, the existence of a stoichiometric relationship between DOC and coagulant demand is commonly cited as support for a direct CNP reaction, although the nature of the stoichiometric relationship is a matter of debate. Narkis and Rebhun (1977) observed direct proportionality between Aldrich humic acid and a cationic polyelectrolyte, but the linear relationship with alum was limited to humic acid concentrations below 10 mg/L. Dempsey and co-workers (1984), studying alum coagulation of fulvic acid, concluded that CNP produced a zone of non-linear stoichiometry between pH 4.0 and 5.0, whereas Edwards and Amirtharajah (1985) observed linear stoichiometry in the CNP coagulation of Aldrich humic acid with alum.

Correspondence between negatively-charge functional groups and the required dose of aluminum or ferric coagulant is also cited as evidence for the CNP mechanism. Since CNP is thought to control alum coagulation at pH less than approximately 6.0 (Dempsey et al. 1984, Edwards and Amirtharajah 1985, Hall and Packham 1965), many have hypothesized that the negative functionality is primarily contributed by ionized carboxyl groups. Narkis and Rebhun (1977) related the required alum dose to carboxyl functional groups on an equivalent basis, and it has been suggested that increasing coagulant requirements at higher pH levels reflect increased demand by ionized phenolic groups (Hall and Packham 1965). Hall and Packham (1965) concluded that precipitates produced by CNP have approximate stoichiometry of $Al(OH)_{2.5}$, which is consistent with the $Al(OH)_{2.7}FA_{0.64}$ stoichiometry proposed by Van Benschoten and Edzwald (1990b). In jar tests conducted by Shin et al. (2008), the authors cited average stoichiometries of $Al(OH)_{2.56}$ at pH 6.0 and $Al(OH)_{2.65}$ at pH 7.0 as evidence that at least some aluminum reacted by CNP.

Adsorption. Humic substances exhibit strong affinity for aluminum and ferric (oxy)hydroxides and readily adsorb to these surfaces via ligand exchange reactions between surface and humic functional groups (Davis 1982, McKnight et al. 1992, Tipping 1981). Humic sorption to aluminum and ferric surfaces resembles that of other anionic ligands with sorption favored at lower pH levels. Given the known tendency for humic and fulvic acids to sorb, many researchers have concluded that adsorption (ADS) to freshly precipitated aluminum or ferric (oxy)hydroxide is a key coagulation mechanism.

While early mechanistic studies ascribed NOM removal to the CNP mechanism at pH less than approximately 6.0, ADS has been proposed as the primary removal mechanism at higher pH (Dempsey et al. 1984, Edwards and Amirtharajah 1985). Van Benschoten and Edzwald (Edzwald 1993, 1990b) postulated parallel reactions in coagulation, with OH^- ions, humates, and fulvates competing for aluminum coordination sites. Thus, higher pH favors rapid precipitation of aluminum hydroxide or ferric oxyhydroxide, whereas lower pH may favor direct precipitation of mixed Al-NOM or Fe-NOM solids. Even under conditions where removal is thought to occur by ADS, several studies have suggested that the sorbing species may actually be soluble Al-NOM or Fe-NOM complexes (Dempsey et al. 1984, Dennett et al. 1996, Van Benschoten and Edzwald 1990b).

Dempsey (1989) subsequently investigated aluminum-fulvic acid interactions and the influence of organic carbon on aluminum speciation. Results indicated that aluminum hydroxide precipitated under all p[Al]-pH conditions associated with FA removal, and that the adsorption reaction is stronger than the complexation of FA by monomeric aluminum. Dempsey (1989) concluded that ADS is the predominant mechanism for alum coagulation of fulvic acids at all pH levels, although he did not discount the possible significance of polymeric aluminum species. These conclusions are consistent with the view of others who have found that ADS as the primary mechanism for NOM removal is consistent with practical observations (Dennett et al. 1996, Edwards 1997, Tseng and Edwards 1999).

Although the existence of a stoichiometric relationship between NOM and the required coagulant dose is commonly cited as evidence for a CNP mechanism, adsorption reactions also exhibit stoichiometry (Equation 1-2):

$$\equiv X - OH + A^{-} = \equiv X - A + OH^{-} \quad (1\text{-}2)$$

where ≡X-OH represents a surface hydroxyl group, and A^{-} represents an anionic ligand. A linear relationship between percent organic carbon removal and coagulant dose is consistent with the ADS mechanism (Dempsey et al. 1984, Shin et al. 2008) and with regions of a Langmuir-based model that has been used to predict TOC removal by ferric and alum coagulation (Edwards 1997).

Coagulation of NOM is consistent with ADS under a wide range of conditions, but removal during coagulation is generally higher than that observed when preformed amorphous (oxy)hydroxides are exposed to humic substances. This trend is commonly attributed to the higher surface area of fresh precipitates (Dempsey et al. 1984, Randtke 1988). As a secondary effect, Dempsey et al. (1984) indicated ADS in alum coagulation may be increased by the presence of soluble aluminum species which complex with FA, thereby reducing electrostatic repulsion.

Coprecipitation. A third explanation exists for the higher contaminant removals achieved by coagulation. In-situ precipitation of the metal (oxy)hydroxide allows entrapment of contaminants, including metals, within the growing solid phase, yielding removals well in excess of those observed when preformed solids are used (Cheng et al. 2004, Dempsey et al. 1984, Fuller et al. 1993, Karthikeyan et al. 1997, Mayer and Jarrell 2000, Waychunas et al. 1993). This coprecipitation (CPT) phenomenon also influences the sorbent's characteristics, including stoichiometry, site density, surface area, and surface charge (Chowdhury et al. 1991, Doelsch et al. 2001, Fuller et al. 1993, Karthikeyan and Elliott 1999, Mayer and Jarrell 1996, Waychunas et al. 1993).

"Coprecipitation" is a broad term, encompassing several possible mechanisms. Randtke's review (1988) of organics removal during coagulation identifies four specific coprecipitation mechanisms, including (1) isomorphic inclusion, (2) nonisomorphic inclusion, (3) occlusion, and (4) surface adsorption. Isomorphic inclusion occurs when an impurity of similar size or chemistry substitutes within the crystal lattice (e.g., Si substitutes for Al) (Randtke 1988, Stumm and Morgan 1996). Given the characteristics and relatively large size of humic substances, however, Randtke (1988) hypothesizes that coprecipitation of NOM occurs by occlusion. This mechanism is described as a process "in which an impurity differing in size or chemical characteristics from the lattice ions is adsorbed at lattice sites as the crystals are growing, producing crystal imperfections."

In contrast, surface adsorption is limited to interactions on the outer surface of the precipitate, with no incorporation into the internal precipitate structure (Randtke 1988). Therefore, surface adsorption is analogous to adsorption to preformed sorbents, while occlusion likely accounts for the additional NOM removal that typically occurs in coagulation.

Heterocoagulation. An additional theory, advanced by Dentel (1988, Dentel and Gossett 1988), suggests that removal of both NOM and turbidity is attributable to heterocoagulation of dissimilar colloids or particles. This model of alum coagulation assumes deposition of aluminum hydroxide precipitates on the surface of solid-phase contaminants. Rapid aggregation of the aluminum-coated particles occurs at circumneutral surface potentials. Humic substances are assumed to exist as colloids, rather than soluble macromolecules, and Dentel (1988) cites their "substantial" surface area in explaining the high coagulant demand exerted by humics. SEM images at pH 6.5 supported the heterocoagulation hypothesis, although it was unclear whether humic substances were sorbed to the surfaces of seed colloids or copreciptated with aluminum; images at pH 7.5 were more consistent with colloid enmeshment with homogenous aluminum hydroxide precipitates (Chowdhury et al. 1991).

Dentel (1988) applied the term "precipitation-charge neutralization" (PCN) to the model, indicating that charge neutralization is accomplished by aluminum hydroxide precipitates, rather than soluble aluminum species. While the model does not specify a mode of aluminum hydroxide precipitation, possible pathways include (1) surface polymerization as a precursor to precipitation, (2) surface-induced precipitation, and (3) precipitation in solution followed by deposition on the surface (Dentel and Gossett 1988). The PCN model accounts for the stoichiometric relationship between colloid surface area and coagulant demand, with Dentel (1988) noting that the direct proportionality actually exists between surface area and the coagulant dosed in excess of the metal hydroxide solubility limit. Thus, the PCN model is in agreement with Dempsey's (1989) conclusion that aluminum hydroxide precipitates under all p[Al]-pH conditions associated successful FA removal. Moreover, it is not inconsistent with studies that have suggested that CNP is accomplished by polymeric or incipiently solid aluminum phases (Dempsey et al. 1984, Edwards and Amirtharajah 1985, Narkis and Rebhun 1977). Applying the PCN model to PACl coagulation data collected by Dempsey et al. (1984), Dentel (1988) concluded that the preformed Al polymers performed the charge neutralization function. This work suggests that prehydrolyzed coagulants may provide superior coagulation at extreme pHs, lower temperatures, or under other conditions that may inhibit aluminum hydroxide precipitation

Factors Influencing NOM Removal

NOM composition and characteristics. The treatability of NOM is determined primarily by its physical and chemical properties, with improved removal associated with increased functionality, MW, and hydrophobic character. AHSs, which are characterized as hydrophobic acids, frequently control coagulant demand, while the minimum DOC residual is limited by non-sorbable NOM, which ranges from 5-60 percent (Edwards and Benjamin 1992).

Numerous studies have established the link between hydrophobic character and coagulation efficacy. White and co-workers (1997) conducted jar tests and organic fractionation on 31 source waters with hydrophobic fractions in the range of 31-63 percent as DOC. They concluded that coagulation preferentially removed the hydrophobic fraction of NOM, although

some hydrophilic NOM was removed at coagulant doses exceeding the hydrophobic demand (White et al. 1997). Pilot- and bench-scale studies of three source waters with ferric sulfate demonstrated that hydrophobic fractions accounted for most of the charge density in each water and controlled coagulant demand, whereas the hydrophilic fractions contributed a maximum of 11 percent of the charge and were less significant (Sharp et al. 2006a, Sharp et al. 2006c). Alum jar tests with five FA fractions showed that DOC removal was related to hydrophobicity, with generally greater reductions observed for more hydrophobic fractions (Dempsey et al. 1984).

Specific ultraviolet absorbance (SUVA) has been proposed as an indicator of possible DOC removals (Edzwald and Van Benschoten 1990). SUVA values of 4 to 5 L/mg·m suggest that (1) NOM is dominated by more hydrophobic, aromatic, higher-MW organics, (2) DOC controls coagulant demand, and (3) high removals can be achieved. In contrast, SUVA values less than 3 L/mg·m are associated with more hydrophilic or non-sorbable DOC and minimal removal by coagulation (Edzwald and Van Benschoten 1990). Research has confirmed that SUVA is an excellent indicator of aromaticity (Weishaar et al. 2003), and Bose and Reckhow (1998) corroborated the relationship between SUVA and removal by demonstrating direct proportionality between SUVA and NOM adsorption to preformed aluminum hydroxide flocs. SUVA has been incorporated into predictive models for DOC removal during coagulation (Edwards 1997, van Leeuwen et al. 2005).

Functionality contributes to hydrophobicity and plays a key role in the adsorption and coagulation of NOM. Studies of simple organic acids as possible analogues for NOM have suggested characteristics that influence removal. For example, the number, position, and acidity of carboxylic and phenolic groups have been shown to influence the extent to which organic acids are sorbed to goethtite (Evanko and Dzombak 1998). While Dempsey (1989) suggested phthalic acid as a representative compound, Evanko and Dzombak (1998) concluded that pyromellitic acid and 2,3-dihydroxy-benzoic acid (2,3-DHBA) exhibited trends similar to those observed for sorption of Aldrich HA and Suwannee River FA. Common features among these compounds include (1) adjacent carboxylic groups, (2) adjacent phenolic groups, and (3) very acidic carboxylic groups ($pK_a<3$) (Evanko and Dzombak 1998). In contrast, others (Bose and Reckhow 1998, Davis 1982) have suggested that weaker acid groups ($4\leq pK_a\leq 8$) on NOM are predominantly responsible for sorption to aluminum (hydr)oxides. However, Edwards et al. (1996) resolved this inconsistency by quantifying very strong carboxylic acid groups ($pKa<3$) and demonstrating that they were preferentially sorbed to ferric oxyhydroxide. Interestingly, weak acid groups with pK_a values between 8 and 11 followed the same sorption pattern as the very strong groups. Edwards et al. (1996) argued that these weaker groups were actually carboxylic acid groups adjacent to very strongly acidic groups, as supported by the observation of Evanko and Dzombak (1998).

A fraction of NOM is observed to be non-sorbing on oxide surfaces, presumably due to a lack of functional groups available for surface complexation (Davis 1982, Edwards 1997, Edwards et al. 1996). Sharp and co-workers (2006a, 2006c) found that the residual DOC remaining after coagulation jar tests was almost exclusively associated with the hydrophilic non-acid (HPINA) fraction and noted that the charge density of this fraction was below detection. The lack of charge in this non-sorbing, hydrophilic fraction is consistent with the hypothesis that this fraction is unable to undergo ligand exchange reactions (Davis 1982, Davis and Gloor 1981).

NOM fractions of higher MW tend to exhibit increased hydrophobicity, and removal by coagulation can often be viewed as a function of MW. Bose and Reckhow (1998) studied sorption of FA to preformed aluminum hydroxide and found that adsorbed concentrations of the higher-MW fraction (>5000 Da) were up to six times greater than that observed for the lower fraction (<500 Da). Similar relationships between MW and removal have been observed for sorption of NOM to crystalline aluminum oxide (Davis and Gloor 1981), for coagulation with alum (Collins et al. 1986, Jekel 1986, Semmens and Staples 1986), and for coagulation with ferric salts (Dennett et al. 1996, Sharp et al. 2006c, Sinsabaugh et al. 1986a, Sinsabaugh et al. 1986b).

Recent studies have employed size exclusion chromatography (SEC) to characterize NOM size and assess removal trends for source waters in China (Wang et al. 2010, Xie et al. 2012), Australia (Allpike et al. 2005, Chow et al. 2008), the U.S. and UK (Sharp et al. 2006c). Chow et al. (2008) associated high performance size exclusion chromatography (HPSEC) peaks with six fractions of NOM and developed a model to predict DOC removal by coagulation. Sequential jar tests with alum followed by HPSEC analysis suggested that certain high-MW fractions are readily removed by coagulation, while an additional fraction of lower-MW humics can be removed by enhanced coagulation. The fractions with the lowest MWs were not amenable to coagulation and were deemed nonremovable. Interestingly, Chow and co-workers (2008) studied three different natural waters and found that the fraction of NOM remaining after the five stages of treatment shared similar characteristics, namely low MW and SUVA less than 2 L/mg·m. Sharp et al. (2006c) also identified strong similarities in HPSEC chromatograms of the HPINA compounds remaining after various coagulation experiments, further supporting the idea that a fraction of aquatic NOM in non-sorbing and cannot be removed by coagulation (Edwards 1997, van Leeuwen et al. 2005, Xie et al. 2012).

Weng et al. (2007, 2006) compared the adsorption of HA and FA to goethite over the pH range of 3-11; average MWs were reported as 13.2 kDa and 0.683 kDa for the HA and FA, respectively. These researchers observed that HA sorption densities were higher on a mass basis (mg/m^2), while FA sorption was much higher on a molar basis ($\mu mol/m^2$). HA is conceptualized as extending from the surface into the double layer, while the considerably smaller size of the FA allows closer interaction with the goethite surface. These size differences are cited to explain the greater sensitivity to pH and ionic strength observed for HA sorption (Weng et al. 2007, Weng et al. 2006).

Randtke (Jacangelo et al. 1995, Randtke 1988, Randtke and Jepsen 1981) discussed organic carbon removal as a function of coagulant dose and identified two patterns that they associated with differences in NOM character. The Type 1 pattern (Figure 1-3) is characterized by a sharp decrease in DOC at some critical coagulant dosage, and the authors hypothesize that Type 1 removal occurs when relatively homogenous solutions of humic substances are removed by a CNP mechanism at relatively low pH. In contrast, the Type 2 trend (Figure 1-3) is marked by a gradual decline in DOC with increasing dose, and removal is presumed to arise from coprecipitation and adsorption of more heterogeneous NOM mixtures at higher pH.

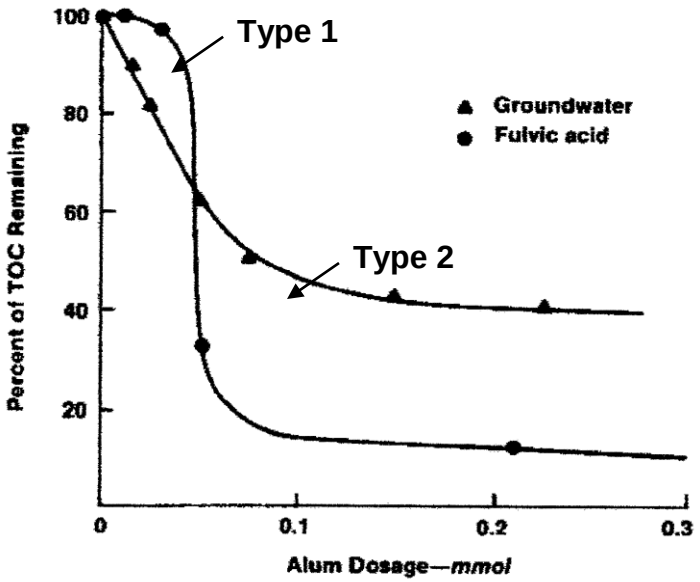

Figure 1-3. TOC removal trends observed by Randtke and Jepsen (1981). Type 1 coagulation was observed for an NOM extracted from groundwater and coagulated in synthetic water. The Type 2 trend was observed for treatment of the groundwater (Randtke 1988). Reprinted from Journal AWWA Vol. 80, No. 5, by permission. Copyright © 1988, American Water Works Association.

Randtke and Jepsen (1981) first advanced this theory after noting that coagulation of a groundwater followed the Type 2 pattern, whereas coagulation of an FA extracted from this groundwater followed a Type 1 pattern when treated in a synthetic tap water matrix. However, this experiment did not eliminate the confounding influence of water quality, which varied along with the NOM type (Table 1-3 and Table 1-4). Randtke (1988) notes that Type 2 removal is typically observed in waters with high turbidity and alkalinity, but he does not identify water quality as a causative factor in determining which trend prevails.

pH. Many studies have shown that pH influences the extent to which NOM is removed during coagulation. Accounting for the effects of other variables (e.g., coagulant dose), NOM removal is generally better at lower pH levels within the range of water treatment. Several authors concluded that optimal removal occurs by CNP at pH≈5-6.25 for alum and ≈4-5.5 for ferric coagulation (Dempsey 1984, Hall and Packham 1965, Randtke 1988). However, improved removal at lower pH is not inconsistent with ADS and CPT. The following factors may influence the relationship between pH and removal, particularly if CPT-ADS mechanisms dominate:

- *Electrostatics:* Below the point of zero charge (pH_{PZC}), the aluminum or ferric (oxy)hydroxide bears a positive charge. Deprotonated functional groups of NOM bear negative charges and are attracted to the positive sorbent surface (Au et al. 1999, Dentel 1988, Evanko and Dzombak 1999, Filius et al. 2003). Evanko and Dzombak (1998) have also stated that the iron-oxygen bond is stronger at higher pH, whereas it is weakened by reduced electron densities in the neutral and positive sites (i.e., ≡Fe-OH and ≡Fe-OH_2^+) that predominate at lower pH. Sites with lower iron-oxygen bond strengths more readily undergo ligand exchange reactions with organic functional groups.

Table 1-3. Water Quality Analysis for Urbana, IL Groundwater Tested by Randtke and Jepsen (1981)

Constituent	Concentration (mg/L)
Iron	1.1
Manganese	0.0
Calcium	59.6
Magnesium	23.7
Ammonium	1.1
Silica	19.6
Fluoride	0.3
Boron	1.0
Chloride	0.0
Nitrate	1.5
Sulfate	1.2
Alkalinity (as $CaCO_3$)	324.0
Sodium	37.0
Phosphate	0.03
Potassium	1.0

Table 1-4. Composition of Synthetic Water Used in Experiments with NOM Extract from Urbana, IL Groundwater

Constituent	Concentration (mM)
Sodium Bicarbonate	1.00
Calcium Chloride	0.25
Magnesium Sulfate	0.25
Sodium Chloride	1.00
Potassium Chloride	0.10

- *Competition:* Aqueous silica readily sorbs to ferric oxyhydroxide surfaces. Unlike other ligands, however, its affinity for the iron surface actually increases with pH, perhaps due to the formation of oligomers (Davis et al. 2002). In waters with appreciable silica concentrations, reducing pH to less than approximately 7 would be expected to improve NOM removal (Davis et al. 2001).

- *Ligand complexation and substitution:* Ligands, such as phosphate and sulfate, can complex soluble aluminum or iron and substitute for OH^- in the hydrolysis and precipitation of the amorphous solid, effectively shifting the pH of precipitation to a lower point (Stumm and Morgan

1962). The formation of a mixed precipitate allows coagulation and adsorption to proceed at a lower pH than would be expected if a pure aluminum or ferric (oxy)hydroxide precipitated.

Coagulant type and dose. Like pH, coagulant type and dose critically influence coagulation efficacy. Yet there is no clear consensus regarding the most effective coagulant for NOM removal, and jar testing remains the method of choice for coagulant selection and treatment optimization. Stoichiometric relationships (Table 1-5) have been published for both alum and ferric coagulants (Edzwald and Van Benschoten 1990, Lefebvre and Legube 1990, Shin et al. 2008, White et al. 1997), but the practical value of such relationships is limited by variations in both NOM and water quality. Sharp and co-workers (2006c) have argued against stoichiometric dosing, and recent research indicates that NOM characteristics such as hydrophobicity, MW, and charge density should guide dosing (Chow et al. 2008, Sharp et al. 2006a, Xie et al. 2012).

Table 1-5. Published Stoichiometric Relationships for Coagulant Dosing

Reference	Coagulant	NOM & Water Matrix	Stoichiometric Relationship
Shin et al. 2008	Alum	Dismal Swamp NOM in synthetic water	0.30 mg Al/mg DOC at pH 6.0 0.47 mg Al/mg DOC at pH 7.0
White et al. 1997	Alum	Six natural source waters	0.20 mg Al/mg TOC at pH 5.3-6.0 represents dose threshold to initiate rapid removal
Edzwald and Van Benschoten 1990	Alum	Multiple data sets including both natural waters and aquatic humics in synthetic waters	0.5 mg Al/mg DOC at pH≈5.5 1.0 mg Al/mg DOC at pH≈7.0
Lefebvre and Legube 1990	Ferric chloride	Moulin Papon FA and Cebron FA in synthetic water	≈2.0 mg Fe/mg DOC at pH 5.5

Key to Abbreviations
NOM: natural organic matter
TOC: total organic carbon
DOC: dissolved organic carbon
FA: fulvic acid

At first examination, the observations summarized in Table 1-5 suggest that alum is more effective than ferric chloride for NOM removal. Randtke and Jepsen (1981) found that alum performed significantly better than ferric sulfate in experiments with fulvic and humic acids suspended in synthetic waters at pH 6.0. However, in experiments with an Illinois groundwater at pH 6.0, alum and ferric sulfate yielded similar removals, with alum only slightly outperforming ferric sulfate at concentrations less than 0.30 mM as Al or Fe (Randtke and Jepsen 1981). The authors suggested that the relatively higher concentration of soluble aluminum polymeric species explained its better performance in the experiments with synthetic water. Compared to alum, ferric chloride yielded similar or greater removals of UV_{254} absorbance in jar tests with samples drawn from an Italian reservoir (Rizzo et al. 2005). Hall and Packham (1965) concluded that dose requirements were similar for alum and ferric chloride on an equivalent basis, but ferric required lower pH and generally yielded a lower organic residual. These experimental observations are consistent with the model advanced by Edwards (1997) for prediction of DOC removal during

coagulation. Inspection of the calibrated model parameters for alum and ferric coagulation suggests that (1) aluminum has a higher affinity for DOC, but (2) a higher fraction of NOM is non-sorbable by aluminum. Thus, aluminum is expected to perform better at lower doses where removal does not exceed the sorbable fraction. When higher doses are applied to remove a larger fraction of NOM, a ferric coagulant may be preferable to minimize the residual DOC. It is also noted that ferric coagulants are more acidic, and that ferric coagulation is optimized at lower pH than aluminum coagulation. Higher doses of ferric coagulant are therefore expected to promote more effective coagulation by further depressing the pH (Edwards 1997).

Floc stability. In natural waters, some fraction of NOM occurs in particulate and colloidal states. As a metal salt coagulant is added, sorbable DOC reacts with the hydrolysis species or precipitates and is transformed to a particulate state. Both naturally-occurring particles and those formed through reactions with coagulants are charged and conceptualized as having an electrical double layer, consisting of the Stern layer and the diffuse layer. The electrical double layer yields an electrostatic potential between the particle surface and bulk solution (Figure 1-4). Although attractive van der Waals forces exist between similarly charged particles, these particles will not collide and aggregate if the repulsive surface potentials exceed attractive forces. Such suspensions are termed stable, and a primary goal of coagulation is to bring about particle destabilization and aggregation to create flocs that can easily be removed.

Zeta potential measurements confirm that rapid aggregation occurs near neutral values. Edwards and Benjamin (1992) treated solutions of 10 mg/L TOC with both ferric chloride and aluminum chloride and found that effective coagulation occurred at zeta potentials between -10 and +10 mV. Tseng et al. (2000) identified -5 mV as the optimal zeta potential for coagulation of Boulder, Colorado water. Their observation was corroborated by subsequent work that identified an "operational window" of -10 to +3 mV (Sharp et al. 2006b, Sharp et al. 2006c). In these studies, residuals of both DOC and turbidity were minimized when zeta potentials of four natural waters were within this window, regardless of dose and pH.

Significance of Water Quality

Water quality—including pH, ionic strength, turbidity, temperature, NOM content, and dissolved constituents—profoundly influences metal salt coagulation. In-situ hydrolysis and precipitation allows certain constituents to coprecipitate with the aluminum or ferric (oxy)hydroxide, allowing removals well in excess of those possible through surface adsorption. Ample evidence from the literature indicates that water quality influences sorption to preformed aluminum or ferric (oxy)(hydr)oxides through phenomena such as competition and electrostatic effects. However, the significance of water quality is magnified for in-situ coagulation, since solution chemistry exerts not only competitive and electrostatic effects, but can also control the characteristics of the resulting metal (oxy)hydroxide coprecipitates. While such relationships clearly exist, the impacts of water quality have never been systematically explored.

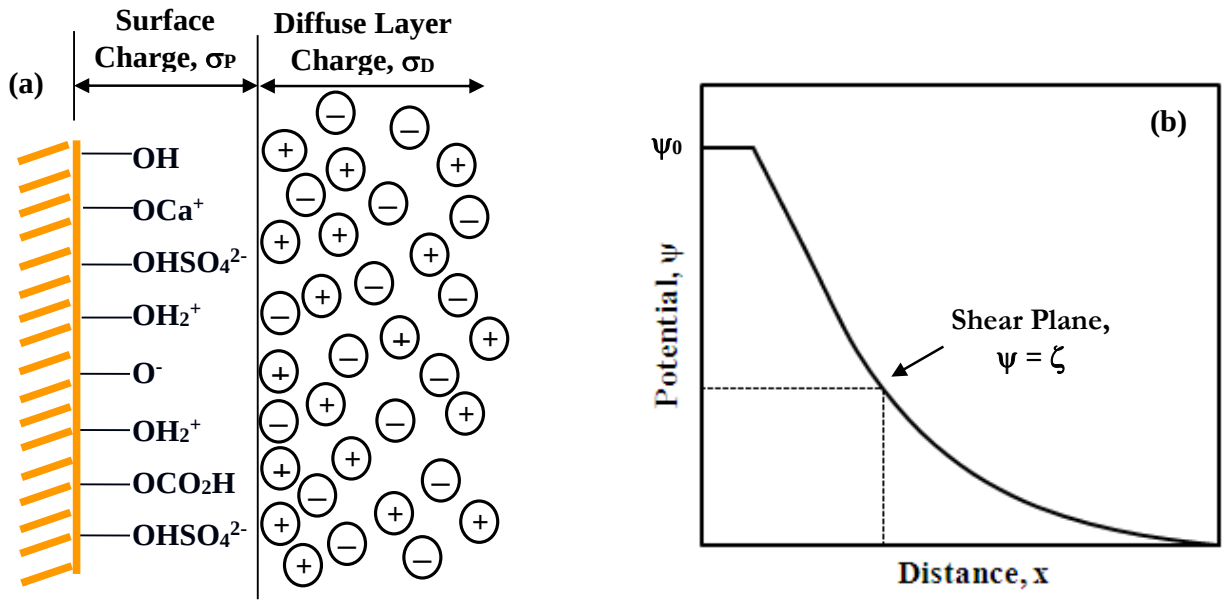

Figure 1-4. (a) Surface complexes on the sorbent surface give rise to net surface charge, which is counterbalanced by a diffuse cloud of ions. (b) Maximum potential occurs at the surface (ψ_o) but exponentially decays with distance from the surface. The experimental measurement of zeta potential corresponds to the potential at the shear plane.

Effects on Metal (Oxy)hydroxide Properties Associated with Coprecipitation

In the pH range of water treatment, metal salt coagulants undergo a series of complex hydrolysis and precipitation reactions. However, the presence of certain ligands can interrupt the normal polymerization and condensation process, yielding significant changes in the properties of the metal (oxy)hydroxide sorbent. Early studies demonstrated that phosphate, fluoride, and simple organic acids inhibited or prevented crystallization of aluminum hydroxide coprecipitated with these ligands (Violante and Huang 1985, Violante and Violante 1980). Aqueous silica has also been identified as a ligand capable of poisoning the polymerization, precipitation, and crystallization of aluminum hydroxide, presumably through the formation of stable aluminosilicate colloids (Brace and Matijevic 1977, Exley and Birchall 1992, Violante and Huang 1985). Schenk and Weber (1968) found that environmentally relevant concentrations of aqueous silica (0.1 and 1.0 mM) significantly inhibited ferric hydrolysis at pH 3.5.

More recently, advanced analytical techniques have provided insight into the mechanisms by which complexing ligands interfere with metal (oxy)hydroxide precipitation and the implications for coagulation. Studies have repeatedly shown that coagulation and coprecipitation remove sorbing species much more efficiently than adsorption to preformed (oxy)hydroxide surfaces (Cheng et al. 2004, Edwards 1994, Fuller et al. 1993, Hering et al. 1997, Karthikeyan et al. 1997).

Fuller et al. (1993) studied the coprecipitation of arsenate and ferrihydrite at As:Fe ratios ranging from 0.01 to 10 M/M and observed sorption densities of up to 0.7 mol As/mol Fe. An Extended X-ray Absorption Fine Structure (EXAFS) investigation of the coprecipitates from this

study revealed decreasing crystallite size as the concentration of arsenic within the crystallites increased (Waychunas et al. 1993). At very low As:Fe ratios, most of the iron atoms did not have neighboring arsenate, and Fe-O-Fe polymerization proceeded with minimal disruption. As the As:Fe ratio increased, however, the authors observed increasing disorder in the ferrihydrite structure. At As:Fe ratios of 0.6 M/M and higher, interchain linking was disturbed or blocked by high concentrations of primarily bidentate arsenate, limiting ferrihydrite growth to short dioctoctahedral chains. The authors argued that the maximum observed sorption density of 0.7 mol As/mol Fe is consistent with EXAFS observations of crystallite size and geometry (Waychunas et al. 1993).

Others have reported that phosphate and aqueous silica also have the ability to interrupt ferrihydrite polymerization and growth. Masion et al. (1997a) found that hydrolysis of ferric chloride in the presence of phosphate (P:Fe=0.2 or 0.5) primarily produced edge-sharing dimers. At higher hydrolysis ratios (h=1.5-2.0), the authors suggested that phosphate ions form bridges between ferric dimers, thereby forming dense clusters (Masion et al. 1997a, Rose et al. 1996). Doelsch et al. (2003, 2001) examined interactions between ferric iron and aqueous silica over the pH range of 3 to 10 and at Si:Fe ratios from 0 to 4 M/M (Fe=0.2 M; Si=0-0.8 M). Interestingly, these authors found that silica inhibited the polymerization of ferrihydrite at Si:Fe ratios between 0.5 and 2.0, with the formation of Si-O-Fe bonds maximized at approximately 1 M Si/M Fe. Beyond this threshold, the aqueous silica and ferrihydrite began to polymerize independently of one another, although ferrihydrite growth in the presence of silica was limited to two-dimensional growth by edge sharing (Doelsch et al. 2003). Thus, the effects of silica appear distinct from those of arsenate and phosphate, which continue to inhibit ferrihydrite growth as ligand concentration increases.

During coagulation of natural waters, As:Fe and P:Fe ratios are expected to be significantly lower than 0.6 M/M (Fuller et al. 1993, Waychunas et al. 1993) and 0.2 M/M (Masion et al. 1997a, Masion et al. 1997b), respectively. And while Si:Fe ratios may easily reach 4 M/M, the absolute concentrations of silica and ferric iron encountered in drinking water coagulation are orders of magnitude lower than the concentrations studied by Doelsch et al. (2003, 2001). Despite the use of artificially high constituent concentrations, however, the data and conceptualizations collectively presented in these studies (Doelsch et al. 2003, Doelsch et al. 2001, Fuller et al. 1993, Masion et al. 1997a, Rose et al. 1996, Waychunas et al. 1993) are useful from the following perspectives:

- These studies illuminate mechanistic interactions that occur between sorbing ligands and ferric coagulants, particularly at ligand concentrations that are high with respect to iron concentration.

- Results support macroscopic observations of increased ligand sorption density and suggest that higher sorption densities are attributable to some combination of increased site density and surface area.

- Finally, these data suggest that ligand:Fe ratios determine whether the influence of coprecipitation is significant in a given system. If a water has low ligand concentrations, but requires a relatively high dose to achieve a strong, separable floc, interactions between the sorbing species and Fe may mimic an adsorption mechanism. Under these conditions, ferrihydrite

polymerization likely resumes after ligand demand is exhausted, and the effects of coprecipitation are negligible. In contrast, waters with higher concentrations of sorbing ligands may be significantly influenced by coprecipitation and its effect on ferric coagulant hydrolysis. The threshold between "adsorption" and "coprecipitation" is likely a dual function of each ligand's concentration and affinity for the iron surface.

Photometric dispersion techniques have also been used to demonstrate that aqueous silica hinders particle aggregation and growth during in-situ hydrolysis of alum (Duan and Gregory 1998, Duan and Gregory 1996) and ferric chloride (Liu et al. 2007b), particularly as silica concentrations and/or pH increase. Duan and Gregory (1996) studied coagulation of kaolinite suspensions, and found that low concentrations of silica were beneficial at lower pH levels; they hypothesized that silica prevented overdosing and restabilization under these conditions. However, modestly higher concentrations (5 mg/L as SiO_2) often suppressed coagulation altogether. These findings of hindered polymerization, growth, and aggregation are consistent with studies that have found that concentrations of "soluble" aluminum or ferric iron tend to increase during coprecipitation with silica at concentrations typical of natural waters (Duan and Gregory 1996, Exley and Birchall 1992, Liu et al. 2007b, Meng et al. 2000, Schenk and Weber 1968).

The effects of NOM on ferrihydrite polymerization have also been examined under a limited set of conditions. Vilge-Ritter et al. (1999) employed X-ray absorption spectroscopy (XAS) and small-angle X-ray scattering (SAXS) to examine flocs formed during jar tests with two natural waters. The jar tests were performed at pH 5.5 and pH 7.5 with ferric chloride dosed at 1.48×10^{-4} M (8.26 mg/L as Fe). The results indicated that ferric iron in the flocs was poorly polymerized, occurring as small monomers, dimers, and trimers. The oligomers were assumed to occur as spheres, and SAXS indicated radii in the range of 2.10-4.53 Å. The authors theorize that ferrihydrite polymerization was hindered by the formation of two or three Fe-O-C bonds per Fe atom, with NOM blocking further growth sites on the Fe octahedral (Vilge-Ritter et al. 1999).

Vilge-Ritter et al. (1999) viewed their data as evidence that coagulation of NOM occurs by complexation of ferric oligomers rather than adsorption of NOM to an amorphous ferric floc. They observed similar Fe speciation in flocs formed at both pH 5.5 and 7.5, leading them to conclude that removal occurs by a charge neutralization/complexation mechanism at both pH levels, in contrast to conventional wisdom that CNP is only relevant at pH less than approximately 6.0 (Dempsey et al. 1984, Edwards and Amirtharajah 1985, Hall and Packham 1965). However, increasing pH led to less dense aggregates, presumably due to electrostatic repulsion and conformational changes in NOM (Vilge-Ritter et al. 1999).

Unfortunately, this study did not include any measurements of particle destabilization, so it is impossible to determine whether effective coagulation occurred. The coagulant doses applied by Vilge-Ritter and co-workers yielded ratios of 2.1 mg Fe/mg TOC for the Seine River water and 1.0 mg Fe/mg TOC for the lake water. Examination of jar test data collected by Singer et al. (1995) indicates that doses up to 3.9 mg Fe/mg TOC may be required to simultaneously accomplish effective TOC removal and particle destabilization. While the poisoned polymerization observed by Vilge-Ritter and co-workers (1999) is likely significant in the coagulation process, this study does not unambiguously confirm the mechanism responsible for NOM removal.

Subsequent investigations have also applied advanced analytical techniques to characterize the flocs formed during ferric coagulation of humic substances at pH 6 and pH 8, and the results have generally supported those of Vilge-Ritter et al. (1999). In jar tests with natural waters and with NOM resuspended in synthetic waters, residual turbidity measurements allowed identification of ferric iron concentrations associated with both optimal coagulation (OCC) and restabilization, leading researchers to suggest coagulation by CNP at both pHs (Jung et al. 2005, Sieliechi et al. 2008). Jung et al. (2005) used electron energy loss spectroscopy (EELS) to analyze flocs and concluded that the Fe/C ratios at both pHs were consistent with the earlier finding that NOM limited Fe hydrolysis to the trimer stage (Vilge-Ritter et al. 1999). Results also suggested that charge neutralization of humic colloids occurs by a reaction in which carboxylic groups release calcium ions in exchange for the ferric hydrolysis species. The higher OCC required for coagulation at pH 8 is explained by a conformational change, specifically "an opening of the deprotonated humic network…thus increasing the number of carboxylic groups available for aggregation" (Sieliechi et al. 2008).

Synergistic and Competitive Effects of Specific Ions

In addition to water quality impacts on the metal (oxy)hydroxide sorbent, specific ions can affect coagulation by either promoting or hindering removal of target contaminants, such as NOM and arsenic. Calcium, sulfate, silica, and carbonate species are among the most prevalent and significant constituents of natural waters, and are therefore most likely to influence the coagulation process. Previous studies have examined the behaviors of these ions during coagulation. However, many aspects have not been investigated, and existing knowledge has not been synthesized to form a comprehensive understanding of water quality effects on coagulation.

Silica. Silica concentrations in natural waters fall within typical ranges of 1-20 mg/L as SiO_2 for surface waters and 7-45 mg/L as SiO_2 for groundwaters (Davis 2000, Frey and Edwards 1997) and are well below the solubility limit of amorphous silica (Davis 2000, Iler 1979, Stumm and Morgan 1996). Aqueous silica exhibits an unusually high affinity for aluminum and ferric (oxy)(hydr)oxides, with some researchers reporting sorption densities in excess of monolayer sorption (Davis et al. 2002, Hingston and Raupach 1967, Huang 1975, Smith and Edwards 2005, Swedlund and Webster 1999). Silica sorption to iron (oxyhydr)oxides typically increases with pH, approaching a maximum at approximately pH 9, although broad plateaus are sometimes observed at pH greater than 6 (Luxton et al. 2006, Swedlund and Webster 1999). Historically, silica in natural waters was thought to occur exclusively as a monomer, but a recent analysis suggests that oligomeric silica, particularly $Si_2O(OH)_5^-$, may be significant at pH levels and silica concentrations normally encountered in natural waters (Davis 2000, Davis et al. 2002). The presence of oligomeric species, which appear to display increased affinities for the metal oxide surface (Taylor et al. 1997), may explain the tendency of silica to sorb strongly and attain very high sorption densities.

There are several mechanisms by which silica may diminish the effective sorption and removal of target contaminants, such as NOM and arsenic. Not surprisingly, sorbed and coprecipitated silica depress the surface potential of both aluminum and ferric (oxy)(hydr)oxides (Davis et al. 2002, Duan and Gregory 1996, Liu et al. 2007b, Luxton et al. 2006, Smith and Edwards 2005). This reduced surface potential may be associated with inhibition of aggregation reactions of the metal (oxy)hydroxide sorbent. Moreover, sorbed silica may interfere with sorption

and removal of other ligands through electrostatic repulsion. Simple site competition also accounts for some of the interference. Sigg and Stumm (1981) developed a surface complexation model that suggested that phosphate and silica dominated goethite surface speciation in natural waters and in the absence of NOM, even at low concentrations of these ligands.

In experiments with preformed ferric (oxyhydr)oxides, silica interfered with sorption of chromate (Zachara et al. 1987) and arsenic (Davis et al. 2001, Luxton et al. 2006, Smith and Edwards 2005, Swedlund and Webster 1999). Significant interference with arsenic removal was also observed in systems typical of coagulation (Holm 2002, Liu et al. 2007b, Meng et al. 2000, Tong 1997). In comparison to arsenic, relatively little research has focused on competition between silica and humic substances. Davis et al. (2001) found that FA sorption to preformed ferric oxyhydroxide was reduced by up to 40 percent when the sorbent was exposed to silica for 1.5 hours prior to the addition of FA; as expected, the extent of interference increased with silica concentration and pH. Tipping (1981) observed a 20 percent reduction in humic sorption to goethtite in the presence of 6 mg/L as SiO_2.

Carbonate Species. Inorganic carbon is ubiquitous in natural waters, occurring at typical concentrations of 0.1-5 mM in river waters and 0.5-8 mM in groundwaters (Stumm and Morgan 1996). Inputs of these species, specifically $CO_{2(aq)}$, H_2CO_3, HCO_3^-, and CO_3^{2-}, include gas transfer from the atmosphere, respiration, and dissolution of carbonate solids and minerals, while primary sinks include sorption and precipitation reactions.

In drinking water treatment, the carbonate system's significance has generally been associated with its capacity for regulating pH through a series of acid-base reactions:

$$H_2O + CO_{2(aq)} \leftrightarrow H_2CO_3 \quad (1\text{-}3)$$

$$H_2CO_3 \leftrightarrow HCO_3^- + H^+ \quad (1\text{-}4)$$

$$HCO_3^- \leftrightarrow CO_3^{2-} + H^+ \quad (1\text{-}5)$$

Along with the hydroxyl ion, bicarbonate and carbonate are dominant contributors to alkalinity in most natural waters.

High-alkalinity waters are generally considered problematic in coagulation of NOM, and recognition of this phenomenon led to the inclusion of alkalinity as a factor in determining required TOC removal via enhanced coagulation (Table 1-6). During development of the 3x3 matrix, EPA rationalized that "[i]n higher alkalinity waters, pH depression to a level at which TOC removal is optimal (e.g., pH between 5.5 and 6.5) is more difficult and cannot be achieved easily through addition of coagulant alone" (USEPA 1999). On the other hand, waters with very low alkalinity may be associated with difficulty in removing turbidity (Tseng et al. 2000), infrastructure corrosion, and increased levels of soluble or colloidal metals in finished water.

The significance of bicarbonate and carbonate as acid-neutralizing species is clear. Yet relatively little effort has been invested in studying other impacts of carbonate species during coagulation. Early research in which model waters were treated with alum indicated that bicarbonate improves the overall performance of the coagulation-flocculation process. In these studies, Letterman and co-workers (1970, 1979) found that increasing bicarbonate concentrations

Table 1-6. Percent Total Organic Carbon Removals Required by the Stage 1 Disinfectants and Disinfection Byproducts Rule

Total Organic Carbon (mg/L)	Alkalinity (mg/L as $CaCO_3$)		
	0-60	*>60-120*	*>120*
>2.0-4.0	35	25	15
>4.0-8.0	45	35	25
>8.0	50	40	30

led to lower residual turbidities, reduced alum dosing requirements, widened the pH range of effective turbidity removal, and improved flocculation efficiency. The authors noted that increases in the flocculation kinetic parameters are associated with increased floc volume and suggested that bicarbonate improves flocculation by serving as a "cross-link" between positively charged aluminum hydrolysis species (Letterman et al. 1979).

More recent work has shown that carbonate displays a moderate affinity for iron (oxyhydr)oxide surfaces, forming inner-sphere complexes and reducing surface potential. In a system with ferrihydrite (0.87 mM=48.6 mg/L as Fe) and 0.0045 mM $C_{T,CO3}$, a maximum of approximately 50 percent of the carbonate species were sorbed in the pH range of 5.5-6.0 (Zachara et al. 1987). Villalobos and Leckie (2000) also observed a broad sorption maxima in the pH range of 6-7 in a closed-system experiment with goethite and various ionic strengths and concentrations of carbonate species. The highest surface coverage was measured in the system with 133 μM CO_2 ($C_{T,CO3}$≈0.04-0.08 mM and I=0.01 M); at the observed sorption density of 0.5 μmol/m^2, the authors calculated that up to 13 percent of surface sites were occupied by carbonate. In experiments with open systems, sorption either increased with pH or displayed a plateau at some pH greater than approximately 6, depending upon the experimental conditions. The maximum sorption density of 1.4 μmol/m^2 (P_{CO2}=5.52 matm, I=0.01 and 0.1 M) suggested that up to 37 percent of sites were bonded with carbonate (Villalobos and Leckie 2000). Although the observed coverages appear modest, a triple layer model (TLM) predicted that up to 80 percent of goethite surface sites may be occupied by carbonate at pH 6-8 and at the higher CO_2 pressures typical of the subsurface (Villalobos and Leckie 2001).

Despite the potential for high carbonate sorption densities, results indicate that carbonate sorption to the iron oxide surface can be easily disrupted and is particularly sensitive to electrostatic effects. For example, decreasing sorption at higher pHs in the closed system suggests an inability to overcome repulsion, despite much higher concentrations of aqueous carbonate (Villalobos and Leckie 2000). Comparing ionic strengths of 0.1 and 0.01 M, higher ionic strength was associated with suppressed sorption in the closed system and at lower pHs in the open system, leading the authors to hypothesize that electrolyte anions may have competed with carbonate for sorption sites (Villalobos and Leckie 2000). Similarly, this work found that carbonate sorption densities were higher in the presence of nitrate than in the presence of chloride electrolyte.

While these behaviors are typical of outer-sphere complexes, spectroscopic evidence has consistently suggested that carbonate forms inner-sphere complexes on goethite (Hiemstra et al. 2004, Villalobos and Leckie 2001, Wijnja and Schulthess 2001). Using the TLM, Villalobos and

Leckie (2001) explained the seemingly anomalous behavior of their proposed inner-sphere monodentate complex by assigning a fraction of the complex's charge to the β-plane. Bargar et al. (2005) used Attenuated Total Reflectance Fourier Transform Infared (ATR-FTIR) spectroscopy to study hematite suspensions equilibrated with atmospheric CO_2. These investigators presented evidence of a monodentate, binuclear complex that was present across the pH range of approximately 4-8 and at $I \leq 0.1$ M. However, they also noted peaks consistent with a second outer-sphere or hydrogen-bonded complex that was dominant at low ionic strength but disappeared at I=0.1 M. The presence of a similar pair of inner- and outer-sphere complexes on goethite could explain the ionic and pH-strength dependencies noted by Villalobos and Leckie (2000). Hiemstra et al. (2004) used existing IR data to affirm an inner-sphere complex but suggested that the primary geometry of carbonate complexes on goethite is bidentate. There was no evidence of bicarbonate complexes on iron oxides in any recent spectroscopic investigation (Bargar et al. 2005, Hiemstra et al. 2004, Villalobos and Leckie 2001, Wijnja and Schulthess 2001).

There is considerable debate in the literature regarding the significance of carbonate as a competitive ion. Zachara et al. (1987) studied chromate (5 μM) sorption to preformed ferrihydrite (0.87 mM = 48.6 mg/L as Fe) in an open system ($P_{CO2}=10^{-2.46}$ atm). In the presence of carbonate species, the chromate sorption edge was shifted lower by approximately 0.5 pH units, and total chromate sorption was suppressed by 30-40 percent at pH 7.0-7.5. Equivalent dissolved carbonate concentrations ($C_{T,CO3}$) at pH 7.0 and 7.5 are calculated as 0.97 and 2.8 mM, respectively, and are well within the typical range of natural waters.

A subsequent study utilized data collected by Zachara and co-workers (1987) to model sorption of carbonate to ferrihydrite. Sorption constants for two surface complexes, $\equiv FeOCO_2^-$ and $\equiv FeOCO_2H$, were fit based on a single-sorbate system of preformed ferrihydrite and low carbonate concentrations ($C_{T,CO3}=0.0046$ mM) (Appelo et al. 2002). When the model was extrapolated to a hypothetical water with pH 7, multiple sorbates, and a much higher inorganic carbon concentration of 5 mM, the model predicted significant interference with As(V) and As(III) sorption, leading the authors to conclude that bicarbonate may be responsible for high subsurface arsenic concentrations under conditions such as those found in Bangladesh (Appelo et al. 2002). Similarly, Holm (2002) measured decreased removal of As(V) (37.5 μg/L) during coagulation with iron (1.4 mg/L as Fe) in the pH range of 7-9 and in the presence of inorganic carbon concentrations of 1 mM and 10 mM. A study of As(V) and As(III) sorption to goethite in the presence of 10 mM inorganic carbon demonstrated a moderate interference with As(V) sorption at pH less than 8.5; the competition was even greater for As(III), with carbonate increasing aqueous As(III) concentrations by up to an order of magnitude at pH less than 8.0 (Stachowicz et al. 2007).

In contrast, others have concluded that competition between carbonate and other oxyanions is minimal. Meng et al. (2000) reported negligible impact of carbonate on arsenic removal during ferric chloride coagulation in air-equilibrated systems from pH 4 to 10. Fuller et al. (1993) also found no discernible interference when arsenate was coprecipitated with ferrihydrite; in their study, experiments were conducted in an "artificial stream water" with an initial inorganic carbon concentration (3 mM) that was subsequently reduced by purging with air. Carbonate exerted only a marginal influence in a column study with arsenate and iron-oxide coated sand at pH 7 (Radu et al. 2005).

Understanding the net impact of carbonate in a competitive sorption system is complicated by the confounding role of proton co-adsorption that is commonly associated with carbonate. For carbonate sorption to goethite, Villalobos and Leckie (2000) calculated co-adsorption of 1.3-1.7 protons per CO_3^{2-}, depending upon ionic strength. Similarly, Schulthess et al. (1998) concluded that carbonate sorption to aluminum oxide was accompanied by 1.1 ± 0.3 protons. Experiments and modeling suggest that, under some water quality conditions, proton co-adsorption actually enhances sorption of other ligands in the presence of carbonate. For example, carbonate promoted the sorption of sulfate and selenate to goethite (Wijnja and Schulthess 2002) and aluminum oxide (Wijnja and Schulthess 2000a), with the stronger effect observed for aluminum oxide. The maximum enhancement of sulfate and selenate sorption to aluminum oxide occurred at pH from 6 to 8 and at an inorganic carbon concentration of 0.3 mM, and the positive effect of carbonate continued to 3 mM (Wijnja and Schulthess 2000a). As carbonate continued to increase, however, carbonate became competitive (Wijnja and Schulthess 2002).

Arai et al. (2004) also found that arsenate sorption to hematite was enhanced under the following conditions: (1) at pH 4 ($C_{T,CO3}$=0.1 mM), (2) at pH 6 and reaction periods greater than 30 minutes ($C_{T,CO3}$=0.1 mM), and (3) at pH 8 and reaction periods greater than 2 hours ($C_{T,CO3}$=5.56 mM). The authors explained their results according to a "shared charge" concept, suggesting that it is more favorable for arsenate to displace bound carbonate than a surface hydroxyl group. However, these results are not inconsistent with the notion that carbonate and proton co-adsorption enhanced arsenate adsorption under certain conditions. A TLM predicted little difference between systems equilibrated with either an air or argon atmosphere between pH 4 and 8; however, it predicts interference with arsenate sorption in a theoretical system equilibrated at $P_{CO2}=10^{-2}$ atm and pH above 5.5 (Arai et al. 2004). The model results indicate that excess surface sites are available, suggesting that carbonate interferes with competing ligands by reducing the surface potential of the iron oxide surface (Arai et al. 2004).

Sulfate. Groundwater sulfate concentrations generally fall within the range of 1-275 mg/L as SO_4^{2-}, whereas the typical range for surface waters is slightly lower (2-250 mg/L as SO_4^{2-}) (Frey and Edwards 1997). Sulfate, which is strongly influenced by electrostatics and ionic strength, exhibits only a weak or moderate affinity for ferric and aluminum (oxy)(hydr)oxides. Sulfate sorption is favored at lower pH, but declines as pH increases, and negligible sorption occurs in the vicinity of the isoelectric point (Ali and Dzombak 1996, Geelhoed et al. 1997, Pommerenk and Schafran 2005, Sigg and Stumm 1981). Sorption is also suppressed at higher ionic strength, regardless of pH (Ali and Dzombak 1996, Geelhoed et al. 1997). Together, these behaviors are often considered indicative of outer-sphere complexation. However, spectroscopic studies indicate that sulfate forms both inner- and outer-sphere complexes, with relative significance of each complex depending upon sorbent type and solution conditions. Monodentate inner-sphere complexes are favored at higher ionic strength and at pH less than 6.0, while outer-sphere complexes become more important at higher pH or lower ionic strength (Peak et al. 1999, Wijnja and Schulthess 2000b). Wijnja and Schulthess (2000b) also found that a relatively small fraction of sulfate formed inner-sphere complexes with aluminum oxide (γ-Al_2O_3) and suggested that sulfate has a higher affinity for goethite than aluminum oxide.

Various studies have explored the extent of competition between sulfate and target contaminants. Ali and Dzombak (1996) investigated competitive sorption between sulfate and model organic acids to goethite. At pH 5.0 and relatively low ionic strength (I=0.01 M) and sulfate

concentration (0.25 mM = 24 mg/L as SO_4^{2-}), sulfate suppressed equimolar concentrations of phthalic acid and chelidamic acid by approximately 25 and 35 percent, respectively. However, the competitive effect diminished as pH increased, perhaps due to a shift from inner-sphere to outer-sphere sulfate complexation (Peak et al. 1999, Wijnja and Schulthess 2000b). Cathalifaud et al. (1993) studied the sorption of Aldrich humic acid to freshly formed ferric oxyhydroxide flocs, and found that the presence of 63 mg/L (0.66 mM) of SO_4^{2-} reduced humic sorption by approximately 30 percent. The pH of the experiments is not clearly stated, but the ferric oxyhydroxide flocs were formed within the pH range of 5.4-6.1. Very high concentrations of sulfate (10 mM = 961 mg/L) have been shown to suppress the sorption of NOM to iron oxide over the pH range of 3-10 (Gu et al. 1994).

The influence of sulfate on arsenic removal has also been studied. Hering et al. (1996) performed adsorption and coagulation (i.e., coprecipitation) experiments with ferric chloride in the pH range of 4-6. Arsenate has a strong affinity for ferric (oxyhydr)oxide, and these authors observed 100 percent As(V) removal (As(V)=20 µg/L and Fe_T = 1.7 mg/L) in coagulation experiments, even with a sulfate concentration of 10 mM (961 mg/L as SO_4^{2-}) at pH 4. Meng et al. (2000) found that sulfate (0-300 mg/L) did not interfere with arsenate removal (300 µg/L) during coagulation with ferric chloride (1 mg/L as Fe) at pH 6.8.

While arsenite is less amenable to sorptive removal, Meng and colleagues (2000) noted no discernible competitive effect on arsenite (100 µg/L) at the same sulfate levels and pH. In contrast, sulfate (250 mg/L) significantly inhibited the removal of low arsenite concentrations (9-10 µg/L) in adsorption and coprecipitation experiments conducted at pH 5 and 6 (Hering et al. 1996). The greatest effect occurred at pH 5, where arsenite removals were reduced by nearly 45 percent. Although arsenite removal was still inhibited at pH 6, the competitive effect was somewhat mitigated. The reduced or negligible effects of sulfate observed at pH 6 and 6.8 are consistent with the decline in sulfate sorption as pH increases and the increasing significance of outer-sphere complexes (Peak et al. 1999, Wijnja and Schulthess 2000b).

Although sulfate can act as an interfering anion under some conditions, several researchers have noted that sulfate can be beneficial during coagulation. Dempsey et al. (1984) compared the coagulation of FA with alum to that achieved with aluminum chloride. Stability domains were designated by shading areas of at least 20 percent removal on dose-pH diagrams. Compared to aluminum chloride, alum extended the zone of coagulation to lower pHs, thereby increasing the overall area of the domain. Increasing concentrations of sulfate also decreased the pH at which maximum FA removal was observed. Similarly, sulfate was found to enhance coagulation of seed colloids at pH 6.5 (Chowdhury et al. 1991). The positive role of sulfate in both of these studies likely stems from its ability to coordinate with aluminum, forming a mixed aluminum hydroxide-sulfate coprecipitate. This reaction would be expected to decrease the pH of precipitation since sulfate is substituting for OH^- ion (Stumm and Morgan 1962). Stoichiometric data for aluminum precipitation supports this idea. In the presence of the colloidal seed particles, the OH^-:Al^{3+} ratio was 2.9:1 using aluminum nitrate; when the suspension was coagulated with alum, the stoichiometry declined to 2.1:1 (Chowdhury et al. 1991).

Letterman and Vanderbrook (1983) are credited with elucidating an additional benefit of sulfate. They studied coagulation of kaolinite suspensions with alum and concluded that the particles were coated by aluminum hydrolysis products. At lower pHs, the aluminum-coated

particles are protonated and positively charged. Under these conditions, sulfate sorption effectively prevents overdosing and restabilization by limiting the positive surface charge. Not surprisingly, the sulfate concentration needed to prevent restabilization decreases with increasing pH; sulfate is unnecessary above pH 7.5 (Letterman and Vanderbrook 1983). This observation is consistent with later work, which showed that sulfate sorption to a preformed, amorphous aluminum hydroxide significantly reduced zeta potential, but did not reverse the sign from positive to negative (Pommerenk and Schafran 2005).

Calcium. Calcium is a prevalent divalent cation, typically occurring at 2-75 mg/L in surface water and 2-150 mg/L in groundwater (Frey and Edwards 1997). While high calcium levels are problematic for aesthetic reasons, low and moderate concentrations frequently prove beneficial to coagulation.

Calcium mitigates the detrimental impacts of silica on coagulation. Duan and Gregory (1996) studied coagulation and particle aggregation in a kaolinite suspension with 15 mg/L of aqueous silica. At pH 7.0 and 40 μM alum (1.08 mg/L as Al), no coagulation occurred until the suspension was dosed with 3 mM (120 mg/L) calcium. Similarly, Liu et al. (2007a) found that calcium at 40 mg/L improved aggregation of ferric oxyhydroxide precipitates and minimized "soluble" iron residual in the presence of silica. Studies have also shown that calcium increases zeta potential in ferric oxyhydroxide particles exposed to aqueous silica (Liu et al. 2007a, Smith and Edwards 2005). By improving ferric oxyhydroxide precipitation and increasing zeta potential, the overall effect of calcium in such systems is to enhance arsenic sorption in the presence of silica (Liu et al. 2007a, Meng et al. 2000, Smith and Edwards 2005). However, this enhancement appears to be related to kinetics, and its significance is greatest at relatively short reaction times (i.e., less than one day) (Smith and Edwards 2005). Smith and Edwards (2005) noted that the presence of calcium (10 mg/L) in their experiment (Fe=20 mg/L, SiO_2=40 mg/L, and As(V)=100 μg/L) did not reduce silica sorption to the amorphous ferric oxyhydroxide surface and concluded that the influence of calcium arose from (1) double-layer compression, (2) sorption to the iron surface, or (3) sorption to the sorbed silica.

Calcium also aids in the coagulation of organic matter. Dempsey and O'Melia (1983) demonstrated that calcium forms complexes with negatively-charged functional groups on fulvic acids. For some conditions, calcium reduced the FA negative charge by more than 50 percent, enabling the FA to sorb to a manganese oxide solid; it was noted that the surface charge of the manganese oxide was negative, and no sorption occurred in the absence of calcium. Calcium was also shown to improve aggregation of alginate polymers and alginate-coated hematite by forming bridging complexes (Chen et al. 2006, Chen et al. 2007). Weng et al. (2005) found that calcium improves adsorption of organic matter to goethite. In the absence of calcium, FA sorption declined rapidly at some pH greater than 6.0, depending on the initial FA concentration (75-300 mg/L). The addition of 40 mg/L of calcium, however, significantly improved FA sorption to goethite at these higher pH levels.

Summary and Identification of Research Needs

The preceding review has explored the influence of water quality and other factors on coagulation with metal salts. Synthesis of relevant research has established the following:

- Hydrolysis and precipitation reactions of metal salt coagulants yield precipitates of aluminum or ferric (oxy)hydroxides. During coagulation, these products destabilize particles and participate in sorption reactions with dissolved species. The composition and characteristics of the hydrolysis products depend upon system-specific conditions, including coagulant dose, pH, water composition, temperature, and mixing.

- In most water systems, NOM removal controls coagulant demand and is a primary objective for systems practicing coagulation. While it is currently impossible to conclusively determine the mechanism(s) responsible for NOM removal in a given system, the following mechanisms have been proposed: charge neutralization/precipitation, adsorption, coprecipitation, and heterocoagulation. The efficacy of NOM removal by coagulation depends on its physical and chemical characteristics, pH, coagulant type and dose, floc properties, and aqueous chemistry.

- Source water quality influences all aspects of coagulation. Contaminant sorption is affected by competitive and electrostatic effects, and solution chemistry influences hydrolysis reactions. Certain naturally-occurring ligands interfere with polymerization and growth of metal (oxy)hydroxides, yielding smaller precipitates with larger surface areas available for sorption. Occlusion of contaminants and other dissolved species within the metal (oxy)hydroxide solids may lead to higher removals than expected by surface adsorption alone.

Current knowledge provides a sound foundation for understanding the mechanisms and interactions that *may* occur during coagulation. Yet significant gaps remain, and there are many examples of waters that are inexplicably difficult to treat. Critical advances in recent years, specifically with respect to the characterization of NOM, have strengthened the ability to quantify the fraction of NOM that is amenable to coagulation and by corollary, the expected residual DOC remaining after treatment. However, data from Randtke and Jepsen (1981) (Figure 1-3) clearly show that water quality can profoundly alter NOM removal, even for a consistent source of NOM. Calcium, silica, sulfate, and inorganic carbon commonly occur in natural waters and may strongly influence coagulation via interactions with NOM, coagulant hydrolysis species, or both. Ideally, design engineers and operators could use NOM characteristics and source water quality data to readily identify the optimal coagulant, dosage, and pH for treatment, thereby minimizing the need for costly and inefficient testing at the bench- and pilot-scales. In the pursuit of this formidable goal, the influence of source water chemistry in coagulation represents a crucial—but relatively unexplored—research need.

Acknowledgements

During the preparation of this review, the first author was supported by graduate fellowships awarded by the US EPA, National Water Research Institute, American Water Works Association, and Virginia Tech Department of Civil and Environmental Engineering. The findings are those of the authors and may not reflect the views of these organizations.

References

Aiken, G.R., McKnight, D.M., Thorn, K.A. and Thurman, E.M. (1992). Isolation of hydrophilic organic acids from water using nonionic macroporous resins. *Organic Geochemistry* 18, 567-573.

Ali, M.A. and Dzombak, D.A. (1996). Competitive sorption of simple organic acids and sulfate on goethite. *Environmental Science & Technology* 30, 1061-1071.

Allpike, B.P., Heitz, A., Joll, C.A., Kagi, R.I., Abbt-Braun, G., Frimmel, F.H., Brinkmann, T., Her, N. and Amy, G. (2005). Size exclusion chromatography to characterize DOC removal in drinking water treatment. *Environmental Science & Technology* 39, 2334-2342.

Amirtharajah, A., Dennett, K.E. and Studstill, A. (1993). Ferric-Chloride Coagulation for Removal of Dissolved Organic-Matter and Trihalomethane Precursors. *Water Science and Technology* 27, 113-121.

Amirtharajah, A. and Mills, K.M. (1982). Rapid-Mix Design for Mechanisms of Alum Coagulation. *Journal American Water Works Association* 74, 210-216.

Appelo, C.A.J., Van der Weiden, M.J.J., Tournassat, C. and Charlet, L. (2002). Surface complexation of ferrous iron and carbonate on ferrihydrite and the mobilization of arsenic. *Environmental Science & Technology* 36, 3096-3103.

Arai, Y., Sparks, D.L. and Davis, J.A. (2004). Effects of dissolved carbonate on arsenate adsorption and surface speciation at the hematite-water interface. *Environmental Science & Technology* 38, 817-824.

Au, K.K., Penisson, A.C., Yang, S.L. and O'Melia, C.R. (1999). Natural organic matter at oxide/water interfaces: Complexation and conformation. *Geochimica Et Cosmochimica Acta* 63, 2903-2917.

Baalousha, M., Motelica-Heino, M. and Le Coustumer, P. (2006). Conformation and size of humic substances: Effects of major cation concentration and type, pH, salinity, and residence time. *Colloids and Surfaces a-Physicochemical and Engineering Aspects* 272, 48-55.

Baes, C.V. and Mesmer, R.E. (1986). *The Hydrolysis of Cations*. Malabar, FL: Robert E. Krieger Publishing Company.

Bargar, J.R., Kubicki, J.D., Reitmeyer, R. and Davis, J.A. (2005). ATR-FTIR spectroscopic characterization of coexisting carbonate surface complexes on hematite. *Geochimica Et Cosmochimica Acta* 69, 1527-1542.

Black, A.P. and Christman, R.F. (1963). Characteristics of Colored Surface Waters. *Journal American Water Works Association* 55, 753-770.

Black, A.P., Singley, J.E., Whittle, G.P. and Maulding, J.S. (1963). Stoichiometry of the Coagulation of Color-Causing Organic Compounds with Ferric Sulfate. *Journal American Water Works Association* 55, 1347-1366.

Bose, P. and Reckhow, D.A. (1998). Adsorption of natural organic matter on preformed aluminum hydroxide flocs. *Journal of Environmental Engineering-Asce* 124, 803-811.

Brace, R. and Matijevic, E. (1977). Coprecipitation of Silica with Aluminum Hydroxide. *Colloid and Polymer Science* 255, 153-160.

Cathalifaud, G., Mossa, M.T.W. and Mazet, M. (1993). Preformed Ferric Hydroxide Flocs as Adsorbents of Humic Substances. *Water Science and Technology* 27, 55-60.

Chen, K.L., Mylon, S.E. and Elimelech, M. (2006). Aggregation kinetics of alginate-coated hematite nanoparticles in monovalent and divalent electrolytes. *Environmental Science & Technology* 40, 1516-1523.

Chen, K.L., Mylon, S.E. and Elimelech, M. (2007). Enhanced aggregation of alginate-coated iron oxide (hematite) nanoparticles in the presence of calcium, strontium, and barium cations. *Langmuir* 23, 5920-5928.

Cheng, Z.Q., Van Geen, A., Jing, C.Y., Meng, X.G., Seddique, A. and Ahmed, K.M. (2004). Performance of a household-level arsenic removal system during 4-month deployments in Bangladesh. *Environmental Science & Technology* 38, 3442-3448.

Chow, C.W.K., Fabris, R., van Leeuwen, J., Wang, D.S. and Drikas, M. (2008). Assessing natural organic matter treatability using high performance size exclusion chromatography. *Environmental Science & Technology* 42, 6683-6689.

Chowdhury, Z.K., Amy, G.L. and Bales, R.C. (1991). Coagulation of Submicron Colloids in Water-Treatment by Incorporation into Aluminum Hydroxide Floc. *Environmental Science & Technology* 25, 1766-1772.

Clark, M.M., Srivastava, R.M. and David, R. (1993). Mixing and Aluminum Precipitation. *Environmental Science & Technology* 27, 2181-2189.

Collins, M.R., Amy, G.L. and Steelink, C. (1986). Molecular Weight Distribution, Carboxylic Acidity, and Humic Substances Content of Aquatic Organic Matter - Implications for Removal During Water-Treatment. *Environmental Science & Technology* 20, 1028-1032.

Cornell, R.M. and Schwertmann, U. (2003). *The Iron Oxides: Structure, Properties, Reactions, Occurences and Uses*. Weinheim, Germany: Wiley-VCH

Crittenden, J.C., Trussell, R.R., Hand, D.W., Howe, K.J. and Tchobanoglous, G. (2005). *Water Treatment: Principles and Design*. Hoboken, N.J.: John Wiley & Sons, Inc.

Davis, C.C. (2000). Aqueous Silica in the Environment: Effects on Iron Hydroxide Surface Chemistry and Implications for Natural and Engineering Systems *Environmental Engineering*. Blacksburg, VA: Virginia Polytechnic Institute and State University.

Davis, C.C., Chen, H.W. and Edwards, M. (2002). Modeling silica sorption to iron hydroxide. *Environmental Science & Technology* 36, 582-587.

Davis, C.C., Knocke, W.R. and Edwards, M. (2001). Implications of aqueous silica sorption to iron hydroxide: Mobilization of iron colloids and interference with sorption of arsenate and humic substances. *Environmental Science & Technology* 35, 3158-3162.

Davis, J.A. (1982). Adsorption of Natural Dissolved Organic-Matter at the Oxide Water Interface. *Geochimica Et Cosmochimica Acta* 46, 2381-2393.

Davis, J.A. and Gloor, R. (1981). Adsorption of Dissolved Organics in Lake Water by Aluminum-Oxide - Effect of Molecular-Weight. *Environmental Science & Technology* 15, 1223-1229.

Dempsey, B.A. (1989). Reactions between Fulvic-Acid and Aluminum - Effects on the Coagulation Process. *Acs Symposium Series* 219, 409-424.

Dempsey, B.A. (1984). Removal of Naturally-Occurring Compounds by Coagulation and Sedimentation. *Crc Critical Reviews in Environmental Control* 14, 311-331.

Dempsey, B.A., Ganho, R.M. and O'Melia, C.R. (1984). The Coagulation of Humic Substances by Means of Aluminum Salts. *Journal American Water Works Association* 76, 141-150.

Dempsey, B.A. and O'Melia, C.R. (1983). Proton and Calcium Complexation of Four Fulvic Acid Fractions In R. F. Christman and E. T. Gjessing (eds.) *Aquatic and Terrestrial Humic Materials*. Ann Arbor, MI: Ann Arbor Science.

Dennett, K.E., Amirtharajah, A., Moran, T.F. and Gould, J.P. (1996). Coagulation: Its Effect on Organic Matter. *Journal American Water Works Association* 88, 129-142.

Dentel, S.K. (1988). Application of the Precipitation Charge Neutralization Model of Coagulation. *Environmental Science & Technology* 22, 825-832.

Dentel, S.K. and Gossett, J.M. (1988). Mechanisms of Coagulation with Aluminum Salts. *Journal American Water Works Association* 80, 187-198.

Diallo, M.S., Glinka, C.J., Goddard, W.A. and Johnson, J.H. (2005). Characterization of nanoparticles and colloids in aquatic systems 1. Small angle neutron scattering investigations of Suwannee River fulvic acid aggregates in aqueous solutions. *Journal of Nanoparticle Research* 7, 435-448.

Doelsch, E., Masion, A., Rose, J., Stone, W.E.E., Bottero, J.Y. and Bertsch, P.M. (2003). Chemistry and structure of colloids obtained by hydrolysis of Fe(III) in the presence of SiO4 ligands. *Colloids and Surfaces a-Physicochemical and Engineering Aspects* 217, 121-128.

Doelsch, E., Stone, W.E.E., Petit, S., Masion, A., Rose, J., Bottero, J.Y. and Nahon, D. (2001). Speciation and crystal chemistry of Fe(III) chloride hydrolyzed in the presence of SiO4 ligands. 2. Characterization of Si-Fe aggregates by FTIR and Si-29 solid-state NMR. *Langmuir* 17, 1399-1405.

Duan, J.M. and Gregory, J. (1998). The influence of silicic acid on aluminium hydroxide precipitation and flocculation by aluminium salts. *Journal of Inorganic Biochemistry* 69, 193-201.

Duan, J.M. and Gregory, J. (1996). Influence of soluble silica on coagulation by aluminium sulphate. *Colloids and Surfaces a-Physicochemical and Engineering Aspects* 107, 309-319.

Eaton, A.D., Clesceri, L.S., Rice, E.W. and Greenberg, A.E. (2005). Standard Methods of the Examination of Water and Wastewater. Washington, D.C.: American Public Health Association.

Edwards, G.A. and Amirtharajah, A. (1985). Removing Color Caused by Humic Acids. *Journal American Water Works Association* 77, 50-57.

Edwards, M. (1994). Chemistry of Arsenic Removal During Coagulation and Fe-Mn Oxidation. *Journal American Water Works Association* 86, 64-78.

Edwards, M. (1997). Predicting DOC Removal During Enhanced Coagulation. *Journal American Water Works Association* 89, 78-89.

Edwards, M. and Benjamin, M.M. (1992). Effect of Preozonation on Coagulant-NOM Interactions. *Journal American Water Works Association* 84, 63-72.

Edwards, M., Benjamin, M.M. and Ryan, J.N. (1996). Role of organic acidity in sorption of natural organic matter (NOM) to oxide surfaces. *Colloids and Surfaces a-Physicochemical and Engineering Aspects* 107, 297-307.

Edzwald, J.K. (1993). Coagulation in Drinking Water Treatment: Particles, Organics and Coagulants. *Water Science and Technology* 27, 21-35.

Edzwald, J.K. and Van Benschoten, J.E. (1990). Aluminum Coagulation of Natural Organic Matter In H. H. Hahn and R. Klute (eds.) *Chemical Water and Wastewater Treatment*. Berlin: Springer-Verlag.

Evanko, C.R. and Dzombak, D.A. (1998). Influence of structural features on sorption of NOM-analogue organic acids to goethite. *Environmental Science & Technology* 32, 2846-2855.

Evanko, C.R. and Dzombak, D.A. (1999). Surface complexation modeling of organic acid sorption to goethite. *Journal of Colloid and Interface Science* 214, 189-206.

Exley, C. and Birchall, J.D. (1992). Hydroxyaluminosilicate Formation in Solutions of Low Total Aluminum Concentration. *Polyhedron* 11, 1901-1907.

Filius, J.D., Meeussen, J.C.L., Lumsdon, D.G., Hiemstra, T. and Van Riemsdijk, W.H. (2003). Modeling the binding of fulvic acid by goethite: the speciation of adsorbed FA molecules. *Geochimica Et Cosmochimica Acta* 67, 1463-1474.

Frey, M.M. and Edwards, M.A. (1997). Surveying Arsenic Occurrence. *Journal American Water Works Association* 89, 105-117.

Fuller, C.C., Davis, J.A. and Waychunas, G.A. (1993). Surface-Chemistry of Ferrihydrite .2. Kinetics of Arsenate Adsorption and Coprecipitation. *Geochimica Et Cosmochimica Acta* 57, 2271-2282.

Geelhoed, J.S., Hiemstra, T. and VanRiemsdijk, W.H. (1997). Phosphate and sulfate adsorption on goethite: Single anion and competitive adsorption. *Geochimica Et Cosmochimica Acta* 61, 2389-2396.

Gu, B.H., Schmitt, J., Chen, Z.H., Liang, L.Y. and McCarthy, J.F. (1994). Adsorption and Desorption of Natural Organic-Matter on Iron-Oxide - Mechanisms and Models. *Environmental Science & Technology* 28, 38-46.

Hall, E.S. and Packham, R.F. (1965). Coagulation of Organic Color with Hydrolyzing Coagulants. *Journal American Water Works Association* 57, 1149-1165.

Hanson, A.T. and Cleasby, J.L. (1990). The Effects of Temperature on Turbulent Flocculation - Fluid-Dynamics and Chemistry. *Journal American Water Works Association* 82, 56-73.

Hering, J.G., Chen, P.Y., Wilkie, J.A. and Elimelech, M. (1997). Arsenic removal from drinking water during coagulation. *Journal of Environmental Engineering-Asce* 123, 800-807.

Hering, J.G., Chen, P.Y., Wilkie, J.A., Elimelech, M. and Liang, S. (1996). Arsenic removal by ferric chloride. *Journal American Water Works Association* 88, 155-167.

Hiemstra, T., Rahnemaie, R. and van Riemsdijk, W.H. (2004). Surface complexation of carbonate on goethite: IR spectroscopy, structure and charge distribution. *Journal of Colloid and Interface Science* 278, 282-290.

Hingston, F.J. and Raupach, M. (1967). The Reaction Between Monosilicic Acid and Aluminium Hydroxide. I. Kinetics of adsorption of Silicic Acid by Aluminium Hydroxide. *Australian Journal of Soil Research* 5, 295-309.

Holm, T.R. (2002). Effects of CO32-/bicarbonate, Si, and PO43- on arsenic sorption to HFO. *Journal American Water Works Association* 94, 174-181.

Huang, C.P. (1975). Removal of Aqueous Silica from Dilute Aqueous Solution. *Earth and Planetary Science Letters* 27, 265-274.

Iler, R.K. (1979). *The Chemistry of Silica: Solubility, Polymerization, Colloid and Surface Properties, and Biochemistry*. New York: John Wiley & Sons.

Jacangelo, J.G., Demarco, J., Owen, D.M. and Randtke, S.J. (1995). Selected Processes for Removing NOM: An Overview. *Journal American Water Works Association* 87, 64-77.

Jekel, M.R. (1986). Interactions of Humic Acids and Aluminum Salts in the Flocculation Process. *Water Research* 20, 1535-1542.

Jolivet, J.-P. (2000). *Metal Oxide Chemistry and Synthesis: From Solution to Solid State*. New York: John Wiley & Sons, Ltd.

Jung, A.V., Chanudet, V., Ghanbaja, J., Lartiges, B.S. and Bersillon, J.L. (2005). Coagulation of humic substances and dissolved organic matter with a ferric salt: An electron energy loss spectroscopy investigation. *Water Research* 39, 3849-3862.

Kang, L.S. and Cleasby, J.L. (1995). Temperature Effects on Flocculation Kinetics Using Fe(III) Coagulant. *Journal of Environmental Engineering-Asce* 121, 893-901.

Karthikeyan, K.G. and Elliott, H.A. (1999). Surface complexation modeling of copper sorption by hydrous oxides of iron and aluminum. *Journal of Colloid and Interface Science* 220, 88-95.

Karthikeyan, K.G., Elliott, H.A. and Cannon, F.S. (1997). Adsorption and coprecipitation of copper with the hydrous oxides of iron and aluminum. *Environmental Science & Technology* 31, 2721-2725.

LaNier, J.M. (1976). Historical Development of Municipal Water Systems in United-States - 1776-1976. *Journal American Water Works Association* 68, 173-180.

Leenheer, J.A. (1981). Comprehensive approach to preparative isolation and fractionation of dissolved organic carbon from natural waters and wastewaters. *Environmental Science & Technology* 15, 578-587.

Leenheer, J.A. and Croue, J.P. (2003). Characterizing aquatic dissolved organic matter. *Environmental Science & Technology* 37, 18A-26A.

Leenheer, J.A. and Huffman, E.W.D. (1976). Classification of Organic Solutes in Water by Using Macroreticular Resins. *Journal of Research of the Us Geological Survey* 4, 737-751.

Lefebvre, E. and Legube, B. (1990). Iron(III) Coagulation of Humic Substances Extracted from Surface Waters - Effect of Ph and Humic Substances Concentration. *Water Research* 24, 591-606.

Letterman, R.D., Quon, J.E. and Gemmell, R.S. (1970). Coagulation of Activated Carbon Suspensions. *Journal American Water Works Association* 60, 652-658.

Letterman, R.D., Tabatabaie, M. and Ames, R.S. (1979). Effect of the Bicarbonate Ion Concentration on Flocculation with Aluminum Sulfate. *Journal American Water Works Association* 71, 467-472.

Letterman, R.D. and Vanderbrook, S.G. (1983). Effect of Solution Chemistry on Coagulation with Hydrolyzed Al(III) - Significance of Sulfate Ion and pH. *Water Research* 17, 195-204.

Liu, R.P., Li, X., Xia, S.J., Yang, Y.L., Wu, R.C. and Li, G.B. (2007a). Calcium-enhanced ferric hydroxide co-precipitation of arsenic in the presence of silicate. *Water Environment Research* 79, 2260-2264.

Liu, R.P., Qu, J.H., Xia, S.J., Zhang, G.S. and Li, G.B. (2007b). Silicate hindering in situ formed ferric hydroxide precipitation: Inhibiting arsenic removal from water. *Environmental Engineering Science* 24, 707-715.

Luxton, T.P., Tadanier, C.J. and Eick, M.J. (2006). Mobilization of arsenite by competitive interaction with silicic acid. *Soil Science Society of America Journal* 70, 204-214.

Malcolm, R.L. (1985). Geochemistry of Stream Fulvic and Humic Substances In G. R. Aiken et al. (eds.) *Humic Substances in Soil, Sediment, and Water: Geochemistry, Isolation, and Characterization*, 181-209). New York: Wiley-Interscience.

Masion, A., Rose, J., Bottero, J.Y., Tchoubar, D. and Elmerich, P. (1997a). Nucleation and growth mechanisms of iron oxyhydroxides in the presence of PO4 ions .3. Speciation of Fe by small angle X-ray scattering. *Langmuir* 13, 3882-3885.

Masion, A., Rose, J., Bottero, J.Y., Tchoubar, D. and Garcia, F. (1997b). Nucleation and growth mechanisms of iron oxyhydroxides in the presence of PO4 ions .4. Structure of the aggregates. *Langmuir* 13, 3886-3889.

Maurice, P.A. and Namjesnik-Dejanovic, K. (1999). Aggregate structures of sorbed humic substances observed in aqueous solution. *Environmental Science & Technology* 33, 1538-1541.

Mayer, T.D. and Jarrell, W.M. (1996). Formation and stability of iron(II) oxidation products under natural concentrations of dissolved silica. *Water Research* 30, 1208-1214.

Mayer, T.D. and Jarrell, W.M. (2000). Phosphorus sorption during iron(II) oxidation in the presence of dissolved silica. *Water Research* 34, 3949-3956.

McKnight, D.M., Bencala, K.E., Zellweger, G.W., Aiken, G.R., Feder, G.L. and Thorn, K.A. (1992). Sorption of Dissolved Organic-Carbon by Hydrous Aluminum and Iron-Oxides Occurring at the Confluence of Deer Creek with the Snake River, Summit County, Colorado. *Environmental Science & Technology* 26, 1388-1396.

Meng, X.G., Bang, S. and Korfiatis, G.P. (2000). Effects of silicate, sulfate, and carbonate on arsenic removal by ferric chloride. *Water Research* 34, 1255-1261.

Morris, J.K. and Knocke, W.R. (1984). Temperature Effects on the Use of Metal-Ion Coagulants for Water-Treatment. *Journal American Water Works Association* 76, 74-79.

Narkis, N. and Rebhun, M. (1977). Stoichiometric Relationship between Humic and Fulvic Acids and Flocculants. *Journal American Water Works Association* 69, 325-328.

Packham, R.F. (1965). Some Studies of the Coagulation of Dispersed Clays with Hydrolyzing Salts. *Journal of Colloid Science* 20, 81-92.

Peak, D., Ford, R.G. and Sparks, D.L. (1999). An in situ ATR-FTIR investigation of sulfate bonding mechanisms on goethite. *Journal of Colloid and Interface Science* 218, 289-299.

Piccolo, A. (2001). The supramolecular structure of humic substances. *Soil Science* 166, 810-832.

Pommerenk, P. and Schafran, G.C. (2005). Adsorption of inorganic and organic ligands onto hydrous aluminum oxide: Evaluation of surface charge and the impacts on particle and NOM removal during water treatment. *Environmental Science & Technology* 39, 6429-6434.

Radu, T., Subacz, J.L., Phillippi, J.M. and Barnett, M.O. (2005). Effects of dissolved carbonate on arsenic adsorption and mobility. *Environmental Science & Technology* 39, 7875-7882.

Randtke, S.J. (1988). Organic Contaminant Removal by Coagulation and Related Process Combinations. *Journal American Water Works Association* 80, 40-56.

Randtke, S.J. and Jepsen, C.P. (1981). Chemical Pretreatment for Activated-Carbon Adsorption. *Journal American Water Works Association* 73, 411-419.

Rizzo, L., Belgiorno, V., Gallo, M. and Meric, S. (2005). Removal of THM precursors from a high-alkaline surface water by enhanced coagulation and behaviour of THMFP toxicity on D-magna. *Desalination* 176, 177-188.

Rook, J.J. (1974). Formation of Haloforms During Chlorination of Natural Waters. *Water Treatment and Examination* 23, 234-243.

Rose, J., Manceau, A., Bottero, J.Y., Masion, A. and Garcia, F. (1996). Nucleation and growth mechanisms of Fe oxyhydroxide in the presence of PO4 ions .1. Fe K-edge EXAFS study. *Langmuir* 12, 6701-6707.

Schenk, J.E. and Weber, W.J. (1968). Chemical Interactions of Dissolved Silica with Iron (II) and (III). *Journal American Water Works Association* 60, 199-212.

Schulthess, C.P., Swanson, K. and Wijnja, H. (1998). Proton adsorption on an aluminum oxide in the presence of bicarbonate. *Soil Science Society of America Journal* 62, 136-141.

Semmens, M.J. and Staples, A.B. (1986). The Nature of Organics Removed During Treatment of Mississippi River Water. *Journal American Water Works Association* 78, 76-81.

Sharp, E.L., Jarvis, P., Parsons, S.A. and Jefferson, B. (2006a). Impact of fractional character on the coagulation of NOM. *Colloids and Surfaces a-Physicochemical and Engineering Aspects* 286, 104-111.

Sharp, E.L., Jarvis, P., Parsons, S.A. and Jefferson, B. (2006b). The impact of zeta potential on the physical properties of ferric-NOM flocs. *Environmental Science & Technology* 40, 3934-3940.

Sharp, E.L., Parson, S.A. and Jefferson, B. (2006c). Coagulation of NOM: linking character to treatment. *Water Science and Technology* 53, 67-76.

Shin, J.Y., Spinette, R.F. and O'Melia, C.R. (2008). Stoichiometry of Coagulation Revisited. *Environmental Science & Technology* 42, 2582-2589.

Sieliechi, J.M., Lartiges, B.S., Kayem, G.J., Hupont, S., Frochot, C., Thieme, J., Ghanbaja, J., de la Caillerie, J.B.D., Barres, O., Kamga, R., Levitz, P. and Michot, L.J. (2008). Changes in humic acid conformation during coagulation with ferric chloride: Implications for drinking water treatment. *Water Research* 42, 2111-2123.

Sigg, L. and Stumm, W. (1981). The Interaction of Anions and Weak Acids with the Hydrous Goethite (Alpha-Feooh) Surface. *Colloids and Surfaces* 2, 101-117.

Simpson, A.J., Kingery, W.L., Hayes, M.H.B., Spraul, M., Humpfer, E., Dvortsak, P., Kerssebaum, R., Godejohann, M. and Hofmann, M. (2002). Molecular structures and associations of humic substances in the terrestrial environment. *Naturwissenschaften* 89, 84-88.

Singer, P.C., Harrington, G.W., Thompson, J. and White, M. (1995). Enhanced Coagulation and Enhanced Softening for the Removal of Disinfection By-product Precursors: An Evaluation. Chapel Hill, NC.

Sinsabaugh, R.L., Hoehn, R.C., Knocke, W.R. and Linkins, A.E. (1986a). Precursor Size and Organic Halide Formation Rates in Raw and Coagulated Surface Waters. *Journal of Environmental Engineering-Asce* 112, 139-153.

Sinsabaugh, R.L., Hoehn, R.C., Knocke, W.R. and Linkins, A.E. (1986b). Removal of Dissolved Organic Carbon by Coagulation with Iron Sulfate. *Journal American Water Works Association* 78, 74-82.

Smith, S.D. and Edwards, M. (2005). The influence of silica and calcium on arsenate sorption to oxide surfaces. *Journal of Water Supply Research and Technology-Aqua* 54, 201-211.

Stachowicz, M., Hiemstra, T. and Van Riemsdijk, W.H. (2007). Arsenic-bicarbonate interaction on goethite particles. *Environmental Science & Technology* 41, 5620-5625.

Stumm, W. and Morgan, J.J. (1996). *Aquatic Chemistry: Chemical Equilibria and Rates in Natural Waters*. New York: John Wiley & Sons, Inc.

Stumm, W. and Morgan, J.J. (1962). Chemical Aspects of Coagulation. *Journal American Water Works Association* 54, 971-992.

Stumm, W. and O'Melia, C.R. (1968). Stoichiometry of Coagulation. *Journal American Water Works Association* 60, 514-569.

Sutton, R. and Sposito, G. (2005). Molecular structure in soil humic substances: The new view. *Environmental Science & Technology* 39, 9009-9015.

Swedlund, P.J. and Webster, J.G. (1999). Adsorption and polymerisation of silicic acid on ferrihydrite, and its effect on arsenic adsorption. *Water Research* 33, 3413-3422.

Swift, R.S. (1999). Macromolecular properties of soil humic substances: Fact, fiction, and opinion. *Soil Science* 164, 790-802.

Taylor, P.D., Jugdaohsingh, R. and Powell, J.J. (1997). Soluble silica with high affinity for aluminum under physiological and natural conditions. *Journal of the American Chemical Society* 119, 8852-8856.

Thurman, E.M. (1985). *Organic Geochemistry of Natural Waters*. Dordrecht: Martinus Nijhoff/Dr W. Junk Publishers.

Thurman, E.M. and Malcolm, R.L. (1981). Preparative isolation of aquatic humic substances. *Environmental Science & Technology* 15, 463-466.

Tipping, E. (1981). The Adsorption of Aquatic Humic Substances by Iron Oxides. *Geochimica Et Cosmochimica Acta* 45, 191-199.

Tong, J. (1997). Development of an Iron (III)-Coagulation-Microfiltration Process for Arsenic Removal from Groundwater. Houston, TX: University of Houston.

Tseng, T. and Edwards, M. (1999). Predicting Full-Scale TOC Removal. *Journal American Water Works Association* 91, 159-170.

Tseng, T., Segal, B.D. and Edwards, M. (2000). Increasing Alkalinity to Reduce Turbidity. *Journal American Water Works Association* 92, 44-54.

USEPA (1999). Enhanced Coagulation and Enhanced Precipitative Softening Guidance Manual. Report No. EPA 815-R-99-012.

Van Benschoten, J.E. and Edzwald, J.K. (1990a). Chemical Aspects of Coagulation Using Aluminum Salts .1. Hydrolytic Reactions of Alum and Polyaluminum Chloride. *Water Research* 24, 1519-1526.

Van Benschoten, J.E. and Edzwald, J.K. (1990b). Chemical Aspects of Coagulation Using Aluminum Salts .2. Coagulation of Fulvic-Acid Using Alum and Polyaluminum Chloride. *Water Research* 24, 1527-1535.

van Leeuwen, J., Daly, R. and Holmes, A. (2005). Modeling the treatment of drinking water to maximize dissolved organic matter removal and minimize disinfection by-product formation. *Desalination* 176, 81-89.

Vilge-Ritter, A., Rose, J., Masion, A., Bottero, J.Y. and Laine, J.M. (1999). Chemistry and structure of aggregates formed with Fe-salts and natural organic matter. *Colloids and Surfaces a-Physicochemical and Engineering Aspects* 147, 297-308.

Villalobos, M. and Leckie, J.O. (2000). Carbonate adsorption on goethite under closed and open CO2 conditions. *Geochimica Et Cosmochimica Acta* 64, 3787-3802.

Villalobos, M. and Leckie, J.O. (2001). Surface complexation modeling and FTIR study of carbonate adsorption to goethite. *Journal of Colloid and Interface Science* 235, 15-32.

Violante, A. and Huang, P.M. (1985). Influence of Inorganic and Organic-Ligands on the Formation of Aluminum Hydroxides and Oxyhydroxides. *Clays and Clay Minerals* 33, 181-192.

Violante, A. and Violante, P. (1980). Influence of pH, Concentration, and Chelating Power of Organic-Anions on the Synthesis of Aluminum Hydroxides and Oxyhydroxides. *Clays and Clay Minerals* 28, 425-434.

Wang, D.S., Xing, L.N., Xie, J.K., Chow, C.W.K., Xu, Z.Z., Zhao, Y.M. and Drikas, M. (2010). Application of advanced characterization techniques to assess DOM treatability of micro-polluted and un-polluted drinking source waters in China. *Chemosphere* 81, 39-45.

Waychunas, G.A., Rea, B.A., Fuller, C.C. and Davis, J.A. (1993). Surface-Chemistry of Ferrihydrite .1. EXAFS Studies of the Geometry of Coprecipitated and Adsorbed Arsenate. *Geochimica Et Cosmochimica Acta* 57, 2251-2269.

Weishaar, J.L., Aiken, G.R., Bergamaschi, B.A., Fram, M.S., Fujii, R. and Mopper, K. (2003). Evaluation of specific ultraviolet absorbance as an indicator of the chemical composition and reactivity of dissolved organic carbon. *Environmental Science & Technology* 37, 4702-4708.

Weng, L., Van Riemsdijk, W.H. and Hiemstra, T. (2007). Adsorption of humic acids onto goethite: Effects of molar mass, pH and ionic strength. *Journal of Colloid and Interface Science* 314, 107-118.

Weng, L.P., Koopal, L.K., Hiemstra, T., Meeussen, J.C.L. and Van Riemsdijk, W.H. (2005). Interactions of calcium and fulvic acid at the goethite-water interface. *Geochimica Et Cosmochimica Acta* 69, 325-339.

Weng, L.P., Van Riemsdijk, W.H., Koopal, L.K. and Hiemstra, T. (2006). Adsorption of humic substances on goethite: Comparison between humic acids and fulvic acids. *Environmental Science & Technology* 40, 7494-7500.

White, M.C., Thompson, J.D., Harrington, G.W. and Singer, P.C. (1997). Evaluating Criteria for Enhanced Coagulation Compliance. *Journal American Water Works Association* 89, 64-77.

Wijnja, H. and Schulthess, C.P. (2001). Carbonate adsorption mechanism on goethite studied with ATR-FTIR, DRIFT, and proton coadsorption measurements. *Soil Science Society of America Journal* 65, 324-330.

Wijnja, H. and Schulthess, C.P. (2002). Effect of carbonate on the adsorption of selenate and sulfate on goethite. *Soil Science Society of America Journal* 66, 1190-1197.

Wijnja, H. and Schulthess, C.P. (2000a). Interaction of carbonate and organic anions with sulfate and selenate adsorption on an aluminum oxide. *Soil Science Society of America Journal* 64, 898-908.

Wijnja, H. and Schulthess, C.P. (2000b). Vibrational spectroscopy study of selenate and sulfate adsorption mechanisms on Fe and Al (hydr)oxide surfaces. *Journal of Colloid and Interface Science* 229, 286-297.

Wilkinson, K.J., Balnois, E., Leppard, G.G. and Buffle, J. (1999). Characteristic features of the major components of freshwater colloidal organic matter revealed by transmission electron and atomic force microscopy. *Colloids and Surfaces a-Physicochemical and Engineering Aspects* 155, 287-310.

Xie, J., Wang, D., van Leeuwen, J., Zhao, Y., Xing, L. and Chow, C.W.K. (2012). pH modeling for maximum dissolved organic matter removal by enhanced coagulation. *Journal of Environmental Sciences* 24, 276-283.

Zachara, J.M., Girvin, D.C., Schmidt, R.L. and Resch, C.T. (1987). Chromate Adsorption on Amorphous Iron Oxyhydroxide in the Presence of Major Groundwater Ions. *Environmental Science & Technology* 21, 589-594.

Chapter 2. Role of Calcium in the Coagulation of NOM with Ferric Chloride

Christina C. Davis and Marc Edwards

Virginia Tech Department of Civil and Environmental Engineering,
407 Durham Hall, Blacksburg, VA 24060

Keywords: calcium, natural organic matter, complexation, coagulation, ferric chloride, Stockholm Humic Model

Abstract

Natural organic matter (NOM) is capable of interfering with Fe hydrolysis and influencing the size, morphology, and identity of Fe precipitates. Conversely, Ca^{2+} is known to raise surface potential and increase the size and aggregation of Fe precipitates, leading to more effective coagulation and widening the pH range of treatment. Experiments and modeling were conducted to investigate the significance the Fe/NOM ratio and the presence of Ca^{2+} in coagulation. At the high Fe/NOM ratio, sufficient or excess Fe was available for NOM removal, and coagulation proceeded according to expectations based upon the literature. At the low Fe/NOM ratio, however, NOM inhibited Fe hydrolysis, reduced zeta potential, and suppressed the formation of filterable Fe flocs, thereby interfering with NOM removal. In these dose-limited systems without Ca^{2+}, complexation of Fe species by NOM appears to be the mechanism by which coagulation is disrupted. Equilibrating NOM with 1 mM Ca^{2+} in dose-limited systems prior to dosing with $FeCl_3$ increased Fe hydrolysis and zeta potential, decreased the fraction of colloidal Fe, and improved NOM removal. In systems with Ca^{2+}, data and modeling indicate that Ca^{2+} complexation by NOM neutralizes some of the negative organic charge and minimizes Fe complexation, making Fe species available for hydrolysis and effective coagulation.

Introduction

Natural organic matter (NOM) is ubiquitous in natural waters and exerts significant influence in geochemical processes and engineered systems. Aquatic humic substances (AHS), a class of NOM comprised of humic acids (HA) and fulvic acids (FA), sorb strongly to aluminum and iron oxides via ligand exchange reactions between humic functional groups and the oxide surface.[1, 2] Sorbed AHSs reduce surface charge and may compete with or disrupt sorption of other ligands, such as arsenic or silica.[3, 4] Previous research has established that NOM is capable of mobilizing iron and aluminum colloids and even promoting reductive or ligand-induced dissolution.[3, 5-11]

NOM also interacts with dissolved metal species, including aluminum, iron, lead, copper, nickel, chromium, cobalt, zinc, manganese, calcium, magnesium, and cadmium.[12] Carboxylic and phenolic functional groups of HAs and FAs can bind metals, thereby affecting mobility, toxicity, and bioavailability. Significant effort has been directed toward developing models to predict metal speciation and competitive binding by humic substances.[13-20] Depending upon concentration, pH, and ionic strength, metal-humic complexation reactions also have the effect of reducing the negative charge on NOM. In the pH range of natural waters, organic acidity generally falls within the range of 5 to 15 meq/g C,[21-24] but Dempsey and O'Melia[21] demonstrated that Ca^{2+} complexation is capable of neutralizing more than 50% of the initial charge as Ca^{2+} concentration and pH increase.

Interactions between NOM and dissolved Fe are of particular interest in iron oxidation, coagulation, and other environments in which Fe^{3+} hydrolyzes in the presence of NOM. In the pH range of natural waters, Fe^{3+} rapidly hydrolyzes to form an amorphous ferric hydroxide precipitate. Historically, NOM adsorption to ferric hydroxide flocs has been viewed as a primary mechanism for DOC removal during coagulation.[25] However, AHS functional groups are capable of binding dissolved Fe^{3+} species, and the presence of NOM can alter the reaction pathways of Fe^{3+} (Figure 2-1). In essence, humates and fulvates compete with OH^- for Fe^{3+} coordination, while Fe^{3+} and its associated hydrolysis species (e.g., $FeOH^{2+}$, $Fe(OH)_2^+$) compete with H^+ for the acidic binding sites of AHS.[26-28]

The occurrence of Fe-NOM reaction(s) (Figure 2-1) depends upon a range of variables, including pH; ionic strength; NOM characteristics; relative concentrations of Fe^{3+}, dissolved organic carbon (DOC), and competing species; temperature; and mixing [29]. In water treatment, these Fe-NOM reactions determine the mechanism(s) and extent of DOC removal. Evidence that NOM interferes with Fe hydrolysis and limits polymerization and growth of ferric hydroxide precipitates has led several researchers to conclude that coagulation of NOM occurs by charge neutralization/precipitation rather than adsorption, even at pH above 7.[30-32] Yet, Dempsey[33] concluded that aluminum hydroxide precipitated under all p[Al]-pH conditions at which successful FA removal was observed.

There is evidence that Ca^{2+} also plays an important role in systems with NOM. Ca^{2+} complexation by NOM is relatively weak, but at concentrations of 2-75 mg/L in surface water and 2-150 mg/L in groundwater,[34] Ca^{2+} may effectively compete with trace metals that occur at significantly lower concentrations.[35] Charge neutralization and bridging by Ca^{2+} promoted

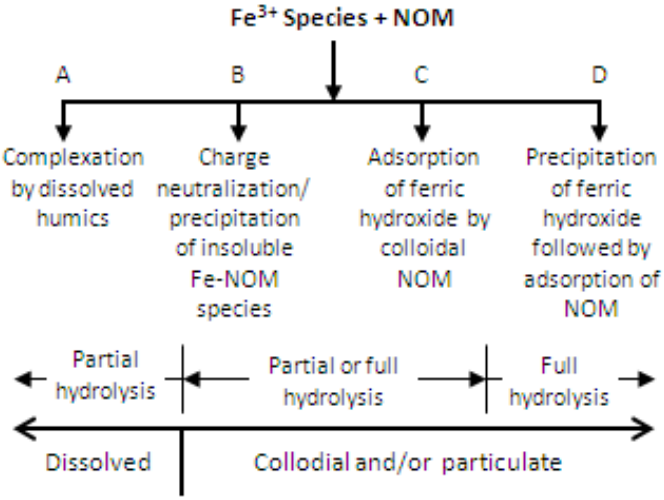

Figure 2-1. Possible reactions between Fe^{3+} species and NOM and characteristics of the resulting products.

aggregation and led to an increase in network size of Suwanee River HA (SRHA), alginate polymers, and alginate-coated hematite.[36-38] In fact, at pH 7.5 and 9.3, Ca^{2+} levels of approximately 9 mg Ca^{2+}/mg SRHA effectively increased the size of the SHRA humic network to greater than 450 nm, thereby altering the operational classification of the SRHA from "dissolved" to "particulate."[36]

In coagulation experiments with Dismal Swamp FA and a low alum dose (0.14 mg Al/mg TOC), Ca^{2+} concentrations of 20-80 mg/L reduced residual FA and substantially widened the pH range of effective treatment.[39] Duan et al.[40] also found that Ca^{2+} widened the pH range of effective treatment and improved removal of small humic molecules, including hydrophilic precursors to haloacetic acids (HAAs). Ca^{2+} has been observed to increase adsorption of FAs to goethite[1, 41] and amorphous aluminum hydroxide.[39] Ca^{2+} also mitigates the negative effects of silica in coagulation, specifically by (a) minimizing residual or colloidal concentrations of Fe or Al[42, 43] and (b) minimizing silica's interference with arsenic removal.[43-45]

There are several mechanisms by which Ca^{2+} may interact with NOM and hydrolyzing metals, and the benefits of Ca^{2+} likely depend upon these interactions. Possible mechanisms include: aggregation of a supramolecular humic network; double layer compression; complexation by AHS; direct adsorption to the metal oxide surface; and the formation of a ternary surface complex between the metal oxide, Ca^{2+}, and sorbing ligand.[1, 36, 39, 41, 45, 46] An increase in surface potential and associated decrease in electrostatic repulsion appear to be a key contributions of Ca^{2+} in many systems.[1, 41, 43, 45]

Methods and Materials

Experiments were conducted to investigate coagulation and removal of FA by ferric chloride. Two DOC concentrations (2 mg/L and 10 mg/L) and three pH levels (5.5, 6.5, and 7.5) were studied. The target Fe^{3+} iron concentration in each sample was 10 mg/L as Fe, yielding ratios of 5 mg Fe/mg DOC at the low-FA condition and 1 mg Fe/mg DOC at the high-FA condition. A

second set of experiments was conducted to investigate the effect of Ca^{2+} (40 mg/L) at both Fe/DOC ratios and each pH level.

Chemicals

Fulvic Acid. FA was isolated from Silver Lake, which serves as a source water for Boulder, Colorado. A concentrated NOM solution was obtained by nanofiltration with a nominal molecular weight cutoff of 300 Da; this solution was then passed through cation exchange resin in the sodium form to remove multivalent cations.[47, 48] The extraction method for FA is described by Aiken.[49] The isolate was preserved by freeze-drying.

Stock Solutions. Stock solutions of $CaCl_2$, $NaNO_3$, and $FeCl_3$ were prepared using reagent-grade chemicals. The $CaCl_2$ (0.50 M) and $NaNO_3$ (4.12 M) solutions were prepared by dissolving the salt in distilled water. $FeCl_3$ (8.59×10^{-3} M) was dissolved in 0.01-M HNO_3 to prevent precipitation in the stock solution. pH adjustment was accomplished with HNO_3 and NaOH solutions of varying concentrations (0.01-0.2 M).

Experimental Protocol

Samples were prepared with distilled water in 500-mL HDPE bottles. Measured DOC concentrations averaged 1.98 $\pm$ 0.12 and 9.60 $\pm$ 0.22 mg/L at the low- and high-FA conditions, respectively. In samples with Ca^{2+}, the average initial concentration was 39.38 $\pm$ 0.73 mg/L. $NaNO_3$ was added as needed to provide a total ionic strength of 0.01 M.

Sample solutions with FA and Ca^{2+} were prepared and equilibrated approximately 12 hours before experiments were conducted. To each sample, the acidified $FeCl_3$ was dosed to initiate the experiment; delivered iron concentrations averaged 10.16 $\pm$ 0.35 mg/L as Fe. pH was adjusted to the target level immediately after the $FeCl_3$ was dosed, and a 10-mL aliquot was withdrawn for an initial zeta potential analysis. The sample was then placed on an end-over-end rotary agitator (Analytical Testing Corp., Warrington, PA) until the first sampling event at 0.5 h after the $FeCl_3$ was dosed. The end-over-end rotary shaker was also used to mix the samples between subsequent sampling events, which were repeated at 4 h and 24 h. During $FeCl_3$ dosing and each sampling event, the samples were mixed with a magnetic stir bar and stir plate.

Sampling followed a standard procedure. pH was measured and adjusted if necessary. After pH was stabilized at the target pH ($\pm$0.05), zeta potential was measured. Next, a syringe filter fitted with a 0.45-µm nylon filter was used to filter 50 mL of sample. The filtrate was analyzed for DOC, UV_{254} absorbance, Fe, and Ca.

Instrumentation

Zeta potential was measured with a Malvern ZetaSizer 3000HS (Malvern Instruments Inc., Westborough, MA). The performance of the instrument was verified using the manufacturer's electrophoresis standard and by comparative measurements with a Zeta Meter 3.0+ (Zeta Meter Inc., Staunton, VA). Additional details are provided elsewhere.[3] DOC was measured with a Sievers Model 800 TOC Analyzer. Analysis was conducted using the persulfate-ultraviolet oxidation according to Standard Method 5310C.[50] UV_{254} absorbance was quantified with a Hach DR5000 UV-Vis Spectrophotometer (Hach, Loveland, CO). Fe and Ca concentrations were

measured using a Thermo Electron X-Series inductively coupled plasma with mass spectrometer (ICP-MS) per Standard Method 3125B.[50] Samples and calibration standards were prepared in a matrix of 2% HNO_3 by volume.

Modeling

Simulations of Fe-FA and Ca-FA complexation were performed using the Stockholm Humic Model (SHM) in Visual MINTEQ 3.0.[18, 51] The default database of generic complexation constants, which includes Fe^{3+} and $Fe(OH)^{2+}$ constants optimized by Sjostedt et al.,[52] was used. Default parameters for FA properties were also used, and the ratio of active dissolved organic matter (ADOM) to DOC was set to 2.0. Model predictions of Ca^{2+} complexation were consistent with measurements reported by others,[21, 24] and no attempt was made to optimize the model. Rather, model simulations were used to aid in interpreting results.

Results and Discussion

Low DOC Concentration (5 mg Fe/mg DOC)

DOC removal followed expected trends with respect to the influence of pH (Figure 2-2). Sorption was maximized at pH 5.5 and 6.5, and removal of UV_{254} absorbance was greater than 90% at these two pH levels (data not shown). At pH 7.5, there was a clear decrease in removal of both DOC and UV_{254} absorbance. Since there is sufficient Fe available to react with the sorbable DOC, the reduced sorption at pH 7.5 is attributed to increased electrostatic repulsion arising from

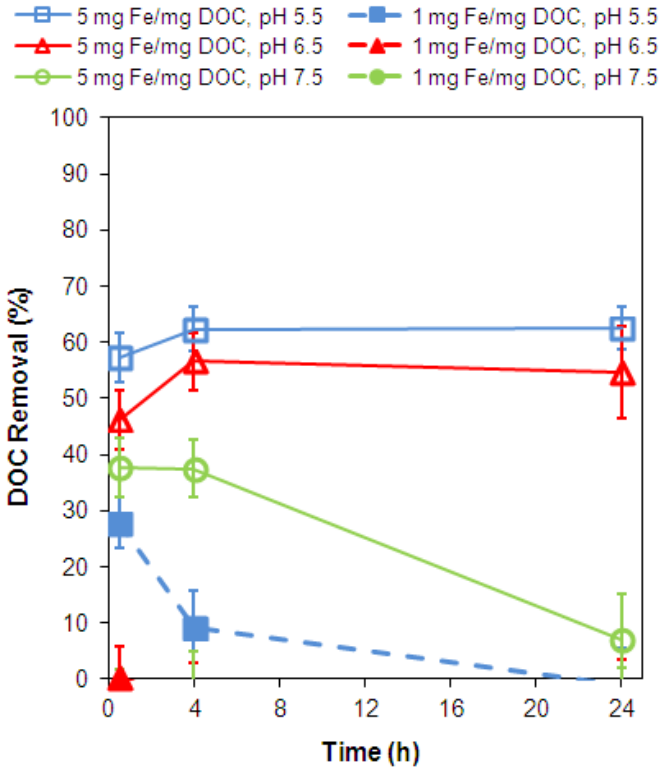

Figure 2-2. DOC removal as a function of pH, Fe/DOC ratio, and reaction time.

deprotonation of Fe and NOM functional groups. Changes in the conformation of FA, which also result from deprotonation of functional groups, may further interfere with sorptive removal at pH 7.5.

FA sorbed rapidly at all three pH levels. By 0.5 h, 92%, 82%, and 100% of the maximum observed DOC removal was attained at pH 5.5, 6.5, and 7.5, respectively (Figure 2-2). At pH 5.5 and 6.5, there was a slight increase in the adsorbed concentration between 0.5 and 4 h, while apparent equilibrium is observed between 4 and 24 h. At pH 7.5, a significant decline in DOC removal was observed between 4 and 24 h, but this trend was not replicated in the UV_{254} absorbance removal data.

High DOC concentration (1 mg Fe/mg DOC)

When DOC was present at a much higher concentration relative to Fe dose, FA removal was severely inhibited (Figure 2-2). At pH 5.5 and 0.5 h, DOC removal was 28%, or roughly half of the removal observed at the higher Fe/DOC ratio. DOC steeply declined to 9.3% at 4 h, and no removal was detected at 24 h. Likewise, no measureable removal was detected during any of the sampling events at pH 6.5 or 7.5.

Examination of zeta potential data provides some insight into DOC removal trends. At the low DOC concentration (5 mg Fe/mg DOC), zeta potential falls within the range of +17.3 mV (pH 5.5) to -17.5 mV (pH 7.5) (Figure 2-3). At the high DOC concentration (1 mg Fe/mg DOC),

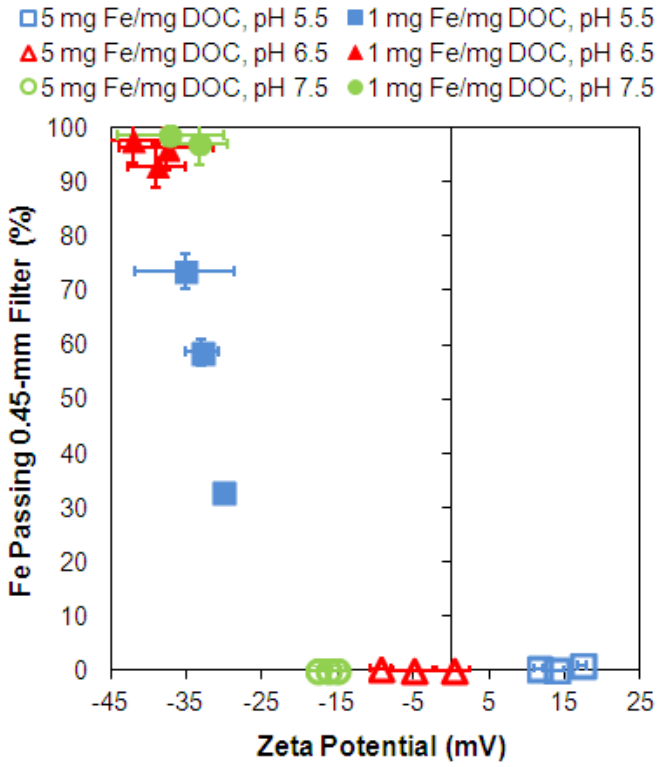

Figure 2-3. The fraction of Fe passing a 0.45-μm filter is correlated with zeta potential and Fe/DOC ratio.

however, products of the Fe-FA interaction exhibit highly negative surface charge, as evidenced by zeta potentials ranging from -30.1 to -42.0 mV. At pH 5.5, the decreasing zeta potential is inversely correlated with the mass of Fe passing through the 0.45-µm filter, which increases from 33% at 0.5 h to 74% at 24 h. At pH 6.5 and 7.5, mobilization of Fe through the filter is always greater than 90%. The highly negative surface charge indicates that FA is sorbed to Fe passing through the filter, and the detectable signal for zeta potential measurements suggests that at least a fraction of the material is present in colloidal form, rather than as dissolved Fe-FA complexes.

Hydrolysis ratios

Calculation of NaOH addition and the resulting OH^-/Fe ratios during hydrolysis provided additional information about the nature of the Fe-FA species (Figure 2-4). At the low DOC concentration (5 mg Fe/mg DOC), the OH^-/Fe ratios are within 3.5% of the theoretical values of an Fe-only system, suggesting that ferric iron in these systems is fully hydrolyzed. In contrast, hydrolysis ratios at the high DOC concentration (1 mg Fe/mg DOC) are 19% (pH 5.5) and 10% (pH 6.5 and 7.5) below the theoretical Fe-only ratios. The corresponding stoichiometries are $Fe(OH)_{2.2}^{0.8+}$, $Fe(OH)_{2.6}^{0.4+}$, and $Fe(OH)_{2.7}^{0.3+}$ at pH 5.5, 6.5, and 7.5, respectively. Taken together with the Fe mobilization results (Figure 2-3), these data suggest that an FA concentration that is high relative to the available Fe dose significantly hinders Fe hydrolysis and polymerization. This finding is corroborated by previous studies in which NOM, SiO_2, or PO_4^{3-} interfered with hydrolysis and growth of aluminum or ferric hydroxides.[29-31, 53]

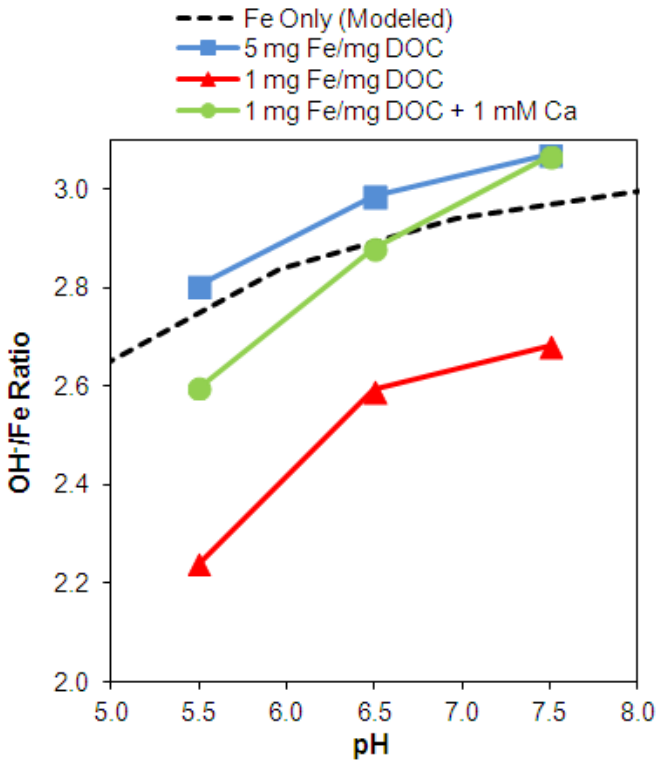

Figure 2-4. Influence of pH, Fe/DOC ratio, and the presence of Ca^{2+} on observed OH^-/Fe ratios. For comparison, the theoretical OH^-/Fe ratio for an Fe-only system is also included.

Influence of Ca^{2+}

In every experiment, the presence of 1 mM Ca^{2+} increased zeta potential (Figure 2-5). At the low DOC concentration (5 mg Fe/mg DOC), zeta potential increased by 4-8 mV at pH 5.5; 4-14 mV at pH 6.5; and 15-22 mV at pH 7.5. Charge reversal was noted at pH 6.5; at pH 7.5, Ca^{2+} shifted zeta potential from an average of -16.3 mV to the circumneutral range (+5.6 to -2.6 mV). Even in systems with a high Fe/DOC ratio, the presence of 1 mM Ca^{2+} exerts a significant influence on zeta potential, and by extension, particle stability. From the perspective of coagulation, these data suggest that a relatively moderate Ca^{2+} concentration can effectively shift the optimal coagulation pH by up to 2 pH units in a system that is not dose-limited.

In experiments at 1 mg Fe/mg DOC, zeta potentials increased by 30%-43% in samples with 1 mM Ca^{2+} (Figure 2-5). The maximum zeta potential attained in a sample with Ca^{2+} was -18.9 mV and was measured at pH 5.5. Although this measurement is more negative than the optimal zeta potential range typically observed in coagulation,[48, 54, 55] the zeta potential increase afforded by Ca^{2+} profoundly affected Fe mobilization (Figure 2-6). At pH 6.5 and 7.5, the Fe passing the 0.45-µm filter exhibited a remarkable decline, from over 90% to less than 5%. This outcome is consistent with previous findings that Ca^{2+} increases the diameter of spherical ferric particles and increases aggregation via the reduction of negative charge.[53] It is possible that a Ca^{2+} concentration greater than 1 mM—but within the range of natural waters—would increase zeta potential to the circumneutral range in which settleable flocs are formed at the tested Fe/DOC ratio. Similarly, an increase in the Fe/DOC ratio at 1 mM Ca^{2+} would be expected to produce settleable flocs.

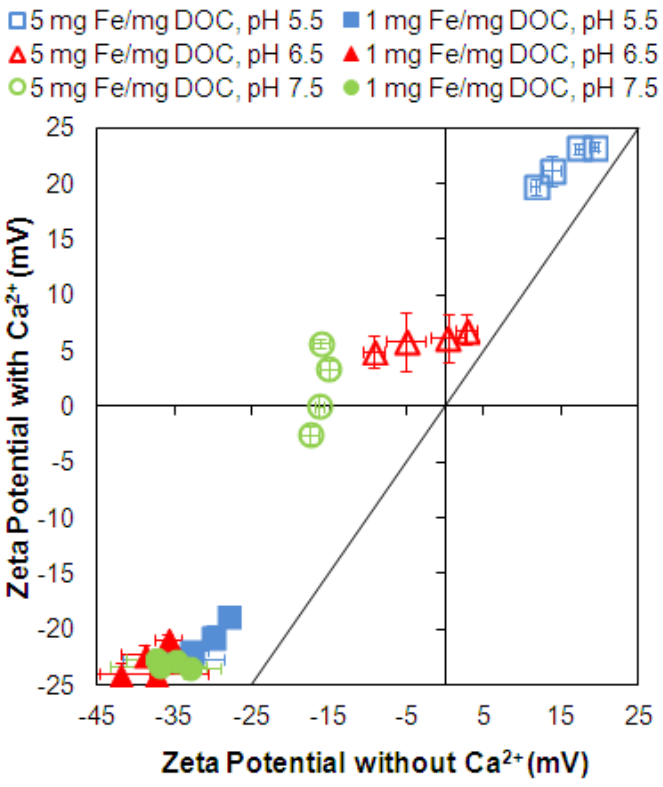

Figure 2-5. Ca^{2+} (1 mM) increases zeta potential at each pH and Fe/DOC ratio.

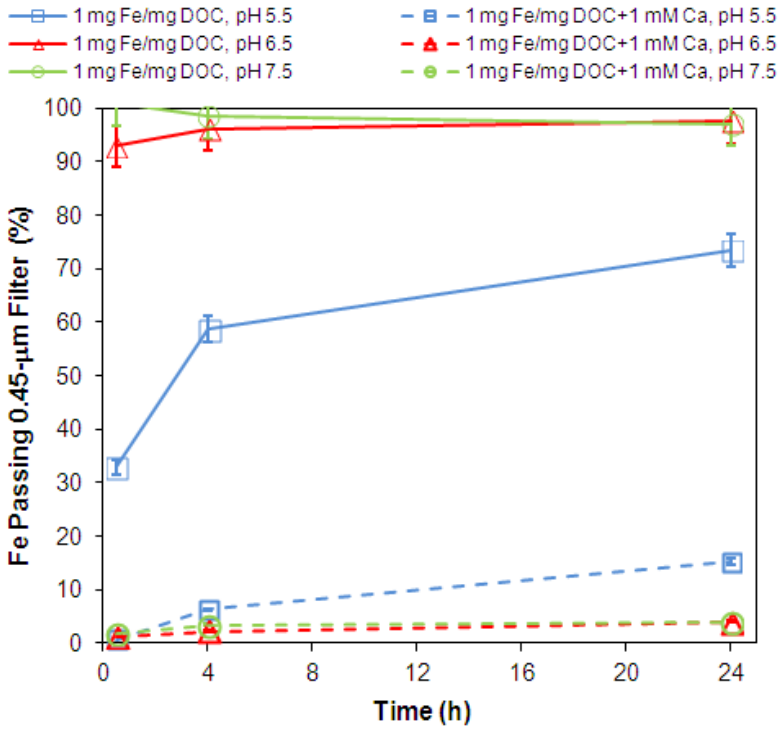

Figure 2-6. The presence of 1 mM Ca^{2+} reduces the fraction of Fe passing a 0.45-µm filter.

The increases in zeta potential in the samples with 1 mM Ca^{2+} led to greater DOC sorption in some cases (Figure 2-7). At 5 mg Fe/mg DOC and pH 7.5, the DOC sorption density (mol C/mol Fe) increased by 63% at 0.5 h and 70% at 4 h. In the experiments without Ca^{2+}, Fe was well hydrolyzed and adequate surface was available for sorption. Thus, it appears that Ca^{2+} improved sorption at pH 7.5 and low DOC primarily by increasing zeta potential and minimizing electrostatic repulsion between FA and the ferric hydroxide surface.

In the 1 mg Fe/mg DOC experiments without Ca^{2-}, DOC removals of 28% (0.5 h) and 10% (4 h) were observed at pH 5.5. Because the concentration of DOC was high relative to Fe concentration, these removals corresponded to rather high DOC sorption densities of 1.76 mol C/mol Fe (0.5 h) and 0.95 mol C/mol Fe (4 h). As previously stated, no DOC sorption was observed at pH 6.5 and 7.5 because more than 90% of Fe passed through the 0.45-µm filter. The inclusion of 1 mM Ca^{2+} and the accompanying increase in Fe particle size yielded drastic increases in observed DOC sorption density at all three pH levels. Averaged across the 24-h experiments, DOC sorption densities in the Fe-FA-Ca systems were 2.55 $\pm$ 0.28 mol C/mol Fe, 2.37 $\pm$ 0.13 mol C/mol Fe, and 2.18 $\pm$ 0.10 mol C/mol Fe at pH 5.5, 6.5, and 7.5, respectively. It is noted that these sorption densities are remarkably high, an outcome that can primarily be attributed to the fact that the Fe was coprecipitated in-situ with FA and Ca^{2+}.

Reduced Fe mobilization and increased DOC sorption in the high-FA samples can be related to changes in the Fe hydrolysis ratio in the presence of Ca^{2+} (Figure 2-4). In samples without Ca^{2+}, FA inhibited Fe hydrolysis and OH^{-}/Fe ratios were 10%-19% below theoretical

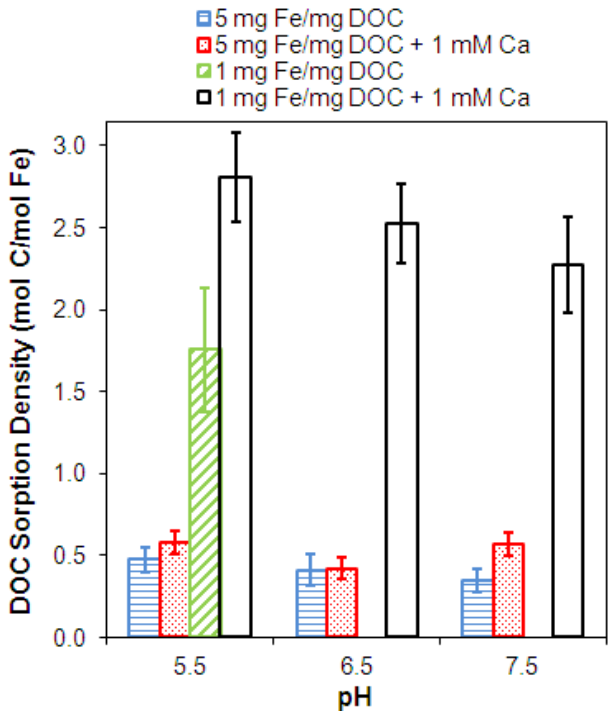

Figure 2-7. DOC sorption densities as a function of pH and Fe/DOC ratio. The presence of 1 mM Ca^{2+} dramatically improves DOC sorption densities in samples with low Fe/DOC ratio.

values. However, the presence of 1 mM Ca^{2+} in the experiments at 1 mg Fe/mg DOC mitigated the interference and increased OH^-/Fe ratios to within 5.5% of theoretical value at pH 5.5 and to within 3% of the theoretical values at pH 6.5 and 7.5. These results are consistent with the hypothesis that more extensive hydrolysis produces larger, more filterable particles.

Mechanistic Interpretation

When Fe^{3+} is dosed to waters in the pH range of 5.5 to 7.5, rapid hydrolysis is initiated, producing species such as $Fe(OH)_2^{+}{}_{(aq)}$ and $Fe(OH)_4^{-}{}_{(aq)}$. Parallel and competing reactions between the hydrolysis species (Figure 2-1) and NOM include: (A) complexation by NOM, (B) charge neutralization/precipitation of insoluble Fe-NOM products, (C) precipitation of ferric hydroxide and charge neutralization of NOM colloids,[56] and (D) precipitation of ferric hydroxide and adsorption of NOM. The size and characteristics of the precipitates that are formed in Pathways B, C, and D depend upon the extent of hydrolysis, condensation, and polymerization. The supply of OH^- at pH 7.5 likely favors pathways (C) and (D), whereas pathways (A) and (B) may wield greater influence at pH 5.5.

At 5 mg Fe/mg DOC, there is sufficient or excess Fe available to meet the coagulant demand exerted by FA. Some fraction of the FA charge is likely neutralized by Fe complexation (Pathway A), yet OH^-/Fe ratios suggest that this fraction is very small. Upon hydrolysis and precipitation, FA ligands or Fe-FA complexes sorb to the ferric hydroxide surface (Pathway D). Alternatively, if large humic colloids are present, removal may occur according to the Precipitation-Charge Neutralization (PCN) model (Pathway C).[56] In this research, however, zeta potential remains positive at pH 5.5, even though UV_{254} absorbance removal exceeded 90% at this

pH. This observation suggests that Pathway D dominates over C and that sorption of FA is not sufficient to reverse surface charge at this Fe/DOC ratio.

At 1 mg Fe/mg DOC, Fe is limited and competition between reaction pathways is more important. The capability of FA to complex Fe species (Pathway A) was assessed with SHM model simulations with 10 mg/L DOC and 10 mg/L as Fe. The lower bound on Fe-FA complexation was estimated by allowing ferrihydrite to precipitate (Scenario 1), while the upper bound on Fe-FA complexation was approximated by excluding precipitation (Scenario 2) (Figure 2-8). In Scenario 1, model output suggests that Fe complexation neutralizes less than 5% of the initial FA charge, which varies from -8.2 meq/g C (pH 5.5) to -10.9 meq/g C (pH 7.5) using default parameter values. Yet, FA is predicted to bind up to 3% of the dosed Fe concentration, yielding soluble Fe concentrations that are 500 to 3000 times higher than soluble concentrations in comparable Fe-only systems. By contrast, Scenario 2 prevents ferrihydrite precipitation, resulting in complexed Fe concentrations of 23%-26% of the total Fe. This scenario suggests that Fe binding neutralizes 48%-53% of the initial FA charge. Interestingly, the SHM predicts that the dominant FA-Fe complex is $FA_2Fe(OH)$, and a high concentration of this species may explain the reduced hydrolysis ratios observed, particularly at pH 5.5.

Vilge-Ritter et al.[30] coagulated two natural waters with $FeCl_3$ and analyzed the resulting Fe-NOM aggregates. These researchers identified the predominant Fe species as trimers with radii of 0.400 to 0.425 nm. They proposed that Fe oligomers are complexed by NOM, and that Fe – O – C bonds inhibit further hydrolysis and polymerization. In our experiments at pH 6.5 and 7.5,

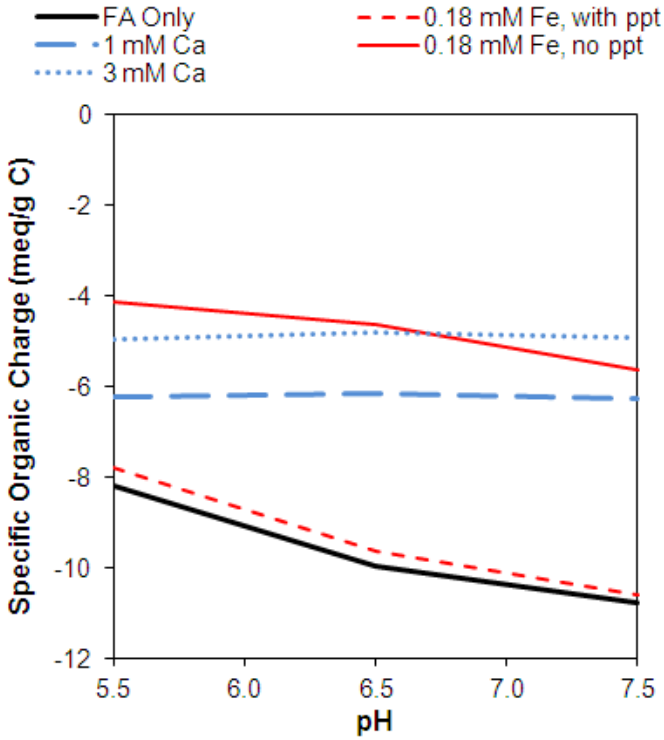

Figure 2-8. The Stockholm Humic Model (SHM) simulates the effects of Ca^{2+} complexation (1 or 3 mM) and Fe complexation (10 mg/L with and without ferric hydroxide precipitation) on the specific organic charge of fulvic acid (FA).

greater than 90% of the Fe passed through the filter. These results are not inconsistent with a complexation (Pathway A) mechanism and may suggest that more Fe is sequestered than predicted by the SHM. On the other hand, we observed only 33%-73% Fe mobilization at pH 5.5, indicating that a significant fraction of Fe was filterable at this pH. These results are more consistent with the notion that some of the Fe precipitated as a colloidal phase, which is then stabilized by sorbed NOM (Pathways B, C, and/or D). While we cannot definitively identify the dominant reaction pathways, the OH^-/Fe ratios, Fe mobilization, and zeta potential measurements are consistent with the idea that a fraction of the Fe is complexed by NOM, leading to a reduced hydrolysis ratio. Free Fe species then interact with unbound ligands of FA, precipitating as a stable, colloidal phase. At pH 5.5, the complexed fraction is likely less than 33%, the concentration of mobilized Fe at 0.5 h.

In experiments with 1 mM Ca^{2+} and 1 mg Fe/mg DOC, there were substantial increases in surface potential and accompanying decreases in Fe mobilization. In these samples, Ca^{2+} and FA were pre-equilibrated before Fe^{3+} was dosed, giving Ca^{2+} complexation a competitive advantage over Fe^{3+} complexation. SHM modeling (Figure 2-9) and experimental data[24] at 1 mM Ca^{2+} and 0.01 M ionic strength independently suggest that 3-5 meq Ca/g C may be complexed by FA in the pH range of 5.5-7.5. As the total Ca^{2+} concentration and pH increase, the extent of complexation and charge neutralization increases. As a result, the influence of pH on organic charge is diminished or eliminated by Ca^{2+} complexation (Figure 2-8 and Figure 2-10). Comparing predictions for pH 5.5 and 7.5, organic charge is predicted to be 24% higher in the absence of Ca^{2+} at pH 5.5. At a total Ca^{2+} concentration of 1 mM, however, the predicted difference in organic charge at pH 5.5 and 7.5 is merely 0.5% (Figure 2-10).

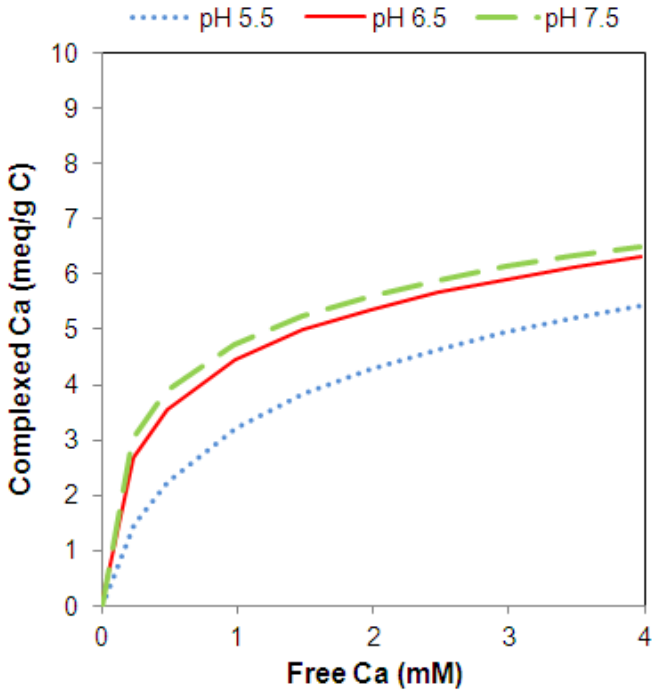

Figure 2-9. Stockholm Humic Model (SHM) simulations indicate that Ca^{2+} complexation increases with pH and Ca^{2+} concentration. Simulations were conducted at I=0.01 M.

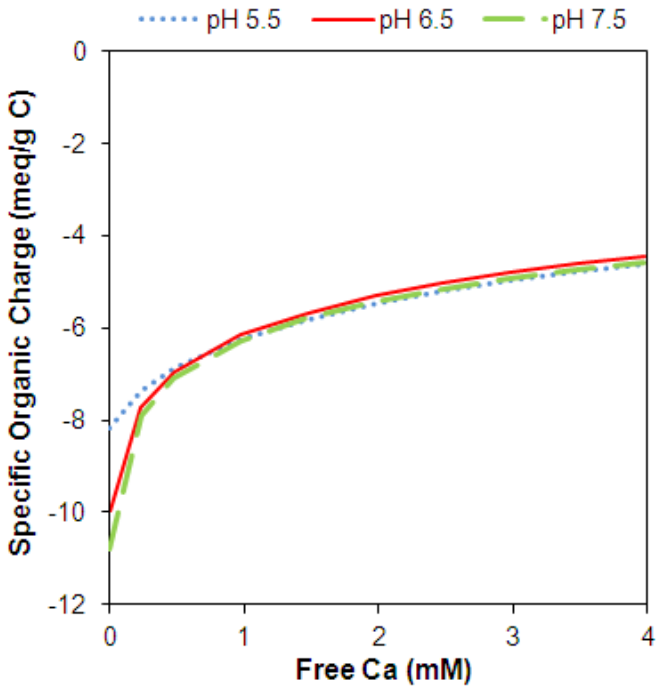

Figure 2-10. Stockholm Humic Model (SHM) simulations suggest that organic charge neutralization increases with increasing Ca^{2+} concentration.

OH^-/Fe ratios calculations indicate that 1 mM Ca^{2+} improved Fe hydrolysis at 1 mg Fe/mg DOC (Figure 2-4). Ratios rose to within 3% of the theoretical values at pH 6.5 and 7.5, suggesting that most Fe was well hydrolyzed in samples with Ca^{2+}. In samples without Ca^{2+}, the most significant interference with Fe hydrolysis occurred at pH 5.5, presumably due to the lower concentration of OH^- to compete with FA ligands. The presence of 1 mM Ca^{2+} at pH 5.5 increased the hydrolysis ratio from 2.2 to 2.6, or to within 5.5% of the theoretical value.

It is postulated that Ca^{2+} complexation and charge neutralization promote Fe hydrolysis in waters with a low Fe/DOC ratio. Since Ca^{2+} satisfies some of the coagulant demand exerted by the FA ligands, more Fe is free to hydrolyze, polymerize, and form filterable flocs. FA-Ca^{2+} complexation may also produce smaller humic conformations, thereby limiting the ability of Fe^{3+} to access binding sites. There is spectroscopic evidence that some previously-complexed Ca^{2+} may be exchanged for Fe^{3+} when the coagulant is dosed.[31, 57] It is expected that such reactions occurred in our samples, particularly at pH 5.5 where a slight interference with hydrolysis is still evident. However, it appears that Ca^{2+} complexation by FA provides a crucial electrostatic and kinetic advantage for Fe hydrolysis.

Acknowledgments

We thank Jeffrey Parks for conducting ICP and TOC analyses. The efforts of Hsiao-wen Chen, who isolated the FA, and Samantha Fisher, who assisted with laboratory experiments, are also acknowledged. While this research was conducted, the first author was supported by graduate fellowships from the National Water Research Institute, and the American Water Works Association (AWWA). Certain equipment and supplies were purchased with STAR fellowship

funds from the US EPA. The findings are those of the authors and may not reflect the views of these organizations.

References

1. Tipping, E., The Adsorption of Aquatic Humic Substances by Iron Oxides. *Geochim. Cosmochim. Acta* **1981,** *45*, (2), 191-199.
2. Davis, J. A., Adsorption of Natural Dissolved Organic-Matter at the Oxide Water Interface. *Geochim. Cosmochim. Acta* **1982,** *46*, (11), 2381-2393.
3. Davis, C. C.; Knocke, W. R.; Edwards, M., Implications of aqueous silica sorption to iron hydroxide: Mobilization of iron colloids and interference with sorption of arsenate and humic substances. *Environ. Sci. Technol.* **2001,** *35*, (15), 3158-3162.
4. Redman, A. D.; Macalady, D. L.; Ahmann, D., Natural organic matter affects arsenic speciation and sorption onto hematite. *Environ. Sci. Technol.* **2002,** *36*, (13), 2889-2896.
5. Knocke, W. R.; Shorney, H. L.; Bellamy, J. D., Examining the Reactions Between Soluble Iron, DOC, and Alternative Oxidants During Conventional Treatment. *J. Am. Water Work Assoc.* **1994,** *86*, (1), 117-127.
6. Kretzschmar, R.; Sticher, H.; Hesterberg, D., Effects of Adsorbed Humic Acid on Surface Charge and Flocculation of Kaolinite. *Soil Sci. Soc. Am. J.* **1997,** *61*, (1), 101-108.
7. Rose, J.; Vilge, A.; Olivie-Lauquet, G.; Masion, A.; Frechou, C.; Bottero, J. Y., Iron speciation in natural organic matter colloids. *Colloid Surf. A-Physicochem. Eng. Asp.* **1998,** *136*, (1-2), 11-19.
8. Choi, S. Y.; Chen, J.; Gu, B. H., Reductive dissolution of iron oxyhydroxides by different fractions of natural organic matter. *Abstr. Pap. Am. Chem. Soc.* **2000,** *220*, U365-U366.
9. Hardin, W. M. Colloid Formation Resulting from Alum Coagulation of Organic-Laden Sourcewaters. Virginia Tech, Blacksburg, VA, 2003.
10. Masters, E. N. Colloid Formation for the Removal of Natural Organic Matter During Iron Sulfate Coagulation. Virginia Polytechnic Institute and State University, Blacksburg, VA, 2003.
11. Wolthoorn, A.; Temminghoff, E. J. M.; Weng, L. P.; van Riemsdijk, W. H., Colloid formation in groundwater: effect of phosphate, manganese, silicate and dissolved organic matter on the dynamic heterogeneous oxidation of ferrous iron. *Appl. Geochem.* **2004,** *19*, (4), 611-622.
12. Malcolm, R. L., Geochemistry of Stream Fulvic and Humic Substances. In *Humic Substances in Soild, Sediment, and Water: Geochemistry, Isolation, and Characterization*, Aiken, G. R.; McKnight, D. M.; Wershaw, R. L.; MacCarthy, P., Eds. John Wiley & Sons: New York, 1985; pp 181-209.
13. Tipping, E.; Backes, C. A.; Hurley, M. A., The complexation of protons, aluminium and calcium by aquatic humic substances: A model incorporating binding-site heterogeneity and macroionic effects. *Water Res.* **1988,** *22*, (5), 597-611.
14. Tipping, E.; Hurley, M. A., A unifying model of cation binding by humic substances. *Geochim. Cosmochim. Acta* **1992,** *56*, (10), 3627-3641.
15. Benedetti, M. F.; Van Riemsdijk, W. H.; Koopal, L. K.; Kinniburgh, D. G.; Gooddy, D. C.; Milne, C. J., Metal ion binding by natural organic matter: From the model to the field. *Geochim. Cosmochim. Acta* **1996,** *60*, (14), 2503-2513.
16. Tipping, E., Humic ion-binding model VI: An improved description of the interactions of protons and metal ions with humic substances. *Aquat. Geochem.* **1998,** *4*, (1), 3-48.
17. Kinniburgh, D. G.; van Riemsdijk, W. H.; Koopal, L. K.; Borkovec, M.; Benedetti, M. F.; Avena, M. J., Ion binding to natural organic matter: competition, heterogeneity, stoichiometry and

thermodynamic consistency. *Colloids and Surfaces A: Physicochemical and Engineering Aspects* **1999,** *151*, (1-2), 147-166.
18. Gustafsson, J. P., Modeling the acid-base properties and metal complexation of humic substances with the Stockholm Humic Model. *J. Colloid Interface Sci.* **2001,** *244*, (1), 102-112.
19. Zhou, P.; Yan, H.; Gu, B. H., Competitive complexation of metal ions with humic substances. *Chemosphere* **2005,** *58*, (10), 1327-1337.
20. Tipping, E.; Lofts, S.; Sonke, J. E., Humic Ion-Binding Model VII: a revised parameterisation of cation-binding by humic substances. *Environmental Chemistry* **2011,** *8*, (3), 225-235.
21. Dempsey, B. A.; O'Melia, C. R., Proton and Calcium Complexation of Four Fulvic Acid Fractions. In *Aquatic and Terrestrial Humic Materials*, Christman, R. F.; Gjessing, E. T., Eds. Ann Arbor Science: Ann Arbor, MI, 1983.
22. Collins, M. R.; Amy, G. L.; Steelink, C., Molecular Weight Distribution, Carboxylic Acidity, and Humic Substances Content of Aquatic Organic Matter - Implications for Removal During Water-Treatment. *Environ. Sci. Technol.* **1986,** *20*, (10), 1028-1032.
23. Edwards, M.; Benjamin, M. M.; Ryan, J. N., Role of organic acidity in sorption of natural organic matter (NOM) to oxide surfaces. *Colloid Surf. A-Physicochem. Eng. Asp.* **1996,** *107*, 297-307.
24. Bose, P.; Reckhow, D. A., Modeling pH and ionic strength effects on proton and calcium complexation of fulvic acid: A tool for drinking water-NOM studies. *Environ. Sci. Technol.* **1997,** *31*, (3), 765-770.
25. Davis, C. C.; Edwards, M., Coagulation With Hydrolyzing Metal Salts: Mechanisms and Water Quality Impacts. *Critical Reviews in Environmental Science and Technology* **2014,** *44*, (4), 303-347.
26. Saar, R. A.; Weber, J. H., Fulvic-Acid - Modifier of Metal-Ion Chemistry. *Environ. Sci. Technol.* **1982,** *16*, (9), A510-A517.
27. Van Benschoten, J. E.; Edzwald, J. K., Chemical Aspects of Coagulation Using Aluminum Salts .2. Coagulation of Fulvic-Acid Using Alum and Polyaluminum Chloride. *Water Res.* **1990,** *24*, (12), 1527-1535.
28. Edzwald, J. K., Coagulation in Drinking Water Treatment: Particles, Organics and Coagulants. *Water Sci. Technol.* **1993,** *27*, (11), 21-35.
29. Davis, C. C.; Edwards, M., Coagulation with Hydrolyzing Metal Salts: Mechanisms and Water Quality Impacts. *Crit. Rev. Environ. Sci. Technol.* **In press**.
30. Vilge-Ritter, A.; Rose, J.; Masion, A.; Bottero, J. Y.; Laine, J. M., Chemistry and structure of aggregates formed with Fe-salts and natural organic matter. *Colloid Surf. A-Physicochem. Eng. Asp.* **1999,** *147*, (3), 297-308.
31. Jung, A. V.; Chanudet, V.; Ghanbaja, J.; Lartiges, B. S.; Bersillon, J. L., Coagulation of humic substances and dissolved organic matter with a ferric salt: An electron energy loss spectroscopy investigation. *Water Res.* **2005,** *39*, (16), 3849-3862.
32. Sieliechi, J. M.; Lartiges, B. S.; Kayem, G. J.; Hupont, S.; Frochot, C.; Thieme, J.; Ghanbaja, J.; de la Caillerie, J. B. D.; Barres, O.; Kamga, R.; Levitz, P.; Michot, L. J., Changes in humic acid conformation during coagulation with ferric chloride: Implications for drinking water treatment. *Water Res.* **2008,** *42*, (8-9), 2111-2123.
33. Dempsey, B. A., Reactions between Fulvic-Acid and Aluminum - Effects on the Coagulation Process. *Acs Symposium Series* **1989,** *219*, 409-424.

34. Frey, M. M.; Edwards, M. A., Surveying Arsenic Occurrence. *J. Am. Water Work Assoc.* **1997,** *89*, (3), 105-117.
35. Iglesias, A.; Lopez, R.; Fiol, S.; Antelo, J. M.; Arce, F., Analysis of copper and calcium-fulvic acid complexation and competition effects. *Water Res.* **2003,** *37*, (15), 3749-3755.
36. Baalousha, M.; Motelica-Heino, M.; Le Coustumer, P., Conformation and size of humic substances: Effects of major cation concentration and type, pH, salinity, and residence time. *Colloid Surf. A-Physicochem. Eng. Asp.* **2006,** *272*, (1-2), 48-55.
37. Chen, K. L.; Mylon, S. E.; Elimelech, M., Aggregation kinetics of alginate-coated hematite nanoparticles in monovalent and divalent electrolytes. *Environ. Sci. Technol.* **2006,** *40*, (5), 1516-1523.
38. Chen, K. L.; Mylon, S. E.; Elimelech, M., Enhanced aggregation of alginate-coated iron oxide (hematite) nanoparticles in the presence of calcium, strontium, and barium cations. *Langmuir* **2007,** *23*, (11), 5920-5928.
39. Hundt, T. R.; O'Melia, C. R., Aluminum Fulvic Acid Interactions - Mechanisms and Applications. *J. Am. Water Work Assoc.* **1988,** *80*, (4), 176-186.
40. Duan, J. M.; Cao, X. T.; Chen, C.; Shi, D. R.; Li, G. M.; Mulcahy, D., Effects of Ca(OH)(2) assisted aluminum sulfate coagulation on the removal of humic acid and the formation potentials of tri-halomethanes and haloacetic acids in chlorination. *Journal of Environmental Sciences-China* **2012,** *24*, (9), 1609-1615.
41. Weng, L. P.; Koopal, L. K.; Hiemstra, T.; Meeussen, J. C. L.; Van Riemsdijk, W. H., Interactions of calcium and fulvic acid at the goethite-water interface. *Geochim. Cosmochim. Acta* **2005,** *69*, (2), 325-339.
42. Duan, J. M.; Gregory, J., Influence of soluble silica on coagulation by aluminium sulphate. *Colloid Surf. A-Physicochem. Eng. Asp.* **1996,** *107*, 309-319.
43. Liu, R. P.; Li, X.; Xia, S. J.; Yang, Y. L.; Wu, R. C.; Li, G. B., Calcium-enhanced ferric hydroxide co-precipitation of arsenic in the presence of silicate. *Water Environ. Res.* **2007,** *79*, (11), 2260-2264.
44. Meng, X. G.; Bang, S.; Korfiatis, G. P., Effects of silicate, sulfate, and carbonate on arsenic removal by ferric chloride. *Water Res.* **2000,** *34*, (4), 1255-1261.
45. Smith, S. D.; Edwards, M., The influence of silica and calcium on arsenate sorption to oxide surfaces. *J. Water Supply Res Technol.-Aqua* **2005,** *54*, (4), 201-211.
46. Ali, M. A.; Dzombak, D. A., Effects of simple organic acids on sorption of Cu2+ and Ca2+ on goethite. *Geochim. Cosmochim. Acta* **1996,** *60*, (2), 291-304.
47. Edwards, M.; Benjamin, M. M., A Mechanistic Study of Ozone-Induced Particle Destabilization. *J. Am. Water Work Assoc.* **1991,** *83*, (6), 96-105.
48. Edwards, M.; Benjamin, M. M., Effect of Preozonation on Coagulant-NOM Interactions. *J. Am. Water Work Assoc.* **1992,** *84*, (8), 63-72.
49. Aiken, G. R., Isolation and Concentration Techniques for Aquatic Humic Substances. In *Humic Subtances in Soil, Sediment, and Water: Geochemistry, Isolation, and Characterization*, Aiken, G. R.; McKnight, D. M.; Wershaw, R. L.; MacCarthy, P., Eds. John Wiley & Sons: New York, 1985; pp 363-385.
50. Eaton, A. D.; Clesceri, L. S.; Rice, E. W.; Greenberg, A. E., *Standard Methods of the Examination of Water and Wastewater*. 21st ed.; American Public Health Association: Washington, D.C., 2005.
51. Gustafsson, J. P. *Visual MINTEQ* 3.0; 2011.

52. Sjostedt, C. S.; Gustafsson, J. P.; Kohler, S. J., Chemical Equilibrium Modeling of Organic Acids, pH, Aluminum, and Iron in Swedish Surface Waters. *Environ. Sci. Technol.* **2010,** *44*, (22), 8587-8593.
53. Kaegi, R.; Voegelin, A.; Folini, D.; Hug, S. J., Effect of phosphate, silicate, and Ca on the morphology, structure and elemental composition of Fe(III)-precipitates formed in aerated Fe(II) and As(III) containing water. *Geochim. Cosmochim. Acta* **2010,** *74*, (20), 5798-5816.
54. Tseng, T.; Segal, B. D.; Edwards, M., Increasing Alkalinity to Reduce Turbidity. *J. Am. Water Work Assoc.* **2000,** *92*, (6), 44-54.
55. Sharp, E. L.; Jarvis, P.; Parsons, S. A.; Jefferson, B., The impact of zeta potential on the physical properties of ferric-NOM flocs. *Environ. Sci. Technol.* **2006,** *40*, (12), 3934-3940.
56. Dentel, S. K., Application of the Precipitation Charge Neutralization Model of Coagulation. *Environ. Sci. Technol.* **1988,** *22*, (7), 825-832.
57. El Samrani, A. G.; Lartiges, B. S.; Montarges-Pelletier, E.; Kazpard, V.; Barres, O.; Ghanbaja, J., Clarification of municipal sewage with ferric chloride: the nature of coagulant species. *Water Res.* **2004,** *38*, (3), 756-768.

Chapter 3. Influence of Silica on Coagulation and Implications for NOM Removal

Christina C. Davis and Marc Edwards

Virginia Tech Department of Civil and Environmental Engineering,
407 Durham Hall, Blacksburg, VA 24060

Keywords: natural organic matter, silica, ferric chloride, coagulation, zeta potential

Abstract

Water quality affects several critical aspects of the coagulation process including particle size distribution, surface charge, floc aggregation, and the extent of contaminant removal. Experiments were conducted to investigate the influence of aqueous silica and pH on the removal of natural organic matter (NOM) by coagulation with ferric chloride. Samples with preformed ferric hydroxide were also compared to samples coagulated in situ to assess the role of coprecipitation. The moderate (10 mg/L) and high (50 mg/L) SiO_2 concentrations both demonstrated interference with NOM removal at pH 6.5-7.5. In turn, NOM at 2 mg/L as DOC interfered with silica sorption at the moderate silica level and in samples with preformed ferric hydroxide at the high silica level. The combination of NOM and high silica led to decreases in DOC sorption and unexpected increases in silica sorption in the coprecipitated samples. The fraction of colloidal Fe passing a 0.45-μm filter also increased in the coprecipitated samples with both NOM and high silica. It is hypothesized that the combination of NOM and high silica synergistically interfered with Fe precipitation and particle growth processes, with NOM having the greater effect at lower pH and shorter reaction times, and silica exerting greater influence at higher pH and longer reaction time. Direct competition for surface sites and electrostatic repulsion were also influential.

Introduction

Interactions between natural organic matter (NOM) and iron hydroxide surfaces are fundamentally important in natural environments, water treatment, and water distribution. Following the discovery and increased regulation of disinfection byproducts in the latter part of the 20th century, extensive research focused on NOM removal by coagulation with alum and ferric salts, and more recently, with alternative coagulants such as polyaluminum chloride (PACl) and polyferric chloride (PFC) (Hussain et al. 2013, Wang et al. 2011, Yan et al. 2008, Zhan et al. 2010). Numerous studies have explored the relationship between NOM character and its amenability to treatment by coagulation. For instance, higher apparent molecular weight, hydrophobicity, and acidity are commonly associated with better removal (Davis and Edwards 2014a). Yet some source waters are difficult to coagulate, yielding poor NOM removal; this behavior is often ascribed to an NOM character that is simply not amenable to coagulation. High pH and alkalinity are also known to hinder coagulation, since sorption of NOM is favored at lower pHs. Recognition of the significant role alkalinity plays in enhanced coagulation led to its inclusion as a parameter affecting the required percentage of total organic carbon (TOC) removal in the US Environmental Protection Agency's (EPA's) Stage 1 Disinfectants/Disinfection Byproducts Rule.

Relatively little research has been devoted to exploring the role that water quality, other than alkalinity, plays in NOM removal during coagulation. In marked contrast, significant effort has been directed toward investigating the effect of water quality on arsenic sorption and coprecipitation with aluminum and iron (hydr)oxides. These studies have established the negative effects of silica (Davis et al. 2001, Holm 2002, Laky and Licsko 2011, Meng et al. 2000, Roberts et al. 2004, Smith and Edwards 2005, Swedlund and Webster 1999), bicarbonate/carbonate (Holm 2002, Laky and Licsko 2011, Stachowicz et al. 2007), phosphate (Holm 2002, Laky and Licsko 2011, Roberts et al. 2004), and NOM (Hering et al. 1997, Pallier et al. 2010, Redman et al. 2002) on arsenic removal. Detecting water quality interferences to arsenic removal is straightforward because the inorganic sorbates, As(III) and As(V), are unchanging, whereas NOM character and amenability to coagulation are known to vary spatially and temporally. NOM variability is widely believed to be responsible for any observed differences in TOC removal (Davis and Edwards 2014a).

For example, in one of the few studies examining the effects of water chemistry on removal of the same NOM sample, Randtke and Jepsen (1981) extracted fulvic acid (FA) from an Illinois groundwater and dissolved the FA in a "synthetic tap water" with $NaHCO_3$, $CaCl_2$, $MgSO_4$, NaCl, and KCl. When this water was coagulated with increasing doses of alum, the authors noted a sudden and rapid decrease in the remaining TOC at a threshold alum dose. This relationship between TOC removal and coagulant dose, which was termed Type 1 behavior, was attributed to the presence of a relatively homogeneous NOM source in the water. When the authors performed the same experiment on the original groundwater from which the FA was extracted, they observed a decrease in the concentration of remaining TOC at the lower range of applied alum dosages. The researchers termed this removal "Type 2," and attributed it the heterogeneous nature of NOM. The possibility that the groundwater matrix, which was characterized by moderately high silica (19.6 mg/L as SiO_2) and very high alkalinity (324 mg/L as $CaCO_3$), could be the major cause of the observed differences in TOC removal was not explored in this or other studies.

NOM and inorganic ligands also influence alum and ferric coagulant precipitation and the properties of the resulting particles. Previous studies have concluded that NOM can limit the Fe hydrolysis ratio (Davis and Edwards 2014b) and inhibit the growth of Fe hydrolysis species beyond the trimer stage (Jung et al. 2005, Vilge-Ritter et al. 1999). The presence of phosphate, arsenate, and silica have been implicated in disrupting ferrihydrite polymerization and growth (Doelsch et al. 2003, Doelsch et al. 2001, Masion et al. 1997, Rose et al. 1996, Waychunas et al. 1993). The practical outcomes of ligand-coagulant coprecipitation include extraordinarily high ligand sorption densities and changes in sorbent characteristics, such as particle size distribution, surface area, and surface charge; these effects are reviewed elsewhere (Davis and Edwards 2014a).

Water quality exerts profound influence on arsenic sorption and coprecipitation, and it is expected that anionic NOM would be subject to similar effects. Thus, the role of water chemistry in key aspects of NOM removal was examined in this research. In general, effective coagulation of NOM may be characterized by: (1) attainment of targeted removal, (2) low levels of colloidal iron or aluminum residuals, and (3) circumneutral surface potential for effective particle destabilization and aggregation. The impact of silica on each of these factors was explored. In order to study the effects on both sorption and sorbent characteristics, experiments were conducted with coprecipitated (CPT) and (PF) ferric hydroxide.

Materials and Methods

Experiments were designed to gauge the effects of three silica concentrations (0, 10, and 50 mg/L as SiO_2) and three pH levels (pH 5.5, 6.5, and 7.5) on the coagulation of FA. The nominal dissolved organic carbon (DOC) concentration in the samples was 2 mg/L. Single-sorbate experiments with only silica (10 and 50 mg/L as SiO_2) were also conducted. Ferric chloride was used as the coagulant at a target dose of 10 mg/L as Fe.

Chemicals

FA was isolated from Silver Lake, which serves as a source water for Boulder, Colorado. The extraction method is described elsewhere (Davis and Edwards 2014b). Stock solutions of Na_2SiO_3, $NaNO_3$, and $FeCl_3$ were prepared using reagent-grade chemicals. The Na_2SiO_3 (0.13 M) and $NaNO_3$ (4.12 M) solutions were prepared by dissolving the salt in distilled water. $FeCl_3$ (8.59×10^{-3} M) was dissolved in 0.01-M HNO_3 to prevent precipitation in the stock solution. HNO_3 and NaOH solutions of varying concentrations (0.01-0.2 M) were used for pH adjustment.

Coprecipitation Studies

Experiments were conducted in 500-mL HDPE bottles with distilled water. Samples were prepared with FA and/or silica and allowed to equilibrate for approximately 12 hours. An initial aliquot was taken to measure total DOC and UV_{254} Abs. To initiate an experiment, a sample was dosed with ferric chloride, and pH was immediately adjusted to the target. Once pH was stabilized to within 0.05 pH units of the target, 10 mL of solution was withdrawn for zeta potential analysis. At this point, an additional control sample was taken to establish the total concentrations of Si and Fe in the sample; this sample was not filtered, but was digested according to the method of Parks et al (2004).

Thereafter, sampling was conducted at 0.5 h, 4 h, and 24 h. During ferric chloride dosing and sample collection, the samples were stirred with a magnetic bar and stir plate. Between sampling events, the samples were mixed on an end-over-end rotary agitator (Analytical Testing Corp., Warrington, PA). At each sampling event, pH was measured and re-adjusted, if necessary, and zeta potential was analyzed. Approximately 50 mL of sample were filtered through a 0.45-μm nylon filter held within a reusable syringe filter holder; the volume of filtrate was determined by measuring its mass. After filtration, the nylon filter was removed and placed in a 25-mL HDPE bottle with 10 mL of distilled water and digested. Filtrate samples were analyzed for UV_{254} Abs, DOC, Si, and Fe. Digestate samples were analyzed for Si and Fe.

Studies with Preformed Ferric Hydroxide

The PF protocol was identical to that of the CPT experiments with the exception of Fe preparation and dosing. Preformed ferric hydroxide was precipitated using the approach described by Davis et al (2001). The pH of an acidified ferric chloride (500 mg/L as Fe) solution was rapidly raised to 6.0 with 3.69-M NaOH, and the precipitates were aged on an end-over-end rotary agitator for 10-12 hours. For dosing, a pipette was used to transfer 10 mL of the PF ferric hydroxide solution to each sample. During the dosing process, the PF ferric hydroxide solution was mixed with a magnetic bar and stir plate. Because the use of a pipette for dosing introduced the possibility of variable Fe concentrations in the final samples, a control sample was taken and digested. The digestate was analyzed to quantify the total Fe and Si in the solution.

Instrumentation

Zeta potential was measured with a Malvern ZetaSizer 3000HS (Malvern Instruments Inc., Westborough, MA). The performance of the instrument was verified using the manufacturer's electrophoresis standard and by comparative measurements with a Zeta Meter 3.0+ (Zeta Meter Inc., Staunton, VA). Uncertainty was estimated as the standard deviation of ten replicate measurements. Additional details are provided elsewhere (Davis et al. 2001).

DOC was measured with a Sievers Model 800 TOC Analyzer using the persulfate-ultraviolet oxidation according to Standard Method 5310C (Eaton et al. 2005). UV_{254} absorbance was quantified with a Hach DR5000 UV-Vis Spectrophotometer (Hach, Loveland, CO). Measurements were made with a 1-cm quartz cell. The standard deviation of triplicate measurements for both DOC and UV_{254} Abs were used to estimate uncertainties. DOC data provide direct measurement of organic carbon concentrations but are subject to greater uncertainty in quantification. UV_{254} Abs, a surrogate indicator of organic carbon concentration, can be affected by colloidal iron and other interferences, but precision in UV_{254} Abs measurements is higher than that for DOC. Statistical comparisons in this research are made on the basis of UV_{254} Abs data unless otherwise stated.

Fe and Si concentrations were measured using a Thermo Electron X-Series inductively coupled plasma with mass spectrometer (ICP-MS) per Standard Method 3125B (Eaton et al. 2005). Samples and calibration standards were prepared in a matrix of 2% HNO_3 by volume. Uncertainty was assumed at 3%.

Results and Discussion

Coagulation of FA

Experiments with FA measured baseline removal as a function of pH and determined the effect of FA on iron coagulation. In CPT experiments at 4 h, DOC removal was 59% or greater pH 5.5 and 6.5, but declined to 38% at pH 7.5 (Figure 3-1). In comparable tests with PF ferric hydroxide. DOC removal was approximately 50% at pH 5.5 and 6.5, while only 41% was removed at pH 7.5. At pH 5.5 and 6.5, DOC removal in the CPT systems exceeded that in the PF systems, but coprecipitation did not improve DOC removal efficiency at pH 7.5.

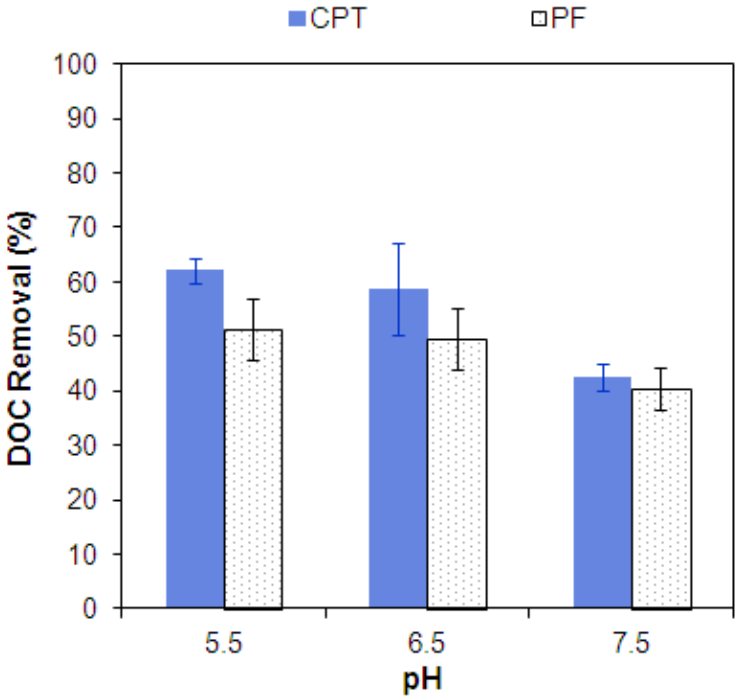

Figure 3-1. Removal of DOC as a function of pH in coprecipitated (CPT) and preformed (PF) experiments at t=4 h.

The "sorption density" (SD) of DOC (mol C/mol Fe) was calculated as:

$$DOC\ SD = \frac{DOC_0 - DOC_{filtrate}}{[Fe]_o - [Fe]_{fltrate}} \quad (3\text{-}1)$$

where DOC_o and $[Fe]_o$ represent the initial DOC (mM) and Fe concentration (mM), respectively, and $DOC_{filtrate}$ and $[Fe]_{filtrate}$ represent those parameters after filtration. For comparison, the SD of UV_{254} Abs (cm^{-1}/mM Fe) was also calculated as:

$$UV_{254}\ Abs\ SD = \frac{UV_o - UV_{soluble}}{[Fe]_o - [Fe]_{soluble}} \quad (3\text{-}2)$$

where UV_o and $[Fe]_o$ represent the initial UV_{254} Abs (cm^{-1}) and Fe concentration (mM) and $UV_{soluble}$ and $[Fe]_{soluble}$ represent those parameters after filtration.

Consistent with the removal data (Figure 3-1), the highest DOC SDs were observed in CPT experiments at pH 5.5 and 6.5 (Figure 3-2a). In CPT experiments, maximum DOC SDs and circumneutral zeta potential measurements suggest that optimal coagulation occurred at pH 6.5 (Figure 3-2). At pH 5.5, however, zeta potentials are positive, indicating a protonated surface that has sites available for further FA sorption. Removal of UV_{254} Abs exceeded 90% (Figure A-1) and DOC removal exceeded 60% at pH 5.5 (Figure 3-1), suggesting that NOM removal was complete. Thus, it is expected that more FA could be sorbed if the ratio of DOC_0/Fe_0 were higher at pH 5.5. In this situation, DOC SDs at pH 5.5 would be expected to exceed those observed at pH 6.5.

Samples coagulated at pH 7.5 exhibited very negative zeta potentials (< -15 mV) and suppression of FA removal (Figure 3-2 and Figure A-1). Compared to measurements at pH 6.5, DOC SDs in the CPT experiment at pH 7.5 were 24%-87% lower, and UV_{254} Abs SDs were 24%-29% lower (Figure A-1). Furthermore, DOC SDs and UV_{254} Abs SDs at pH 7.5 were equivalent to or less than those in PF experiments, suggesting that the increased removals expected with CPT flocs do not extend to higher pHs, where sorption is less favorable.

Zeta potential trends provide some insight into the mechanisms of FA removal in CPT and PF experiments (Figure 3-2b). In the CPT experiments at pHs 5.5 and 6.5, initial zeta potential measurements are positive (i.e., 19.19 mV and 2.76 mV, respectively), but decrease over the 24-h test period. The most significant declines in zeta potential occur in the first 4 h. At pH 5.5 and 6.5, DOC SDs (Figure 3-2a) suggest a slight increase in FA sorption between 0.5 and 4 h that correlates with the decrease in zeta potential during the same period. This increase between 0.5 and 4 h at pH 5.5 is also apparent in the UV_{254} Abs SD data (Figure A-1). Under conditions in which Fe is coprecipitated with NOM, evidence suggests that charge neutralization is an important reaction mechanism as NOM molecules interact with Fe species during precipitation (Davis and Edwards 2014b, Jung et al. 2005, Sieliechi et al. 2008, Vilge-Ritter et al. 1999). Particularly at pH 5.5 and 6.5, FA competes with OH^- for Fe coordination. These zeta potential and SD data are consistent with the notion that in the first 0.5 h, there is rapid coprepipitation as ferric hydrolysis species are complexed by negatively-charged FA ligands. Following this initial Fe-FA complexation reaction, ferric hydroxide precipitation and aggregation are expected to become more important. Adsorption of FA likely plays a critical role during this period, as indicated by increasing DOC and UV_{254} Abs SDs (Figure 3-2a and Figure A-1) and decreasing zeta potential (Figure 3-2b) between 0.5 and 4 h at pH 5.5 and 6.5.

When FA solutions were dosed with PF ferric hydroxide particles, the resulting zeta potential trends differed significantly from those in the CPT experiments. In the PF case, zeta potential measurements taken within the first 5 min were highly negative at less than -20 mV at each pH. Within the first 0.5 h, however, zeta potential increased and began to approach zeta potential measurements from the CPT experiments. This "rebound effect" was most dramatic at pH 5.5, with zeta potential increasing from -20.17 mV at 2 min to +9.35 mV at 0.5 h. Although FA removal was not measured within the first 5 min, the very negative zeta potential in PF data clearly indicates a high level of FA sorption on the Fe surface. It is hypothesized that the sorbed FA dissolves a fraction of Fe via reductive or ligand-induced dissolution (Afonso et al. 1990, Choi

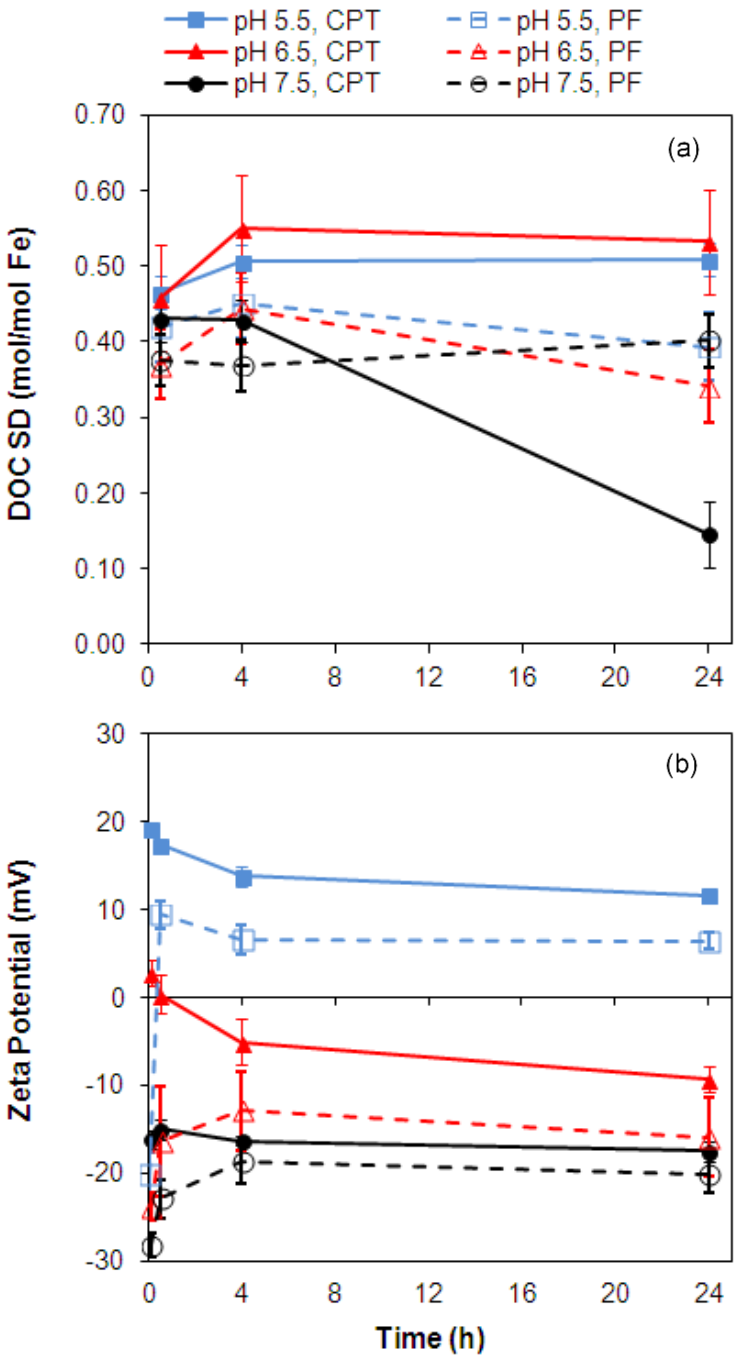

Figure 3-2. (a) DOC sorption densities (SD) in coprecipitated (CPT) and preformed (PF) systems as a function of pH and reaction time. (b) Zeta potential measurements depend upon pH, reaction time, and the use of coprecipitated or preformed Fe.

et al. 2000). To some extent, the presence of dissolved Fe simulates in-situ coagulation, with zeta potential measurements in the PF systems approaching those of the CPT samples. To shed light on this phenomenon, future research should be devoted to monitoring zeta potential, mobilized Fe, and sorbed FA at frequent intervals within the first 0.5 h of contact between FA and PF ferric hydroxide.

Effect of Silica on Coagulation of FA

Low Silica. Similar to DOC SDs, silica sorption densities (mol SiO_2/mol Fe) were calculated as:

$$SiO_2\ SD_{fil} = \frac{[SiO_2]_o - [SiO_2]_{filtrate}}{[Fe]_o - [Fe]_{fltrate}} \quad (3\text{-}3)$$

where $[SiO_2]_o$ and $[Fe]_o$ represent the initial SiO_2 and Fe concentrations (mM) and $[SiO_2]_{filtrate}$ and $[Fe]_{filtrate}$ represent those parameters after filtration.

In single-sorbate experiments in which ferric hydroxide was coprecipitated with 10 mg/L of silica, SiO_2 SD_{fil} varied from 0.14 mol SiO_2/mol Fe at pH 5.5 to 0.22 mol SiO_2/mol Fe at pH 7.5 (Figure 3-3). Silica decreased zeta potential at pH 5.5 and 6.5 and reversed the surface charge at pH 7.5. Dual-sorbate experiments with both FA and silica (10 mg/L as SiO_2) elucidated the competitive interactions between the two ligands. Not surprisingly, the presence of FA at 2 mg/L as DOC interfered with silica sorption, reducing SD_{fil} to less than 0.07 mol SiO_2/mol Fe at pH 5.5 and 6.5 (Figure 3-3). At pH 7.5, where silica sorption is more favorable, interference from FA was less severe; SiO_2 SD_{fil} was reduced by 16%-27% to 0.14-0.16 mol SiO_2/mol Fe. The combination of silica and FA yielded more negative zeta potentials than either sorbate alone (Figure 3-2b and Figure 3-3).

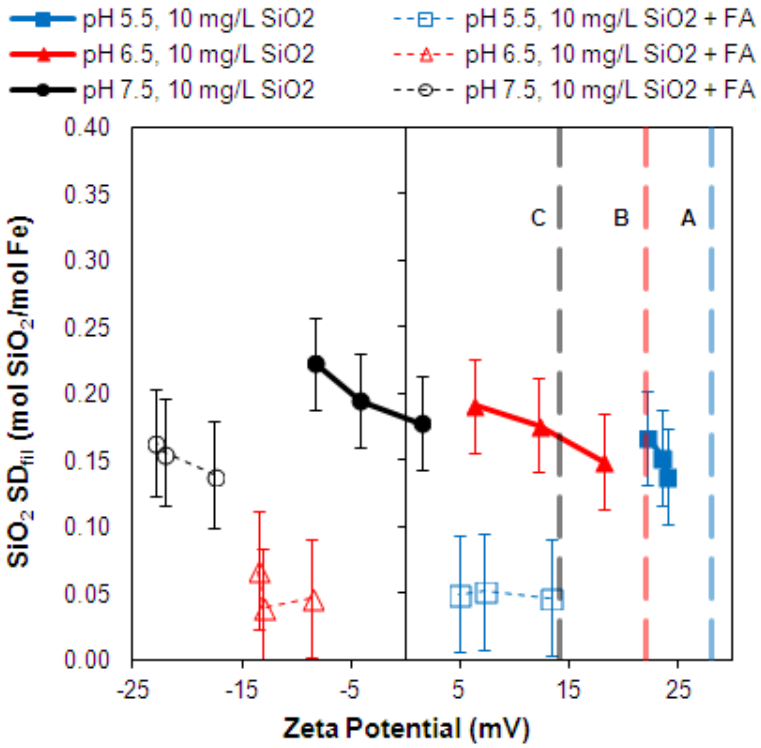

Figure 3-3. Influence of silica sorption density (SD) and pH on zeta potential in coprecipitated systems. Samples contain 10 mg/L as Fe and 10 mg/L as SiO_2. Open symbols represent systems that also include 2 mg/L of DOC. Vertical lines A, B, and C depict zeta potential in Fe-only controls at pH 5.5, 6.5, and 7.5, respectively. The three points in each series represent reaction times of 0.5, 4, and 24 hours.

Silica oligomerization and affinity for the ferric hydroxide surface increase with pH (Davis et al. 2002, Swedlund et al. 2010b), and the ability of silica to interfere with FA sorption appears to follow a similar trend. At lower pH, DOC removals and SDs are generally high (Figure 3-4), and the presence of 10 mg/L as SiO_2 yields no discernible effect on the sorption of DOC at pH 5.5. At pH 6.5, the results suggest that 10 mg/L as SiO_2 may interfere with DOC sorption at 4 h, although this data point appears to be an anomaly since interference is not evident at 24 h and only minimal interference appears in the UV_{254} SD data for pH 6.5 (Figure A-2). In the single-sorbate CPT experiments, pH 7.5 is associated with decreasing FA sorption and increasing silica sorption. When both sorbates are present at pH 7.5, 10 mg/L as SiO_2 acts as a significant (90% confidence level) interferent to FA sorption, reducing DOC SDs by 16%-28% at 0.5 and 4 h (Figure 3-4b) and UV_{254} Abs SDs by 33%-38% at all reaction times (Figure A-2b). This result suggests that a moderate concentration of silica can influence NOM removal above a threshold pH during coagulation.

High Silica. In experiments with 50 mg/L as SiO_2, the higher silica concentration made calculation of SiO_2 SD_{fil} less reliable and subject to higher error. In these experiments, sorption density was calculated directly from digestate:

$$SiO_2\ SD_{dig} = \frac{[SiO_2]_{digestate}}{[Fe]_{digestate}} \tag{3-4}$$

where $[SiO_2]_{digestate}$ and $[Fe]_{digestate}$ represent the concentrations of silica and iron recovered from the digested filters.

When ferric hydroxide was coprecipitated with the higher silica concentration (50 mg/L as SiO_2), exceptionally high sorption densities of 0.28-0.47 mol SiO_2/mol Fe were measured (Figure 3-5). Assuming a site density of 0.2 mol/mol Fe for hydrous ferric oxide (HFO) (Dzombak and Morel 1990), greater than a monolayer of sorbed silica was observed at pH 5.5; at pH 6.5 and 7.5, sorption densities of approximately a bilayer (0.35-0.47 mol SiO_2/mol Fe) were measured. In PF experiments, SiO_2 SD_{dig} values were limited to about a monolayer (0.17-0.25 mol SiO_2/mol Fe). When CPT and PF data points are paired according to pH and sampling time, SiO_2 SD_{dig} was 32-130% higher in the CPT samples. This outcome is consistent with previous research showing that CPT often leads to extraordinarily high sorption densities of arsenate, silica, and phosphate (Cheng et al. 2004, Fuller et al. 1993, Mayer and Jarrell 2000, Waychunas et al. 1993). Comparison of CPT and PF sorption data also indicates that pH plays a more important role in a CPT environment.

Consistent with our earlier study of silica sorption to PF ferric hydroxide (Davis et al. 2002), zeta potentials at pH 5.5 were positive in the CPT sample with SiO_2 SD_{dig} values of 0.28-0.33 mol/mol Fe and in the PF sample with SiO_2 SD_{dig} values of 0.19-0.21 mol/mol Fe (Figure 3-5). Since SiO_2 SD_{dig} values are equivalent to or greater than monolayer coverage while zeta potential remains positive, a fraction of the sorbed silica in the current work is oligomeric as there are no positively charged silica species (Davis et al. 2002, Sigg and Stumm 1981, Swedlund et al. 2010a, Swedlund and Webster 1999). In the CPT experiments, higher silica sorption densities may have been attained through coprecipitation and occlusion of silica within the interior of the floc, yielding unoccupied $\equiv FeOH_2^+$ sites on the surface.

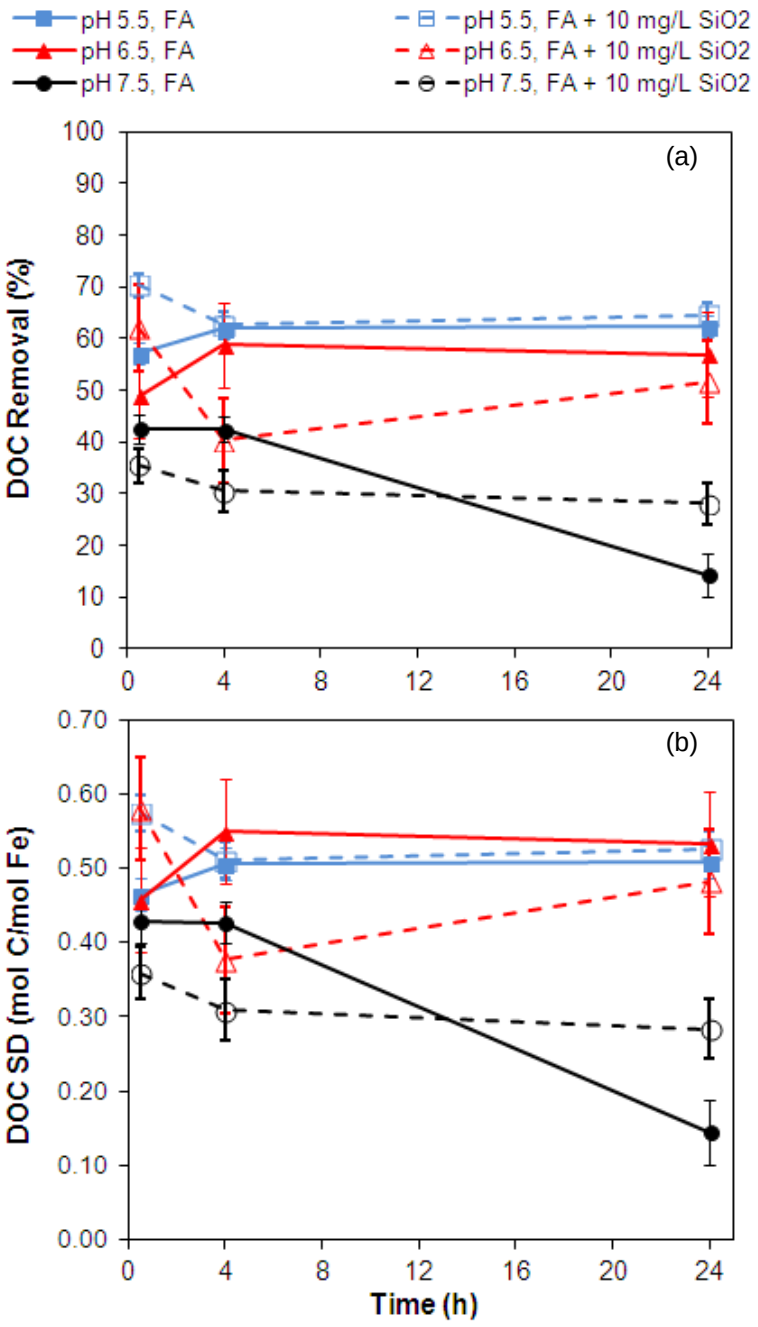

Figure 3-4. (a) DOC removal and (b) DOC sorption density (SD) as a function of pH and time in coprecipitated systems. Samples contain 10 mg/L as Fe and fulvic acid (FA) at 2 mg/L as DOC. Open symbols represent systems that also include 10 mg/L of SiO_2.

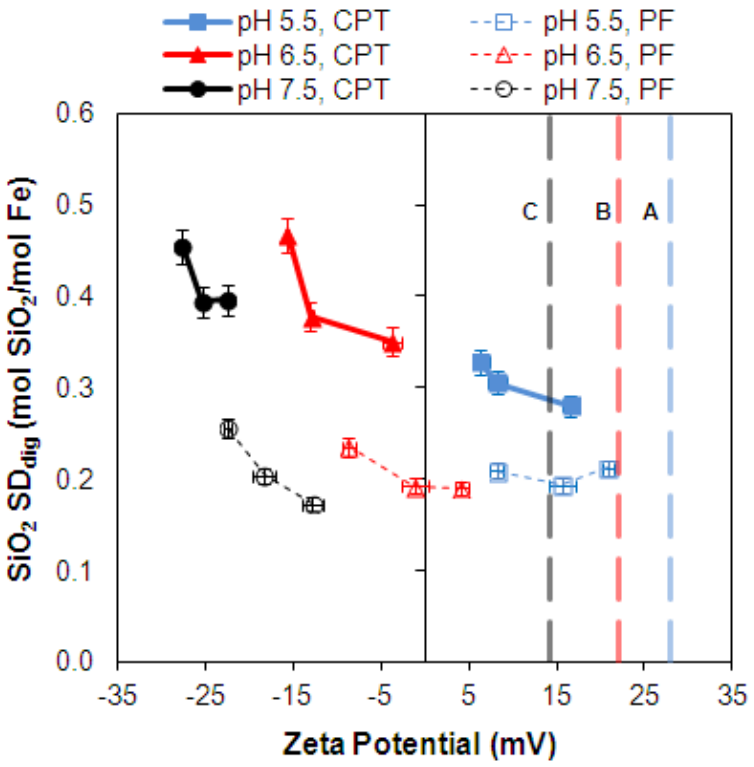

Figure 3-5. The influence of silica sorption density (SD) and pH on zeta potential in coprecipitated (CPT) and preformed (PF) systems. Samples contain 10 mg/L as Fe and 50 mg/L as SiO_2. Vertical lines A, B, and C depict zeta potential in Fe-only controls at pH 5.5, 6.5, and 7.5, respectively. The three points in each series represent reaction times of 0.5, 4, and 24 hours.

Davis et al. (2001) previously showed that certain combinations of pH and silica concentration led to the formation and release of colloidal Fe from PF ferric hydroxide after 50 days. In the current work, Fe was not detected in filtrate within the 24-h test period with PF iron. In the single-sorbate CPT experiment at pH 7.5, however, Fe concentrations of 0.1-0.2 mg/L were measured in the filtrate of samples with 50 mg/L as SiO_2 (Figure 3-6). SiO_2 SD_{dig} values at pH 7.5 were similar to those at pH 6.5, yet no filtrate Fe was measured at pH 6.5. Comparison of the results at pHs 6.5 and 7.5 suggests that mobilization of Fe is primarily influenced by pH and zeta potential, rather than SiO_2 SD_{dig}. The extent of silica polymerization also increases with pH (Choppin et al. 2008, Davis 2000, Iler 1979) and influences the concentration of Fe passing the 0.45-µm filter.

Similar to the behavior observed with PF ferric hydroxide at 50 days (Davis et al. 2001), it is possible that filtrate Fe in the 24-h CPT experiments arises from Fe colloids mobilized from a ferric hydroxide precipitate. Yet, the mechanism is more likely rooted in the differences between the CPT and PF environments. Studies have shown that aqueous silica interferes with Fe hydrolysis, forms Fe-Si coprecipitates, and limits the size of ferric hydroxide growth (Doelsch et al. 2003, Doelsch et al. 2001, Kaegi et al. 2010, Liu et al. 2007, Pokrovski et al. 2003). It is hypothesized that the small fraction of mobilized Fe in the pH 7.5 CPT sample with 50 mg/L as SiO_2 is in the form of a stable, colloidal Fe-Si coprecipitate.

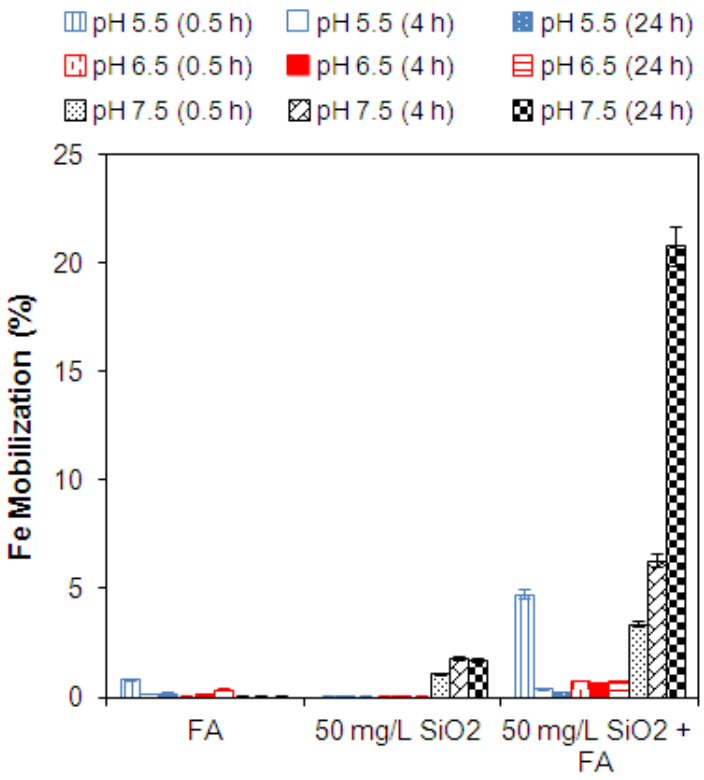

Figure 3-6. Mobilization of Fe through a 0.45-µm filter as a function of pH, reaction time, and water composition. Initial Fe concentration was 10 mg/L. Samples with fulvic acid (FA) included a nominal concentration of 2 mg/L as DOC.

The inclusion of FA (2 mg/L as DOC) in samples coprecipitated with high (50 mg/L as SiO_2) silica unexpectedly yielded much higher SiO_2 SD_{dig} values, with maximum sorption densities of 0.64 at pH 6.5 and 0.88 at pH 7.5 (Figure 3-7a). Inspection of silica sorption densities in single-sorbate experiments with only FA (i.e., no added silica) revealed that some silica was in the FA isolate (Figure 3-7a), and this background silica mathematically accounted for the higher observed dual-sorbate SiO_2 SD in the following five cases: pH 5.5 (all three sample times); pH 6.5 at 0.5 h; and pH 6.5 at 4 h (Table 3-1). However, SiO_2 SDs in the dual-sorbate samples still appear significantly higher after accounting for the silica in the organic matter in three other cases. Specifically, the dual-sorbate SiO_2 SD is at least 25% higher at pH 6.5 and 24 h; 32% higher at pH 7.5 and 0.5 h; and 91% higher at pH 7.5 and 4 h. While an increase in SiO_2 SD was not observed in the dual-sorbate sample at pH 7.5 and 24 h, it is noted that Fe mobilization increased with time at pH 7.5, reaching a maximum of 21% at 24 h (Figure 3-6). While the additive calculation is equivalent to the measured SiO_2 SD in the dual-sorbate sample at pH 7.5 and 24 h (Table 3-1), it is hypothesized that the observed dual-sorbate sorption density is artificially low given the significant fraction of iron passing through the 0.45-µm filter. In other words, it is possible that the increase in colloidal Fe between the 4 and 24-h samples is associated with a disproportionately high quantity of silica; therefore, the particulate Fe that is captured by the filter at 24 h exhibits a lower SiO_2 SD_{dig} than measured at 4 h.

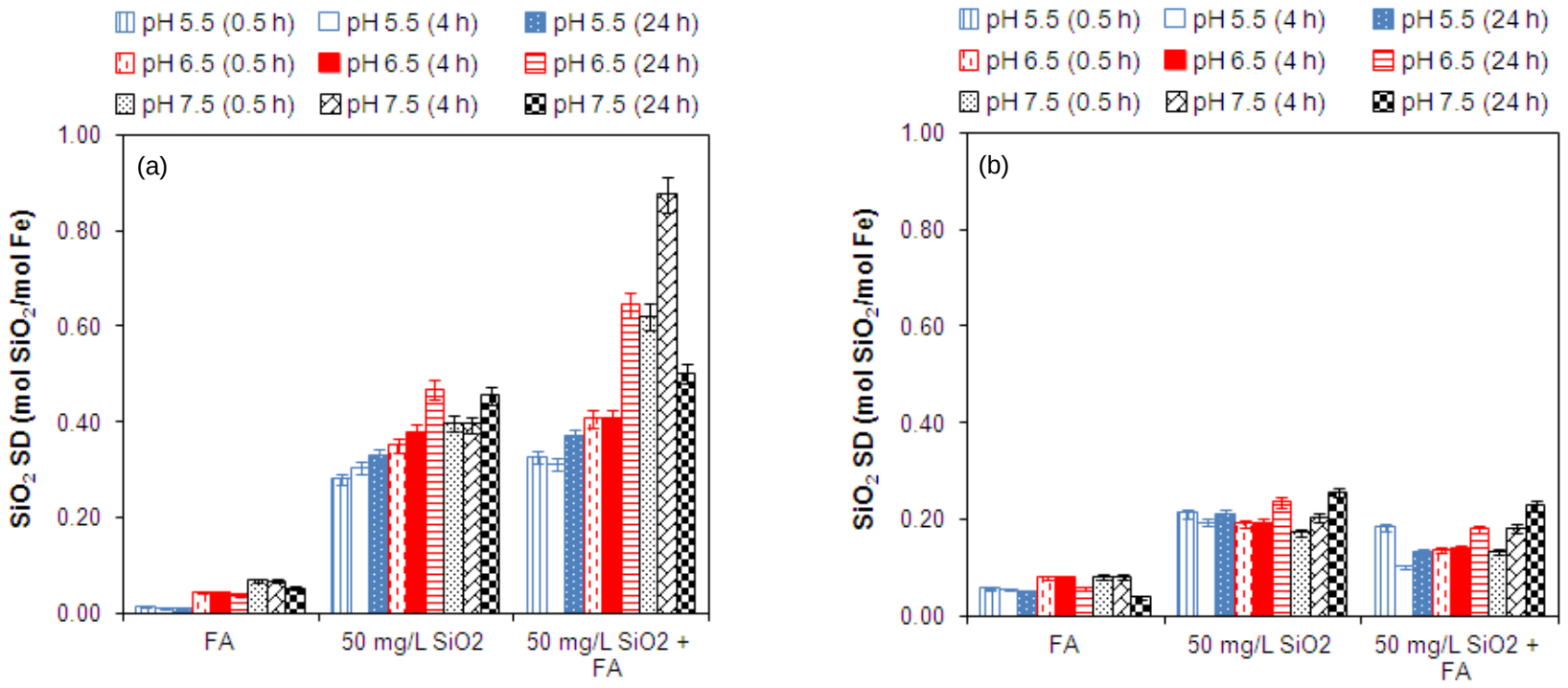

Figure 3-7. Silica sorption densities (SD) as a function of pH, reaction time, and water composition for (a) coprecipitated and (b) preformed systems. Initial Fe concentration was 10 mg/L. Samples with fulvic acid (FA) included a nominal concentration of 2 mg/L as DOC.

Table 3-1. Silica Sorption Densities in Single- and Dual-sorbate Samples with Fulvic Acid and 50 mg/L as SiO_2

pH	Time	Silica Sorption Density (mol SiO_2/mol Fe)				Difference (%)
		Single-Sorbate 2 mg/L as DOC	*Single-Sorbate 50 mg/L SiO2*	*Additive Result of Single-Sorbate Samples*	*Dual-Sorbate 2 mg/L as DOC + 50 mg/L SiO2*	
5.5	0.5	0.01 ± 0.00	0.28 ± 0.01	0.29 ± 0.01	0.33 ± 0.01	12%
	4	0.01 ± 0.00	0.31 ± 0.01	0.32 ± 0.01	0.31 ± 0.01	-3%
	24	0.01 ± 0.00	0.33 ± 0.01	0.34 ± 0.01	0.37 ± 0.02	9%
6.5	0.5	0.04 ± 0.00	0.35 ± 0.01	0.39 ± 0.01	0.41 ± 0.02	5%
	4	0.04 ± 0.00	0.38 ± 0.02	0.42 ± 0.02	0.41 ± 0.02	-2%
	24	0.04 ± 0.00	0.47 ± 0.02	0.51 ± 0.02	0.64 ± 0.03	25%
7.5	0.5	0.07 ± 0.00	0.40 ± 0.01	0.47 ± 0.02	0.62 ± 0.03	32%
	4	0.07 ± 0.00	0.39 ± 0.02	0.46 ± 0.02	0.88 ± 0.04	91%
	24	0.05 ± 0.00	0.45 ± 0.02	0.50 ± 0.02	0.50 ± 0.02	0%

The higher SiO_2 SDs observed in the dual-sorbate samples raised the question of whether FA catalyzed the formation of silica polymers on the ferric hydroxide surface. In experiments with PF ferric hydroxide particles, however, there was no evidence for enhanced silica sorption due to the presence of FA. In fact, at each pH-time combination, SiO_2 SD_{dig} was 11%-48% lower in the dual-sorbate sample than in the comparable single-sorbate sample with only 50 mg/L as SiO_2 (Figure 3-7b). The PF results indicate that competition with FA for sorption sites actually suppresses silica sorption, with the greatest competition generally occurring at shorter reaction times and lower pH. These observations are consistent with behavior reported in the literature, namely that NOM sorption is favored at lower pH and tends to be fast (Avena and Koopal 1999, Ochs et al. 1994), whereas the silica sorption is favored at higher pH and the growth of surface polymers is slower (Davis et al. 2002, Smith and Edwards 2005).

Since FA does not appear to directly catalyze surface polymerization of silica, it is inferred that the co-occurrence of FA and high silica increases SiO_2 SDs through some other mechanism. It is well known that both NOM and aqueous silica can interfere with the hydrolysis, precipitation, growth, and aging of ferric (hydr)oxides (Davis and Edwards 2014b, Doelsch et al. 2003, Doelsch et al. 2001, Knocke et al. 1994, Vilge-Ritter et al. 1999). In this study, a relatively high ratio of Fe-to-DOC (5 mg Fe/mg DOC) was used, yielding only minimal influence on Fe particle sizes in single-sorbate samples (Figure 3-6). As previously discussed, 50 mg/L as SiO_2 in single-sorbate samples led to an Fe mobilization concentration of just 1.1%-1.8% at pH 7.5. Together, these results do not indicate a high level of interference by either FA (at 2 mg/L as DOC) or silica (at 50 mg/L as SiO2) in the Fe growth and aggregation processes. However, comparing single-sorbate CPT to the paired PF experiments, sorption densities of DOC were greater in the CPT samples (Figure 3-2a), and SiO_2 SD was greater at all pHs (Figure 3-5). Higher sorption densities in single-sorbate CPT samples are consistent with the likelihood of smaller Fe particles with greater surface area available for ligand exchange and silica polymer growth, although particles were generally still large enough to be removed by the 0.45-µm filter under most conditions.

In the CPT experiments with both FA and 50 mg/L as SiO_2 present, the Fe mobilization rate was always higher than in the single-sorbate samples with either FA or high silica alone. It is hypothesized that the combination of FA and high silica in dual-sorbate samples exerted a stronger inhibitory influence on the hydrolysis and growth of ferric particles than exhibited by either ligand alone, and this interference yielded smaller particles with greater surface area available for ligand sorption. In these results, a monolayer equivalent of sorbed silica was exceed by 0.5 h, but notably higher SiO_2 SDs were observed at either 24 h (pH 5.5 and 6.5) or 4 h (pH 7.5) (Figure 3-7a); these increases in SiO_2 SD are presumably attributable to the slow growth of silica oligomers on the ferric hydroxide surface. In the dual-sorbate experiment with FA and 50 mg/L as SiO_2 at pH 7.5, zeta potentials decrease below -25 mV, yielding mobilization of a significant concentration of Fe colloids through the 0.45-μm filter (Figure 3-6).

Single-sorbate samples with only 50 mg/L as SiO_2 at pH 7.5 also exhibited highly negative zeta potentials (-23 to -28 mV), but with substantially less Fe mobilization than the dual-sorbate sample with FA (Figure 3-6). The higher SiO_2 SD and Fe mobilization in the dual-sorbate samples is attributed to the synergistic effect of co-occurring FA and high silica, with FA likely playing a more significant role in interrupting Fe hydrolysis at shorter reaction times and lower pH. At pH 5.5, FA can actually reduce the iron hydrolysis ratio by successfully competing with OH^- for Fe coordination (Davis and Edwards 2014b), a phenomenon which presumably contributed to the higher Fe mobilization rates at pH 5.5 and 0.5 h (Figure 3-6). At longer reaction times, Fe mobilization decreases as ferric hydroxide particle growth and aggregation occur in the single-sorbate experiments with FA, consistent with the notion that FA's interference is more significant at shorter reaction time. In the dual-sorbate experiments with high SiO_2, however, silica also sorbs strongly to ferric hydroxide and likely interferes with Fe particle growth and aggregation, particularly at higher pH. Silica sorption and surface polymerization appear to be slower than FA sorption, as evidenced by SiO_2 SDs and mobilized Fe concentrations that generally increase with time (Figure 3-6 and Figure 3-7a).

Similar to the results with SiO_2 at 10 mg/L, high silica interfered with FA removal, and the extent of this interference increased with pH. At pH 6.5, high silica in the CPT sample significantly (95% confidence) decreased DOC SD by 8%-31% and UV_{254} Abs SD by 22%-30% (Figure 3-8a and Figure A-3a). In the dual-sorbate CPT sample at pH 7.5, which was characterized by extraordinarily high SiO_2 SDs and mobilized Fe concentrations, UV_{254} Abs SD decreased by 85% at 0.5 h, but filtrate Fe concentrations in excess of 5% prevented the calculation of a UV_{254} Abs SD at longer reaction times. DOC SDs in the same sample were 28%-45% lower; this result was significant at 90% confidence and confirms that high silica concentrations are important interferents to NOM removal at pH 7.5. In CPT experiments, suppression of FA removal was influenced by pH, competition with silica, and changes in Fe particle characteristics.

While coprecipitation and inhibition of Fe precipitation and aggregation was not a factor in PF experiments, these results exhibited a similar trend with respect to pH and silica interference (Figure 3-8b). Notable interference was observed at pHs 6.5 and 7.5, at which DOC SDs declined by 22%-54% and 13%-46%, respectively, in the presence of 50 mg/L as SiO_2. High silica reduced UV_{254} Abs SD by 12-15% while decreases of 32%-43% and 33-51% were observed at pHs 6.5 and 7.5, respectively (Figure A-3b). These differences were significant at 90% confidence for pH 5.5 and greater than 99% confidence for pHs 6.5 and 7.5. At pH 7.5 and 24 h, the decrease in DOC

SD (Figure 3-8b), coupled with an increase is SiO_2 SD (Figure 3-7b) is consistent with the hypothesis that continued, slow growth of surface silica polymers may lead to release of sorbed NOM. Thus reaction time, as well as pH and floc characteristics, is an important factor in understanding competitive ligand removal.

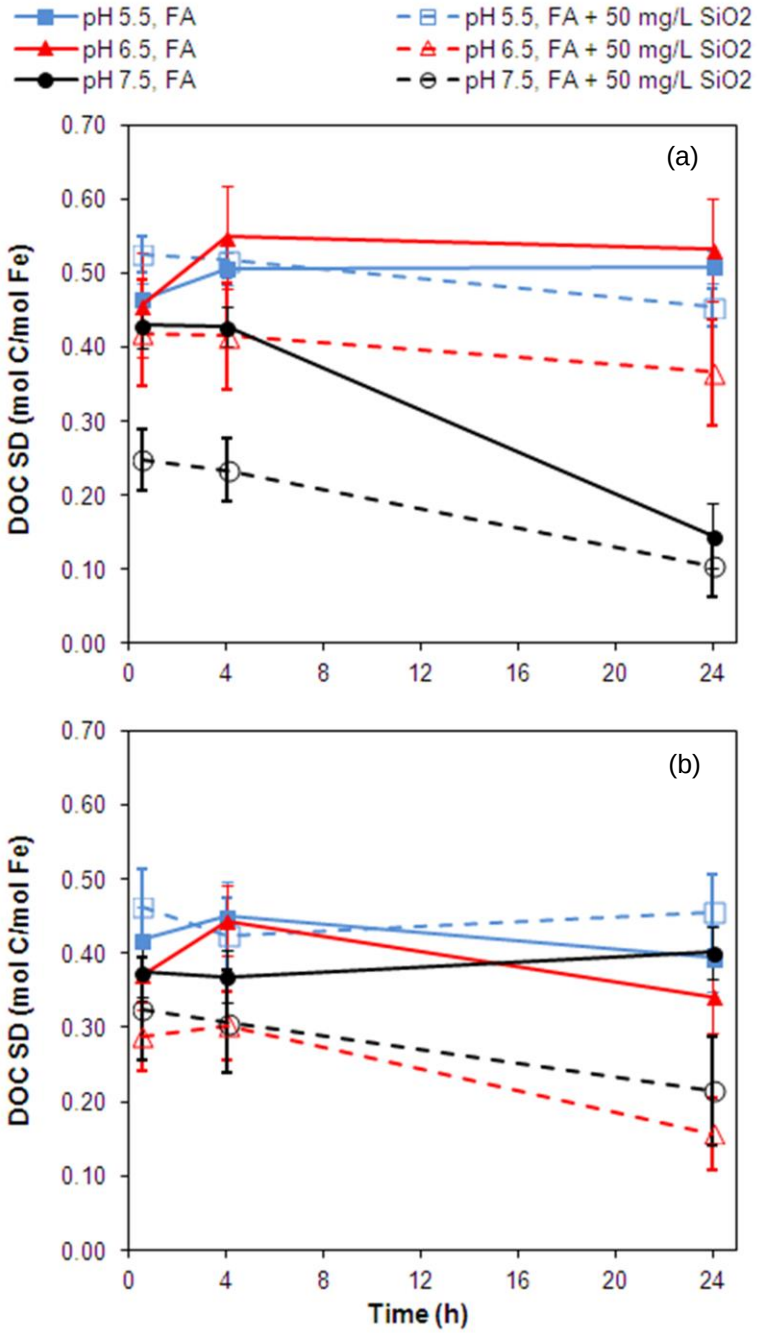

Figure 3-8. DOC sorption densities (SD) in (a) coprecipitated and (b) preformed systems as a function of pH and reaction time. Samples contain 10 mg/L as Fe and fulvic acid (FA) at 2 mg/L as DOC. Open symbols represent systems that also include 50 mg/L of SiO_2.

Conclusions

Silica, a common ligand in natural waters, interfered with the removal of FA in the neutral pH range (pHs 6.5 and 7.5). The moderate SiO_2 concentration (10 mg/L) exhibited the ability to interfere with NOM sorption in the CPT experiment, reducing DOC SD by up to 28% at pH 7.5. The high SiO_2 concentration (50 mg/L) reduced DOC SD in CPT samples by up to 31% at pH 6.5 and 45% at pH 7.5; significant interference was also observed when using PF ferric hydroxide.

The ratio of coagulant-to-ligand concentration proved critical as the mechanisms of coagulation and interference varied with the relative concentrations of ferric iron, FA, and silica. At low silica (i.e., a high dose-to-ligand ratio), interference with FA removal occurred at pH 7.5. Fe mobilization was not a factor at this relatively high Fe dose, and interference was attributed to site competition and electrostatic repulsion. At high SiO_2 (i.e., a low dose-to-ligand ratio), FA and silica synergistically inhibited Fe hydrolysis, precipitation, and aggregation, altering the Fe particle size distribution and providing greater surface area for silica polymerization. These mechanisms, coupled with direct competition for surface sites and electrostatic repulsion, severely hindered FA removal and compromised coagulation efficacy in the samples with co-occurring FA and high silica.

The PF experiments elucidated mechanisms of sorption and competition without the confounding effects of Fe mobilization or complications of coprecipitation. However, PF particles do not represent a good model for in-situ coagulation, in which water quality influences the particle size distribution and chemical composition of the coagulant products. In most experiments, ligand removal was greater in CPT systems than in samples with PF ferric hydroxide.

This research with a single FA isolate demonstrates that competitive ligand concentrations, pH, and coagulant dose strongly influence coagulation efficacy in practice. Depending upon pH, SiO_2 negatively influenced coagulation in each of the three areas that were studied: (1) silica directly competed with NOM for sorption sites, (2) silica interfered with Fe hydrolysis and growth, contributing to the formation of Fe colloids and (3) silica depressed zeta potential. These results confirm that NOM character or pH buffering alone cannot explain difficulties in removing NOM by coagulation. Rather, water quality interferences must be considered as contributing factors.

Acknowledgements

Caitlin Grotke and Samantha Fisher provided valuable assistance in executing laboratory experiments, and Jeffrey Parks completed ICP and TOC analyses. Hsiao-wen Chen isolated the FA used in this study. During this research, the first author was supported by fellowship funding from the National Water Research Institute and the Edna Bailey Sussman Foundation. Certain equipment and supplies were purchased with STAR fellowship funds from the US EPA. The findings are those of the authors and may not reflect the views of these organizations.

References

Afonso, M.D., Morando, P.J., Blesa, M.A., Banwart, S. and Stumm, W. (1990) The Reductive Dissolution of Iron-Oxides by Ascorbate - The Role of Carboxylate Anions in Accelerating Reductive Dissolution. Journal of Colloid and Interface Science 138(1), 74-82.

Avena, M.J. and Koopal, L.K. (1999) Kinetics of humic acid adsorption at solid-water interfaces. Environmental Science & Technology 33(16), 2739-2744.

Cheng, Z.Q., Van Geen, A., Jing, C.Y., Meng, X.G., Seddique, A. and Ahmed, K.M. (2004) Performance of a household-level arsenic removal system during 4-month deployments in Bangladesh. Environmental Science & Technology 38(12), 3442-3448.

Choi, S.Y., Chen, J. and Gu, B.H. (2000) Reductive dissolution of iron oxyhydroxides by different fractions of natural organic matter. Abstracts of Papers of the American Chemical Society 220, U365-U366.

Choppin, G.R., Pathak, P. and Thakur, P. (2008) Polymerization and Complexation Behavior of Silicic Acid: A Review. Main Group Metal Chemistry 31(1-2), 53-71.

Davis, C.C. (2000) Aqueous Silica in the Environment: Effects on Iron Hydroxide Surface Chemistry and Implications for Natural and Engineering Systems, Virginia Polytechnic Institute and State University, Blacksburg, VA.

Davis, C.C., Chen, H.W. and Edwards, M. (2002) Modeling silica sorption to iron hydroxide. Environmental Science & Technology 36(4), 582-587.

Davis, C.C. and Edwards, M. (2014a) Coagulation With Hydrolyzing Metal Salts: Mechanisms and Water Quality Impacts. Critical Reviews in Environmental Science and Technology 44(4), 303-347.

Davis, C.C. and Edwards, M. (2014b) Role of Calcium in the Coagulation of NOM with Ferric Chloride. Manuscript submitted for publication.

Davis, C.C., Knocke, W.R. and Edwards, M. (2001) Implications of aqueous silica sorption to iron hydroxide: Mobilization of iron colloids and interference with sorption of arsenate and humic substances. Environmental Science & Technology 35(15), 3158-3162.

Doelsch, E., Masion, A., Rose, J., Stone, W.E.E., Bottero, J.Y. and Bertsch, P.M. (2003) Chemistry and structure of colloids obtained by hydrolysis of Fe(III) in the presence of SiO4 ligands. Colloids and Surfaces a-Physicochemical and Engineering Aspects 217(1-3), 121-128.

Doelsch, E., Stone, W.E.E., Petit, S., Masion, A., Rose, J., Bottero, J.Y. and Nahon, D. (2001) Speciation and crystal chemistry of Fe(III) chloride hydrolyzed in the presence of SiO4 ligands. 2. Characterization of Si-Fe aggregates by FTIR and Si-29 solid-state NMR. Langmuir 17(5), 1399-1405.

Dzombak, D.A. and Morel, F.M.M. (1990) Surface Complexation Modeling: Hydrous Ferric Oxide, Wiley-Interscience, New York.

Eaton, A.D., Clesceri, L.S., Rice, E.W. and Greenberg, A.E. (eds) (2005) Standard Methods of the Examination of Water and Wastewater, American Public Health Association, Washington, D.C.

Fuller, C.C., Davis, J.A. and Waychunas, G.A. (1993) Surface-Chemistry of Ferrihydrite .2. Kinetics of Arsenate Adsorption and Coprecipitation. Geochimica Et Cosmochimica Acta 57(10), 2271-2282.

Hering, J.G., Chen, P.Y., Wilkie, J.A. and Elimelech, M. (1997) Arsenic removal from drinking water during coagulation. Journal of Environmental Engineering-Asce 123(8), 800-807.

Holm, T.R. (2002) Effects of CO32-/bicarbonate, Si, and PO43- on arsenic sorption to HFO. Journal American Water Works Association 94(4), 174-181.

Hussain, S., van Leeuwen, J., Chow, C., Beecham, S., Kamruzzaman, M., Wang, D.S., Drikas, M. and Aryal, R. (2013) Removal of organic contaminants from river and reservoir waters by three different aluminum-based metal salts: Coagulation adsorption and kinetics studies. Chemical Engineering Journal 225, 394-405.

Iler, R.K. (1979) The Chemistry of Silica: Solubility, Polymerization, Colloid and Surface Properties, and Biochemistry, John Wiley & Sons, New York.

Jung, A.V., Chanudet, V., Ghanbaja, J., Lartiges, B.S. and Bersillon, J.L. (2005) Coagulation of humic substances and dissolved organic matter with a ferric salt: An electron energy loss spectroscopy investigation. Water Research 39(16), 3849-3862.

Kaegi, R., Voegelin, A., Folini, D. and Hug, S.J. (2010) Effect of phosphate, silicate, and Ca on the morphology, structure and elemental composition of Fe(III)-precipitates formed in aerated Fe(II) and As(III) containing water. Geochimica Et Cosmochimica Acta 74(20), 5798-5816.

Knocke, W.R., Shorney, H.L. and Bellamy, J.D. (1994) Examining the Reactions Between Soluble Iron, DOC, and Alternative Oxidants During Conventional Treatment. Journal American Water Works Association 86(1), 117-127.

Laky, D. and Licsko, I. (2011) Arsenic removal by ferric-chloride coagulation - effect of phosphate, bicarbonate and silicate. Water Science and Technology 64(5), 1046-1055.

Liu, R.P., Qu, J.H., Xia, S.J., Zhang, G.S. and Li, G.B. (2007) Silicate hindering in situ formed ferric hydroxide precipitation: Inhibiting arsenic removal from water. Environmental Engineering Science 24(5), 707-715.

Masion, A., Rose, J., Bottero, J.Y., Tchoubar, D. and Elmerich, P. (1997) Nucleation and growth mechanisms of iron oxyhydroxides in the presence of PO4 ions .3. Speciation of Fe by small angle X-ray scattering. Langmuir 13(14), 3882-3885.

Mayer, T.D. and Jarrell, W.M. (2000) Phosphorus sorption during iron(II) oxidation in the presence of dissolved silica. Water Research 34(16), 3949-3956.

Meng, X.G., Bang, S. and Korfiatis, G.P. (2000) Effects of silicate, sulfate, and carbonate on arsenic removal by ferric chloride. Water Research 34(4), 1255-1261.

Ochs, M., Ćosović, B. and Stumm, W. (1994) Coordinative and hydrophobic interaction of humic substances with hydrophilic Al2O3 and hydrophobic mercury surfaces. Geochimica Et Cosmochimica Acta 58(2), 639-650.

Pallier, V., Feuillade-Cathalifaud, G., Serpaud, B. and Bollinger, J.C. (2010) Effect of organic matter on arsenic removal during coagulation/flocculation treatment. Journal of Colloid and Interface Science 342(1), 26-32.

Parks, J.L., McNeill, L., Frey, M., Eaton, A.D., Haghani, A., Ramirez, L. and Edwards, M. (2004) Determination of total chromium in environmental water samples. Water Research 38(12), 2827-2838.

Pokrovski, G.S., Schott, J., Garges, F. and Hazemann, J.L. (2003) Iron (III)-silica interactions in aqueous solution: Insights from X-ray absorption fine structure spectroscopy. Geochimica Et Cosmochimica Acta 67(19), 3559-3573.

Randtke, S.J. and Jepsen, C.P. (1981) Chemical Pretreatment for Activated-Carbon Adsorption. Journal American Water Works Association 73(8), 411-419.

Redman, A.D., Macalady, D.L. and Ahmann, D. (2002) Natural organic matter affects arsenic speciation and sorption onto hematite. Environmental Science & Technology 36(13), 2889-2896.

Roberts, L.C., Hug, S.J., Ruettimann, T., Billah, M., Khan, A.W. and Rahman, M.T. (2004) Arsenic removal with iron(II) and iron(III) waters with high silicate and phosphate concentrations. Environmental Science & Technology 38(1), 307-315.

Rose, J., Manceau, A., Bottero, J.Y., Masion, A. and Garcia, F. (1996) Nucleation and growth mechanisms of Fe oxyhydroxide in the presence of PO4 ions .1. Fe K-edge EXAFS study. Langmuir 12(26), 6701-6707.

Sieliechi, J.M., Lartiges, B.S., Kayem, G.J., Hupont, S., Frochot, C., Thieme, J., Ghanbaja, J., de la Caillerie, J.B.D., Barres, O., Kamga, R., Levitz, P. and Michot, L.J. (2008) Changes in humic acid conformation during coagulation with ferric chloride: Implications for drinking water treatment. Water Research 42(8-9), 2111-2123.

Sigg, L. and Stumm, W. (1981) The Interaction of Anions and Weak Acids with the Hydrous Goethite (Alpha-Feooh) Surface. Colloids and Surfaces 2(2), 101-117.

Smith, S.D. and Edwards, M. (2005) The influence of silica and calcium on arsenate sorption to oxide surfaces. Journal of Water Supply Research and Technology-Aqua 54(4), 201-211.

Stachowicz, M., Hiemstra, T. and Van Riemsdijk, W.H. (2007) Arsenic-bicarbonate interaction on goethite particles. Environmental Science & Technology 41(16), 5620-5625.

Swedlund, P.J., Hamid, R.D. and Miskelly, G.M. (2010a) Insights into H4SiO4 surface chemistry on ferrihydrite suspensions from ATR-IR, Diffuse Layer Modeling and the adsorption enhancing effects of carbonate. Journal of Colloid and Interface Science 352(1), 149-157.

Swedlund, P.J., Miskelly, G.M. and McQuillan, A.J. (2010b) Silicic Acid Adsorption and Oligomerization at the Ferrihydrite-Water Interface: Interpretation of ATR-IR Spectra Based on a Model Surface Structure. Langmuir 26(5), 3394-3401.

Swedlund, P.J. and Webster, J.G. (1999) Adsorption and polymerisation of silicic acid on ferrihydrite, and its effect on arsenic adsorption. Water Research 33(16), 3413-3422.

Vilge-Ritter, A., Rose, J., Masion, A., Bottero, J.Y. and Laine, J.M. (1999) Chemistry and structure of aggregates formed with Fe-salts and natural organic matter. Colloids and Surfaces a-Physicochemical and Engineering Aspects 147(3), 297-308.

Wang, Y.L., Feng, J., Dentel, S.K., Lu, J., Shi, B.Y. and Wang, D.S. (2011) Effect of polyferric chloride (PFC) doses and pH on the fractal characteristics of PFC-HA flocs. Colloids and Surfaces a-Physicochemical and Engineering Aspects 379(1-3), 51-61.

Waychunas, G.A., Rea, B.A., Fuller, C.C. and Davis, J.A. (1993) Surface-Chemistry of Ferrihydrite .1. EXAFS Studies of the Geometry of Coprecipitated and Adsorbed Arsenate. Geochimica Et Cosmochimica Acta 57(10), 2251-2269.

Yan, M.Q., Wang, D.S., Yu, J.F., Ni, J.R., Edwards, M. and Qu, H.H. (2008) Enhanced coagulation with polyaluminum chlorides: Role of pH/Alkalinity and speciation. Chemosphere 71(9), 1665-1673.

Zhan, X.A., Gao, B.Y., Yue, Q.Y., Wang, Y. and Cao, B.C. (2010) Coagulation behavior of polyferric chloride for removing NOM from surface water with low concentration of organic matter and its effect on chlorine decay model. Separation and Purification Technology 75(1), 61-68.

Chapter 4. Simultaneous Prediction of NOM Removal and Particle Destabilization in Coagulation

Christina C. Davis[1]; Hsiao-wen Chen[2]; and Marc Edwards[1]

[1]Virginia Tech Department of Civil and Environmental Engineering
407 Durham Hall, Blacksburg, VA 24060

[2]Water Research Foundation
6666 W. Quincy Ave., Denver, CO 80235

Keywords: coagulation, natural organic matter, diffuse layer model, surface complexation, zeta potential, ferric chloride

Abstract

Coagulation is a complex, but crucial, process in water treatment, wastewater treatment, and natural systems. Previous attempts to model coagulation have been limited by variability in water quality and composition and the inherent complexities of simultaneously predicting ligand sorption, metal complexation, and particle removal. In this research, a diffuse layer (DLM) surface complexation model was formulated to predict natural organic matter (NOM) sorption and surface potential. Predictions of surface potential were used to estimate zeta potential and ultimately correlated to residual turbidity, which serves as an indicator of particle removal. The model was formulated on the basis of data from bench-scale experiments with synthetic water and evaluated with data from jar tests of nine U.S. source waters. Under most conditions, the model provides excellent capability for predicting NOM sorption, calcium sorption, and particle destabilization and adequate capability for predicting silica sorption. Model simulations of hypothetical water scenarios and experimental results help to explain practical observations from the literature. The DLM can be optimized to site-specific conditions and expanded to include sorption of additional species, such as arsenic.

Introduction

Coagulation, a common process in water treatment plants throughout the U.S. and around the world, plays a critical role in the removal of turbidity, pathogens, natural organic matter (NOM), and inorganic contaminants (Davis and Edwards, 2014). Historically, conventional treatment (i.e., coagulation, flocculation, and sedimentation) was employed to remove turbidity and improve filtration. Over the last several decades, however, the significance of coagulation increased as the focus expanded from simple turbidity removal to NOM and arsenic removal for regulatory compliance, and more recently, for removal of a limited subset of endocrine-disrupting compounds (EDCs) and pharmaceuticals and personal care products (PPCPs) (Huerta-Fontela et al. 2011; Westerhoff et al. 2005). Newer technologies, such as dissolved air flotation (DAF) and membrane filtration, rely on coagulation as an important pretreatment process for improving operations and finished water quality (Edzwald 2010; Lee et al. 2009; Wang and Wang 2006; Xia et al. 2007). Many industrial and municipal wastewater treatment systems also incorporate coagulation in their treatment trains. In natural systems, coagulation-like processes occur when aluminum or ferric hydroxides precipitate, and these reactions have implications for contaminant sorption and transport.

Given the established importance of coagulation, researchers have long sought to develop models to predict coagulation efficacy and required chemical doses. Some researchers have created "domains" describing treatment conditions where optimal coagulation is expected for waters conforming to the assumptions used to formulate the domains (Amirtharajah et al. 1993; Amirtharajah and Mills 1982). Empirical and semi-empirical (Tseng et al. 2000; van Leeuwen et al. 2005; Xie et al. 2012) correlations and linear relationships between coagulant dose and organic carbon (Edzwald and Van Benschoten 1990; Lefebvre and Legube 1990; Shin et al. 2008; White et al. 1997) or alkalinity (Tseng et al. 2000) have been developed to predict treatability, but these models are typically able to predict only one variable, such as minimum coagulant dose or coagulation pH.

Previous research has indicated that surface complexation models (SCMs) are capable of making accurate predictions of contaminant sorption, including removal of arsenic (Boccelli et al. 2006; Chen et al. 2005; Luxton et al. 2006; Wilkie and Hering 1996), silica (Davis et al. 2002; Luxton et al. 2006; Sigg and Stumm 1981; Swedlund and Webster 1999), and organic acids (Evanko and Dzombak 1999; Pommerenk 2001). Langmuir-based equations, which are simplified SCMs, have proven useful for predicting removals of the sorbable dissolved organic carbon (DOC) fraction (Edwards 1997; Kastl et al. 2004) and even for predicting critical coagulant dose during full-scale treatment at individual treatment plants (Tseng and Edwards 1999). Stumm and Sigg (1979) applied an SCM approach to predict sorption and particle stability, but the focus of their work was limited to phosphate removal, and the model was not experimentally validated. Other efforts to apply SCM to coagulation have not developed the ability to predict particle destabilization, which is necessary to achieve effective particle and contaminant removal. The practical usefulness and accuracy of prior models of DOC or arsenic removal have been limited by the necessary assumption that coagulation would effectively remove particles with sorbed contaminants, regardless of dose.

An SCM with the capability to predict combinations of coagulant dose and pH leading to effective contaminant removal and successful particle destabilization would represent a significant

advance in understanding and yield benefits for practitioners. Such predictive ability would assist engineers in evaluating the treatability of water sources and in optimizing treatment conditions. Operators would benefit from a coagulation model that limits dependence on jar tests, especially during storm events when water quality can change rapidly. Additionally, a coagulation model may prove useful in developing maximum contaminant levels (MCLs) in future regulations that rely on coagulation and assist in explicitly considering costs associated with pH adjustment, residual disposal, and corrosion control.

It is further anticipated that a coagulation model would function as a tool to investigate phenomena that have been observed in practice. Examples of such observations include the role of calcium in improving coagulation and NOM removal (Davis and Edwards 2014b; Dempsey and O'Melia 1983; Dowbiggin and Singer 1989; Duan et al. 2012; Kaegi et al. 2010; Weng et al. 2005); interference with NOM sorption attributable to silica (Davis and Edwards 2014a; Davis et al. 2001; Tipping 1981); and linear correlations between optimal coagulant concentration (OCC) and organic carbon (Edzwald and Van Benschoten 1990; Lefebvre and Legube 1990; Shin et al. 2008; White et al. 1997) and alkalinity (Tseng et al. 2000). Modeling could also be used to explore the influence of water quality on the effectiveness of coagulation. For instance, Randtke and Jepsen (1981) studied the removal of NOM from a groundwater characterized by high alkalinity, high hardness, and moderately high silica. They then extracted fulvic acid (FA) from the groundwater NOM and repeated the coagulation experiment in a "synthetic tap water" matrix characterized by low alkalinity, low hardness, and the absence of silica. The two experiments produced different relationships between final total organic carbon (TOC) and coagulant dose, and the investigators attributed the variation to differences between groundwater NOM and the extracted FA. However, the possible role of the differing concentrations alkalinity, hardness, and silica was not considered.

The overarching goal of this research was the formulation, calibration, assessment, and application of a robust coagulation model. An SCM was formulated and calibrated to data derived from laboratory experiments that examined the effects of pH and water composition on zeta potential and the sorption of DOC, silica, and calcium. Thereafter, the model's accuracy and limitations were explored with an independent data set collected during jar tests of nine U.S. source waters (Singer et al. 1995). Finally, model simulations were executed to demonstrate the capabilities of the model as a predictive tool and to explore explanations for practical observations from the literature.

Materials and Methods

The diffuse layer model (DLM) was selected for this study because it is the simplest SCM capable of predicting both sorption and particle destabilization at the lower ionic strengths encountered in natural waters (Dzombak and Morel 1990). Preliminary efforts to develop a DLM for ferric coagulation demonstrated that it was possible to accurately predict DOC removal with a very basic DLM that only considered the surface acidity of hydrous ferric oxide (HFO) and NOM complexation. This observation suggests that variability in water quality and NOM character is not a critical factor in predicting DOC removal, a result that is consistent with the accuracy of the simplified Langmuir-based models proposed by Edwards (1997) and Kastl et al. (2004). However, attempts to use the preliminary model to identify OCCs for particle destabilization were unsuccessful for most waters. A set of experiments was therefore devised to investigate the influence of water quality—specifically pH, calcium, and silica—on the coagulation of NOM.

Data collected during these experiments guided the selection of model species and served as the data set to which the model was calibrated.

Stock Solutions

FA was isolated from Silver Lake, which serves as a source water for Boulder, Colorado. The extraction method is described elsewhere (Davis and Edwards 2014b). The charge density (meq/g C) of the FA was estimated by titration from ambient pH to pH 8 (Figure B-1). Titrations were conducted on carbonate-free solutions with TOC concentrations of 2.21 mg/L and 10.98 mg/L.

Stock solutions of $CaCl_2$, Na_2SiO_3, $NaNO_3$, and $FeCl_3$ were prepared using reagent-grade chemicals. The $CaCl_2$ (0.50 M), Na_2SiO_3 (0.13 M), and $NaNO_3$ (4.12 M) solutions were prepared by dissolving the salt in distilled water. $FeCl_3$ (8.59×10^{-3} M) was dissolved in 0.01-M HNO_3 to prevent precipitation in the stock solution. HNO_3 and NaOH solutions of varying concentrations (0.01-0.2 M) were used for pH adjustment.

Experimental Procedure

Single-sorbate experiments with FA (2 or 10 mg/L as TOC) and SiO_2 (10 or 50 mg/L) were conducted to measure the extent of sorption and the corresponding effect on surface potential (Table 4-1). Thereafter, dual-sorbate experiments were completed to examine competition between FA and SiO_2. A second set of dual-sorbate experiments investigated the influence of Ca^{2+} (40 mg/L) on FA sorption at both concentrations (2 and 10 mg/L as TOC) (Table 4-1). Each set of experiments was conducted at pH 5.5, 6.5, and 7.5.

Table 4-1. Experimental Sorbate Concentrations

Experiment Description	pH	TOC (mg/L)	SiO_2 (mg/L)	Ca^{2+} (mg/L)
Single-sorbate				
Fulvic Acid only	5.5, 6.5, 7.5	2, 10		
SiO_2 only	5.5, 6.5, 7.5		10, 50	
Dual-sorbate				
Fulvic Acid + SiO_2	5.5, 6.5, 7.5	2, 10	10, 50	
Fulvic Acid + Ca^{2+}	5.5, 6.5, 7.5	2, 10		40

Experiments were conducted in 500-mL HDPE bottles with distilled water. Temperatures varied between 22°C and 26°C. $NaNO_3$ was added to each sample to provide a background ionic strength of 0.01 M. Samples were prepared with target sorbate concentration(s) and allowed to equilibrate for approximately 12 hours. A t=0 aliquot was taken to measure initial DOC. To initiate an experiment, a sample was dosed with $FeCl_3$, and pH was immediately adjusted to the target. Once pH was stabilized to within 0.05 pH units of the target, 10 mL of solution were withdrawn for zeta potential analysis. At this point, an additional control sample was taken to establish the total concentrations of Fe, Si, and Ca in the sample; this control sample was not filtered but was digested according to the method of Parks et al. (2004).

Thereafter, sampling was conducted at 0.5 h, 4 h, and 24 h. At each sampling event, pH was measured and re-adjusted, if necessary, and zeta potential was analyzed. Approximately 50 mL of sample were filtered through a 0.45-μm nylon filter held within a reusable syringe filter holder; the volume of filtrate was determined by measuring its mass. After filtration, the nylon filter was removed and placed in a 25-mL HDPE bottle with 10 mL of distilled water and digested. Filtrate samples were analyzed for DOC, Si, Ca, and Fe; digestate samples were analyzed for Si, Ca, and Fe. During $FeCl_3$ dosing and sample collection, the samples were stirred with a magnetic bar and stir plate. Between sampling events, the samples were mixed on an end-over-end rotary agitator (Analytical Testing Corp., Warrington, PA).

Instrumentation

Zeta potential was measured with a Malvern ZetaSizer 3000HS (Malvern Instruments Inc., Westborough, MA). The performance of the instrument was verified using the manufacturer's electrophoresis standard and by comparative measurements with a Zeta Meter 3.0+ (Zeta Meter Inc., Staunton, VA). Additional details are provided elsewhere (Davis et al. 2001). DOC was measured with a Sievers Model 800 TOC Analyzer using the persulfate-ultraviolet oxidation according to Standard Method 5310C (Eaton et al. 2005). Fe, Ca, and Si concentrations were measured by a Thermo Electron X-Series inductively coupled plasma with mass spectrometer (ICP-MS) per Standard Method 3125B (Eaton et al. 2005). Samples and calibration standards were prepared in a matrix of 2% HNO_3 by volume.

Model Formulation and Calibration

The model includes a total of 19 surface species (Table 4-2). Complexation constants were optimized in FITEQL 4.0 (Herbelin and Westall 1999). Ionic strength and activity coefficients were calculated in FITEQL 4.0 using the Davies equation.

NOM Solution Reactions

Although NOM is known to exist as complex, heterogeneous mixtures in natural waters, the model assumes a general triprotic acid of the form H_2A^-.

$$H_2A^- \rightleftharpoons HA^{2-} + H^+ \qquad K_{a,2\_NOM} \tag{4-1}$$

$$H_2A^- \rightleftharpoons A^{3-} + 2H^+ \qquad K_{a,3\_NOM} \tag{4-2}$$

A molecular weight (MW) of 500 g/mol and humic organic carbon fraction of 45% are assumed, yielding a humic organic carbon content (HOCC) of 225 g C/mol H_2A^-. On the basis of experiments performed at the highest coagulant-to-DOC ratio (5 mg Fe:1 mg DOC) and lowest pH (5.5) used in this study, the fraction of non-sorbable DOC was set at 65%. Values of the dissociation constants, $K_{a,2\_NOM}$ and $K_{a,3\_NOM}$ (Table 4-2), were selected to fit the organic charge of the FA (Figure B-1).

In solution, NOM is capable of binding calcium. The formation of Ca-NOM complexes neutralizes negative organic charge (Bose and Reckhow 1997; Dempsey and O'Melia 1983) and increases the size of humic networks via supramolecular aggregation (Baalousha et al. 2006). Ca-NOM complexation aids ferric coagulation under some conditions by mitigating NOM's

Table 4-2. Solution and Surface Complexation Reactions with Equilibrium Constants

Equation	Species	Reaction	Log K
Solution Reactions			
4-1	FA	$H_2A^- \rightleftharpoons HA^{2-} + H^+$	-3.9
4-2	FA	$H_2A^- \rightleftharpoons HA^{3-} + 2H^+$	-9.9
4-3	$Ca^{2+} - FA$	$H_2A^- + Ca^{2+} \rightleftharpoons HCaA + H^+$	-0.375
4-4	$Ca^{2+} - FA$	$H_2A^- + Ca^{2+} \rightleftharpoons CaA^- + 2H^+$	-6.5
4-5	SiO_2	$H_4SiO_4 \rightleftharpoons H_3SiO_4{}^- + H^+$	-9.5
4-6	SiO_2	$2H_4SiO_4 \rightleftharpoons H_5Si_2O_7{}^- + H^+ + H_2O$	-5.0[1]
4-7	$CO_3{}^{2-}$	$CO_3{}^{2-} + 2H^+ \rightleftharpoons H_2CO_3$	16.76
4-8	$CO_3{}^{2-}$	$CO_3{}^{2-} + H^+ \rightleftharpoons HCO_3{}^-$	10.38
Surface Reactions			
4-9	H^+	$\equiv FeOH + H^+ \rightleftharpoons \equiv FeOH_2^+$	7.29[2]
4-10	H^+	$\equiv FeOH \rightleftharpoons \equiv FeO^- + H^+$	-8.93[2]
4-11	H^+	$\equiv Fe_sOH + H^+ \rightleftharpoons \equiv Fe_sOH_2{}^+$	7.29[2]
4-12	H^+	$\equiv Fe_sOH \rightleftharpoons \equiv Fe_sO^- + H^+$	-8.93[2]
4-13	FA	$\equiv FeOH + H_2A^- \rightleftharpoons \equiv FeHA^- + H_2O$	8.59
4-14	FA	$\equiv FeOH + H_2A^- \rightleftharpoons \equiv FeA^{2-} + H^+ + H_2O$	4.65
4-15	Ca^{2+}	$\equiv Fe_sOH + Ca^{2+} \rightleftharpoons \equiv Fe_sOHCa^{2+}$	4.97[2]
4-16	Ca^{2+}	$\equiv FeOH + Ca^{2+} \rightleftharpoons \equiv FeOCa^{2+} + H^+$	-5.85[2]
4-17	$Ca - FA$	$\equiv FeOH + Ca^{2+} + H_2A^- \rightleftharpoons \equiv FeOH_3CaA^+$	11.47
4-18	$Ca - FA$	$\equiv FeOH + Ca^{2+} + H_2A^- \rightleftharpoons \equiv FeOH_2CaA + H^+$	5.92
4-19	$Ca - FA$	$\equiv FeOH + Ca^{2+} + H_2A^- \rightleftharpoons \equiv FeOHCaA^- + 2H^+$	1.023
4-20	H_4SiO_4	$\equiv FeOH + H_4SiO_4 \rightleftharpoons \equiv FeSiO(OH)_3 + H_2O$	1.27
4-21	H_4SiO_4	$\equiv FeOH + H_4SiO_4 \rightleftharpoons \equiv FeSiO_2(OH)_2{}^- + H^+ + H_2O$	-6.70
4-22	H_4SiO_4	$\equiv FeOH + 2H_4SiO_4 \rightleftharpoons \equiv FeSi_2O_2(OH)_5 + 2H_2O$	8.00
4-23	H_4SiO_4	$\equiv FeOH + 2H_4SiO_4 \rightleftharpoons \equiv FeSi_2O_3(OH)_4{}^- + 2H^+$	0.40
4-24	$CO_3{}^{2-}$	$\equiv FeOH + CO_3{}^{2-} + H^+ \rightleftharpoons \equiv FeOCO_2{}^- + H_2O$	12.78[3]
4-25	$CO_3{}^{2-}$	$\equiv FeOH + CO_3{}^{2-} + 2H^+ \rightleftharpoons \equiv FeOCO_2H + H_2O$	20.37[3]
4-26	$SO_4{}^{2-}$	$\equiv FeOH + SO_4{}^{2-} + H^+ \rightleftharpoons \equiv FeSO_4{}^- + H^+$	7.78[2]
4-27	$SO_4{}^{2-}$	$\equiv FeOH + SO_4{}^{2-} \rightleftharpoons \equiv FeOHSO_4{}^{2-}$	3.61[2]

[1] Svensson et al. 1986
[2] Dzombak and Morel 1990
[3] Appelo et al. 2002

interference with Fe hydrolysis and precipitation (Davis and Edwards 2014b; Kaegi et al. 2010). Therefore, the formation and sorption of hypothetical Ca-NOM complexes was included in the DLM.

Because Ca-NOM complexation was not measured in the calibration data set, predictions from the Stockholm Humic Model (SHM) (Gustafsson 2001; Gustafsson 2011) were used as the basis for identifying plausible Ca-NOM species and optimizing the corresponding complexation

constants. The SHM was used to simulate Ca-FA complexation at Ca^{2+} concentrations of 0-4 mM and a DOC concentration of 10 mg/L at pHs 5.5, 6.5, and 7.5. The species HCaA, and CaA^- (Table 4-2) were incorporated into the DLM, and the constants were optimized to approximate SHM predictions (Figure B2a). Calculations of FA charge neutralization attributable to complexed calcium were comparable between the two models (Figure B-2b).

Sorbent Properties

Surface area and site density are expected to vary between experiments because water quality influences Fe hydrolysis, precipitation, and particle properties. In the model, values used by Dzombak and Morel (1990) for surface area (600 m^2/g), site density (0.20 mol sites/mol Fe or 2.26 sites/nm^2), and weak site density (0.005 mol/mol Fe) were initially assumed to apply.

NOM and Calcium Sorption Reactions

In systems without calcium, modeled NOM species include $\equiv FeHA^-$ and $\equiv FeA^{2-}$ (Table 4-2). Single-sorbate data with only FA were used to fit the complexation constants for these species. The optimization procedure yielded a pair of constants that provided excellent prediction of DOC sorption, but failed to accurately predict surface potential. Attempts to vary site density did not improve surface potential predictions.

Since surface potential predictions were more positive than expected on the basis of zeta potential measurements, carbonate sorption was incorporated using constants from Appelo et al. (2002) (Table 4-2). Including the $\equiv FeOCO_2^-$ and $\equiv FeOCO_2H$ species yielded slight improvements in the correlations between measured zeta potential and predicted surface potential, but surface potential predictions were still generally too positive. The log K^{int} constant for $\equiv FeOCO_2^-$ was manually increased from 12.37 to 14.6, and this change improved surface potential predictions for all conditions except low DOC at pH 6.5 (Figure 4-1). Further increases in this constant did not improve the surface potential prediction for the low DOC sample at pH 6.5.

The species of $\equiv FeOH_3CaA^+$, $\equiv FeOH_2CaA$, and $\equiv FeOHCaA^-$ were used to model the sorption of Ca-NOM complexes. In addition, species and constants proposed by Dzombak and Morel (1990) for calcium sorption were used (Table 4-2). The resulting model yields excellent prediction capability for DOC and calcium sorption (Figure 4-2a and Figure 4-3a). Surface potential predictions correlate well with zeta potential measurements, as indicated by agreement in sign (i.e., positive vs. negative potential) and the fact that absolute values of surface potential exceed the absolute values of corresponding zeta potentials (Figure 4-2b).

Silica Sorption Reactions

Silica sorption was modeled using the two monomeric (i.e., $\equiv FeSiO(OH)_3$ and $\equiv FeSiO_2(OH)_2^-$) and two dimeric (i.e., $\equiv FeSi_2O_2(OH)_5$ and $\equiv FeSi_2O_3(OH)_4^-$) surface species (Table 4-2) proposed by Davis et al. (2002). The monomeric complexation constants optimized for the current model are comparable to those in the 2002 model, but those for the dimeric species are 3-5 orders of magnitude lower than the 2002 model. The difference in the optimized complexation constants most likely lies with the lower surface area used in the current model versus the previous version (6.49×10^3 m^2/g). The optimized constants provide satisfactory capability for predicting

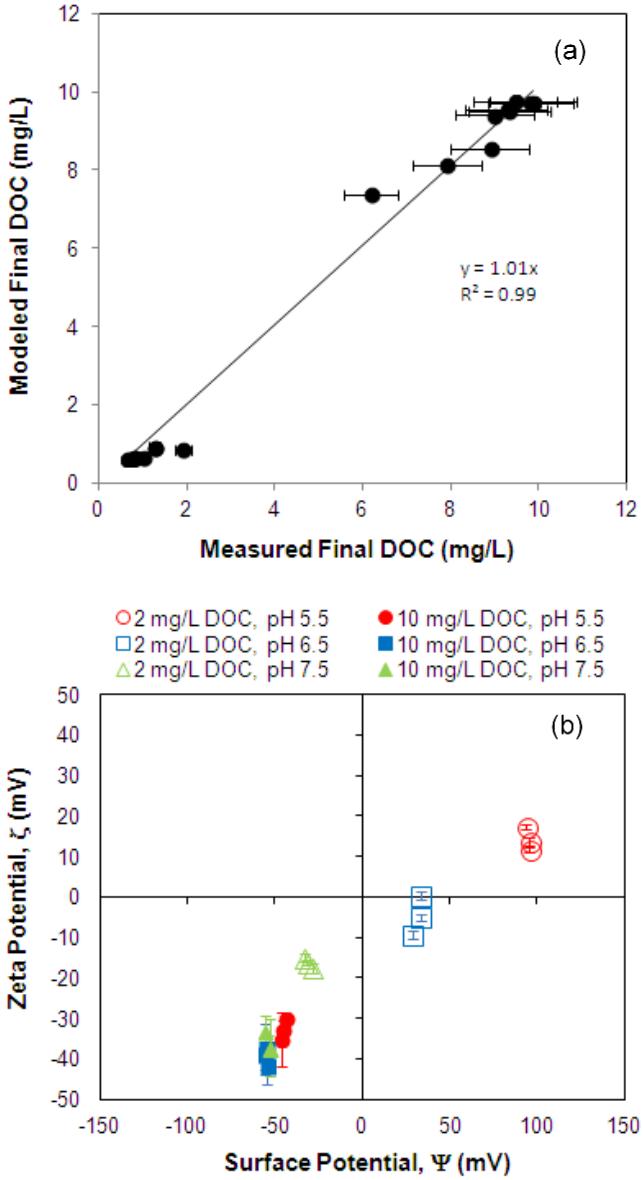

Figure 4-1. (a) DLM prediction of final DOC in single-sorbate samples with fulvic acid (FA) only. Error in TOC measurement is estimated at 10%. (b) Correlation between measured zeta potential and predicted surface potential in single-sorbate samples with FA only.

final DOC, silica sorption density, and surface potential in samples with SiO_2 sorption densities up to 0.6 mol/mol Fe (Figure 4-3b and Figure 4-4).

Swedlund et al. (2010) used Attenuated Total Reflectance-Infared (ATR-IR) spectroscopy and adsorption isotherm data to propose a DLM for silica sorption to ferrrihydrite that employs two monomeric and two trimeric surface species. Swedlund et al.'s (2010) species and best-fit constants were used to model the experimental data in the current study, and while predictions of final DOC and surface potential were acceptable, predictions of silica sorption density were significantly lower than those measured. This difference is likely attributable to the use of digestate concentrations to calculate sorption densities, whereas Swedlund et al.'s (2010) model

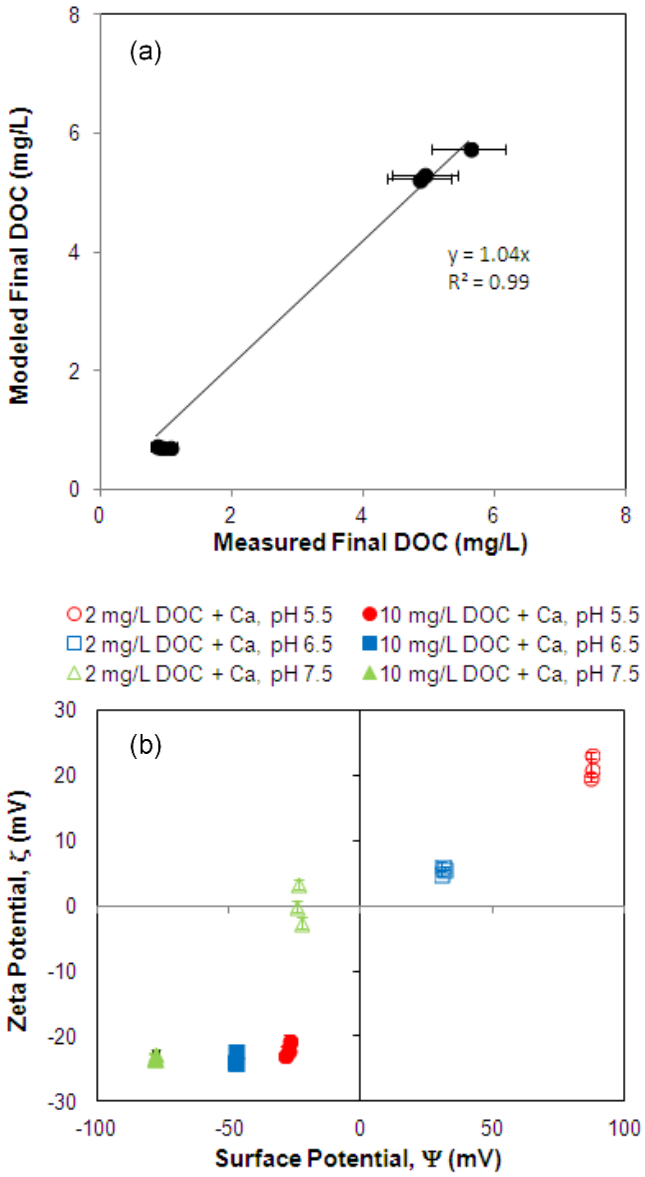

Figure 4-2. (a) DLM prediction of final DOC in dual-sorbate samples with fulvic acid (FA) and 1 mM Ca^{2+}. Error in TOC measurement is estimated at 10%. (b) Correlation between measured zeta potential and predicted surface potential in dual-sorbate samples with FA and 1 mM Ca^{2+}.

was calibrated to filtrate data. For example, in single-sorbate samples with high silica (50 mg/L as SiO_2) and pH 7.5, the Swedlund et al. (2010) model predicts a silica sorption density of 0.18 mol Si/mol Fe, whereas the measured sorption density is 0.47 mol Si/mol Fe in this study. Since the silica complexation reactions originally proposed by Davis et al. (2002) provided a better fit (standard error of 20% or 0.08 mol SiO_2/mol Fe) than the Swedlund et al. (2010) model (standard error of 41% or 0.17 mol/mol Fe), the Davis et al. (2002) species were used in this DLM. While it is possible, and even likely, that the trimeric species employed by Swedlund et al. (2010) are a more accurate representation of oligomeric silica species arrangement, the DLM in the current study emphasizes accuracy in practical predictions, such as sorption density and surface potential.

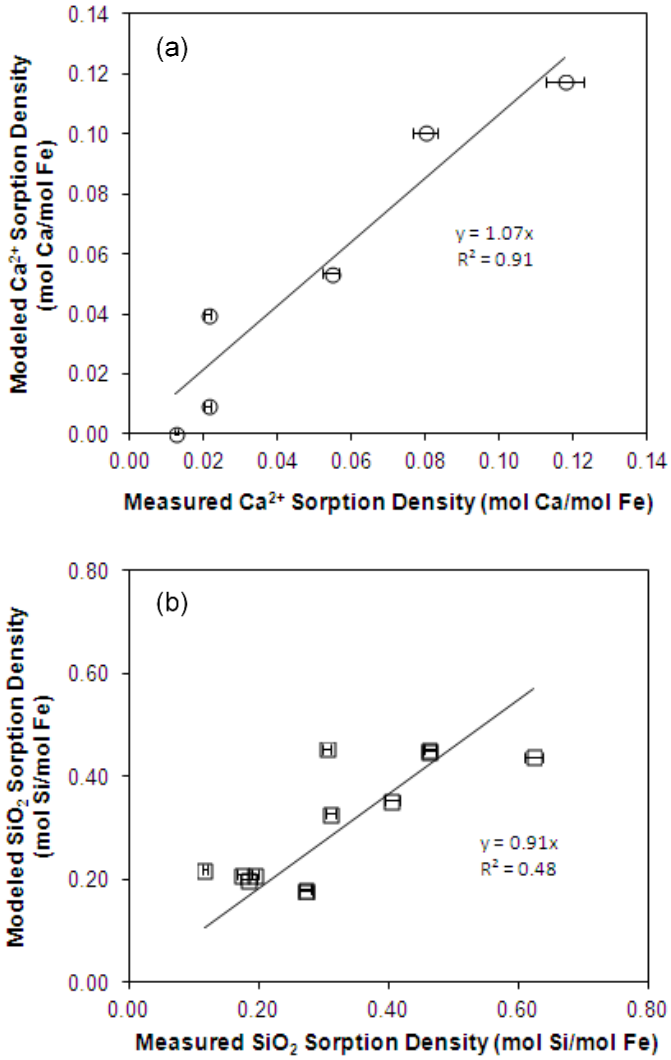

Figure 4-3. DLM prediction of (a) Ca^{2+} sorption density in dual-sorbate samples with fulvic acid (FA) and (b) SiO_2 sorption density in single-sorbate and dual-sorbate samples with FA. All data and predictions are at t=4 h. Measured sorption densities were directly calculated from analyte concentrations in digestate. Error bars assume 3% error in ICP measurement of each analyte.

Model Assessment

The model's predictive capability was assessed using jar test data collected during an enhanced coagulation survey of U.S. waters (Singer et al. 1995). Ferric sulfate was used as the coagulant, and each water represents one of the nine categories in the enhanced coagulation 3x3 matrix. Raw water quality data are provided in Table 4-3. Non-sorbable fractions (Table 4-4) were selected by observing the DOC remaining at the maximum applied coagulant dose in the jar tests conducted by Singer and co-workers (1995).

Since Singer et al. (1995) did not measure zeta potentials (ζ) for this data set, settled water turbidity was used as a surrogate indicator of particle stability. Predicted potentials and settled water turbidities were graphically compared to ensure reasonable consistency between the two

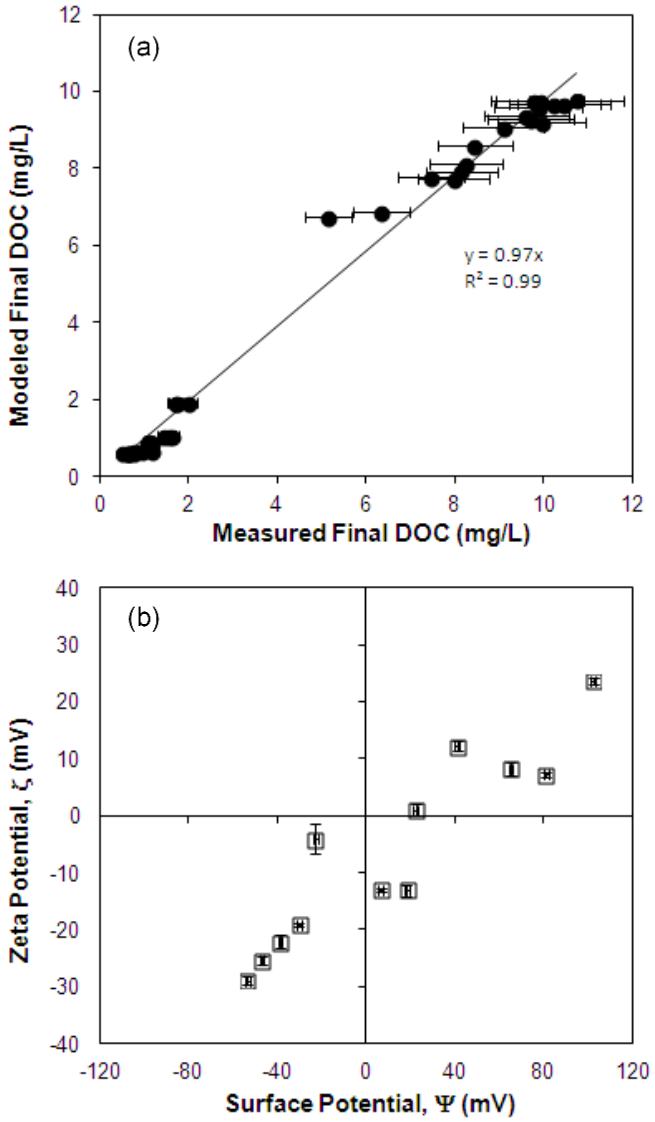

Figure 4-4. (a) DLM prediction of final DOC in dual-sorbate samples with fulvic acid (FA) and SiO_2. Error in TOC measurement is estimated at 10%. (b) Correlation between measured zeta potential and predicted surface potential in single-sorbate SiO_2 samples and dual-sorbate samples with FA and SiO_2. All data and predictions are at t=4 h.

values. This approach assumes that electrostatic destabilization is required for effective aggregation and settling; thus, data points with very low settled water turbidities are believed to correspond to circumneutral surface potential. This assumption is supported by literature indicating that effective particle destabilization and TOC removal typically occur at zeta potentials ranging from -10 to +10 mV (Edwards and Benjamin 1992; Sharp et al. 2006a; Sharp et al. 2006b; Tseng et al. 2000).

While it is impossible to determine the location of the shear plane—the point at which potential is equal to the observed zeta potential (i.e., $\psi = \zeta$)—it is known that the shear plane occurs at some distance from the surface. Therefore, settled water turbidity was also compared to calculated potentials occurring at two points in the diffuse layer, specifically at distances of

Table 4-3. Water Quality Characteristics[1] of Source Waters Comprising the Validation Data Set

Source	pH	Total Organic Carbon (mg/L)	Specific UV Absorbance (SUVA) (L/mg·m)	Alkalinity (mg/L as $CaCO_3$)	Hardness (mg/L as $CaCO_3$)		Silica (mg/L)	Turbidity (ntu)
					Total	Ca		
Low Alkalinity								
Columbus	7.1	2.3	3.0	18	20	14	3	7.2
Flagstaff	7.0	6.1	4.7	26	29	14	19	35
Chesapeake	6.7	25.8	5.1	36	64	40	11	4.5
Moderate Alkalinity								
WSSC	7.7	2.4	2.9	105	149	110	2.2	2.5
Houston	8.5	6.7	3.4	86	67	52	22	24
Tampa	7.2	14.7	4.7	86	106	93	10	0.8
High Alkalinity								
MWD-CRW[2]	8.3	2.6	1.4	123	329	203	9.3	0.9
New Orleans	7.7	4.5	2.8	128	171	111	5.7	58
Ft. Lauderdale	7.3	12.0	3.6	228	249	223	4.2	1.8

[1]Singer et al. 1995
[2]Metropolitan Water District-Colorado River Water

Table 4-4. Source-Specific Model Parameters and Optimal Coagulant Concentrations

Source	Non-sorbable Fraction	Optimized Site Density (mol/mol Fe)	Optimal Coagulant Concentration (OCC) Range (mg/L as Fe)	
			Observed from Reduced Turbidity	Predicted from Potential-0.50 between -5 and 0 mV
Low Alkalinity				
Columbus	47.8%	0.15	5.58 – 7.37	5.58
Flagstaff	38.3%	0.15	11.06 – 12.73	14.52
Chesapeake	26.9%	0.30	not available	not available
Moderate Alkalinity				
WSSC	54.2%	0.15	9.27	7.37 – 9.27
Houston	36.9%	0.15	23.23 – 26.69	25.02
Tampa	23.8%	0.35	28.15	28.15
High Alkalinity				
MWD-CRW	68.0%	0.20	not available	19.88
New Orleans	47.1%	0.20	12.84 – 16.31	14.63
Ft. Lauderdale	63.8%	0.35	12.84 – 14.63	18.21

25 percent (Potential-0.25) and 50 percent (Potential-0.50) of the double layer "thickness" (κ^{-1}). The potential (ψ_x) at some distance from the surface (x) is related to the surface potential (ψ_0) by Guoy-Chapman theory (Hiemenz 1986):

$$\frac{exp\left(ze\psi_x/2kT\right)-1}{exp\left(ze\psi_x/2kT\right)+1} = \frac{exp\left(ze\psi_0/2kT\right)-1}{exp\left(ze\psi_0/2kT\right)+1} exp(-\kappa x) \quad (4\text{-}28)$$

where: z = valence of the symmetrical electrolyte
e = electron charge (1.602 x 10^{-19} C)
k = Boltzmann constant (1.3805 x 10^{-23} J/K)
κ = Debye parameter = $\left(\frac{2F^2 I \times 10^3}{\varepsilon\varepsilon_0 RT}\right)^{1/2}$
I = ionic strength (mol/L)
ε = relative dielectric constant of water (78.5 at 25°C)
ε_0= permittivity of free space (8.854 x 10^{-12} $C^2/J \cdot m$).

Model predictions of final DOC and potential were compared to DOC and turbidity measurements collected by Singer et al. (1995). In the initial model run, the assumed surface area and site density were set to the same values used in model calibration (i.e., 600 m^2/g and 0.20 mol/mol Fe, respectively). With the exception of Houston, waters with moderate or high alkalinity had surface potential predictions that were deemed too negative to be reasonable (< -17.7 mV) in the region of particle destabilization. Various combinations of surface area (500-900 m^2/g) and site density (0.20-0.60 mol/mol Fe) were evaluated, but the resulting surface potential predictions consistently appeared too negative to be plausible for waters from WSSC, Tampa, MWD-CRW, New Orleans, and Ft. Lauderdale.

Since alkalinity was implicated as a factor in the excessively negative surface potential predictions, the log K^{int} constant for $\equiv FeOCO_2^-$ was reset to the value of 12.37 published by Appelo et al. (2002) for subsequent model runs (Table 4-2). Recognizing that surface area may vary as a function of water quality, it was assumed to be 600 m^2/g. With surface area fixed, site density was varied between 0.15 mol/mol Fe (1.70 sites/nm^2) and 0.35 mol/mol Fe (3.96 sites/nm^2).

With the change in the $\equiv FeOCO_2^-$ sorption constant and the variation in site densities, model predictions of potential were consistent with Singer et al.'s (1995) turbidity measurements for seven of the nine waters (Figure 4-5, Figure C-1, and Figure C-2). Most waters have an optimized site density of 0.15 or 0.20 mol/mol Fe, but high site densities (0.30-0.35 mol/mol Fe) were required to approach circumneutral potentials in waters with exceptionally high TOC levels (i.e., Ft. Lauderdale, Tampa, and Chesapeake) (Table 4-4). Evaluation of surface potential predictions for MWD-CRW water was impossible since all turbidity measurements were less than 2 NTU, and the data did not reveal the OCC for Chesapeake since turbidity remained very high (27 NTU) at the highest tested dose (37.86 mg/L as Fe).

For the remaining seven waters, OCCs from turbidity data were compared to OCCs selected on the basis of predicted potentials. Observed OCCs are presented as ranges of tested doses at which turbidity is substantially reduced and further increases in dose do not appear to appreciably decrease turbidity. Predicted OCCs based on potential were selected by identifying doses at which the calculated Potential-0.50 is in the range of -5 to 0 mV (Table 4-4). Comparing OCCs selected by these independent methods reveals a strong linear correlation (R^2=0.96; m=1.05) and validates the accuracy of the model for predicting particle destabilization (Figure 4-6).

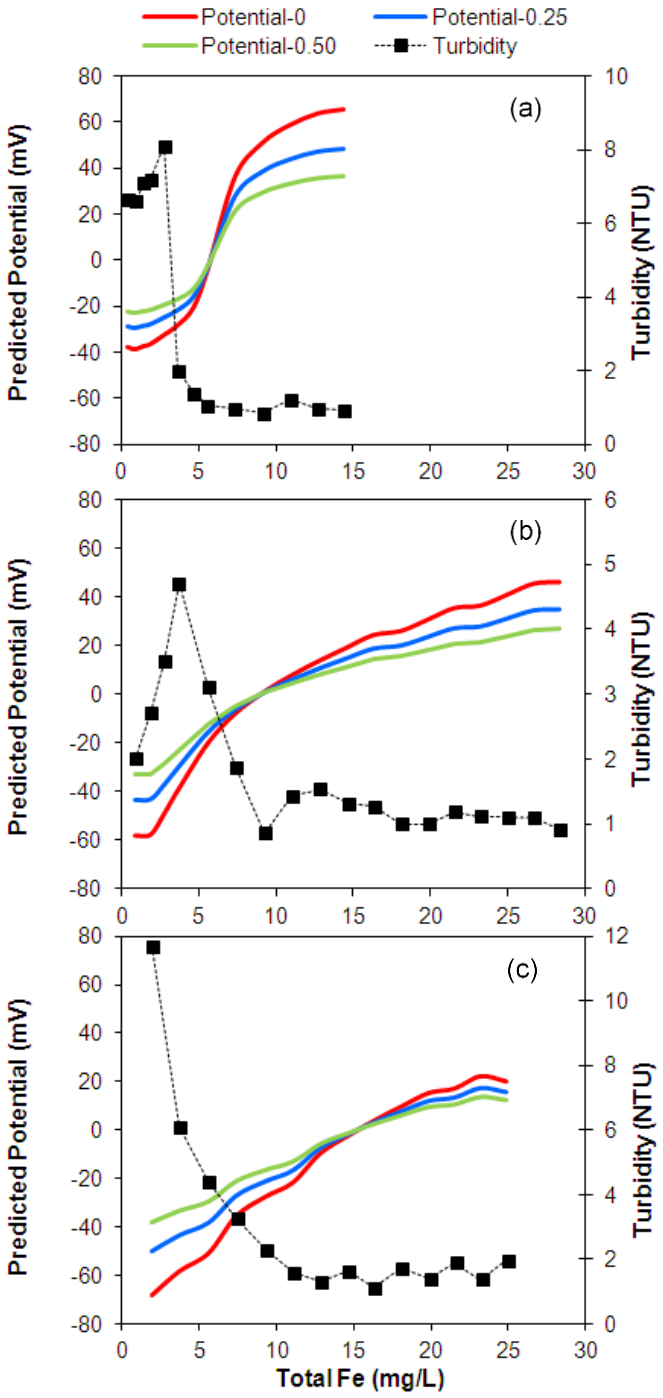

Figure 4-5. Measured turbidities and predicted potentials at the surface (Potential-0) and at 25% and 50% of the double-layer "thickness" (Potential-0.25 and Potential-0.50, respectively) for (a) Columbus, (b) WSSC, and (c) New Orleans.

Early approaches to predicting coagulant dose relied upon linear relationships between initial turbidity and coagulant demand (Stumm and O'Melia 1968), but later work demonstrated that demand attributable to turbidity was often insignificant compared to that of NOM (Edzwald

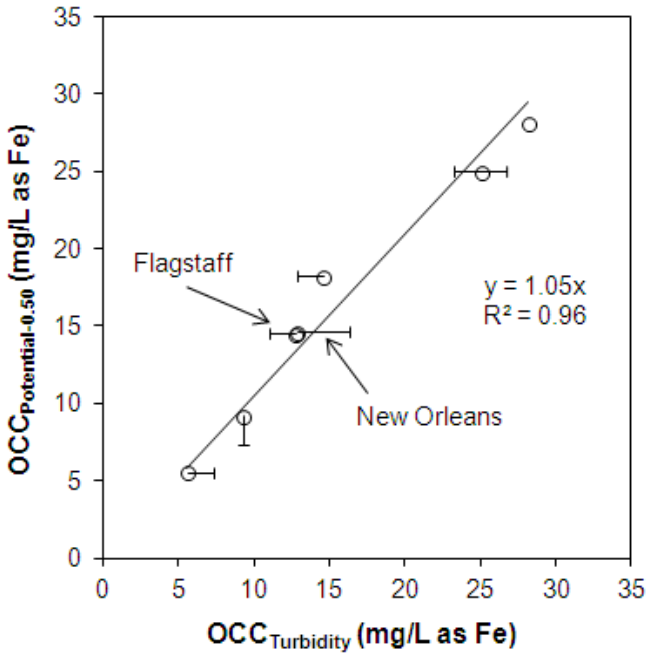

Figure 4-6 Correlation between optimal coagulant concentrations (OCCs) predicted by Potential-0.50 and turbidity measurements. Error bars represent ranges of possible OCCs in waters where a single OCC could not be readily identified. Turbidity OCCs were selected by visual inspection. $OCC_{Potential\text{-}0.50}$ was selected as doses with predicted Potential-0.50 between -5 mV and 0 mV.

and Van Benschoten 1990; Shin et al. 2008; Tseng et al. 2000). Consistent with this observation, a linear regression verifies that there is no relationship between observed OCC and initial turbidity (R^2=0) in the current work, supporting the decision to exclude turbidity as a source of coagulant demand in model development. At both the observed and DLM-predicted OCCs, measured and predicted TOC removals exceed required removals under the Stage 1 Disinfectant and Disinfection Byproducts Rule, consistent with the conceptualization that effective TOC removal is dependent upon particle destabilization.

Various researchers have developed stoichiometric guidelines for estimating OCC as a linear function of initial DOC concentration (Edzwald and Van Benschoten 1990; Lefebvre and Legube 1990; Shin et al. 2008; White et al. 1997) or initial DOC and alkalinity (Tseng et al. 2000). Although some of these linear relationships exhibit high correlations ($R^2 \geq 0.79$) (Shin et al. 2008; Tseng et al. 2000; White et al. 1997), they are typically limited to a single pH or narrow pH range. Furthermore, many of these stoichiometric guidelines were developed for synthetic waters and are not readily applicable to natural waters. When observed OCCs (Table 4-4) were plotted against initial DOC for the seven natural waters in this analysis, linear regression yielded the relationships:

$$OCC_{Turbidity}\left(\frac{mg}{L} as\ Fe\right) = 2.0 \cdot DOC_0\left(\frac{mg}{L}\right) \qquad R^2=0.30 \qquad (4\text{-}29)$$

$$OCC_{Turbidity}\left(\frac{mg}{L} as\ Fe\right) = 1.3 \cdot DOC_0\left(\frac{mg}{L}\right) + 7.0 \qquad R^2=0.57 \qquad (4\text{-}30)$$

The form of Equation 4-29 is frequently encountered in the literature, and although the observed slope of 2.0 agrees with Lefebvre's and Legube's (1990) stoichiometric dose for Fe coagulation at

pH 5.5, the correlation is quite low (R^2=0.30). Equation 4-30 adds a y-intercept of 7.0 mg Fe/L, which accounts for some of the unknown source(s) of coagulant demand and increases the R^2 value to 0.57. However, the overall poor correlations for Equations 4-29 and 4-30 suggest that initial DOC explains only 30%-57% of the variation in observed OCC for the natural waters in the Singer et al. (1995) data set. In contrast, a linear regression of $OCC_{Turbidity}$ as a function of DLM-predicted OCC yields:

$$OCC_{Turbidity}\left(\frac{mg}{L}as\ Fe\right) = 0.95 \cdot OCC_{Potential-0.50}\left(\frac{mg}{L}\ as\ Fe\right) \quad R^2=0.97 \tag{4-31}$$

By incorporating coagulation pH, sorbable DOC fraction, Ca-NOM complexation, sorption of inorganic ligands, and surface potential, the DLM extends the accuracy and capability of prior models for predicting OCC by 40%-67% (Figure 4-6).

As a fitting parameter, site density influences predictions of both potential and DOC sorption. When all other variables are held constant, increasing site density (1) increases DOC sorption and (2) increases predicted surface potential at pHs less than the point of zero charge (PZC). Thus, it is not always possible to select an optimum site density that accurately predicts both particle destabilization and DOC sorption. When site densities were optimized to predict particle destabilization in the region where Singer et al. (1995) observed minimal residual turbidity (Table 4-4 and Figure 4-5), the model overpredicted DOC sorption under certain conditions in five of the nine waters. However, the overpredictions in DOC sorption were limited to regions of lower coagulant doses and more negative surface potentials (Figure 4-7b, Figure 4-7c, Figure A3b, Figure A4b, and Figure A4c). In every water, the model predictions of final DOC were in excellent agreement with measurements in the regions of lower residual turbidity and predicted circumneutral surface potential (Figure 4-6 and Figure 4-7).

It is interesting to note that the model did not overpredict DOC sorption in waters with low alkalinity and low calcium. Maximum deviations between model predictions and measured final DOC were 0.25 and 0.20 mg/L of DOC for Flagstaff and Columbus, respectively, and 16% for Chesapeake (Figure 4-7a, Figure C-3a, and Figure C-4a). By contrast, deviations of 23% to 35% were observed for various waters in the moderate and high alkalinity categories of the 3x3 matrix, specifically WSSC, Houston, Tampa, New Orleans, and Ft. Lauderdale (Figure 4-7b, Figure 4-7c, Figure C-3b, Figure C-4b, and Figure C-4c).

Several possible explanations exist for the overpredictions in DOC sorption in certain waters. Factors that may have influenced predictions of DOC sorption include: (1) particle removal, (2) alkalinity, and (3) hardness. In the case of particle removal, the laboratory calibration data and Singer et al.'s (1995) data set were both treated with 0.45-μm filters prior to measuring DOC. However, filtration can be unreliable, particularly at doses where residual turbidity is high and surface potential is very negative. In these situations, it is possible that DOC sorbed to colloidal particles that were not effectively removed by the filtration step in the work by Singer and co-workers. Since the model assumes that 100% of sorbed DOC is removed, inefficiencies in filtration and particle removal can lead to discrepancies between predicted and measured final DOC.

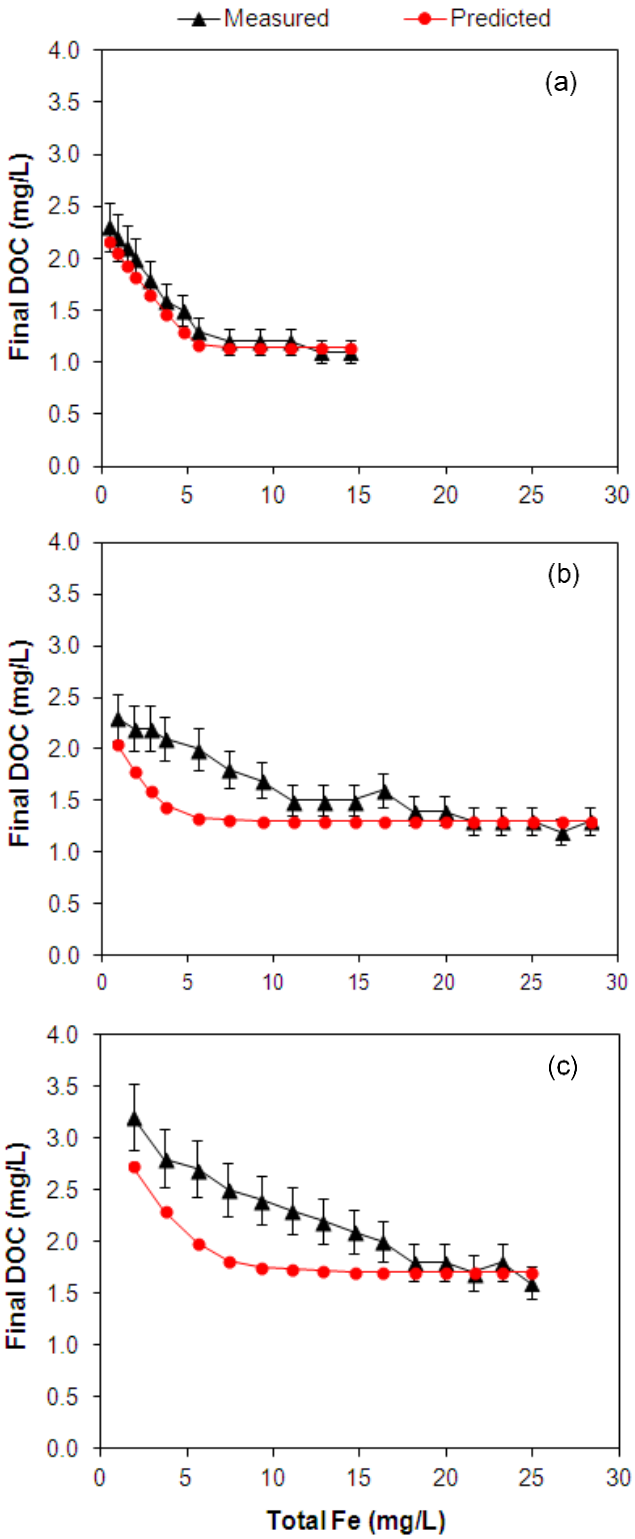

Figure 4-7. The model provides excellent predictions of final DOC in certain waters, such as (a) Columbus. At lower Fe doses, the model overpredicts DOC sorption in waters with moderate and high alkalinity, including (b) WSSC and (c) New Orleans. Error in TOC measurement is estimated at 10%.

It is also plausible that higher concentrations of carbonate alkalinity and/or hardness may have contributed to the apparent overpredictions of DOC sorption in certain waters. If alkalinity is the culprit, it would suggest that carbonate species interfere with DOC sorption to a greater extent than is captured by the model. This hypothesis would be consistent with the observation that DOC overpredictions are not observed in the low-alkalinity waters of Columbus, Flagstaff, and Chesapeake (Figure 4-7a, Figure C-3a, and Figure C-4a). Calcium's roles in the model include (1) direct sorption to the Fe surface and (2) complexation with NOM, followed by sorption of the Ca-NOM complexes. Higher calcium concentrations raise the possibility that the model overpredicts the synergistic effects of Ca-NOM complexation and sorption. However, this scenario is less likely since only one of the problematic waters (i.e., Ft. Lauderdale) has a substantially higher calcium concentration than the 40 mg/L (100 mg/L as $CaCO_3$) used in the calibration data set, yet the model fit the calibration data very well with respect to final DOC, Ca sorption density, and surface potential trends (Figure 4-2 and Figure 4-3a). Furthermore, it is noted that the model does not take magnesium hardness into consideration. If magnesium provides similar synergistic benefits to coagulation and NOM sorption, the differences between predicted and measured final DOC concentrations would be smaller since magnesium would presumably improve NOM sorption in the Singer et al. (1995) data set.

Given the fact that the nine natural waters from the Singer et al. (1995) data set were modeled with only two adjustable parameters (i.e., site density and sorbable DOC fraction), it is not surprising that the model exhibited limitations in its ability to predict NOM sorption in certain regions for five of the waters. Since the DLM is a rather simple model and water quality is known to vary between the source waters, it is actually quite remarkable that the model satisfactorily predicted (1) OCCs in each of the seven waters that demonstrated destabilization (Figure 4-6), (2) final DOC concentrations at coagulant doses coinciding with particle destabilization in those seven waters (Figure 4-8), and (3) final DOC concentration over the entire Fe dose range for four of the waters (i.e., Columbus, Flagstaff, Chesapeake, and MWD-CRW). It is anticipated that the model could be optimized to any particular raw water by characterizing the source-specific NOM and optimizing the related parameters, such as HOCC; sorbable DOC fraction; and organic charge density and the relevant H_2A^- dissociation constants. Further improvements could be expected by optimizing sorption constants for carbonate species and source-specific surface area and site density.

Model Applications

Desktop Testing for Planning and Operations

This model, which simultaneously predicts surface potential and DOC sorption, may serve as a basis for planning and utility operations. A desktop analysis can quickly identify the coagulant dose-pH combinations associated with required TOC removal and particle destabilization and facilitate calculation of costs associated with chemicals and residuals management. A similar analysis could be used to analyze possible treatment adjustments in response to water quality changes arising from seasonal water quality changes or storm events. For example, model simulations were executed to investigate treatment options for a hypothetical storm runoff event in Flagstaff water. At pH 5.5, the simulations suggest that a nearly threefold increase in coagulant dose would be required to achieve particle destabilization in the hypothetical storm event (Figure B-3).

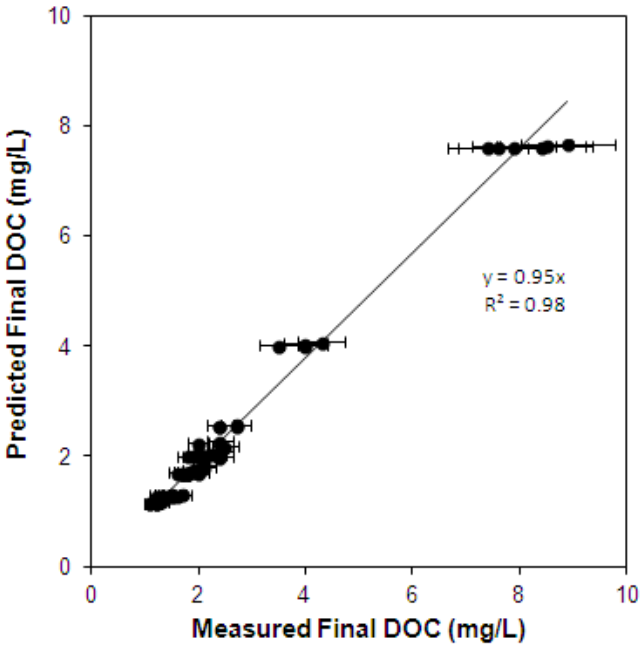

Figure 4-8. Predicted and measured final DOC concentrations for the Singer et al. (1995) data set at points characterized by higher coagulant doses and lower measured turbidities. Error in TOC measurement is estimated at 10%.

Simulations to Improve Understanding

The model can also be applied to answer practical questions about sorbate behavior and interactions during coagulation. For example, model simulations were used to investigate the effects of Fe dose, pH, and varying sorbate concentrations (Table 4-5) on DOC sorption and surface potential. The simulation runs assumed an initial DOC of 4.00 mg/L, a sorbable DOC content of 80% or 3.20 mg/L, a pH range of 5.5 to 7.5, and Fe dose range of 0.50 to 40 mg/L.

Calcium. Previous research has shown that calcium improves the polymerization and aggregation of ferric hydroxides (Davis and Edwards 2014b; Kaegi et al. 2010; Voegelin et al. 2010), forms complexes with NOM (Bose and Reckhow 1997; Dempsey and O'Melia 1983), increases surface potential (Davis and Edwards 2014b; Kaegi et al. 2010; Smith and Edwards 2005), and enhances NOM removal (Davis and Edwards 2014b; Duan et al. 2012; Weng et al. 2005). Consistent with these observations, the model simulations indicate that calcium always improves DOC sorption and under most conditions, yields more positive surface charge compared to waters with only DOC (Figure 4-9, Figure C-5, and Figure C-6). With respect to the coagulation of NOM, the model suggests that calcium's benefits derive from the formation and subsequent sorption of Ca-NOM complexes.

For competitive co-sorbates, interference with DOC sorption can be calculated as:

$$Interference = Final\ DOC_{co-sorbate} - Final\ DOC \quad (4\text{-}32)$$

where: $Final\ DOC_{co-sorbate}$= predicted Final DOC with co-sorbate(s) (mg/L)
$Final\ DOC$= predicted Final DOC in a system with only DOC and Fe coagulant (mg/L)

Table 4-5. Sorbate Concentrations Used in Model Simulations

Set No.	Sorbate Combinations	pH	DOC[(1)] (mg/L)	Ca^{2+} (mg/L)	Carbonate Alkalinity (mg/L as $CaCO_3$)	SiO_2 (mg/L)
Single-sorbate						
1	Fulvic Acid only	5.5, 6.5, 7.5	4.00			
Dual-sorbate						
2	Fulvic Acid + Ca^{2+}	5.5, 6.5, 7.5	4.00	10, 40, 80, 120, 150		
3	Fulvic Acid + Alkalinity		4.00		30, 75, 125, 175, 225	
4	Fulvic Acid + SiO_2		4.00			5, 10, 20, 40, 60
Tri-sorbate						
5	Fulvic Acid + Ca^{2+} + Alkalinity	5.5, 6.5, 7.5	4.00	40, 100	30, 75, 125, 175, 225	

Thus, the calculated value of interference represents the mg/L of DOC that are not sorbed due to the presence of a competitive species. In the case of calcium, which promoted DOC sorption at all calcium concentrations and pHs, values of interference are negative and represent the additional DOC sorbed due to the synergistic influence of calcium (Figure 4-10 and Figure 4-11).

Model predictions of surface speciation at each Fe dose and pH provide some insight into DOC sorption trends. In systems without calcium, the dominant NOM surface species is predicted to be $\equiv FeA^{2-}$. As expected, the prevalence of this species decreases with increasing pH and the accompanying decline in DOC sorption. The percentage of sites as $\equiv FeA^{2-}$ also decreases as dose, and therefore the total quantity of ≡FeOH sites, increases. Yet, $\equiv FeA^{2-}$ is predicted to remain the most significant form of sorbed DOC at all pHs and doses analyzed in systems with only DOC. In this scenario, a maximum of 5% of the total ≡FeOH sites are expected to take the form of $\equiv FeHA^{-}$

In the scenarios with calcium, the percentage of ≡FeOH sites in the form of either $\equiv FeA^{2-}$ or $\equiv FeHA^{-}$ generally decreases as a fraction of NOM sorbs in the form of Ca-NOM complexes. This trend is more apparent as pH and/or calcium concentration increase. Of the three Ca-NOM surface species, $\equiv FeOH_3CaA^{+}$ is predicted to be the most significant at pH 5.5 whereas $\equiv FeOHCaA^{-}$ is expected to be more important at pH 6.0 to 7.5. Although a sizeable fraction of sites still occur as $\equiv FeA^{2-}$, the more positive charge associated with $\equiv FeOHCaA^{-}$ and $\equiv FeOH_3CaA^{+}$ accounts for the surface potential increase observed in systems with calcium (Figure 4-9b) and for the increased synergistic influence of calcium at higher pH (Figure 4-11). It is also interesting to note that calcium's ability to promote DOC sorption is eliminated above a threshold Fe dose between 12 and 27 mg/L, depending upon pH (Figure 4-10). Above this threshold, there is enough Fe surface to remove all sorbable DOC (3.20 mg/L in these scenarios), and sorption of Ca-NOM complexes becomes less significant from the perspective of removal. However, the sorption of

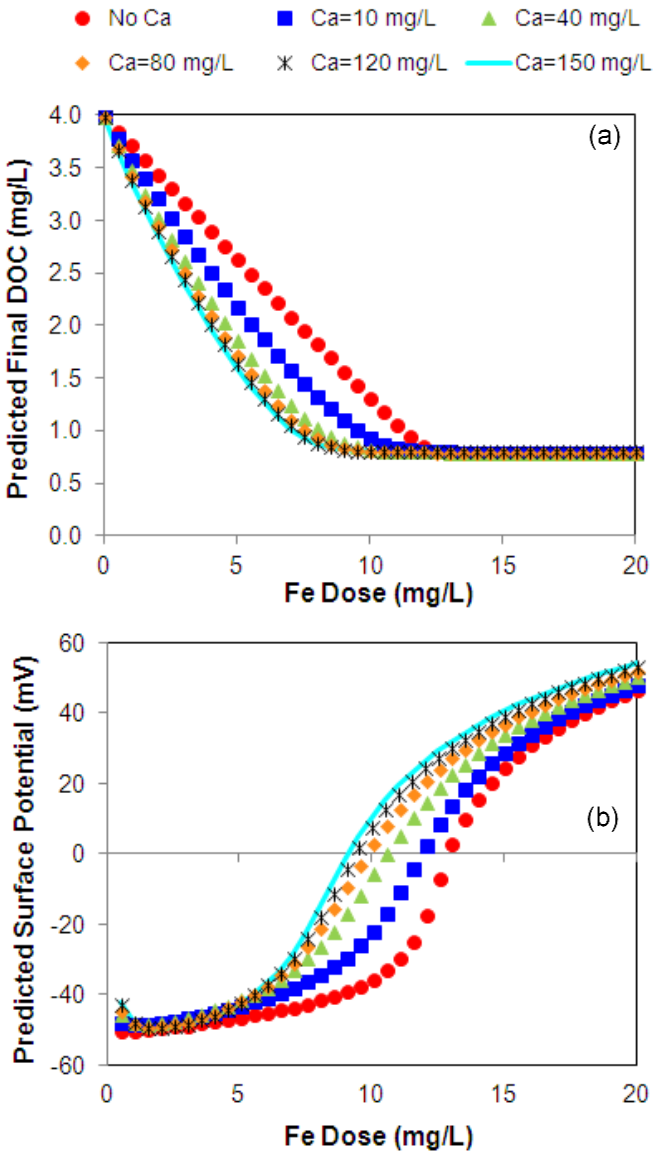

Figure 4-9. (a) Effect of calcium concentration on predicted final DOC. This simulation assumes pH 6.5 and 3.20 mg/L of sorbable DOC. DOC sorption is expected to improve at all calcium concentrations up to a threshold Fe dose of 13.5 mg/L. (b) Predicted surface potential as a function of calcium concentration and Fe dose at pH 6.5. Calcium is expected to decrease the PZC by approximately 10-30%.

calcium species continues to increase surface potential at Fe doses above the threshold for pHs from 6.0 to 7.5 (Figure 4-9b).

Carbonate Alkalinity. Previous studies indicate that carbonate sorbs to iron (hydr)oxide surfaces as an inner-sphere complex and may attain high surface coverages in the absence of competitive sorbates (Villalobos and Leckie 2000; Zachara et al. 1987). Model simulations at pH 6.5 and with varying levels of alkalinity (30-225 mg/L as $CaCO_3$) were consistent with these

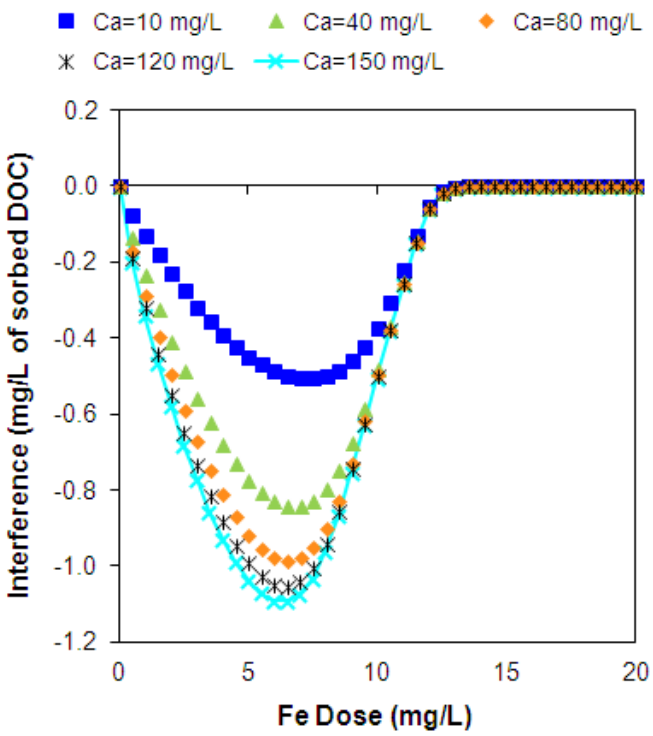

Figure 4-10. Simulated interference with DOC sorption as a function of calcium concentration and Fe dose at pH 6.5. Analysis assumes a sorbable DOC concentration of 3.20 mg/L. Negative values of interference indicate the extent to which calcium promoted DOC sorption compared to a hypothetical water with only DOC and Fe coagulant.

experimental observations and suggested that 37-71% of available ≡FeOH sites could be occupied by carbonate species in the absence of competitive ligands (data not shown).

There is disagreement in the literature regarding carbonate's ability to interfere with the sorption of target contaminants, such as arsenic (Appelo et al. 2002; Holm 2002; Meng et al. 2000; Stachowicz et al. 2007; Zachara et al. 1987), and we are not aware of any studies that have examined direct competition between carbonate and NOM sorption. Thus, model simulations were used to examine the possible effects of carbonate species on coagulation of DOC (Table 4-5, Set No. 3). Predictions indicate that carbonate species are not strongly competitive sorbates, even at high alkalinity concentrations (e.g., 225 mg/L as $CaCO_3$) or pHs up to 7.5 (Figure 4-12a, Figure C-7a, and Figure C-8a). The peak value of interference in simulations was just 0.33 mg/L, or approximately 10% of the sorbable DOC concentration (Figure 4-11).

Although carbonate species do not strongly compete with NOM for sorption sites, model simulations suggest that they may affect coagulation by significantly shifting surface potential curves (Figure 4-12b, Figure C-7b, and Figure C-8b). At pH 6.5, for example, the Fe dose at the PZC increases by 15-54% for alkalinity levels of 75-225 mg/L as $CaCO_3$. Consistent with the observation of Tseng et al. (2000), the model predicts a linear correlation between OCC and alkalinity (Figure B-4). Examination of the predicted surface speciation indicates that surface potential decreases associated with carbonate alkalinity occur at higher Fe doses after the sorbable fraction of DOC (i.e., 3.20 mg/L) is fully removed. As Fe dose increases beyond what is necessary

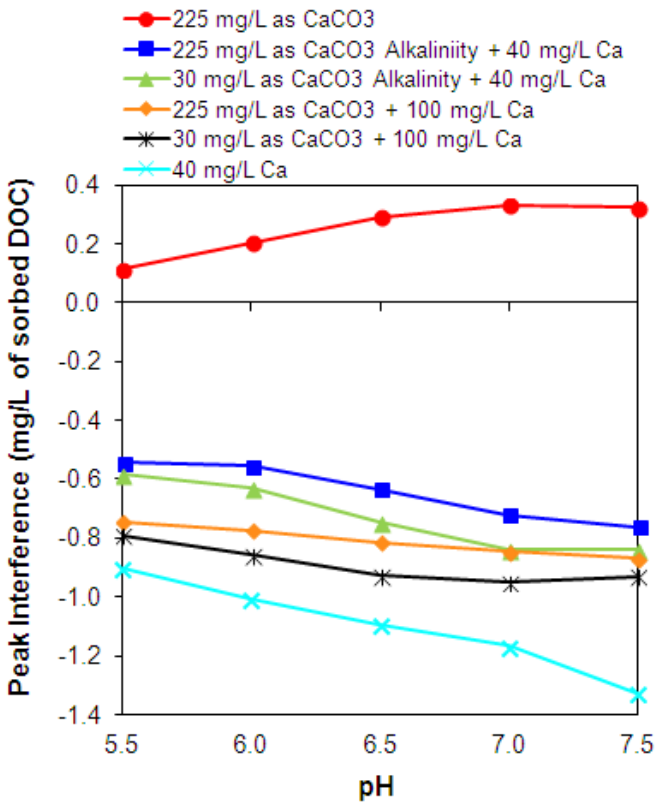

Figure 4-11. Simulated interference with DOC sorption as a function of pH, alkalinity, and calcium concentration. Analysis assumes a sorbable DOC concentration of 3.20 mg/L. Negative values of interference indicate the extent to which calcium promoted DOC sorption compared to a hypothetical water with only DOC and Fe.

to sorb DOC, more Fe surface sites become available for the sorption of the carbonate species $\equiv FeOCO_2^-$ and $\equiv FeOCO_2H$. The result is a decrease in surface potential at higher Fe doses, while carbonate alkalinity appears to have very little effect on sorption or surface potential at lower Fe doses.

While it is instructive to consider the influence of carbonate species in coagulation of DOC, hardness co-occurs with alkalinity in natural waters and is generally correlated with carbonate alkalinity. Considering the nine waters in the Singer et al. (1995) data set, a linear regression yields R^2=0.62 for the relationship:

$$Total\ Hardness\ \left(\frac{mg}{L}\ as\ CaCO_3\right) = 1.37 \cdot Alkalinity\ \left(\frac{mg}{L} as\ CaCO_3\right) \quad (4\text{-}33)$$

and R^2=0.83 for the relationship:

$$Ca\ Hardness\ \left(\frac{mg}{L}\ as\ CaCO_3\right) = 1.04 \cdot Alkalinity\ \left(\frac{mg}{L} as\ CaCO_3\right) \quad (4\text{-}34)$$

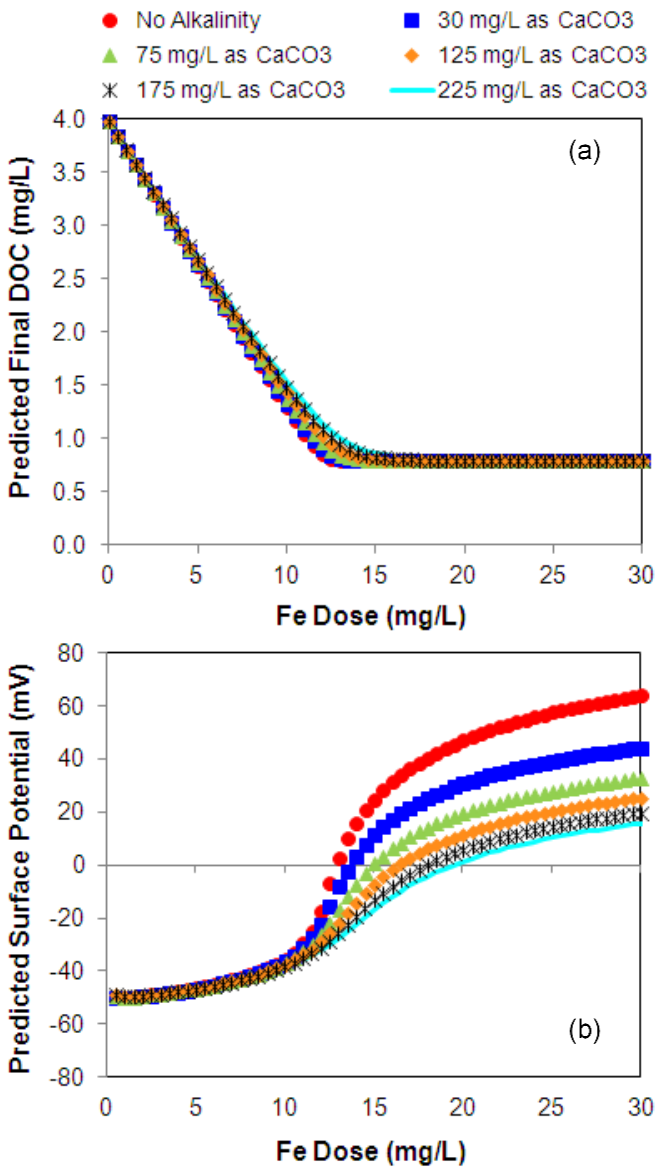

Figure 4-12. (a) Effect of carbonate alkalinity on predicted final DOC. This simulation assumes pH 6.5 and 3.20 mg/L of sorbable DOC. High alkalinity concentrations are associated with slight interference with DOC sorption. (b) Predicted surface potential as a function of carbonate alkalinity and Fe dose at pH 6.5. Alkalinity is expected to increase the PZC by approximately 8-53%.

Thus, a second set of simulations (Table 4-5, Set No. 5) was completed to examine the significance of carbonate species when they co-occur with calcium. Hypothetical calcium concentrations were selected to simulate moderately hard (40 mg/L as Ca) and hard (100 mg/L as Ca) waters since higher alkalinity concentrations (75-225 mg/L as $CaCO_3$) were of primary interest.

Both calcium concentrations effectively eliminated the minor interference with DOC sorption that was observed with alkalinity alone (Figure 4-11). When combined with the highest alkalinity concentration (225 mg/L as $CaCO_3$), both calcium concentrations led to a maximum, but

negligible, interference of 0.05 mg/L of DOC over the entire pH range of 5.5-7.5 (data not shown). At lower coagulant doses (i.e., 5.0-6.5 mg/L as Fe), negative interference, or improvement, with DOC sorption was observed for both calcium concentrations (Figure 4-11).

Although calcium promotes DOC sorption, alkalinity influences surface potential in tri-sorbate systems with NOM, calcium, and alkalinity. The presence of 40 or 100 mg/L of Ca tends to decrease the Fe dose at the PZC in waters with alkalinity $\leq$ 125 mg/L as $CaCO_3$ (Figure 4-13, Figure C-9, and Figure C-10). Compared to simulated waters with only NOM, the combination of calcium and alkalinity yields more positive surface potentials at doses below the PZC; these increases in surface potential are observed because the improved DOC sorption comes in the form of $\equiv FeOHCaA^-$ and at the expense of $\equiv FeA^{2-}$. At Fe doses beyond that necessary to react with the sorbable DOC fraction, sorbed carbonate species, $\equiv FeOCO_2^-$ and $\equiv FeOCO_2H$, become more prevalent and tend to depress surface potential (Figure 4-13, Figure C-9, and Figure C-10).

This simulation analysis indicates that carbonate species do not strongly compete with NOM for sorption sites, and the presence of moderate or high levels of calcium hardness is expected to overcome any minor interference from carbonate alkalinity. However, sorption of carbonate species may strongly influence surface potential and particle stability, depending upon coagulant dose and pH. Consistent with established thought, high concentrations of alkalinity may also hinder DOC sorption by complicating pH control. It is noted that the DLM and this simulation analysis could possibly be enhanced by collecting and using experimental data to validate and/or optimize the carbonate sorption constants proposed by Appelo et al. (2002). It is possible that different sorption constants may suggest scenarios in which carbonate species inhibit NOM sorption through direct competition and/or electrostatic repulsion.

Silica. Aqueous silica is known to inhibit Fe polymerization and growth (Doelsch et al. 2003; Doelsch et al. 2001; Liu et al. 2007), interfere with sorption of NOM to iron (hydr)oxide surfaces (Davis and Edwards 2014a; Davis et al. 2001; Tipping 1981), and form oligomeric complexes on the ferrihydrite surface (Swedlund et al. 2011). A third set of simulations (Table 4-5, Set 4) was therefore completed to investigate the role of aqueous silica in the sorptive removal of NOM. Although activated silica may be used as a coagulant aid (Baylis 1937; Letterman et al. 1999), the model does not reveal any scenario in which aqueous silica improves or promotes DOC sorption. While the effects of aqueous silica on DOC sorption are minor at lower silica concentrations ($SiO_2 \leq 10$ mg/L) and lower pH (5.0-6.0), increasing silica concentration and/or pH generates notable interference (Figure 4-14). At the highest silica concentration (60 mg/L as SiO_2) and pH (7.5) simulated, interference of 2.86 mg/L of sorbed DOC—or 89% of the sorbable DOC—is expected.

Aqueous silica's effect on predicted surface potential also depends on concentration and pH. At lower silica concentrations, lower pH, and lower coagulant doses, silica exerts little influence on surface potential (Figure 4-15a). In this region, the surface is predicted to be dominated by unoccupied $\equiv FeOH_2^+$ and sorbed DOC in the form of $\equiv FeA^{2-}$. As Fe dose increases, the supply of sorbable DOC declines and is ultimately exhausted. In waters without silica, the

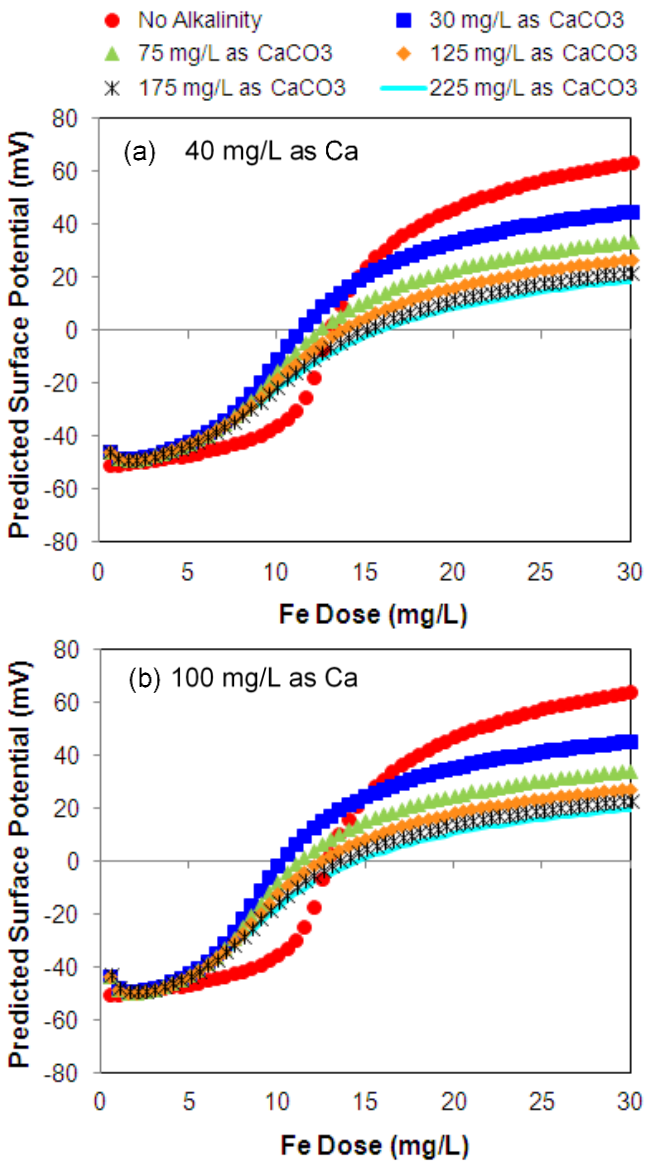

Figure 4-13. (a) The influence of carbonate alkalinity, calcium (40 mg/L), and NOM (3.20 mg/L of sorbable DOC) on predicted surface potential at pH 6.5. (b) The influence of carbonate alkalinity, calcium (100 mg/L), and NOM (3.20 mg/L of sorbable DOC) on predicted surface potential at pH 6.5. In both (a) and (b), sorption of Ca-NOM complexes tends to increase surface potential at lower Fe doses. At higher Fe doses, sorbed carbonate species limit increases in surface potential.

surface acidity reactions (Table 4-2) then control surface speciation and potential as coagulant dose continues to increase. In waters with aqueous silica, silica species begin to sorb in significant concentrations and limit surface potential increases. Model predictions indicate that the neutral dimer, $\equiv FeSi_2O_2(OH)_5$, is predicted to be the dominant silica species, but the negative dimer, $\equiv FeSi_2O_3(OH)_4^-$, occupies up to 10% of the surface sites in some scenarios (e.g., Figure 4-16).

Even at pH 5.5, high silica concentrations (e.g., 40-60 mg/L as SiO_2) can increase the Fe dose associated with the PZC by 44-91% (Figure 4-15a). However, as pH increases, the

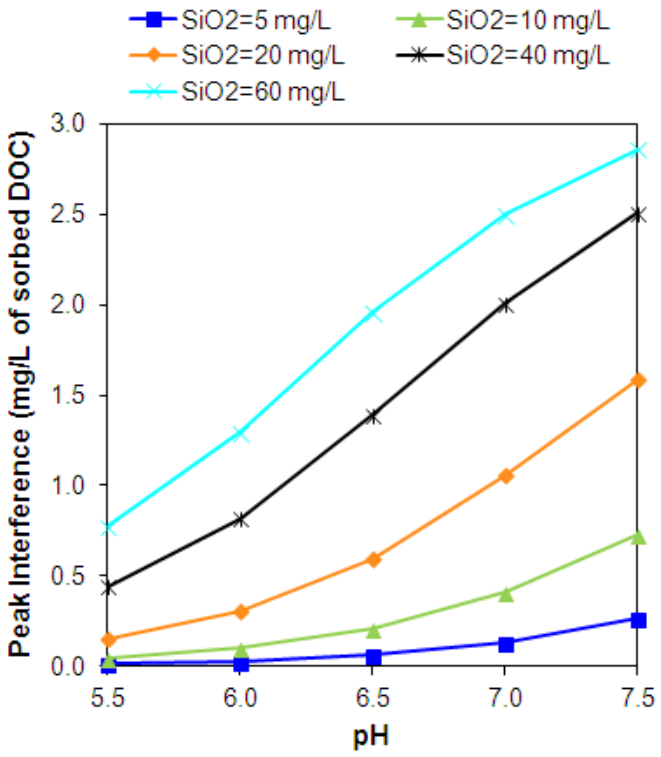

Figure 4-14. Simulated interference with DOC sorption as a function of pH and aqueous silica concentration. Analysis assumes a sorbable DOC concentration of 3.20 mg/L.

concentration of silica required to reduce surface potential decreases. For example, at pH 6.5, the Fe dose required to attain the PZC increases by 23% at 10 mg/L as SiO_2 and by 81% at 20 mg/L as SiO_2; at higher concentrations of 40 and 60 mg/L as SiO_2, surface potential is not predicted to even reach the PZC at the maximum Fe dose simulated (40 mg/L) (Figure 4-15b). Silica's effect is even more striking at pH 7.5, at which only 5 mg/L as SiO_2 is expected to increase the Fe dose at the PZC by 12.5 mg/L as Fe, or 48% (Figure 4-15c). Interestingly, the predicted distribution of surface species at pH 6.5 resembles that at pH 5.5, but at pH 7.5, silica species are highly significant. At 10 mg/L as SiO_2 and pH 7.5, the neutral dimer, $\equiv FeSi_2O_2(OH)_5$, occupies a higher fraction of surface sites than sorbed NOM species. At silica concentrations of 20 mg/L and higher, this species is predicted to dominate the surface, occupying a maximum of 54% of the available surface sites at 20 mg/L as SiO_2 and 83% at 60 mg/L as SiO_2 at pH 7.5. The negative dimer, $\equiv FeSi_2O_3(OH)_4^-$, continues to occupy up to 10% of the sites at pH 7.5, depending on Fe dose. The predominance of silica species on the surface at pH 7.5 suppresses not only sorbed NOM, but also the concentration of $\equiv FeOH_2^+$, yielding a more negative surface.

Multi-sorbate Groundwater. Model simulations are useful in investigating the possible interference from the combined effects of high carbonate alkalinity (324 mg/L as $CaCO_3$), high calcium (59.6 mg/L), and moderately high silica (19.6 mg/L) in the groundwater studied by Randtke and Jepsen (1981). Interference was calculated in a similar fashion as Equation 4-35:

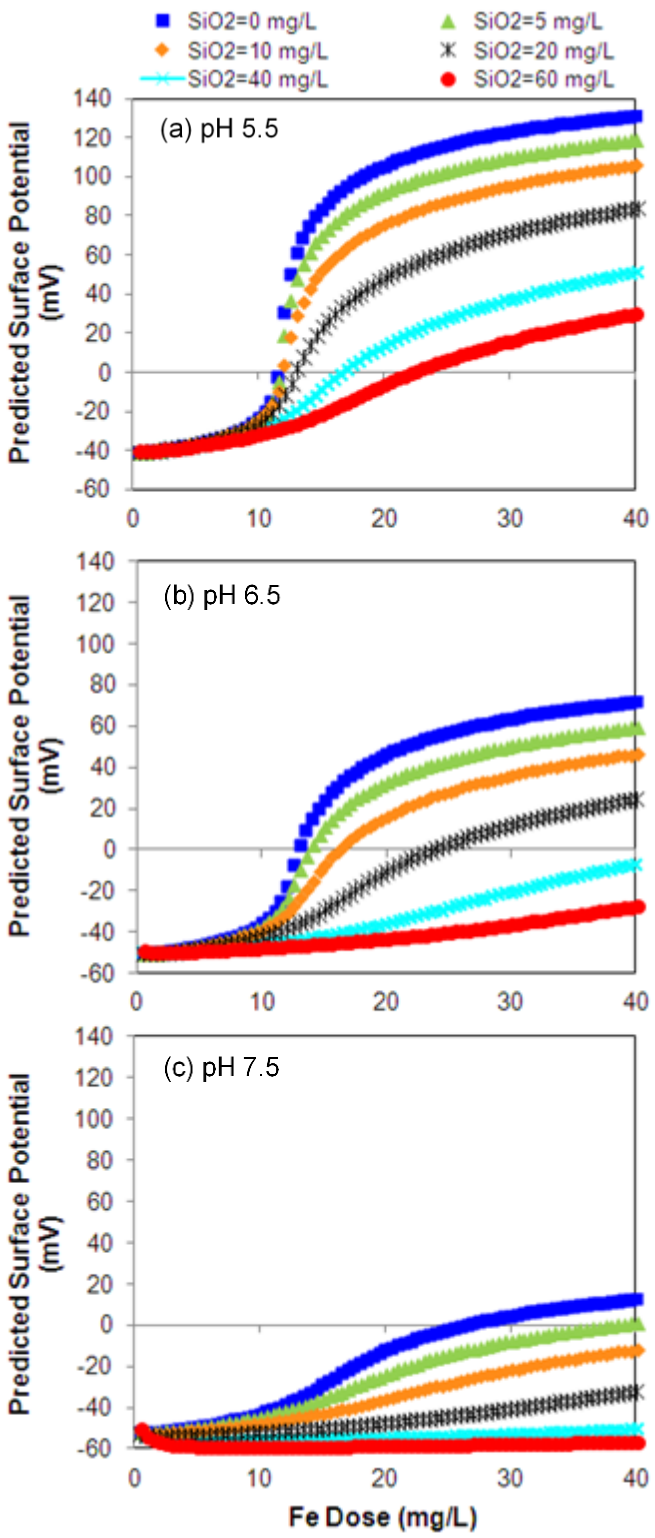

Figure 4-15. The influence of aqueous silica and NOM (3.20 mg/L of sorbable DOC) on predicted surface potential at (a) pH 5.5, (b) pH 6.5, and (c) pH 7.5.

$$Interference = TOC\ Removal - TOC_{co-sorbate}\ Removal \quad (4\text{-}35)$$

where: $TOC\ Removal$ = TOC Removal without co-sorbate(s) (%)
$TOC_{co-sorbate}Removal$ = TOC Removal with co-sorbate(s) (%)

The calculated value of interference represents the percentage of TOC that is not removed due to the presence of carbonate alkalinity, calcium, and/or silica species. Interference with removal is plotted as a function of coagulant dose normalized to the initial TOC concentration (Edwards and Benjamin 1992).

The observed interference for Randtke's and Jepsen's (1981) original experiment was calculated by subtracting TOC removal (%) in the groundwater from TOC removal (%) in the "synthetic tap water" experiment (Figure 4-17). The comparison indicates that TOC removal was higher in the groundwater matrix at lower alum doses (≤0.10 mmol/mmol TOC), whereas groundwater constituents appear to interfere with TOC removal at higher alum doses. With only 10 mg/L of calcium available to neutralize negative FA charge in the "tap water," it is hypothesized that FA extensively complexed aluminum hydrolysis species at low coagulant doses, interfering with coagulation and preventing FA removal (Davis and Edwards 2014b). At a critical coagulant dose between 0.06 and 0.10 mmol Al/mmol TOC, a precipitous decrease in final TOC is observed in the "tap water" experiment. This dose likely represents the threshold at which the FA's charge neutralization/complexation demand is satisfied; beyond this critical dose, aluminum hydroxide precipitation and coagulation proceed efficiently, and FA is effectively removed by adsorption.

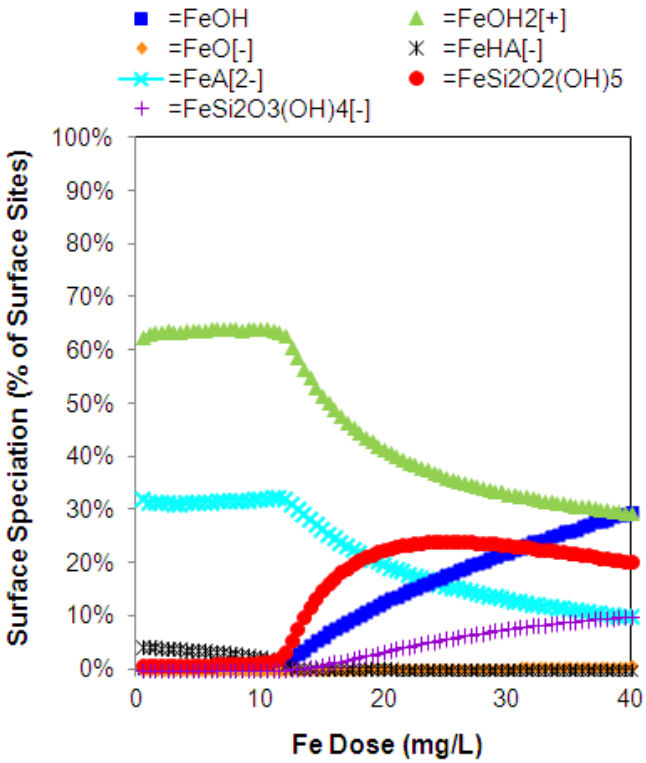

Figure 4-16. Predicted surface speciation at pH 5.5 and 10 mg/L as SiO_2. Analysis assumes a sorbable DOC concentration of 3.20 mg/L. Monomeric silica species, $\equiv FeSiO(OH)_3$ and $\equiv FeSiO_2(OH)_2^-$, are expected to occupy less than 0.05% of surface sites and are excluded.

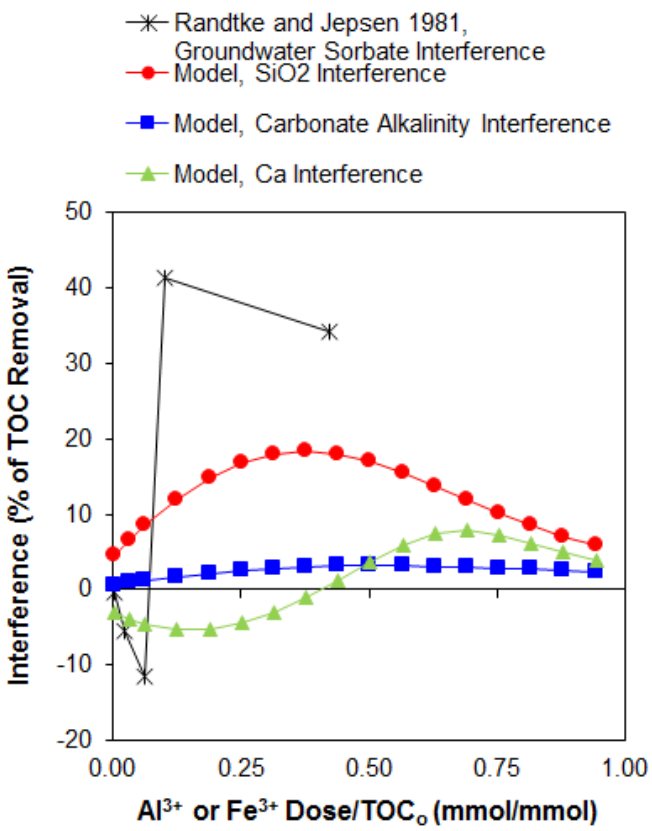

Figure 4-17. Interference in percentage TOC removal as a function of coagulant dose at pH 6.0. The comparison between groundwater and tap water experiments is based on observed data with alum (Randtke and Jepsen 1981). Predicted interference arising from individual co-sorbates in groundwater is based on diffuse layer model (DLM) simulations with ferric coagulant.

NOM removal from the groundwater was better at the low coagulant doses, presumably because the high calcium concentration satisfied most or all of NOM's initial complexation demand, allowing sufficient aluminum hydroxide precipitation and sorption of Ca-FA complexes at low coagulant doses. At the higher alum doses, however, Randtke and Jepsen's (1981) data are consistent with the hypothesis that moderately high silica and/or high carbonate alkalinity in the groundwater interfere with NOM removal.

Model simulations were completed at pH 6.0 to examine the predicted, independent effects of carbonate alkalinity, silica, and calcium on NOM removal from the groundwater. Initial model runs simulating Randtke's and Jepsen's (1981) groundwater data were used to select a non-sorbable TOC fraction of 22.5% (Figure B-5). A surface area of 600 m^2/g and site density of 0.20 mol/mol Fe were assumed. All model simulations were conducted with the initial TOC concentration (3.85 mg/L) used in Randtke's and Jepsen's (1981) groundwater experiment. Since the model is based upon ferric coagulation, predicted interference was calculated by comparing model simulations of TOC removal (%) without the co-sorbate in question to model predictions of Randtke's and Jepsen's (1981) data with groundwater coagulation by ferric sulfate (Figure B-6). In the original study, negligible differences were noted between alum and ferric sulfate performance at pH 6.0 (Randtke and Jepsen 1981).

The simulations predicted interference in TOC removal ranging from 4-18% due to SiO_2 and 0.7-3% attributable to carbonate alkalinity in the groundwater (Figure 4-17). Taken together, the combined, maximum interference in TOC removal from these two ligands is predicted to be 21% at a dose of 0.38 mmol Fe/mmol TOC, suggesting that interference from silica and carbonate alkalinity can explain a majority of the 35% interference in TOC removal that Randtke and Jepsen (1981) observed at this dose. Consistent with Randtke and Jepsen's (1981) data, model simulations predicted that calcium is expected to improve TOC removal by up to 5% at lower coagulant doses (Figure 4-17). In contrast with previous studies indicating that calcium is beneficial for NOM removal (Davis and Edwards 2014b; Dowbiggin and Singer 1989; Duan et al. 2012; Weng et al. 2005), model simulations appear to suggest that calcium contributes to interference with TOC removal at coagulant doses of 0.44 mmol Fe/mmol TOC and higher. However, inspection of the predicted surface speciation does not indicate that calcium acts as a direct source of interference. Rather, the model simulation suggests that calcium promotes the sorption of silica at higher coagulant doses, and extensive surface coverage by silica species is the likely source of interference with TOC removal. Further research is necessary to test this hypothesis.

Conclusions

With only two adjustable parameters—non-sorbable DOC fraction and site density—a general DLM proved successful at predicting DOC sorption and particle destabilization under a wide range of water quality conditions. For synthetic single- and dual-sorbate waters tested at bench scale, the model was calibrated to provide excellent predictions of calcium sorption and adequate predictions of silica sorption. The primary limitation observed with the DLM rested with its capability to predict DOC sorption at lower coagulant doses in waters with higher alkalinity and hardness. The model tended to overpredict DOC sorption in these waters, although it is unclear whether the deficiency should be attributed to carbonate alkalinity, hardness, or inadequate particle separation.

Using the model to simulate treatment of various hypothetical waters suggests that calcium significantly improves DOC sorption across a range of calcium concentrations and pHs. In addition to improving Fe hydrolysis and precipitation, calcium appears to promote NOM sorption in the form of $\equiv FeOHCaA^-$ and $\equiv FeOH_3CaA^+$. Simulations also suggest that carbonate species do not compete with NOM for sorption sites, but may strongly influence surface potential, depending upon alkalinity concentration, pH, and Fe dose. Calcium that co-occurs with carbonate alkalinity eliminates the minor competition between NOM and carbonate species and tends to increase surface potential at lower Fe doses where DOC sorption is critical. However, the model indicates that even in the presence of calcium, carbonate alkalinity may suppress surface potential at Fe doses higher than those required to remove sorbable DOC. Furthermore, calcium has no effect on the pH buffering capability of alkalinity and the associated implications for coagulation. With respect to aqueous silica, model simulations suggest that its effects strongly depend upon pH and silica concentration. At lower concentrations and pH, silica may exert little influence on DOC sorption or surface potential. As concentration and/or pH increase, however, sorbed oligomeric silica concentrations increase and can significantly limit NOM sorption and decrease surface potential.

In previous studies (Randtke and Jepsen 1981; White et al. 1997), reported variations in TOC removal by coagulation were often associated with differences in NOM character. Applying the model to a real groundwater with high carbonate alkalinity, high calcium, and moderately high silica suggests that water quality interferences can explain part of the variation in TOC removal. While confirmation experiments are desirable, this analysis of a multi-sorbate groundwater demonstrates the model's capabilities as a tool for problem-solving and furthering understanding of water quality effects on coagulation.

The DLM could be further optimized to provide better predictions of DOC removal and particle destabilization for a particular source water or blend. Site-specific NOM parameters include the sorbable DOC fraction, MW, humic fraction, and the organic charge density. The sorbent parameters of site density and surface area could be calibrated to data from bench-scale tests that examine the influence of water quality on floc properties. Similarly, the optimum zeta potential or streaming current for a particular source water could be compared to potential predictions to identify the target potential in future modeling runs. It is noted that extreme temperatures affect various aspects of coagulation and sorption processes, and methods for temperature correction are not readily available. End users that are interested in seasonal variations may need to conduct bench-scale studies in the target temperature range and develop temperature-specific equilibrium constants. Example applications for a site-specific DLM include: planning for seasonal or sudden water quality changes; evaluating treatment options for blended water sources; assessing possible treatment strategies while limiting the need for extensive testing; and managing costs associated with chemicals, residuals management, and corrosion control. It is anticipated that such efforts to optimize the DLM for site-specific conditions would yield a powerful tool for planning, design, and operations.

Acknowledgments

We appreciate the contributions of Caitlin Grotke, Samantha Fisher, and Jeffrey Parks, who provided assistance with laboratory experiments and analysis. Certain equipment and supplies were purchased with STAR fellowship funds from the US EPA. While this research was conducted, the first author was supported by graduate fellowships granted by US EPA, Virginia Tech, National Water Research Institute, and the Virginia Water Resources Research Center. The findings are those of the authors and may not reflect the views of these organizations.

References

Amirtharajah, A., Dennett, K. E., and Studstill, A. (1993). "Ferric-Chloride Coagulation for Removal of Dissolved Organic-Matter and Trihalomethane Precursors." *Water Sci. Technol.*, 27(11), 113-121.

Amirtharajah, A., and Mills, K. M. (1982). "Rapid-Mix Design for Mechanisms of Alum Coagulation." *J. Am. Water Work Assoc.*, 74(4), 210-216.

Appelo, C. A. J., Van der Weiden, M. J. J., Tournassat, C., and Charlet, L. (2002). "Surface complexation of ferrous iron and carbonate on ferrihydrite and the mobilization of arsenic." *Environ. Sci. Technol.*, 36(14), 3096-3103.

Baalousha, M., Motelica-Heino, M., and Le Coustumer, P. (2006). "Conformation and size of humic substances: Effects of major cation concentration and type, pH, salinity, and residence time." *Colloid Surf. A-Physicochem. Eng. Asp.*, 272(1-2), 48-55.

Baylis, J. R. (1937). "Silicates as Aids to Coagulation." *J. Am. Water Work Assoc.*, 29(9), 1355-1395.

Boccelli, D. L., Small, M. J., and Dzombak, D. A. (2006). "Effects of water quality and model structure on arsenic removal simulation: An optimization study." *Environ. Eng. Sci.*, 23(5), 835-850.

Bose, P., and Reckhow, D. A. (1997). "Modeling pH and ionic strength effects on proton and calcium complexation of fulvic acid: A tool for drinking water-NOM studies." *Environ. Sci. Technol.*, 31(3), 765-770.

Chen, H. W., Davis, C. C., and Edwards, M. (2005). "Using surface complexation modeling to assess the role of silica in arsenate adsorption onto metal oxides." *J. Water Supply Res Technol.-Aqua*, 54(6), 339-348.

Davis, C. C., Chen, H. W., and Edwards, M. (2002). "Modeling silica sorption to iron hydroxide." *Environ. Sci. Technol.*, 36(4), 582-587.

Davis, C. C., and Edwards, M. (2014a). "Influence of Silica on Coagulation and Implications for NOM Removal." *Manuscript submitted for publication*.

Davis, C. C., and Edwards, M. (2014b). "Role of Calcium in the Coagulation of NOM with Ferric Chloride." *Manuscript submitted for publication*.

Davis, C. C., Knocke, W. R., and Edwards, M. (2001). "Implications of aqueous silica sorption to iron hydroxide: Mobilization of iron colloids and interference with sorption of arsenate and humic substances." *Environ. Sci. Technol.*, 35(15), 3158-3162.

Dempsey, B. A., and O'Melia, C. R. (1983). "Proton and Calcium Complexation of Four Fulvic Acid Fractions." *Aquatic and Terrestrial Humic Materials*, R. F. Christman, and E. T. Gjessing, eds., Ann Arbor Science, Ann Arbor, MI.

Doelsch, E., Masion, A., Rose, J., Stone, W. E. E., Bottero, J. Y., and Bertsch, P. M. (2003). "Chemistry and structure of colloids obtained by hydrolysis of Fe(III) in the presence of SiO4 ligands." *Colloid Surf. A-Physicochem. Eng. Asp.*, 217(1-3), 121-128.

Doelsch, E., Stone, W. E. E., Petit, S., Masion, A., Rose, J., Bottero, J. Y., and Nahon, D. (2001). "Speciation and crystal chemistry of Fe(III) chloride hydrolyzed in the presence of SiO4 ligands. 2. Characterization of Si-Fe aggregates by FTIR and Si-29 solid-state NMR." *Langmuir*, 17(5), 1399-1405.

Dowbiggin, W. B., and Singer, P. C. (1989). "Effects of Natural Organic-Matter and Calcium on Ozone-Induced Particle Destabilization." *J. Am. Water Work Assoc.*, 81(6), 77-85.

Duan, J. M., Cao, X. T., Chen, C., Shi, D. R., Li, G. M., and Mulcahy, D. (2012). "Effects of Ca(OH)(2) assisted aluminum sulfate coagulation on the removal of humic acid and the formation potentials of tri-halomethanes and haloacetic acids in chlorination." *Journal of Environmental Sciences-China*, 24(9), 1609-1615.

Dzombak, D. A., and Morel, F. M. M. (1990). *Surface Complexation Modeling: Hydrous Ferric Oxide*, Wiley-Interscience, New York.

Eaton, A. D., Clesceri, L. S., Rice, E. W., and Greenberg, A. E. (2005). "Standard Methods of the Examination of Water and Wastewater." American Public Health Association, Washington, D.C.

Edwards, M. (1997). "Predicting DOC Removal During Enhanced Coagulation." *J. Am. Water Work Assoc.*, 89(5), 78-89.

Edwards, M., and Benjamin, M. M. (1992). "Effect of Preozonation on Coagulant-NOM Interactions." *J. Am. Water Work Assoc.*, 84(8), 63-72.

Edzwald, J. K. (2010). "Dissolved air flotation and me." *Water Res.*, 44(7), 2077-2106.

Edzwald, J. K., and Van Benschoten, J. E. (1990). "Aluminum Coagulation of Natural Organic Matter." *Chemical Water and Wastewater Treatment*, H. H. Hahn, and R. Klute, eds., Springer-Verlag, Berlin.

Evanko, C. R., and Dzombak, D. A. (1999). "Surface complexation modeling of organic acid sorption to goethite." *J. Colloid Interface Sci.*, 214(2), 189-206.

Gustafsson, J. P. (2001). "Modeling the acid-base properties and metal complexation of humic substances with the Stockholm Humic Model." *J. Colloid Interface Sci.*, 244(1), 102-112.

Gustafsson, J. P. (2011). "Visual MINTEQ ".

Herbelin, A., and Westall, J. (1999). "FITEQL 4.0: A Computer Program for Determination of Chemical Equilibrium Constants from Experimental Data." Oregon State University, Corvallis, OR.

Hiemenz, P. C. (1986). *Principles of Colloid and Surface Chemistry*, Marcel Dekker, New York.

Holm, T. R. (2002). "Effects of CO32-/bicarbonate, Si, and PO43- on arsenic sorption to HFO." *J. Am. Water Work Assoc.*, 94(4), 174-181.

Huerta-Fontela, M., Galceran, M. T., and Ventura, F. (2011). "Occurrence and removal of pharmaceuticals and hormones through drinking water treatment." *Water Res.*, 45(3), 1432-1442.

Kaegi, R., Voegelin, A., Folini, D., and Hug, S. J. (2010). "Effect of phosphate, silicate, and Ca on the morphology, structure and elemental composition of Fe(III)-precipitates formed in aerated Fe(II) and As(III) containing water." *Geochim. Cosmochim. Acta*, 74(20), 5798-5816.

Kastl, G., Sathasivan, A., Fisher, I., and Van Leeuwen, J. (2004). "Modeling DOC removal by enhanced coagulation." *J. Am. Water Work Assoc.*, 96(2), 79-89.

Lee, B.-B., Choo, K.-H., Chang, D., and Choi, S.-J. (2009). "Optimizing the coagulant dose to control membrane fouling in combined coagulation/ultrafiltration systems for textile wastewater reclamation." *Chemical Engineering Journal*, 155(1-2), 101-107.

Lefebvre, E., and Legube, B. (1990). "Iron(III) Coagulation of Humic Substances Extracted from Surface Waters - Effect of pH and Humic Substances Concentration." *Water Res.*, 24(5), 591-606.

Letterman, R. D., Amirtharajah, A., and O'Melia, C. R. (1999). "Coagulation and Flocculation." *Water Quality and Treatment: A Handbook of Community Water Supplies*, R. D. Letterman, ed., McGraw-Hill, Inc., New York, 6.1-6.66.

Liu, R. P., Qu, J. H., Xia, S. J., Zhang, G. S., and Li, G. B. (2007). "Silicate hindering in situ formed ferric hydroxide precipitation: Inhibiting arsenic removal from water." *Environ. Eng. Sci.*, 24(5), 707-715.

Luxton, T. P., Tadanier, C. J., and Eick, M. J. (2006). "Mobilization of arsenite by competitive interaction with silicic acid." *Soil Sci. Soc. Am. J.*, 70(1), 204-214.

Meng, X. G., Bang, S., and Korfiatis, G. P. (2000). "Effects of silicate, sulfate, and carbonate on arsenic removal by ferric chloride." *Water Res.*, 34(4), 1255-1261.

Parks, J. L., McNeill, L., Frey, M., Eaton, A. D., Haghani, A., Ramirez, L., and Edwards, M. (2004). "Determination of total chromium in environmental water samples." *Water Res.*, 38(12), 2827-2838.

Pommerenk, P. (2001). "Adsorption of Inorganic and Organic Ligands onto Aluminum Hydroxide and Its Effect in Water Treatment." Ph.D., Old Dominion University, Norfolk, VA.

Randtke, S. J., and Jepsen, C. P. (1981). "Chemical Pretreatment for Activated-Carbon Adsorption." *J. Am. Water Work Assoc.*, 73(8), 411-419.

Sharp, E. L., Jarvis, P., Parsons, S. A., and Jefferson, B. (2006a). "The impact of zeta potential on the physical properties of ferric-NOM flocs." *Environ. Sci. Technol.*, 40(12), 3934-3940.

Sharp, E. L., Parson, S. A., and Jefferson, B. (2006b). "Coagulation of NOM: linking character to treatment." *Water Sci. Technol.*, 53(7), 67-76.

Shin, J. Y., Spinette, R. F., and O'Melia, C. R. (2008). "Stoichiometry of Coagulation Revisited." *Environ. Sci. Technol.*, 42(7), 2582-2589.

Sigg, L., and Stumm, W. (1981). "The Interaction of Anions and Weak Acids with the Hydrous Goethite (Alpha-Feooh) Surface." *Colloids and Surfaces*, 2(2), 101-117.

Singer, P. C., Harrington, G. W., Thompson, J., and White, M. (1995). "Enhanced Coagulation and Enhanced Softening for the Removal of Disinfection By-product Precursors: An Evaluation." Univeristy of North Carolina at Chapel Hill, Chapel Hill, NC.

Smith, S. D., and Edwards, M. (2005). "The influence of silica and calcium on arsenate sorption to oxide surfaces." *J. Water Supply Res Technol.-Aqua*, 54(4), 201-211.

Stachowicz, M., Hiemstra, T., and Van Riemsdijk, W. H. (2007). "Arsenic-bicarbonate interaction on goethite particles." *Environ. Sci. Technol.*, 41(16), 5620-5625.

Stumm, W., and O'Melia, C. R. (1968). "Stoichiometry of Coagulation." *J. Am. Water Work Assoc.*, 60(5), 514-569.

Stumm, W., and Sigg, L. (1979). "Colloid-Chemical Basis of Phosphate Removal by Chemical Precipitation, Coagulation and Filtration." *Zeitschrift Fur Wasser Und Abwasser Forschung-Journal for Water and Wastewater Research*, 12(2), 73-83.

Swedlund, P. J., Hamid, R. D., and Miskelly, G. M. (2010). "Insights into H4SiO4 surface chemistry on ferrihydrite suspensions from ATR-IR, Diffuse Layer Modeling and the adsorption enhancing effects of carbonate." *J. Colloid Interface Sci.*, 352(1), 149-157.

Swedlund, P. J., Sivaloganathan, S., Miskelly, G. M., and Waterhouse, G. I. N. (2011). "Assessing the role of silicate polymerization on metal oxyhydroxide surfaces using X-ray photoelectron spectroscopy." *Chem. Geol.*, 285(1-4), 62-69.

Swedlund, P. J., and Webster, J. G. (1999). "Adsorption and polymerisation of silicic acid on ferrihydrite, and its effect on arsenic adsorption." *Water Res.*, 33(16), 3413-3422.

Tipping, E. (1981). "The Adsorption of Aquatic Humic Substances by Iron Oxides." *Geochim. Cosmochim. Acta*, 45(2), 191-199.

Tseng, T., and Edwards, M. (1999). "Predicting Full-Scale TOC Removal." *J. Am. Water Work Assoc.*, 91(4), 159-170.

Tseng, T., Segal, B. D., and Edwards, M. (2000). "Increasing Alkalinity to Reduce Turbidity." *J. Am. Water Work Assoc.*, 92(6), 44-54.

van Leeuwen, J., Daly, R., and Holmes, A. (2005). "Modeling the treatment of drinking water to maximize dissolved organic matter removal and minimize disinfection by-product formation." *Desalination*, 176(1-3), 81-89.

Villalobos, M., and Leckie, J. O. (2000). "Carbonate adsorption on goethite under closed and open CO2 conditions." *Geochim. Cosmochim. Acta*, 64(22), 3787-3802.

Voegelin, A., Kaegi, R., Frommer, J., Vantelon, D., and Hug, S. J. (2010). "Effect of phosphate, silicate, and Ca on Fe(III)-precipitates formed in aerated Fe(II)- and As(III)-containing water studied by X-ray absorption spectroscopy." *Geochim. Cosmochim. Acta*, 74(1), 164-186.

Wang, J., and Wang, X.-c. (2006). "Ultrafiltration with in-line coagulation for the removal of natural humic acid and membrane fouling mechanism." *Journal of Environmental Sciences*, 18(5), 880-884.

Weng, L. P., Koopal, L. K., Hiemstra, T., Meeussen, J. C. L., and Van Riemsdijk, W. H. (2005). "Interactions of calcium and fulvic acid at the goethite-water interface." *Geochim. Cosmochim. Acta*, 69(2), 325-339.

Westerhoff, P., Yoon, Y., Snyder, S., and Wert, E. (2005). "Fate of endocrine-disruptor, pharmaceutical, and personal care product chemicals during simulated drinking water treatment processes." *Environ. Sci. Technol.*, 39(17), 6649-6663.

White, M. C., Thompson, J. D., Harrington, G. W., and Singer, P. C. (1997). "Evaluating Criteria for Enhanced Coagulation Compliance." *J. Am. Water Work Assoc.*, 89(5), 64-77.

Wilkie, J. A., and Hering, J. G. (1996). "Adsorption of arsenic onto hydrous ferric oxide: Effects of adsorbate/adsorbent ratios and co-occurring solutes." *Colloid Surf. A-Physicochem. Eng. Asp.*, 107, 97-110.

Xia, S. J., Li, X., Zhang, Q. L., Xu, B., and Li, G. B. (2007). "Ultrafiltration of surface water with coagulation pretreatment by streaming current control." *Desalination*, 204(1-3), 351-358.

Xie, J., Wang, D., van Leeuwen, J., Zhao, Y., Xing, L., and Chow, C. W. K. (2012). "pH modeling for maximum dissolved organic matter removal by enhanced coagulation." *Journal of Environmental Sciences*, 24(2), 276-283.

Zachara, J. M., Girvin, D. C., Schmidt, R. L., and Resch, C. T. (1987). "Chromate Adsorption on Amorphous Iron Oxyhydroxide in the Presence of Major Groundwater Ions." *Environ. Sci. Technol.*, 21(6), 589-594.

Appendix A. Supplemental Information

to accompany manuscript submission for

Chapter 3. Influence of Silica on Coagulation and Implications for NOM Removal

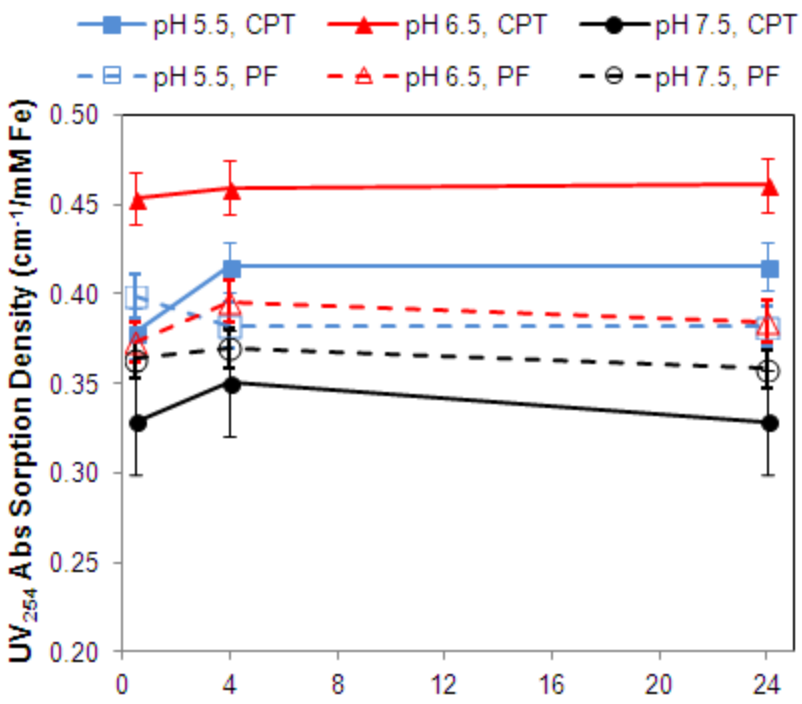

Figure A-1. UV_{254} Abs sorption densities in coprecipitated (CPT) and preformed (PF) systems as a function of pH and reaction time.

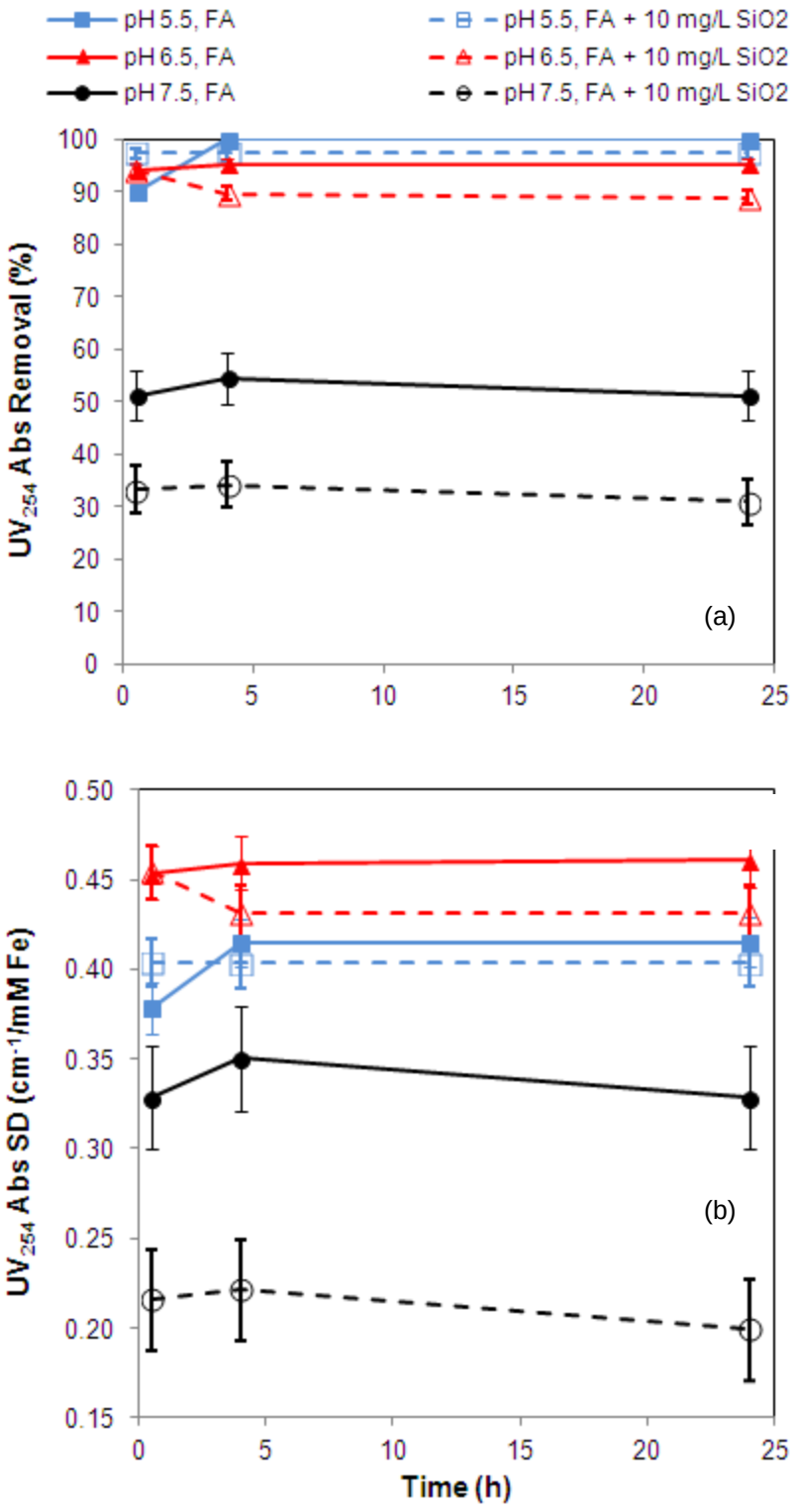

Figure A-2. (a) UV_{254} Abs removal and (b) UV_{254} Abs sorption density (SD) as a function of pH and time in coprecipitated systems. Samples contain 10 mg/L as Fe and fulvic acid (FA) at 2 mg/L as DOC. Open symbols represent systems that also include 10 mg/L of SiO_2.

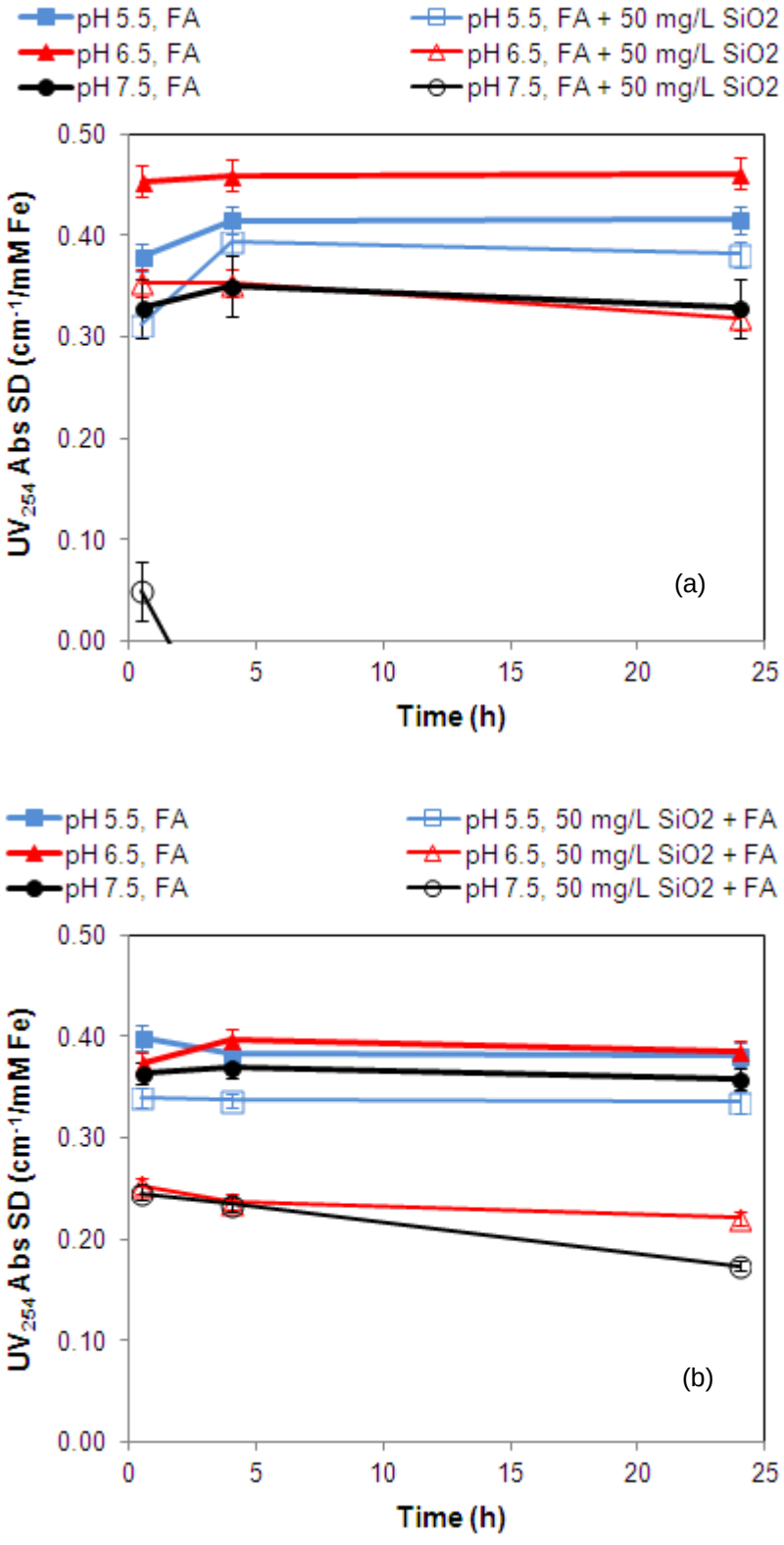

Figure A-3. UV_{254} Abs sorption densities (SD) in (a) coprecipitated and (b) preformed systems as a function of pH and reaction time. Samples contain 10 mg/L as Fe and fulvic acid (FA) at 2 mg/L as DOC. Open symbols represent systems that also include 50 mg/L of SiO_2.

Appendix B. Supplemental Information

to accompany manuscript submission for

Chapter 4. Simultaneous Prediction of NOM Removal and Particle Destabilization in Coagulation

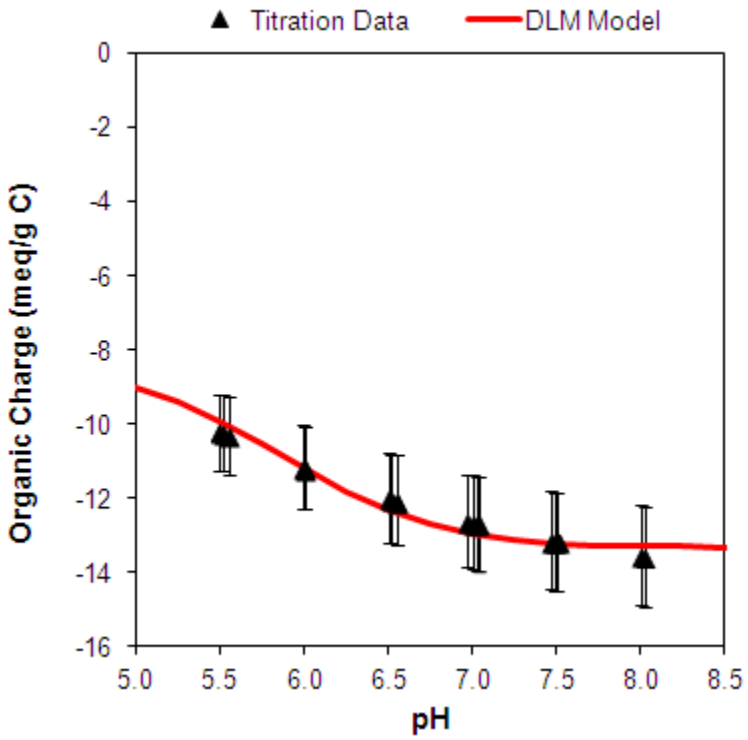

Figure B-1. Organic charge density of Silver Lake fulvic acid (FA) as determined by titration and predicted by the DLM. Error bars represent an estimated 10% error.

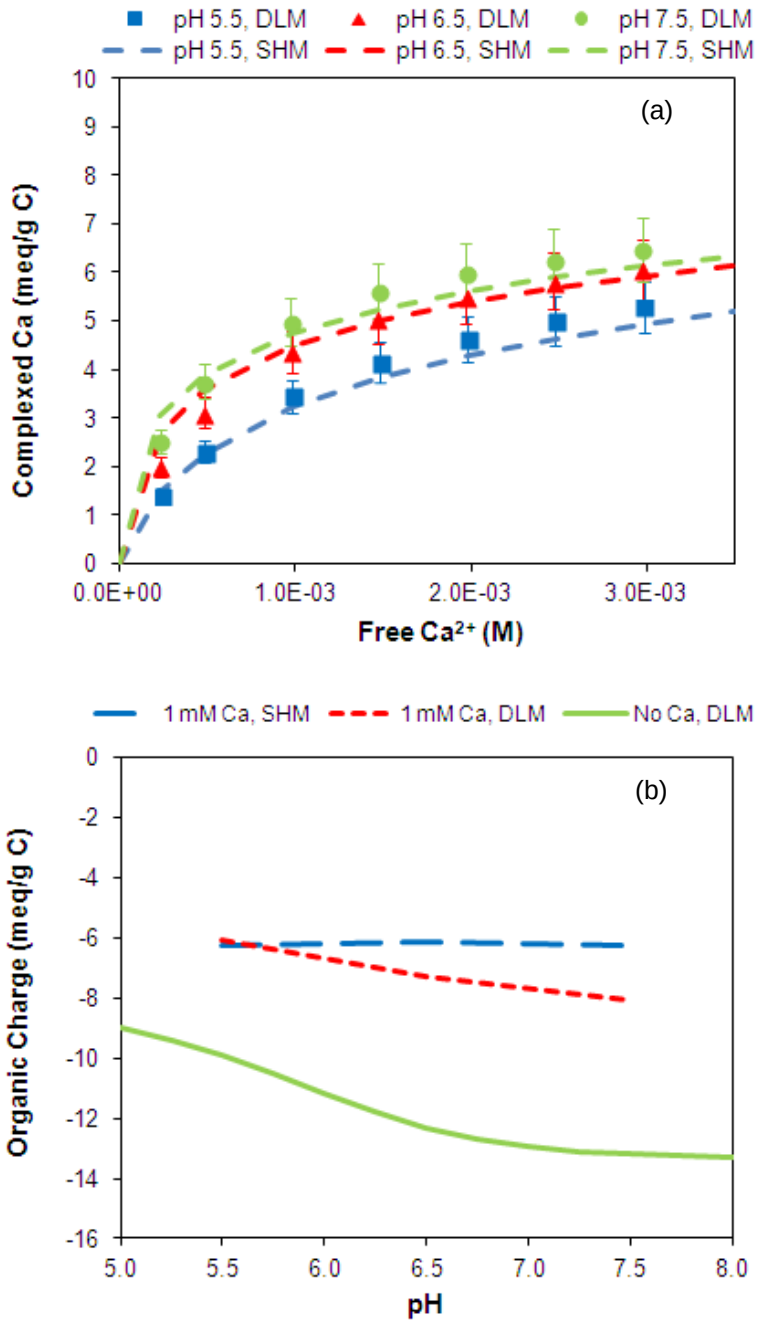

Figure B-2. (a) DLM and Stockholm Humic Model (SHM) predictions of complexed calcium as a function of free calcium and pH. (b) DLM and SHM predictions of organic charge neutralization by 1 mM Ca^{2+}.

Desktop Testing for Planning and Operations

A model simulation of Flagstaff water and calculation of Potential-0.50 suggests that minimum doses of 12.5 mg/L as Fe at pH 5.5 to 30 mg/L as Fe at pH 6.8 are required to attain minimum Potential-0.50 values of –10 mV, the assumed threshold for particle destabilization and effective settling (Figure B-3a). The model simulation also indicates that the expected TOC removal for Flagstaff meets or exceeds the regulatory requirement of 45% under all conditions where Potential-0.50 is greater than or equal to -10 mV if restabilization does not occur. A second simulation was run to assess treatment options in response to a hypothetical storm runoff event; this scenario was characterized by an increase in DOC (12.9 mg/L), and decreases in alkalinity (8.7 mg/L as $CaCO_3$) and calcium hardness (4.7 mg/L as $CaCO_3$). Model output suggests that much higher coagulant concentrations would be required to treat this hypothetical raw water with at least 35 mg/L as Fe required at pH 5.5 (Figure B-3b). Again, the model suggests that at least 45% TOC removal can be achieved at all Potential-0.50 values greater than or equal to -10 mV.

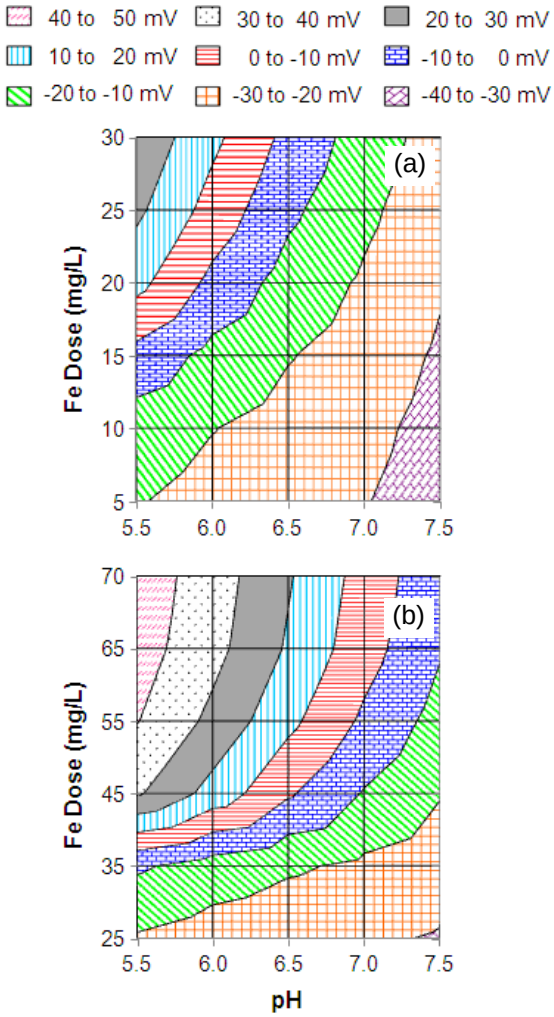

Figure B-3. (a) Predicted Potential-0.50 as a function of Fe dose and pH for Flagstaff source water. (b) Predicted Potential-0.50 as a function of Fe dose and pH for a hypothetical storm event yielding water with high DOC (12.9 mg/L), low alkalinity (8.7 mg/L as $CaCO_3$) and low calcium hardness (4.7 mg/L as $CaCO_3$).

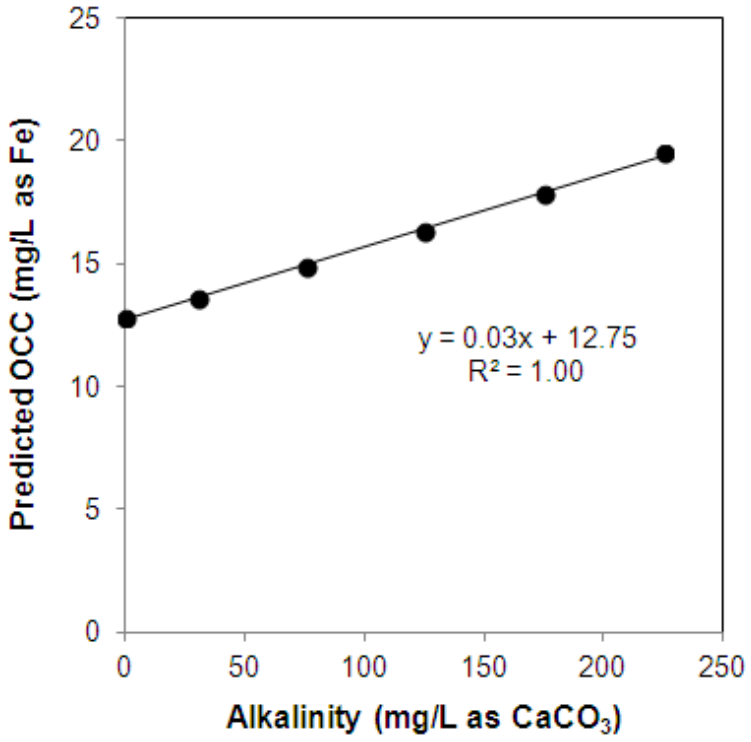

Figure B-4. Effect of carbonate alkalinity on predicted optimal coagulant concentration (OCC). This simulation assumes pH 6.5 and 3.20 mg/L of sorbable DOC. OCCs were selected as the doses with surface potential of 0 (PZC). Modeling predicts that OCC increases linearly with carbonate alkalinity.

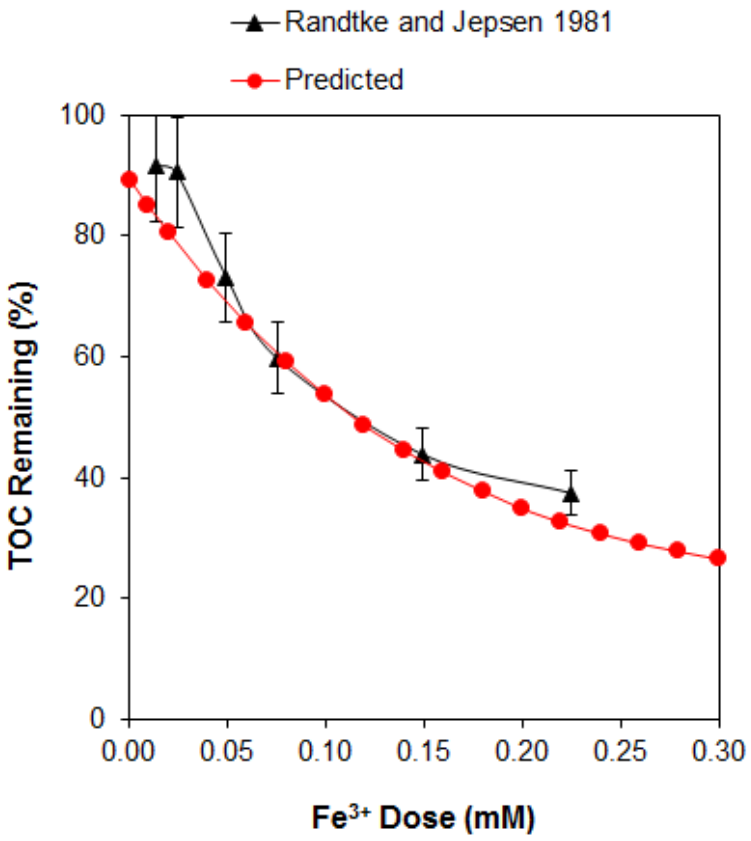

Figure B-5. TOC Remaining as a function of ferric sulfate dose for an Illinois groundwater. Data were collected by Randtke and Jepsen (1981), and predictions were made with the DLM assuming a non-sorbable TOC fraction of 22.5%, surface area of 600 m^2/g, and site density of 0.20 mol/mol Fe. Experiments and modeling were conducted at pH 6.0 with an initial TOC concentration of 3.85 mg/L. Error bars represent an estimated 10% error.

Appendix C. Additional Information

for

Chapter 4. Simultaneous Prediction of NOM Removal and Particle Destabilization in Coagulation

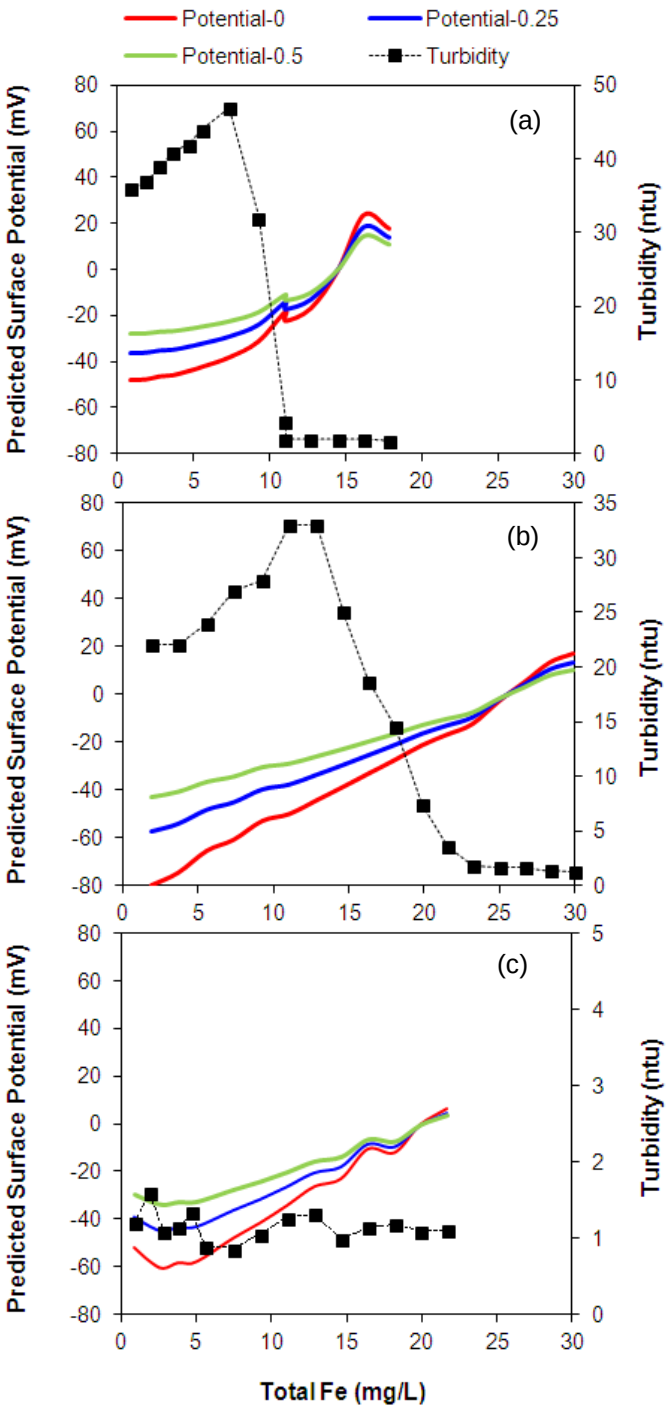

Figure C-1. Measured turbidities and predicted potentials at the surface (Potential-0) and at 25% and 50% of the double-layer "thickness" (Potential-0.25 and Potential-0.50, respectively) for (a) Flagstaff, (b) Houston, and (c) MWD-CRW.

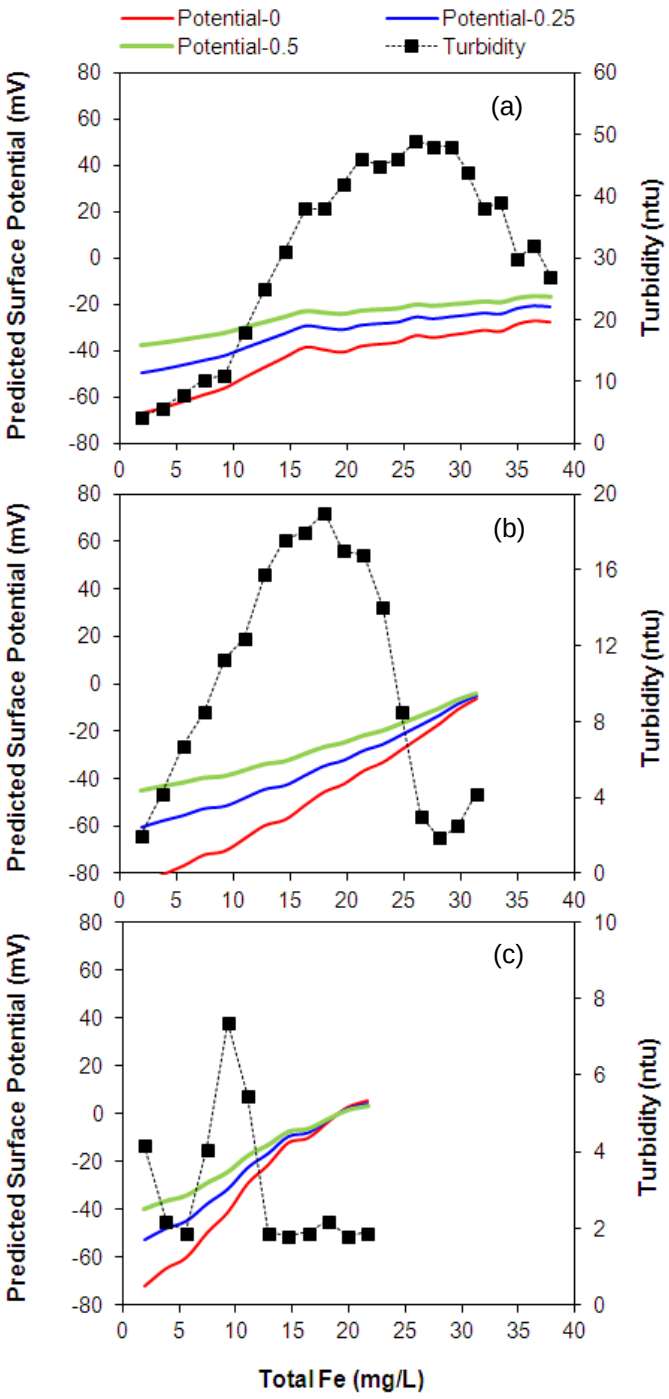

Figure C-2. Measured turbidities and predicted potentials at the surface (Potential-0) and at 25% and 50% of the double-layer "thickness" (Potential-0.25 and Potential-0.50, respectively) for (a) Chesapeake, (b) Tampa, and (c) Ft. Lauderdale.

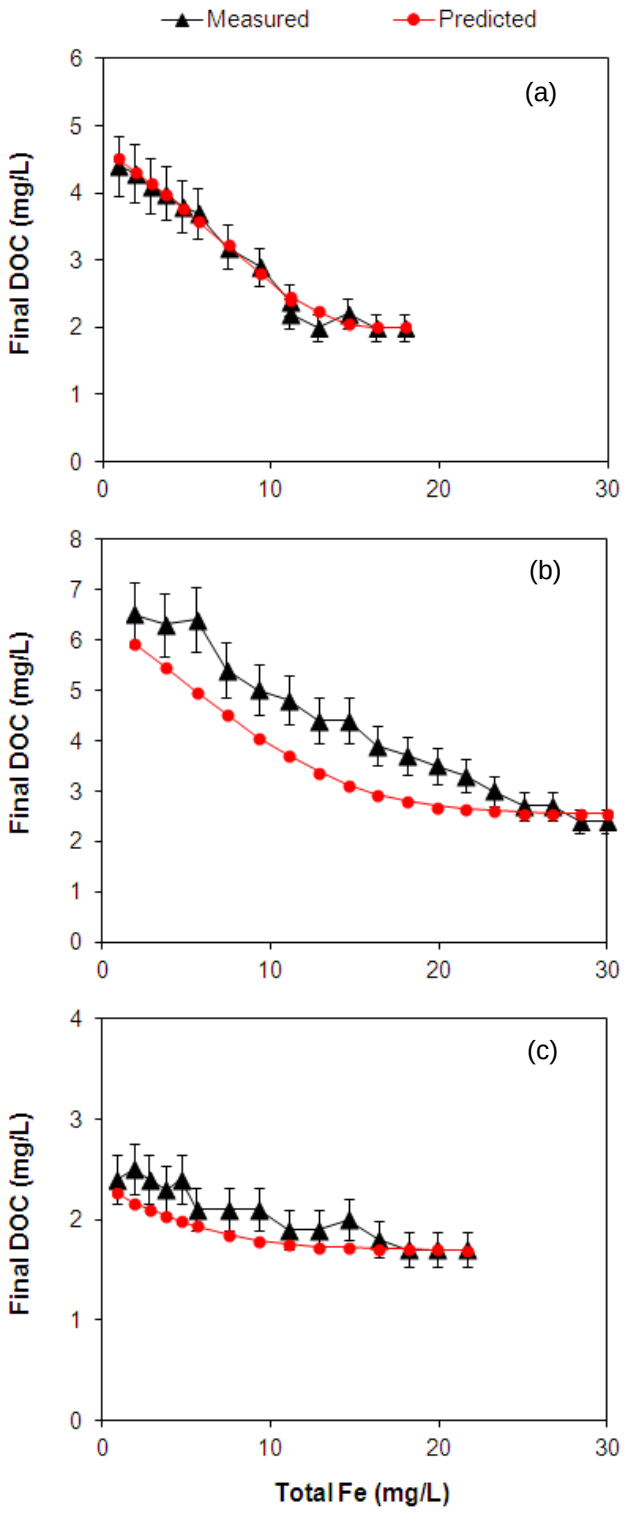

Figure C-3. The model provides excellent predictions of final DOC in certain waters, such as (a) Flagstaff and (c) MWD-CRW. At lower Fe doses, the model overpredicts DOC sorption in some waters with moderate or high alkalinity, including (b) Houston. Error in TOC measurement is estimated at 10%.

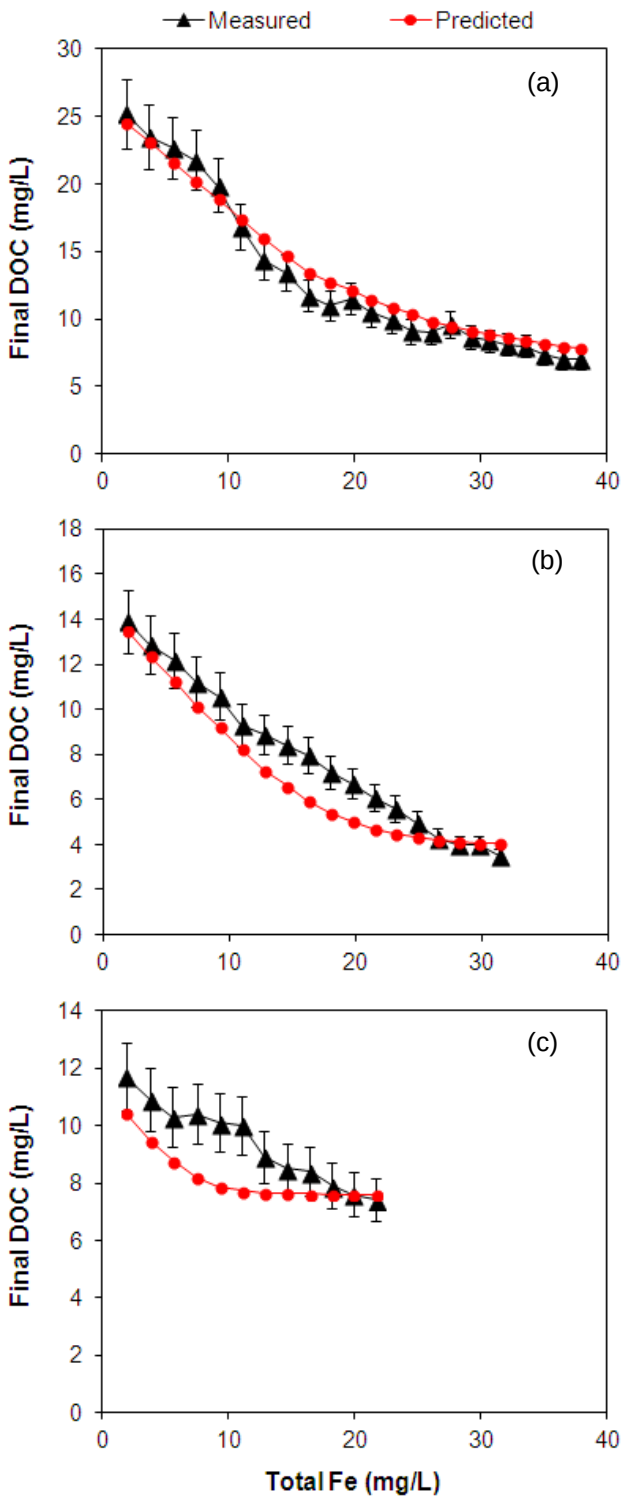

Figure C-4. The model provides excellent predictions of final DOC in certain waters, such as (a) Chesapeake. At lower Fe doses, the model overpredicts DOC sorption in some waters with moderate or high alkalinity, including (b) Tampa and (c) Ft. Lauderdale. Error in TOC measurement is estimated at 10%.

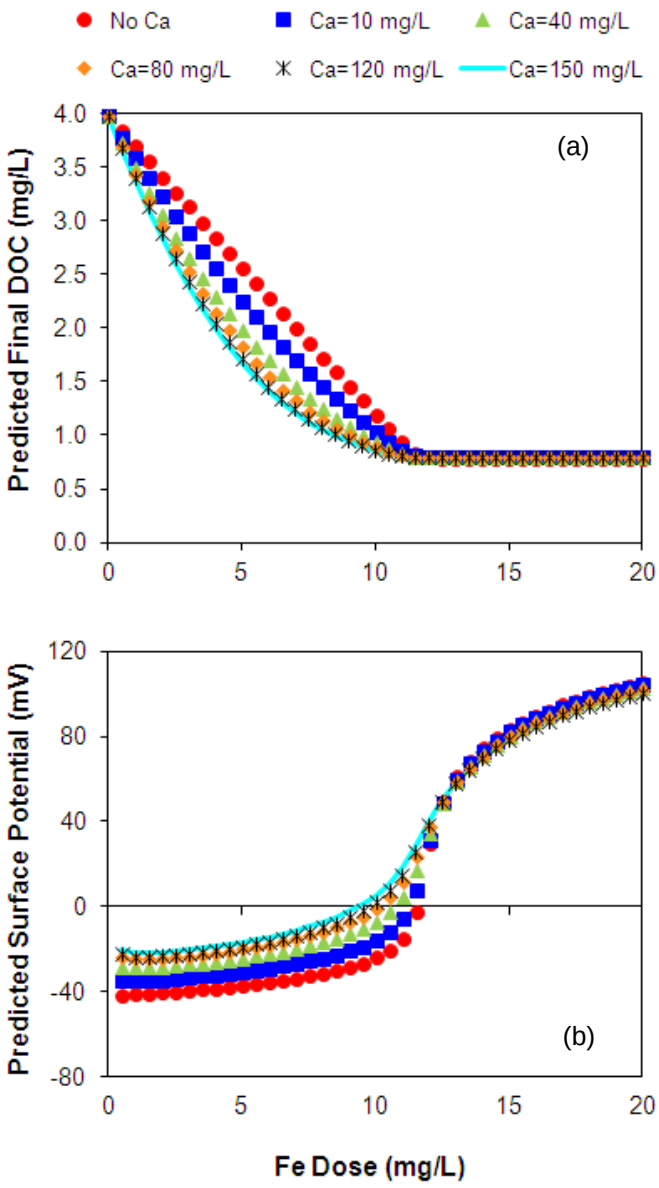

Figure C-5. (a) Effect of calcium concentration on predicted final DOC. This simulation assumes pH 5.5 and 3.20 mg/L of sorbable DOC. DOC sorption is expected to improve at all calcium concentrations. (b) Predicted surface potential as a function of calcium concentration and Fe dose at pH 5.5.

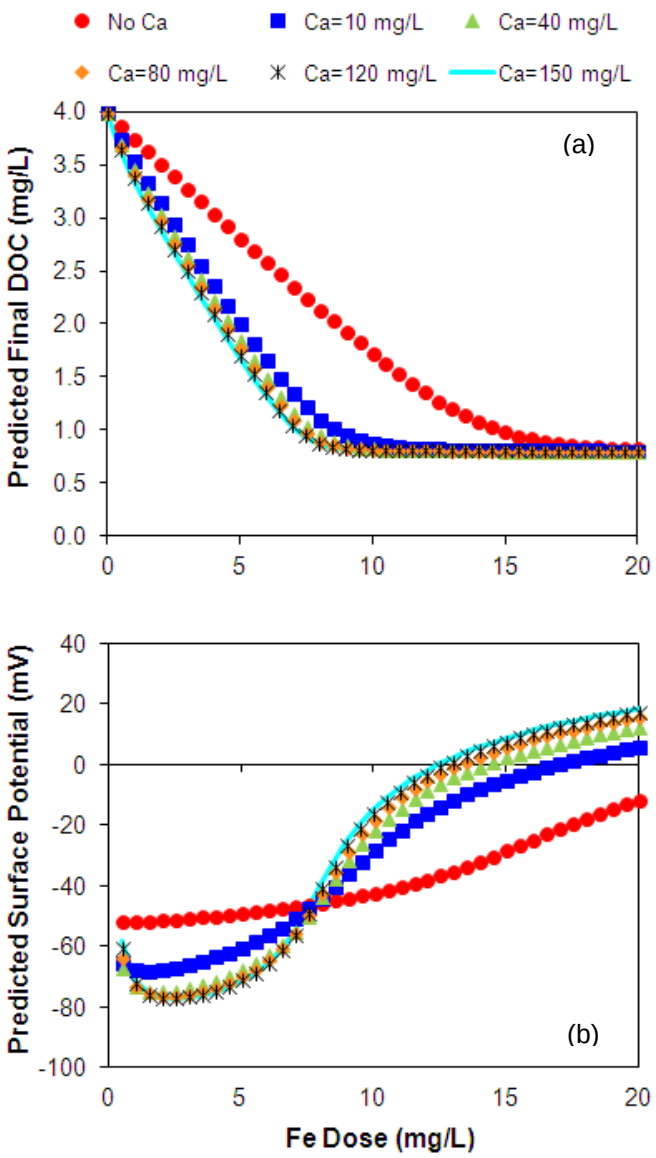

Figure C-6. (a) Effect of calcium concentration on predicted final DOC. This simulation assumes pH 7.5 and 3.20 mg/L of sorbable DOC. DOC sorption is expected to improve at all calcium concentrations. (b) Predicted surface potential as a function of calcium concentration and Fe dose at pH 7.5.

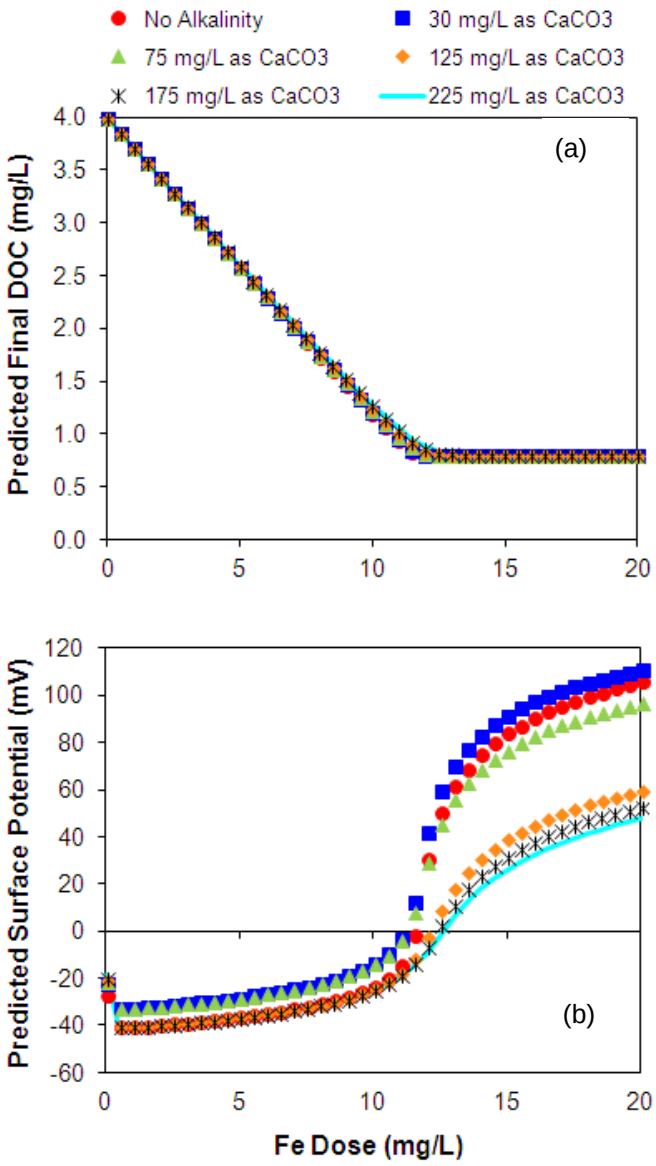

Figure C-7. (a) Effect of carbonate alkalinity on predicted final DOC. This simulation assumes pH 5.5 and 3.20 mg/L of sorbable DOC. (b) Predicted surface potential as a function of carbonate alkalinity and Fe dose at pH 5.5.

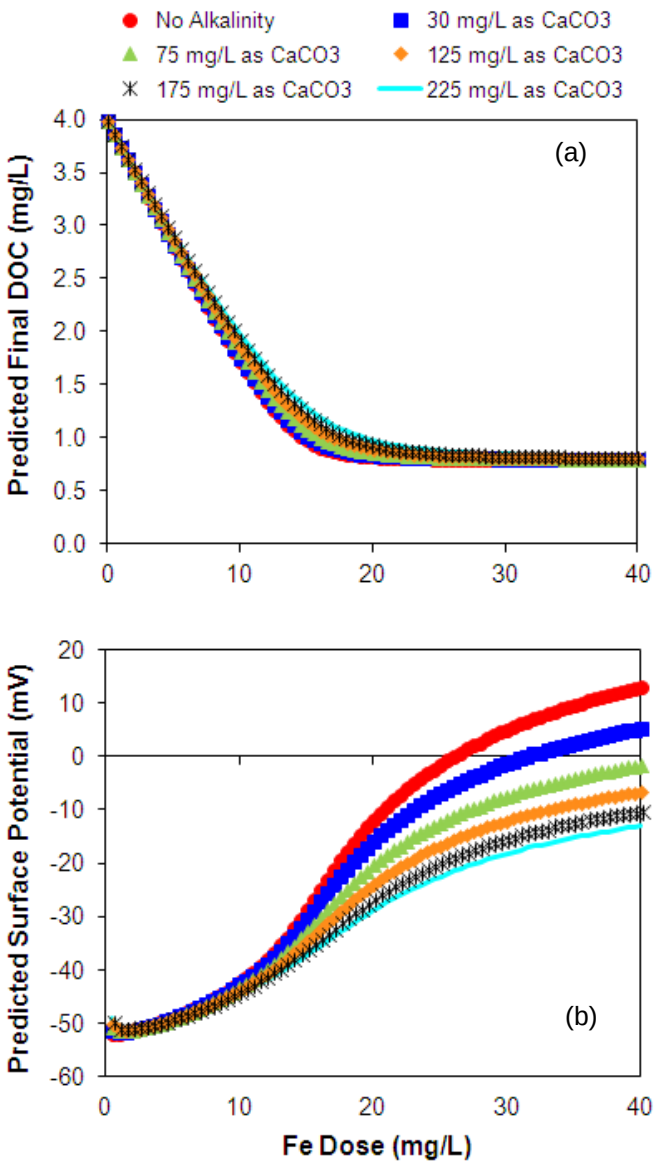

Figure C-8. (a) Effect of carbonate alkalinity on predicted final DOC. This simulation assumes pH 7.5 and 3.20 mg/L of sorbable DOC. (b) Predicted surface potential as a function of carbonate alkalinity and Fe dose at pH 7.5.

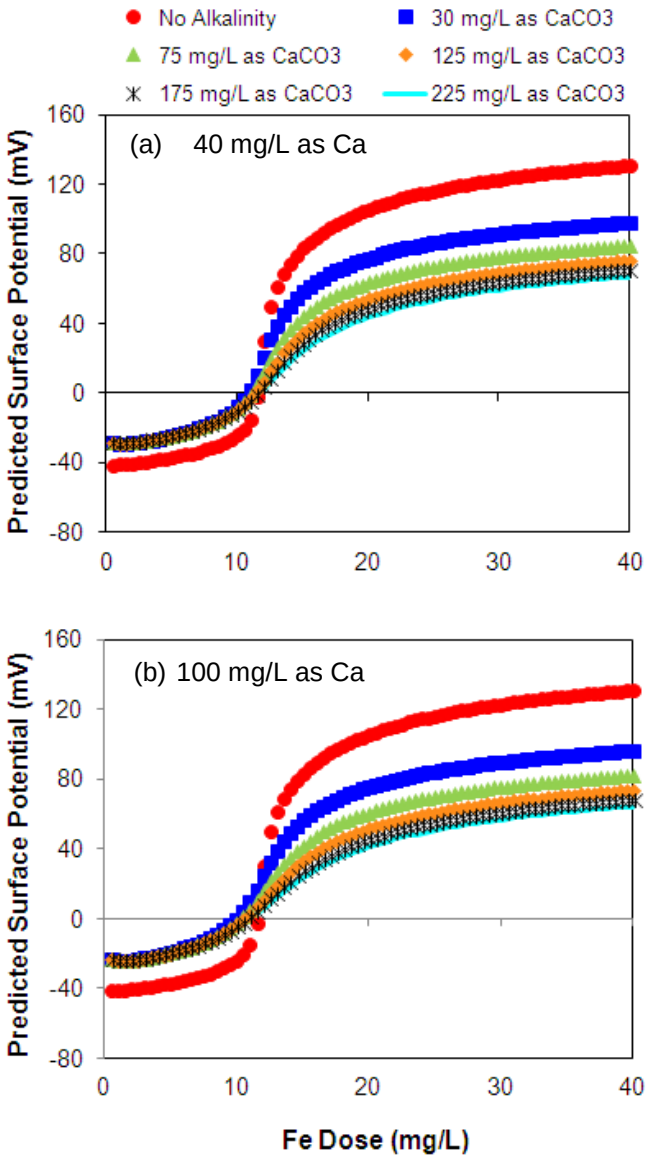

Figure C-9. (a) The influence of carbonate alkalinity, calcium (40 mg/L), and NOM (3.20 mg/L of sorbable DOC) on predicted surface potential at pH 5.5. (b) The influence of carbonate alkalinity, calcium (100 mg/L), and NOM (3.20 mg/L of sorbable DOC) on predicted surface potential at pH 5.5.

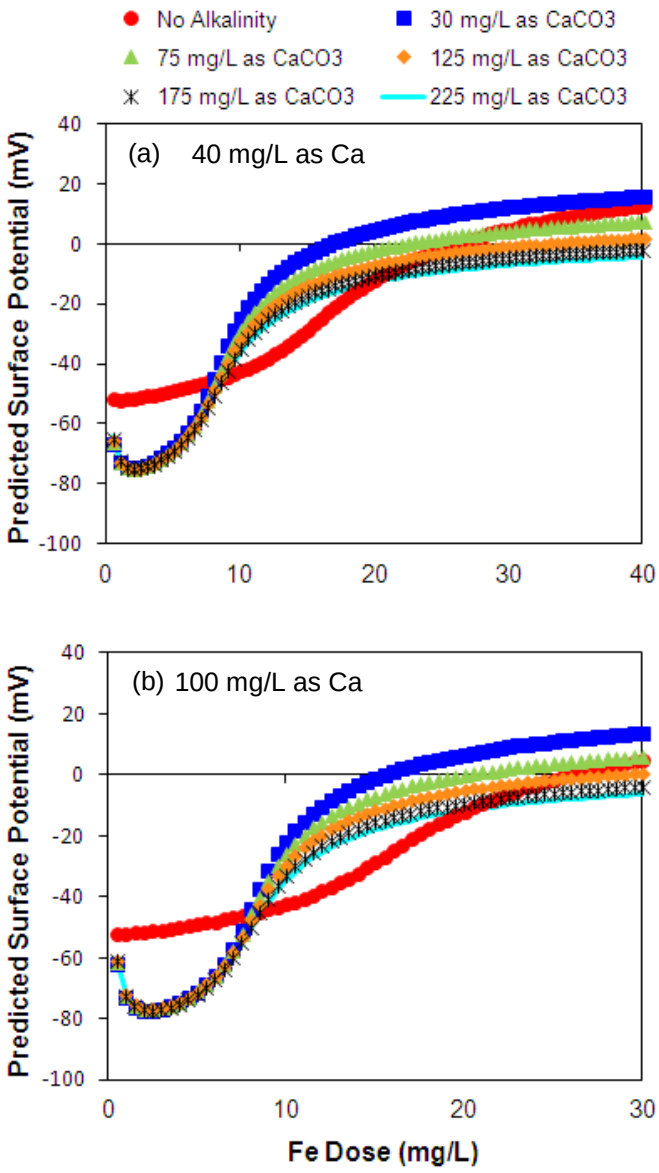

Figure C-10. (a) The influence of carbonate alkalinity, calcium (40 mg/L), and NOM (3.20 mg/L of sorbable DOC) on predicted surface potential at pH 7.5. (b) The influence of carbonate alkalinity, calcium (100 mg/L), and NOM (3.20 mg/L of sorbable DOC) on predicted surface potential at pH 7.5.